Decoding cultured meat production

DECODING CULTURED MEAT PRODUCTION

The transcriptomic landscape of bovine satellite cells in proliferation and differentiation

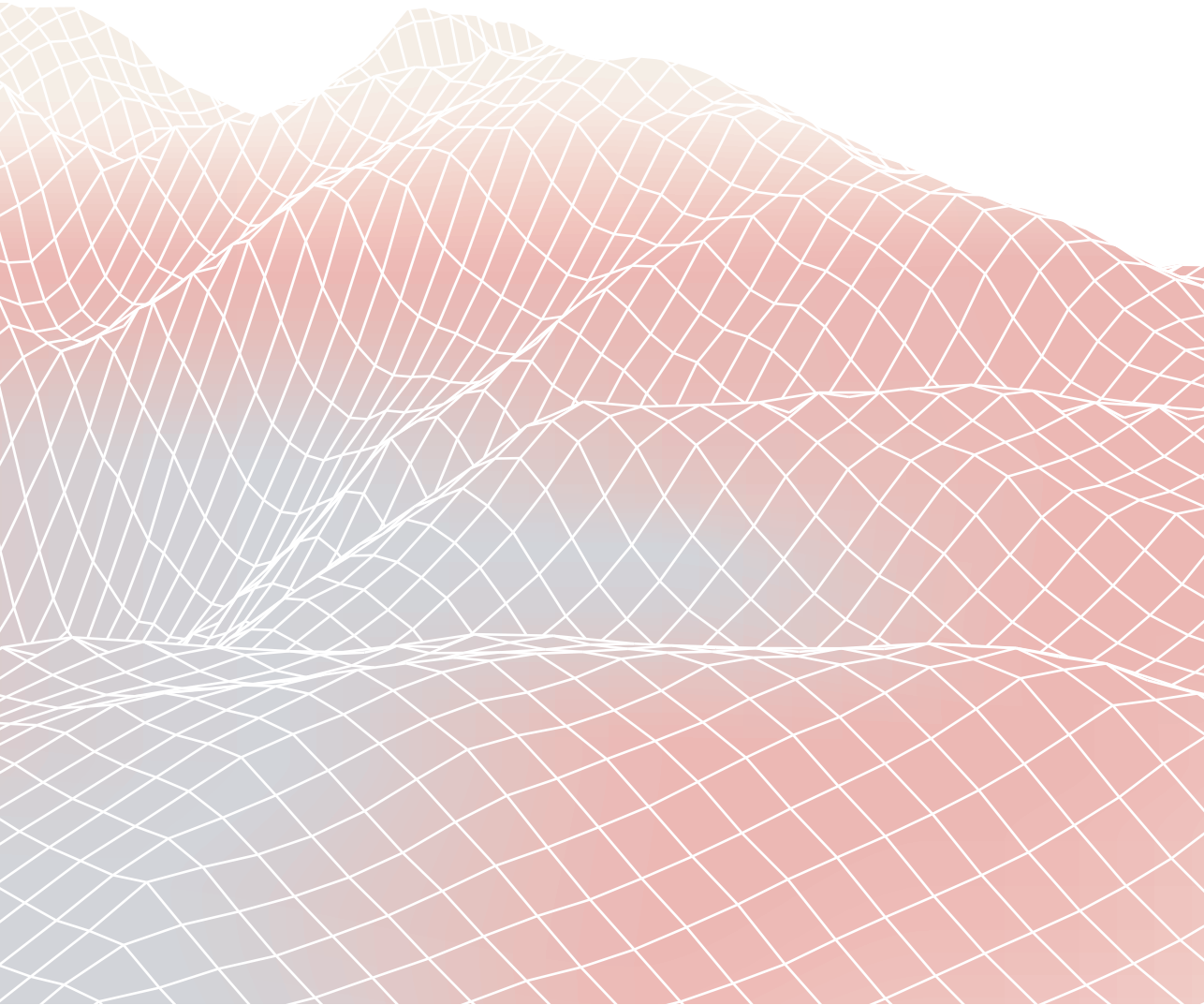

Tobias Meßmer

DECODING CULTURED MEAT PRODUCTION

The transcriptomic landscape of bovine satellite cells in proliferation and differentiation

Tobias Meßmer

The work presented in this thesis was performed within Maastricht University and Mosa Meat B.V.

ISBN: 978-94-6458-781-4
Cover design: Sandra Tukker
Lay-out: Publiss | www.publiss.nl
Printed: Ridderprint | www.ridderprint.nl

DECODING CULTURED MEAT PRODUCTION

The transcriptomic landscape of bovine satellite cells in proliferation and differentiation

DISSERTATION

to obtain the degree of Doctor at the Maastricht University,
on the authority of the Rector Magnificus,
Prof.dr. Pamela Habibović
in accordance with the decision of the Board of Deans,
to be defended in public on
Friday, 21st of April 2023 at 13:00 hours

by

Tobias Meßmer

Supervisors
Prof. Dr. M.J. Post
Dr. J.E. Flack

Assessment Committee
Prof. Dr. J. Sluimer (Chair)
Prof. Dr. C. Evelo
Prof. Dr. M. Henkel, Technische Universität München, Germany
Prof. Dr. F. Le Grand, Université Claude Bernard Lyon, France
Dr. T. Snijders

Financial support for the publication of this thesis as provided by Maastricht University and Mosa Meat B.V. is gratefully acknowledged.

TABLE OF CONTENTS

Chapter 1

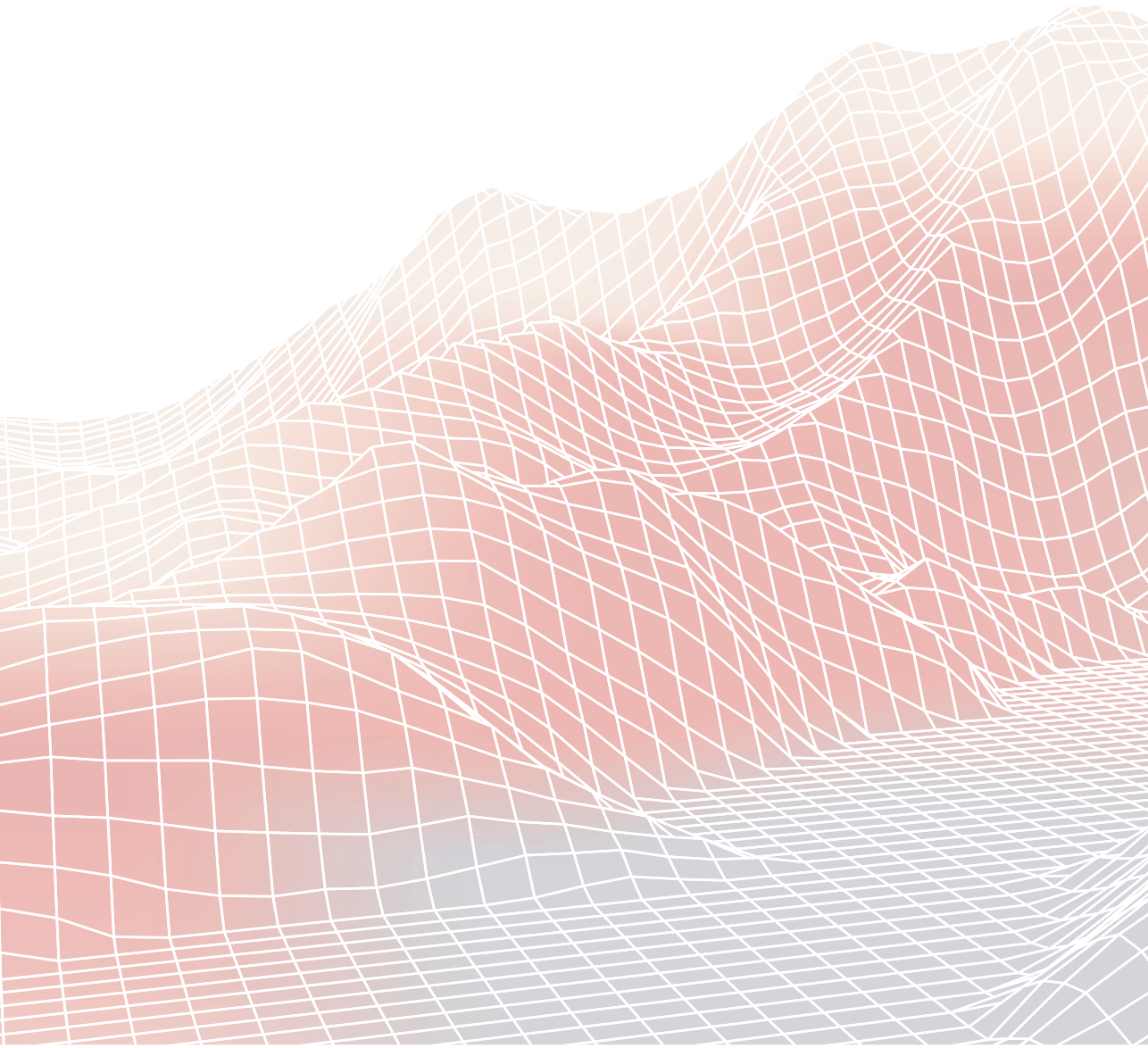

GENERAL INTRODUCTION

1.1 THE PROMISE OF CULTURED MEAT

Meat is an integral part of human diet and its consumption – not merely influenced by nutrition and taste but also by the societal, cultural, and religious environment of consumers - has been steadily increasing since the beginning of the 20th century.[1] Particularly through the introduction of industrial farming, global meat production considerably increased from 70.5 megatons at an average yearly consumption of 23.1 kg per person in 1960 to 337.5 megatons at 43.2 kg per capita in 2020 (Fig. 1). Over 71 billion animals, including 320 million cattle, are slaughtered each year to satisfy the global demand for meat, and their production requires 38.5% of habitable land and 30.2% of fresh water usage. Livestock production leads to 13.5% of global greenhouse gas emissions and is a major cause of deforestation and loss of biodiversity.[2,3]

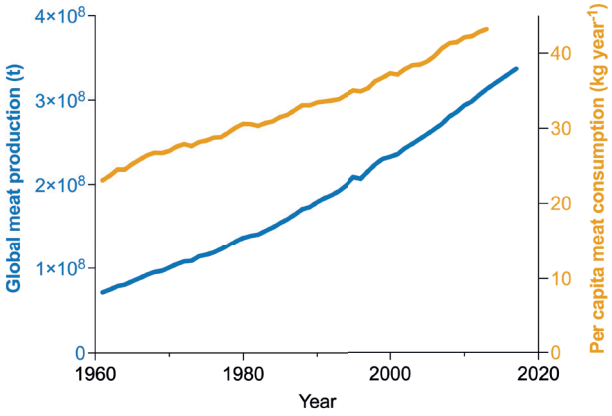

Figure 1: Increase in meat consumption since 1960.
Due to rising meat consumption per capita (orange) and a growing world population, global meat production has more than quadrupled within the past 60 years; adapted from Ritchie et al., 2017.[2]

There is a broad consensus that reduction in livestock is imperative to achieve sustainable levels of greenhouse gas emissions, preserve biodiversity and, of course, improve animal welfare.[4–8] However, despite the emergence of alternative proteins such as plant-based meat substitutes, many consumers fail to adopt a primarily vegetarian diet.[9,10]

A potential solution is the development of more sustainable and animal-friendly meat production methods. Meat is derived from skeletal muscle, which is primarily

composed of muscle fibres that are interspersed with adipose, connective, vascular and nervous tissues.[11] The field of tissue engineering has made it conceivable to create organs and functional tissues outside of an organism by the use of specialised stem cells and bioactive scaffolds.[12] Applied to skeletal muscle, this has resulted in the emergence of a food technology called 'cultured' or 'cultivated' meat, which aims to resolve many of the adverse implications of meat production.[13–16]

1.1.1 Concept

Production of meat has traditionally involved breeding, husbandry and slaughter of livestock animals. Optimisation of this process, for instance through feeding strategies or selective breeding, primarily focused on improving feed efficiency, tissue composition, growth speed, and total mass.[17] However, the energy required for the development and metabolism of an animal considerably exceeds the energy conserved in its edible tissue.[18] Instead of growing the entire animal, cultured meat technologies utilise in vitro culture techniques to isolate stem cells from livestock animals, expand them in bioreactors using specific growth media, and differentiate them into edible, skeletal muscle-like tissues.

The origins of this concept date back to the beginning of the 20th century, and technological feasibility has come within reach with the emergence of tissue engineering.[14] However, it was not until 2013 that the manual production of a burger from bovine skeletal muscle-derived cells has provided proof of principle.[13] This has led to the formation of numerous commercial and academic parties dedicated to realising an upscaled production process of cultured meat,[19] seeking to reduce the environmental impact of meat consumption.

1.1.2 Environmental prospects

Cultured meat aims to drastically reduce livestock by circumventing animal husbandry and slaughter for meat production, and replacing it with the in vitro production of cell-derived tissues.

Due to the large environmental footprint associated with conventional meat, especially beef, cultured meat promises to considerably reduce greenhouse gas emissions. Cultured cells have a higher feed conversion rate than cattle and hence require significantly fewer crops to produce the same amount of beef.[20] Compared to beef cattle, land and water consumption per kilogram of meat may be

reduced by up to 15 and 5 times, respectively.[21,22] Reduction of livestock would also drastically reduce the emission of methane from enteric fermentation. However, manufacture, operation and sterilisation of bioreactors necessary in cultured meat production make it a highly energy-intensive process. Therefore, only by the use of renewable energy in production facilities, the carbon footprint of cultured meat can be significantly lowered compared to conventionally grown meat, by up to 2- to 30-fold fewer CO_2-equivalents per kg of produced protein.[21,22] Moreover, as up to 70% of antibiotics in the US are used in animal production and livestock is a major source of zoonotic disease, the prospect of an antibiotic-free and animal component-free bioprocess in a sterile environment suggests positive effects on global health.[23,24]

While promising, it is noteworthy that life cycle assessment studies underlying these comparisons are based on assumptions, including many of which contain a wide margin of error due to multiple degrees of freedom and lack of commercial-scale operational facilities.[25] Therefore, whether and to what extent cultured meat technologies may lower the environmental impact of meat production needs to be re-examined when first commercial bioprocesses approach operation.

1.1.3 Technical overview

In its most common definition, meat refers to skeletal muscle with associated connective and fat tissues of non-human animals. Cultured meat technologies attempt to recreate this tissue through a variety of approaches that generally share four principal steps (section 1.2).[26]

First, a cell source that possesses the potential to proliferate in vitro and form muscle, fat, or other meat-associated tissues is derived from an animal by sample extraction, tissue digestion, cell purification, and, if necessary, cell modification. Suitable starting cells can be primary stem cells such as muscle-resident satellite cells (SCs), fibro-adipogenic progenitors (FAPs), or mesenchymal stem cells (MSCs), or engineered cell lines such as pluripotent stem cells or genetically modified somatic cells. Second, during the proliferation phase of the process, this starting population of cells needs to be multiplied in vitro to reach substantial amounts of mass by continuous stimulation of cell division.[27,28] Defined growth media provide nutrients and growth stimuli that enable manifold cell proliferation and need to be adapted for the specific cell type, species, and other bioprocess requirements.[29]

When a sufficient mass is reached, the (thus far) undifferentiated cells are transferred onto biomaterials that, together with a switch to a differentiation medium, allow functionalisation towards muscle fibres or fat.[30] There is a wide variety of approaches to perform differentiation, varying in duration (between 5-28 days), extent of maturation, underlying biomaterials (hydrogels vs. scaffolds) and tissue complexity (mono-culture vs. co-culture system).[31–37] The process is then finalised by harvesting the produced tissues and by assembly and post-processing of the end product.

This general bioprocess has been described in variations in small-scale dimensions. However, transferring the technology from a laboratory to a commercially relevant scale requires overcoming a multitude of technological challenges.[38]

1.1.4 Challenges

To bring cultured meat to market, it is necessary to design a bioprocess that yields a product that is affordable, safe to consume, and resembles the sensation and taste of conventionally grown meat.[39] The challenges that need to be addressed to meet these criteria include removal of animal components from cell culture, increase in structural complexity of the product, bioprocess design that is robustly scalable and reduction of cost.

1.1.4.1 Removal of animal components

Eukaryotic cell culture has traditionally involved use of animal compounds, e.g. as media supplements or plate coatings, to improve cell survival and growth.[40–42] However, there are scientific concerns over use of animal-derived components such as foetal bovine serum (FBS), insulin, gelatin, collagen or albumin, including batch-to-batch variation and introduction of undefined byproducts.[43,44] Furthermore, they are antithetical to the aim of livestock reduction, increase costs of culture media, and raise concerns related to consumer appeal and safety[39]. Thus, a viable bioprocess for cultured meat production must eliminate reliance on non-replicative animal components in cell culture.

1.1.4.2 Increase in structural complexity

The complexity of conventionally grown meat arises from a diversity of cell types, the involvement and relative composition of several tissues, and the shape, size and

location of the muscle.[11] First-generation cultured meat prototypes were limited to bioartificial muscle constructs resembling myofibres, lacking pronounced maturation or associated tissues such as fat.[13,19] Since tissue maturation and the involvement of fat or connective tissue influence the colour, taste, and texture of meat,[11] increasing efforts need to be directed towards producing meat-associated tissues other than skeletal muscle, or involving cell types that may support muscle fibre maturation.[31,37] This requires the identification of cell types present in the muscle microenvironment, as well as the ability to culture and efficiently differentiate them into mature tissues in vitro.

1.1.4.3 Upscaling

Amongst the most critical challenges in the realisation of cultured meat commercialisation is the ability to manufacture sufficient amounts of cell mass.[38,45] It is estimated that approximately 2 x 10^6 L of bioreactor volume is required to produce 10 kilotons of cultured meat per year, corresponding to 0.014% of global beef production.[2,22,27] In comparison, total eukaryotic cell culture in pharmaceutical applications amounts to a world-wide bioreactor volume of 3 x 10^6 L.[46] In addition to the logistical challenges of these dimensions, such as the building of operational facilities, underlying bioprocesses must be both scalable and robust. From a cellular perspective, this means that cell growth and functionality must be maintained over a long period in three-dimensional (3D) suspension cultures. Moreover, variability in cell behaviour, such as proliferation rate and differentiation capacity, must be sufficiently low to allow for a controlled large-scale production process.

1.1.4.4 Cost efficiency

Due to small-scale production and the use of expensive, high-purity pharmaceutical-grade ingredients, current cost of cultured meat is estimated to range from 2000 to 400000 USD kg^{-1}, indicating that a primary challenge of cultured meat commercialisation is the reduction of cost along the bioprocess. For current production processes, culture media components such as recombinantly-produced proteins make up the majority of the cost. Thus, the development of cost-effective media as well as the optimisation of media consumption offer vast saving potentials.[29] However, similar to the analyses of environmental impact, assessment of future cost for cultured meat relies on the estimation of many unknown parameters, such as advances in the core technology as well as along

the supply chain for product ingredients. Between worst and best-case scenarios, future cost of cultured meat products on a commercial scale varies from 2 up to 100 USD kg^{-1}. Here, biological variables such as cell proliferation rate, stemness, or variation between cell batches have a stark impact on bioprocess efficiency, and hence will make the difference between technological success or failure.[47–49]

1.2 THE PROCESS OF CULTURED MEAT PRODUCTION

There are a variety of in vitro approaches that aim to produce skeletal muscle and meat-associated tissues from stem cells.[13,19,31,32,50,51] Most design concepts consist of four major phases: cell sourcing and banking (section 1.2.1), proliferation (section 1.2.2), differentiation (section 1.2.3), and post-culture processing (section 1.2.4), where each phase involves the definition and optimisation of multiple variables that determine downstream process requirements (Fig. 2).

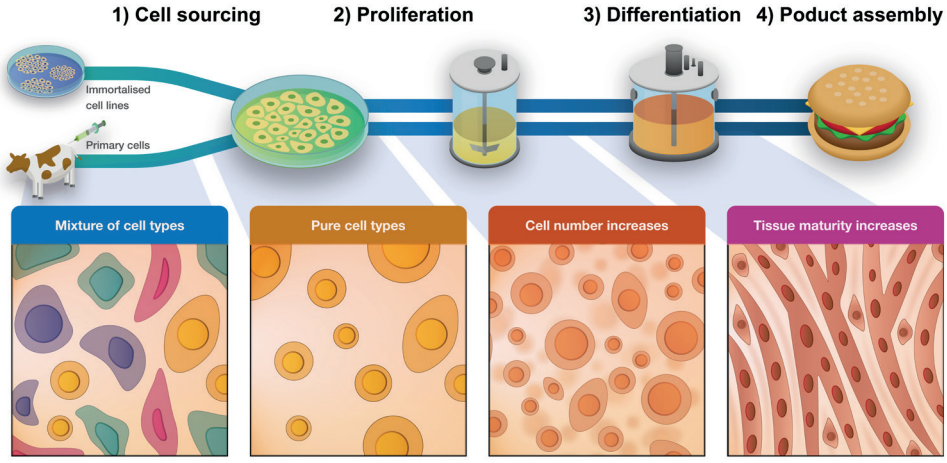

Figure 2: Main steps of cultured meat production processes.
Cells are the starting material to produce cultured meat. Potential cell sources are continuous cell lines (top), which can be established by immortalisation, or primary cells (bottom), which are isolated from donor animals as a mixture of different cell types and need to be purified for the cell type of interest (step 1). The purified cells are banked by cryopreservation to then be proliferated on tissue culture plates, followed by batch or continuous bioreactors (step 2). Next, the progenitor cells differentiate into meat-associated tissues such as muscle or fat using bioactive scaffolds or hydrogels in tissue bioreactors (step 3). A product is then assembled, post-culture processed, and packaged (step 4). Squares show cellular perspective of the bioprocess. To model this bioprocess on a smaller scale, cells can be proliferated and differentiated on tissue culture plates; adapted from Stout et al., 2022.[52]

1.2.1 Cell sourcing

The starting material for cultured meat is cells that have the potential to differentiate towards muscle, fat, or other meat-associated tissues. Cell selection is one of the most fundamental choices in the cultured meat bioprocess, critically defining downstream proliferation and differentiation conditions, and two principal approaches can be distinguished.

The first approach is the generation of continuous cell lines that possess near-unlimited proliferative potential, such as pluripotent stem cells or immortalised somatic cells. Induced pluripotent stem cells (iPSCs) or embryonic stem cells can differentiate into multiple functionalised cell types including muscle and fat cells but require complex protocols for their establishment, growth and/or differentiation.[53–57] Continuous cell lines derived from primary somatic cells are immortalised by spontaneous mutation, overexpression of telomerase genes, impediment of cell cycle inhibitors, or a combination thereof (amongst other methods). While non-integrative, transgene-free methods for reprogramming and differentiation exist, most current methods require genetic modification, and are therefore more difficult to establish as a food product from a regulatory and consumer-acceptance perspective.[58–61]

In contrast, primary cells derived from animal tissue may grow and differentiate in vitro without the need for genetic manipulation. The most common primary cells used in cultured meat applications are adult stem cells, which can only differentiate towards one or few cell types. The precursor-cells that make up muscle tissue are called satellite cells (SCs), whereas fat tissue can be produced from FAPs (derived from skeletal muscle) or MSCs (derived from bone marrow or intramuscular fat).[13,36,37,62] Primary cells are derived from tissues usually containing a variety of cell types, and therefore require protocols for their purification following isolation, e.g. by fluorescent activated cell sorting, magnetic cell sorting or other methods.[63,64] Optimisation of these practices, as well as donor animal considerations such as age, sex or breed of the animal, may play a crucial role in development of bioprocesses using primary cells as starting material.[28,65]

Regardless of whether continuous cell lines or primary cells are used in the production, cryopreservation is a necessary tool for the logistical coordination of the bioprocess by allowing intermediate storage of cells. The necessary size of these cell banks is dependent on the proliferation phase that follows thawing, as

this determines the maximum multiplication factor of a culture and thus the final mass that can be produced from a batch of the initial cell source.[66]

1.2.2 Proliferation

The purpose of the proliferation phase is to multiply the initial cell population by manifold cell division to reach sufficient mass for dietary consumption. Proliferation of primary cells in vitro requires distinct culture conditions that must be tailored to each specific cell type, species, and downstream application. These conditions include growth media (solutions that provide nutrients to the cells), physical parameters such as temperature or atmospheric composition, coatings and other attachment factors and, for large-scale applications, additional culture vessel considerations.

Growth media are aqueous solutions of minerals, vitamins, buffers, amino acids, fatty acids, proteins, and other compounds that affect cell behaviour.[67] Growth media are intended to provide cells with a similar nutrient profile that they would experience in vivo, and thus, traditional formulations often contain animal-derived compounds or solutions such as albumins or FBS. More recently, these have been replaced with proteins that support cell growth (therefore referred to as 'growth factors'), peptides or hydrolysates, enabling the formulation of serum-free media. A variety of proteins that can be recombinantly produced have been proposed to stimulate the growth of bovine SCs including albumin, fibroblast growth factor 2 (FGF2), hepatocyte growth factor (HGF), vascular endothelial growth factor (VEGF) and platelet-derived growth factor (PDGF).[68,69] Next to culture media, modification of culture surfaces to mimic the extracellular environment, e.g. through coating with extracellular matrix (ECM) proteins including collagen, laminin, or fibronectin, or other bioactive substances such as polyethylene glycol have been shown to stimulate cell growth by increasing cell attachment and mobility.[70,71] Similarly, physical parameters such as temperature or oxygen levels may strongly influence cell proliferation.[72,73]

Additional considerations must be taken into account when transitioning from culture flasks to bioreactors. To accommodate the exponentially increasing number of cells during the proliferative phase, increasing volumes need to be employed, either by bioreactor parallelisation or by upscaling vessel sizes. Different types of bioreactors including perfusion, stir tank, rocking platform, or hollow-fibre

bioreactors have been tested for mammalian cell culture, both as batch-fed or continuous systems (the latter in the case of immortalised cell lines). By providing a strictly controlled environment (e.g. pH, temperature, oxygen concentrations), monitoring and supplying nutrients, removing waste products, and ensuring homogenous distribution through intermittent or continuous stirring, mammalian cell cultures up to 2 x 10^4 L have been reported, although no protocols have been published in the cultured meat field that achieve similar dimensions.[74–78] In addition, most adult stem cells including SCs and FAPs are adherent cell types. Therefore, protocols to grow these cells in vessels such as bioreactors or spinner flasks usually require the use of microcarriers. These are synthetic or naturally occurring particles with diameters of 100-3000 µm that support cell attachment and either must be removed or dissolved before the differentiation phase or, if made from an edible material such as alginate, may remain present until the end of the process.[77]

Optimisation of proliferation phase parameters is imperative to generate sufficient cell mass to produce commercially relevant quantities of cultured meat. Cells need to divide up to approximately 30 times to produce 1 ton of cell mass from a starting population of 1 mg. Assuming a proliferation rate of 20-80 h, the proliferation phase for such a bioprocess may take between 25-100 days.[28,79] In some cultured meat concepts, this cell mass is then harvested and transferred to a separate culture system for differentiation.

1.2.3 Differentiation

Once sufficient cell numbers are produced, progenitor cells are differentiated towards the desired tissue type. To create cultured meat constructs that mimic the visual and contextual sensation of in vivo grown skeletal muscle, adult stem cells are differentiated towards muscle fibres, fat, or other meat-associated tissues such as vasculature or connective tissue.[30]

The differentiation phase equirees an altered media composition, and in most concepts involves a biomaterial that serves as a substrate for cell attachment and retention. For satellite cells, myogenic differentiation is traditionally achieved by an abrupt switch from pro-mitotic to anti-proliferative conditions, e.g. by serum-starvation, exogenous expression of myogenic transcription factors, or abrupt cell cycle inhibition.[44,80,81] In addition, the SCs are embedded in edible biomaterials to create 3D tissue constructs, either by encapsulation in hydrogels (e.g. alginate,

recombinant ECM proteins) or by seeding onto porous scaffolds (derived from plants or fungi, or from synthetic materials). Interaction with the biomaterial is necessary for cell survival and allows for myogenic differentiation and accumulation of a similar protein composition as in myofibres in vivo.[31–33] Analogous methods exist for fat tissue, where the induction of adipogenic pathways leads to the accumulation of intracellular triglycerides.[36,37]

Multiple examples of small-scale techniques for 3D muscle tissue construction have been reported, with culture durations of 5-12 days.[31–35] However, tissue reactors that provide a controlled hydrogel- or scaffold-based culture environment for differentiation in industrial dimensions remain in development. First patented solutions indicate use of edible porous scaffolds, which may be axially arranged in bioreactors and allow flow of differentiation media.[82,83] Alternative approaches employ 3D-bioprinting to create larger and more complex structures, although at the current stage of development these techniques are limited by biological and technical challenges including vascularisation, cell ink printability and biocompatibility, and heterogeneous cell dispersion.[84,85]

Another pivotal bioprocess decision is the choice between mono-culture or co-culture differentiation systems. Mono-cultures (which employ only one cell type per differentiation environment) have the advantage of lower system complexity, for instance concerning media formulations or biomaterials, which don't need to support the simultaneous differentiation of multiple cell types. However, co-culture tissues might better capture the heterocellular complexity of skeletal muscle and small-scale co-culture experiments indicate that cross-communication between cell types may have positive effects on the respective differentiation.[32,51]

1.2.4 Product assembly

After the differentiation phase, mature muscle, fat, and other tissues are harvested and further processed into final food products. Differentiated mono-cultures of muscle fibres may be assembled with other tissues such as fat into minced meat or steak-like structures. As an intermediate step towards the commercial establishment and cost parity of cultured meat, hybrid products that combine cultured tissues with plant-based proteins or conventionally produced meat are being considered to lower the price and support market entry. For instance, supplementing a plant-based burger with cultured fat might considerably

improve taste and succulence .[86] Following the harvesting of tissue bioreactors and product assembly, additional food processing steps such as seasoning or flavour enhancement may further improve product taste or optics.

Conventionally reared meat often involves a post mortem 'ripening' step (also referred to as 'dry ageing'), consisting of anaerobic enzymatic digestion of residual glucose and glycogen, accumulation of lactic acid following *rigor mortis*, and proteolytic digestion of myofibres upon pH decrease, which impacts meat tenderness and taste.[87,88] The ability of bioengineered skeletal muscle to contract in vitro implies the presence of sarcomeres and suggests that a similar process may be applied to cultured meat, although there have been no reports yet.[85] Finally, processed cultured meat products need to be packaged for distribution. Performing post-culture steps in a sterile environment would allow for aseptic packaging, extending shelf life and allowing higher temperature storage conditions compared to conventional meat, which has been shown in a cultured beef proof-of-principle for up to 2 weeks at room temperature.[32,89]

1.3 SATELLITE CELL BIOLOGY

Skeletal muscle is a complex tissue that involves multiple multi- and mononucleated cell types and their extracellular environment for its development, functionality, and maintenance. The most abundant cells in skeletal muscle are multinucleated muscle cells (myofibres), which are each surrounded by a basal lamina (endomysium). Myofibres arrange in parallel to form fascicles, which together make up the entire muscle. Between the membrane of the myofibre (sarcolemma) and the endomysium reside muscle precursor cells called satellite cells (SCs). Vital for development, maintenance, and regeneration of skeletal muscle, SCs are orchestrated through a myogenic cycle that involves phases of quiescence, proliferation, and differentiation by an intricate interplay of intrinsic and extrinsic mechanisms.[90,91]

1.3.1 Extrinsic regulation of satellite cells by their microenvironment

In homeostasis, when muscle is unperturbed, SCs are maintained in a quiescent state by their microenvironment, which comprises the extracellular matrix of the sarcolemma and the basal lamina, as well as a variety of other cell types. These include FAPs, smooth muscle and endothelial cells of intramuscular vasculature,

resident macrophages, glial and neural cells, and other low-abundance cell types such as tenocytes or MSCs.[92,93] In addition to their inherent functions, these cell types extrinsically regulate SCs, e.g. by ECM production and maintenance, paracrine signalling, and direct cell-cell interaction (Fig. 3).[92,94–96] SC quiescence is spatiotemporally controlled through interaction with many of the basal lamina's most prevalent ECM proteins such as laminin-211 (formerly merosin), collagen IV and VI, fibronectin, or different heparan sulphate proteoglycans (HSPGs) such as syndecan-3. HSPGs impair the progression of the cell cycle by sequestering pro-mitotic growth factors such as FGF2 or HGF.[96–98] In addition, the quiescent state of SCs is further supported by their interaction with the sarcolemma of the myofibres e.g. through Delta-Notch or M-Cadherin-CD34 signalling.[99]

On a cellular level, the disruption of muscle fibres and surrounding tissue, e.g. following exercise or injury, leads to dissociation of SCs from their niche and gives rise to three consecutive phases of regeneration: immediate local inflammation, mitogenic response, and differentiation cascade.[100–102] During acute inflammation, the remnant basal lamina is remodelled and ECM is synthesised by remaining mononuclear cells, most prominently FAPs and pro-inflammatory macrophages, mastocytes, and neutrophils.[92] These first-response immune cells promote the activation of SCs and FAPs through cytokines such as CLL1, IL4, or TNF-α, leading to the mitogenic response - a strong induction of proliferation. Several mechanisms in the immediate environment of activated, fusion-competent SCs (also referred to as myoblasts) and FAPs support this proliferation phase. First, both cell types produce pro-mitotic ECM proteins such as laminin-511 or laminin-111, creating a feed-forward signal that potentiates proliferation. Second, the disruption of HSPGs leads to a release of previously bound growth factors such as FGF2 and HGF. Third, resident macrophages remove cellular and extracellular debris by phagocytosis and subsequent efferocytosis, allowing the formation of de novo ECM and vasculature. This enables the release of additional pro-mitotic signals such as IGFs by endothelial cells and smooth muscle cells. Five days after injury, a re-established microenvironment including anti-inflammatory macrophages, lymphocytes and FAPs promotes the transition of myoblasts towards committed myocytes, e.g. by the secretion of differentiation-stimulating proteins. During this differentiation phase, the multiplied SCs align and fuse to form de novo myofibres or replenish existing damaged myofibres. Meanwhile, the ECM is reorganised towards the homeostatic condition prior to injury by the help of surrounding cells, predominantly FAPs.[92,93,103,104]

1.3.2 Intracellular satellite cell biology during muscle regeneration

SCs utilise a tightly controlled sequence of transcription factors to navigate the myogenic cycle of quiescence, proliferation, and differentiation. These transcription factors include paired homeobox factors Pax3 and Pax7, and so-called myogenic regulatory factors (MRFs) Myf5, MyoD, Myogenin, and Mrf4.[105–109] The regulation of this intrinsic machinery is mediated by an interplay of upstream pathways such as p38 MAPK, Notch, TGF-β, and Wnt, as well as epigenetic mechanisms, posttranslational modifications, and microRNA (miR) interactions.[110,111]

During quiescence, SCs are maintained in a reversible G_0 state at low metabolic activity by several internal pathways. These include negative regulators of cell cycle such as Sprouty,[112] which acts as an antagonist to the FGF-pathway, impairing MEK/ERK signalling and halting progression to G1. Reduced receptor tyrosine kinase signalling is supported by sequestration of pro-proliferative intracellular signals, for example, through upregulation of IGF-binding proteins (Igfbp6)[113] or through miRs that repress myogenic signals such as miR-1, -33, or -206.[114–116] Furthermore, upregulated expression of Notch ensures that extracellular signals efficiently suppress inadvertent SC activation.[94] Quiescence has long been regarded as a binary state, in which SCs have lower cytoplasmic volume than when activated, and are defined by high expression of Pax7 and low abundance of MRFs.[101] Detailed characterisation of quiescent SCs on a single-cell level has been hindered by their rapid activation upon muscle injury, preventing the establishment of accurate in vitro models due to the distortion of quiescence by common isolation protocols.[97,117,118] However, recent technological advances have now enabled a more nuanced understanding of SC quiescence that involves heterogeneous expression of Pax7 and Pax3 and suggests a gradient rather than a binary switch that leads from quiescence to activation.[117,119,120]

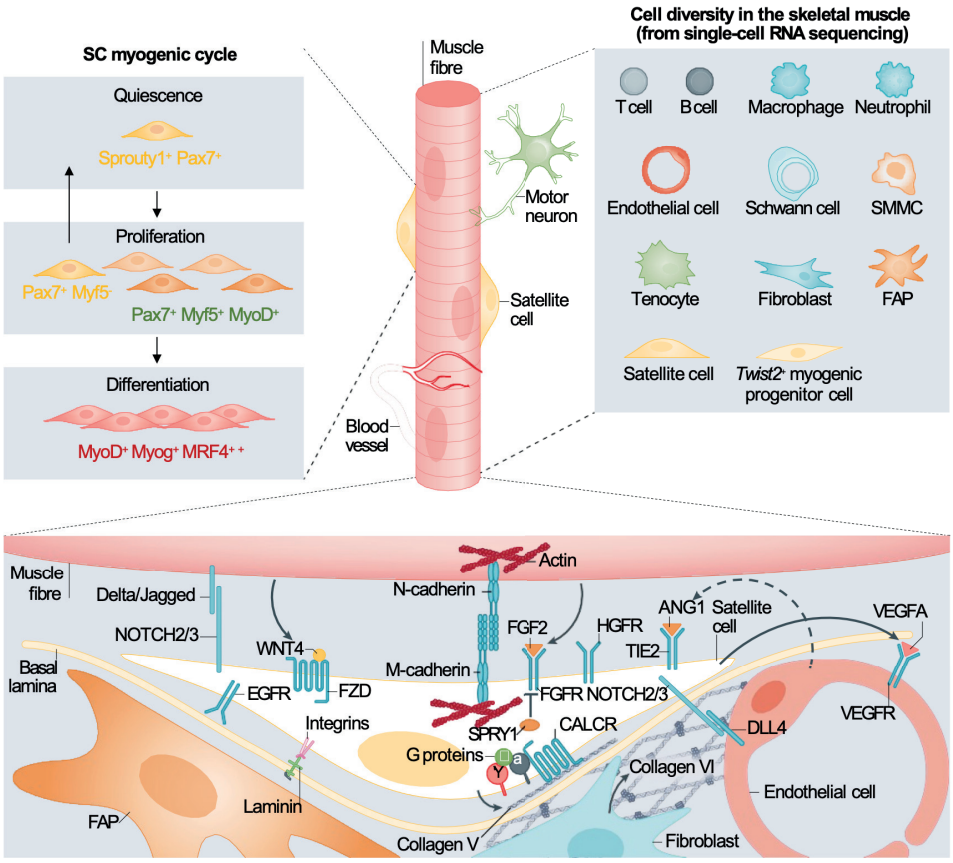

Figure 3: Extrinsic regulation of the SC myogenic cycle.
SCs are maintained in a quiescent state by extrinsic signals from their extracellular environment comprising a multitude of different cell types (top right) and the interplay with proteins from basal lamina and sarcolemma (bottom). Disruption of the quiescent niche through muscle injury induces the myogenic cascade - a sequence of transcription factors that cause activation and differentiation of SCs to reform the perturbed myofibres; adapted from Sousa-Victor et al., 2022.[121]

The proliferation phase that follows quiescence is essential for effective muscle regeneration.[122] Released from repression by anti-proliferative signals of the extracellular environment, activation of pathways such as MAPK/ERK, mTORC, and PI3K/Akt leads to both symmetric and asymmetric division of the SCs. In asymmetric division, SCs that express Pax7 but not Myf5 generate one daughter cell that remains Pax7^{+} Myf5^{-} and returns to quiescence to preserve the SC pool (thus also referred to as Satellite stem cell), whereas the other daughter cell expresses Pax7^{+} Myf5^{+} and commits to proliferation.[123,124] These Pax7^{+} Myf5^{+} myoblasts generate

progeny exclusively by symmetric division, exhibit increased mobility and express high levels of MyoD, eventually leading to the induction of the myogenic cascade.

In the last phase, a sequence of feed-forward signalling MRFs is initiated by the expression of MyoD. After multiple cell divisions, the proliferation rate of activated SCs decreases, Pax7 is downregulated, and the accumulation of MyoD leads to the induction of Myogenin (Myog).[125] Phosphorylation of myocyte enhancement factor 2 (MEF2) downstream of p38-α/β MAPK initiates the terminal differentiation phase of the myoblasts. Marked by an irreversible cell cycle exit (as opposed to the reversible G0 state during quiescence), committed myoblasts express proteins necessary for fusion such as myomerger (MYMX) and myomaker (MYMK) and for the formation of functional muscle such as desmin, actin, or myosin-2.[125–127]

1.3.3 Satellite cell ageing in vivo and in vitro

Stem cells are characterised by their ability to self-renew and to undergo efficient fate commitment towards a differentiated phenotype, a characteristic referred to as stemness. For SCs, the ability to generate daughter cells that can either replenish the SC pool or follow a myogenic fate enables the regeneration of skeletal muscle throughout the lifetime of vertebrates.[67,128] However, ageing and disease lead to a decline of the regenerative potential of SCs in vivo, which manifests in muscle atrophy and reduction of strength (sarcopenia). A similar decline in proliferation and differentiation potential of SCs can be observed in vitro, which may limit their applicability in a cultured meat production process that relies on the multiplication of a starting cell population (Fig. 4). Therefore, in order to produce large quantities of functional SCs, it is necessary to understand SC ageing and its underlying mechanisms, both in vivo and in vitro.

1.3.3.1 In vivo

The phenotype of aged skeletal muscle is well described, and is characterised by decreasing numbers and cross-sectional areas of myofibres, fibrosis and fat infiltration, inflammation and decreased protein expression.[129] Many interconnected factors, both on cellular and organismal level, contribute to this ageing process but it is evident that alterations within SCs and their microenvironment play a pivotal role.[130]

Geriatric skeletal muscle contains fewer SCs per myofibre than muscles in young animals.[131–134] Yet, onset of sarcopenia has also been observed when SC numbers

remained constant. It was thus suggested that loss of SC stemness, resulting both from intrinsic changes and from extrinsic signals of the ageing SC niche, is a major contributing factor to the decline of skeletal muscle.[132,135–138]

The aged microenvironment exposes SCs to an altered profile of external signals compared to young muscles. Elevated levels of TGF-β1 and myostatin have been measured in skeletal muscle and the serum of aged patients, resulting in impaired activation and differentiation of SCs and intramuscular fibrosis through increased SMAD3 phosphorylation.[139,140] Concurrently, diminished levels of Delta decreases SMAD3-antagonistic Notch signalling.[141,142] In a similar fashion, chronic release of interleukins (ILs) present during inflammation, such as IL-6, may be responsible for the increased activation of the JAK/STAT pathway in aged animals.[143,144] Furthermore, the aged ECM contains an altered heparan sulphate composition that fails to sufficiently sequester pro-mitotic growth factors. This impairs the return of SCs to the quiescent state, and may thus contribute to the exhaustion of the SC pool.[145]

In addition to changes mediated by organismal ageing, SCs acquire alterations on a molecular level that affect self-renewal and functionality, referred to as cellular ageing. These include genomic instability and DNA damage caused by endogenous stress such as reactive oxygen species (ROS),[146] telomere shortening[147] and epigenetic drift including hypermethylated CpG islands.[148–150] Moreover, dysfunctional autophagy in aged SCs can lead to aggregation of misfolded proteins and damaged mitochondria. This results in cellular senescence that limits the self-renewal capacity, and ultimately impairs muscle regeneration.[57,132,151]

There is conflicting data on the in vitro proliferation and differentiation capacity of SCs isolated from geriatric animals or patients. These show either a minor reduction or no difference compared to younger controls, although experimental differences such as donor species, isolation procedures or the measured readouts limit the comparability between studies.[57,131,132,152] This highlights that only a combination of intracellular and extracellular changes can sufficiently explain the aged SC phenotype.

1.3.3.2 In vitro ageing

It was first described by Hayflick et al. that human foetal fibroblasts had a finite proliferative capacity of approximately 50 population doublings (PDs) – an observation later known as Hayflick limit.

While senescence is considered a binary, non-reversible state of cell cycle arrest, cellular ageing is a gradual process that is characterised in various cell types including adult stem cells by five major hallmarks.[153] First, ageing cells exhibit a prolonged cell cycle duration, and thus a reduction of proliferation rate prior to entering senescence.[154,155] Second, similar to ageing cells in vivo, telomere length decreases with each cell division and below a critical threshold leads to DNA-damage responses and senescence. While this supports the hypothesis of a binary switch to senescence, telomere-associated regulators of downstream pathways such as NF-κB also indicate a role of telomere-shortening in the gradual progression of cellular ageing.[156,157] Third, cultured cells accumulate intracellular damage that negatively affect cell function, including DNA damage and genetic instability, aggregation of misfolded proteins, accumulation of carbohydrates and fatty acids due to reduced autophagy, and oxidative modifications. Due to constant cell replication, mutations, double-strand breaks, and other DNA damage accumulate in ageing cells and can eventually result in functional decay and cellular senescence.[158–160] Fourth, cellular ageing induces a hypertrophic phenotype in vitro, as cell size is negatively correlated with proliferation rate. Although it is unclear whether cause or effect of decreased proliferation, cell size during early culture has been suggested as a predictor for in vitro proliferation capacity.[161,162] Fifth, ageing cells have a higher consumption of glucose but produce lower levels of lactate and ATP through oxidative phosphorylation. This suggests that products of glycolysis are directed towards increasing cell size, for example through mTOR, rather than towards proliferation. This is consistent with the observation that the concentration of NAD^+, a product of oxidative phosphorylation, decreases when cells approach senescence.[163,164]

In addition to their ability for self-renewal, adult stem cells are characterised by their ability to differentiate and exit the cell cycle independently of senescence. It is therefore necessary to differentiate between cellular ageing occurring for all in vitro cultures, and the loss of stemness that is specific to SCs and other adult stem cells. The ability of SCs to perform efficient myogenic differentiation in vitro may decrease long before they become senescent, suggesting that stemness is defined by both proliferation and differentiation capacity.[165,166] However, while there is ample evidence for age-related alterations that may affect stemness in vivo, e.g. in p38-α/β MAPK, Notch, Wnt, or JAK/STAT signalling, literature that focuses on the particular effect of long-term in vitro culture of SCs is sparse – a potential result of the scepticism surrounding in vitro models for capturing in vivo cell behaviour.[167]

SCs use a complex transcriptional program to navigate through quiescence, proliferation and differentiation including several reversible and irreversible cellular states. In vivo, failure to restore the quiescent state leads to the exhaustion of the regenerative capacity of the SCs, suggesting that constant activation in vitro might lead to an analogous depletion of a SC subpopulation with higher differentiation potential.[149] Furthermore, as described above, SCs are strongly influenced by their extracellular environment.[168] In vitro, plate coatings and culture media constitute the extracellular environment of the cells. Since they are replaced with every new passage, they can be considered largely constant during long-term proliferation. Nevertheless, paracrine signalling and cell-cell interactions of ageing SCs may affect surrounding cells and create positive feedback loops that decrease stemness, similar to mechanisms observed for senescent cells in vitro.[169]

Transgene-free interventions that maintain or restore the SC stemness in vitro focus on providing culture conditions that target pivotal myogenic pathways in SCs. For instance, culturing SCs from old mice with serum of young mice increases proliferation capacity in vitro by activating Notch signalling.[138] Similarly, inhibition of p38-α/β MAPK with the small molecule SB203580 increases proliferation and late differentiation capacity.[166] Providing an optimised extracellular environment, e.g. by coating with laminin, can additionally improve SC in vitro behaviour through p38-α/β or JNK.[168,170] Together, these studies highlight the potential of targeting intracellular pathways to improve SC stemness.

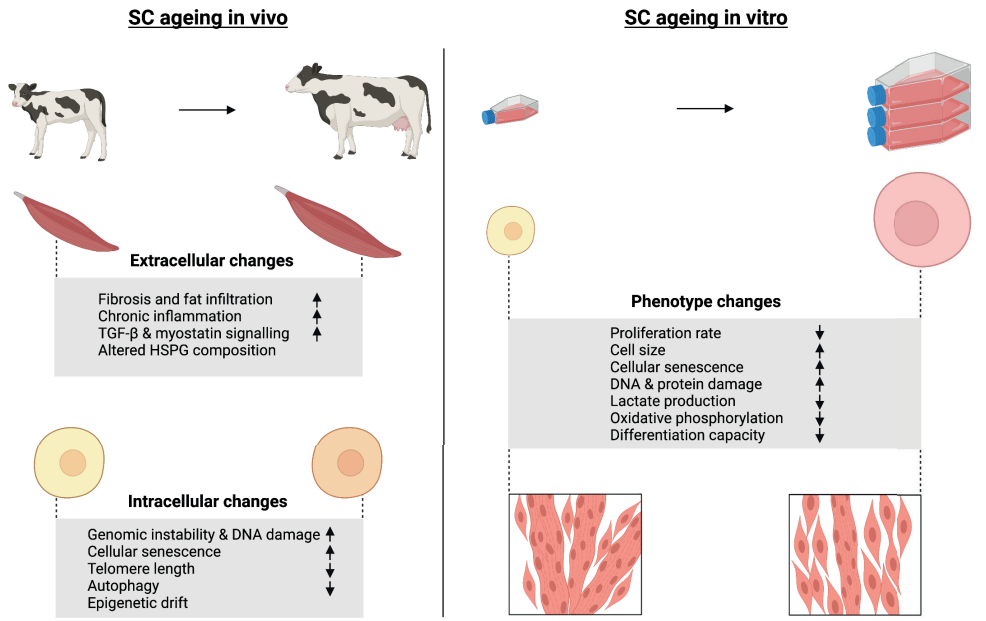

Figure 4: SC ageing in vivo and in vitro.
In vivo, SCs accumulate intracellular changes and are exposed to an altered extracellular environment of an aged organism, which leads to hampered muscle regeneration and sarcopenia. In vitro, the extracellular conditions are constant but SCs gradually age with prolonged culture. The aged in vitro phenotype manifests in a loss of stemness, i.e. the decline of proliferation and differentiation capacity.

1.3.4 Main challenges of using primary SCs for cultured meat production

Due to their high proliferative capacity upon activation, and their inclination to readily differentiate in vitro, SCs are theoretically a highly suitable cell type to produce cultured meat. However, there are biological limitations that may restrict their applicability in consideration of producing a food product on an industrial scale.

Both proliferation and differentiation media have traditionally used FBS. However, animal-derived media components, particularly FBS, are incompatible with a robust, cost-effective and animal-friendly bioprocess and undefined ancillary components have raised concerns about their usage for cell culture beyond cultured meat application.[43,45] Therefore, increasing effort is put into the development of serum-free media formulations, especially focusing on proliferation.[68,69] However, it is currently unclear whether efficient myogenic differentiation of bovine SCs, both in 2D and 3D, can be achieved with serum-free and transgene-free protocols.

Loss of stemness in cultured SCs is a limiting factor for producing cultured meat on a commercial scale. Cellular ageing, and concomitant loss of stemness, is a complex, multifactorial process that causes sarcopenia in ageing human and non-human animals. In vitro, the aged SC phenotype is primarily characterised by a decline in proliferation and differentiation capacity. The precise boundaries of this decline for SC cultures has not yet been systematically studied, i.e. after how many PDs their proliferation and differentiation capacities decrease below a threshold that is prohibitive for cultured meat production. In any case, limited proliferation and differentiation capacities restrict the producible quantity of meat coming from a given source sample. It is therefore necessary to regularly source new batches from donor animals, which includes the selection and purification of cell types of interest from the gathered muscle sample. We only have a limited understanding of the cell types present in the bovine skeletal muscle niche, and whether current selection methods are capable of exclusively purifying intended cell types. In addition, this regular sourcing introduces variability to the bioprocess, as proliferation or differentiation capacity might differ between SC batches.

Therefore, optimization of culture media, plate coatings, and other parameters to preserve a functional SC phenotype using only process-compatible components is a key challenge for the cultured meat production approach from primary SCs. This requires the identification of a serum-free myogenic differentiation method, selective protocols for purification, and scalable interventions to maintain SC stemness.

1.4 THE POTENTIAL OF BIOINFORMATICS IN CULTURED MEAT RESEARCH

Next-generation sequencing (NGS) has fundamentally broadened the understanding of biological systems by providing high-resolution insights into the genome, epigenome and transcriptome of cells, tissues, and organisms. NGS technologies are based on determining the nucleotide sequence of DNA fragments and a wide variety of technical approaches has been developed in the past 20 years to address biological questions beyond the identification and mapping of genes.[171]

Quantification of gene expression through RNA sequencing has served as a powerful tool box to understand intracellular processes.[172,173] Most RNA sequencing technologies are based on the isolation of RNA from biological samples, the enrichment of mRNA, and the synthesis of complementary DNA (cDNA) prior to

sequencing. For common RNA sequencing technologies (Fig. 5), the cDNA is further processed by ligation of DNA adapters that enable their binding to flow cells for clonal bridge amplification. Sequences of the amplified cDNA fragments are then determined by synthesis of conjugated nucleotides and massive parallel detection of fluorescent signals. Finally, mapping the resulting reads to a reference genome allows the quantification of expressed RNA molecules corresponding to distinct genes in the analysed samples.[174] By this, it is possible to measure differences in gene expression between different cell types, tissues or other biological samples – an analysis referred to as differential expression analysis.[175] In recent years, the introduction of local separation and barcoding of single cells prior to library preparation, for example by bead encapsulation (10X sequencing) has advanced these bulk-sequencing technologies to single-cell or single-nucleus resolution, allowing study of the transcriptomic variability of single cells.[176,177]

Next to NGS technologies, there are other bioinformatic tools that are not based on nucleotide sequencing but share the principle of generating large amounts of data for the comparison of biological samples, for example proteomics, lipidomics, or metabolomics. Most methods are based on lipid chromatography coupled with mass-spectrometry to separate and determine cellular components, such as the proteome. While the downstream analysis that follows data acquisition and quantification is similar to transcriptomics, they offer additional information on cell states and functions that are not merely captured by gene expression.[178]

Bioinformatic tools, in particular bulk and single-cell RNA-sequencing, have offered great insight into the complexity of skeletal muscle and the inter- and intracellular mechanisms of muscle regeneration (sections 1.3.1 & 1.3.2), as well as into the pathways involved in SC states and cellular ageing (section 1.3.3). However, they have only been minimally applied to biological questions in the field of cultured meat. The bioprocess of cultured meat production includes cell sourcing, proliferation and differentiation. During each of these steps, transcriptomics and other bioinformatic analyses may help to understand and ultimately improve the cellular behaviour in vitro.

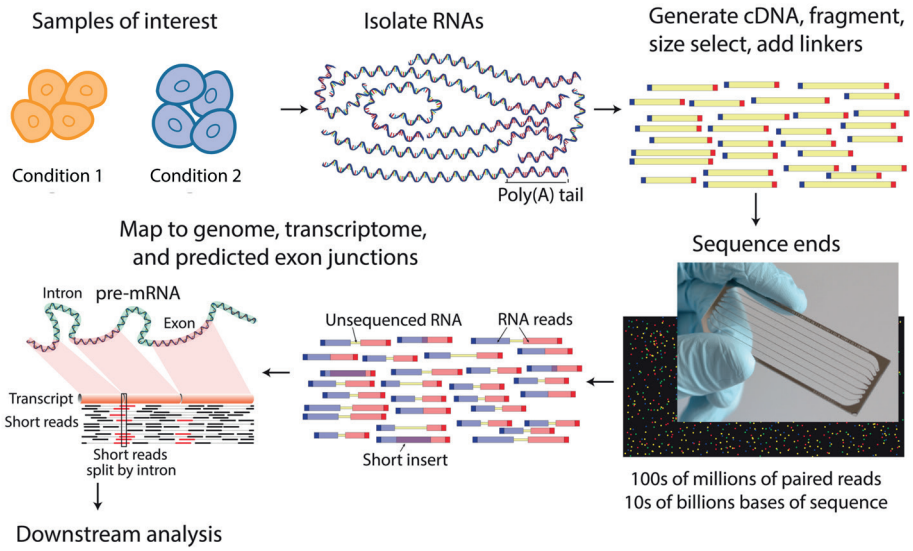

Figure 5: Steps of a RNA sequencing workflow.
To analyse gene expression in samples of interest, mRNA is isolated and reverse-transcribed into cDNA. Libraries are constructed by fragmentation and ligation of adapters, amplified, and sequenced. The resulting reads are aligned to a reference genome to generate the final gene count matrix; adapted from Griffith et al., 2015.[179]

1.5 AIMS OF THE THESIS

Cultured meat has the potential to drastically decrease the environmental footprint and animal suffering related to industrial meat production, but many technical and biological challenges must be overcome to enable its realisation. Most downstream bioprocess parameters are dependent on the selection of cell type and it is therefore imperative to develop a deep understanding of both the initial cell type, and changes during in vitro culture. SCs are a promising choice to produce cultured muscle but intrinsic cellular mechanisms may restrict their applicability to produce substantial amounts of cultured meat in a robust, cost-effective, animal-component-free manner. Bioinformatic technologies, in particular RNA sequencing, are powerful tools to gain insight into biological systems. It is the aim of this thesis to harness these tools to establish a deep understanding of the biology of bovine SCs at each in vitro step of the cultured meat bioprocess. This analysis may illuminate paths towards improving their isolation, proliferation, and differentiation.

In particular, the thesis aims to address the following challenges of using bovine SCs for cultured meat production:

1) *Reliance on FBS for myogenic differentiation*. The removal of animal components such as FBS is necessary to reduce cost and variability of cultured meat production. However, there are no serum-free and transgene-free protocols for inducing myogenic differentiation in SCs. Therefore, it is necessary to characterise in vitro differentiation in detail to be able to recreate this process in a serum-free environment.

2) *Heterogeneity of bovine skeletal muscle and derived cultures*. Cultured meat aims to reproduce skeletal muscle but there is only limited knowledge about involved cell types in bovine tissue. Furthermore, while SCs are a highly dynamic cell type in vivo, it is unclear how much cellular heterogeneity remains when SCs are cultured in vitro, and whether variability on a single-cell level may have implications for a robust proliferation process.

3) *Variability between batches of SCs*. The limited lifespan of SCs in vitro requires regular sourcing of new batches of SCs from bovine muscle. This necessarily introduces variability to the bioprocess, but it is not known to what extent phenotypic differences manifest during prolonged in vitro culture and which underlying cellular properties may explain these potential differences.

4) *Loss of stemness during long-term culture in vitro*. To upscale cultured meat production, cultures of functional SCs need to be maintained for a long period of time in vitro. However, their ability to proliferate and differentiate efficiently decreases over time, a process described as loss of stemness. Therefore, it is essential to develop methods that allow the identification and assessment of interventions that may improve the stemness of SCs.

1.6 OVERVIEW OF THE THESIS

This thesis characterises bovine SCs through bioinformatic tools in order to address the limitations of this cell type for cultured meat applications.

The second chapter focuses on the removal of FBS during myogenic differentiation. We assess transcriptomic and proteomic changes that occur upon serum-starvation, and analyse the cellular mechanisms that orchestrate myogenic differentiation in vitro. Next, we determine genes that encode surface receptors and are significantly upregulated during differentiation to develop a formulation for serum-free differentiation media by supplementing ligands to those receptors. Finally, we study whether the proposed serum-free differentiation media can be used to create 3D muscle constructs.

In the third chapter, we use single-cell RNA sequencing to study the transcriptional heterogeneity of bovine skeletal muscle and derived cell cultures. We determine the various cell types that can be isolated from skeletal muscle before and after a serum-free culture, and develop a simple flow cytometry-based protocol to sort for four principal cell types. We further describe an overgrowth phenomenon of contaminating cell types in the SC cultures due to selective growth conditions, and adjust the serum-free growth media to favour SCs. Finally, we characterise heterogeneity within purified SCs and note three cellular states between which SCs dynamically transit in vitro.

In the fourth chapter, we analyse the variability of SC performance in vitro by studying extent and dynamics of proliferation and myogenic differentiation between different SC cultures. We seek to find early in vitro readouts that may predict the observed phenotypic differences in ageing SCs. Finally, we analyse genetic structural variation, DNA methylation and the transcriptional profiles of multiple passages of SCs in order to understand the phenotypic variability.

In the fifth chapter, we establish a workflow to screen candidate compounds that may maintain the stemness of bovine SCs and to assess their compatibility within a cultured meat production process. We study the effects of p38-α/β inhibitor SB203580 on proliferation and differentiation during a long-term serum-free culture and use RNA sequencing to gain insights into the effect of p38-inhibition on stemness. Finally, we test the application of p38 inhibition in an upscaled bioprocess and describe a context-dependency of the efficacy of p38-inhibitory compounds.

1.7 BIBLIOGRAPHY

1. Chiles, R. M. & Fitzgerald, A. J. Why is meat so important in Western history and culture? A genealogical critique of biophysical and political-economic explanations. *Agric. Hum. Values* **35**, 1–17 (2018).
2. Ritchie, H. & Roser, M. Meat and Dairy Production. *Our World Data* (2017).
3. Heinke, J. *et al.* Water Use in Global Livestock Production—Opportunities and Constraints for Increasing Water Productivity. *Water Resour. Res.* **56**, e2019WR026995 (2020).
4. Tilman, D. & Clark, M. Global diets link environmental sustainability and human health. *Nature* **515**, 518–522 (2014).
5. Hedenus, F., Wirsenius, S. & Johansson, D. J. A. The importance of reduced meat and dairy consumption for meeting stringent climate change targets. *Clim. Change* **124**, 79–91 (2014).
6. Bonnet, C., Bouamra-Mechemache, Z., Réquillart, V. & Treich, N. Viewpoint: Regulating meat consumption to improve health, the environment and animal welfare. *Food Policy* **97**, 101847 (2020).
7. Shepon, A., Eshel, G., Noor, E. & Milo, R. The opportunity cost of animal based diets exceeds all food losses. *Proc. Natl. Acad. Sci.* **115**, 3804–3809 (2018).
8. Muller, A. *et al.* Strategies for feeding the world more sustainably with organic agriculture. *Nat. Commun.* **8**, 1290 (2017).
9. Rubio, N. R., Xiang, N. & Kaplan, D. L. Plant-based and cell-based approaches to meat production. *Nat. Commun.* **11**, 6276 (2020).
10. Sanchez-Sabate, R. & Sabaté, J. Consumer Attitudes Towards Environmental Concerns of Meat Consumption: A Systematic Review. *Int. J. Environ. Res. Public. Health* **16**, 1220 (2019).
11. Listrat, A. *et al.* How Muscle Structure and Composition Influence Meat and Flesh Quality. *Sci. World J.* **2016**, 3182746 (2016).
12. Badylak, S. F., Taylor, D. & Uygun, K. Whole-Organ Tissue Engineering: Decellularization and Recellularization of Three-Dimensional Matrix Scaffolds. *Annu. Rev. Biomed. Eng.* **13**, 27–53 (2011).
13. Post, M. J. Cultured beef: medical technology to produce food. *J. Sci. Food Agric.* **94**, 1039–1041 (2014).
14. Datar, I. & Betti, M. Possibilities for an in vitro meat production system. *Innov. Food Sci. Emerg. Technol.* **11**, 13–22 (2010).
15. Vein, J. Method for producing tissue engineered meat for consumption. (2004).
16. Eelen, W. F. V., Kooten, W. J. V., Westerhof, W. & Mummery, C. Industrial production of meat from in vitro cell cultures. (2003).
17. Kenny, D. A., Fitzsimons, C., Waters, S. M. & McGee, M. Invited review: Improving feed efficiency of beef cattle – the current state of the art and future challenges. *Animal* **12**, 1815–1826 (2018).
18. Cabezas-Garcia, E. H., Lowe, D. & Lively, F. Energy Requirements of Beef Cattle: Current Energy Systems and Factors Influencing Energy Requirements for Maintenance. *Anim. Open Access J. MDPI* **11**, 1642 (2021).
19. Choudhury, D., Tseng, T. W. & Swartz, E. The Business of Cultured Meat. *Trends Biotechnol.* **38**, 573–577 (2020).

20. Tuomisto, H. L. & Teixeira de Mattos, M. J. Environmental Impacts of Cultured Meat Production. *Environ. Sci. Technol.* **45**, 6117–6123 (2011).
21. Parodi, A. *et al.* The potential of future foods for sustainable and healthy diets. *Nat. Sustain.* **1**, 782–789 (2018).
22. Sinke. *LCA of cultivated meat. Future projections for different scenarios*. (2019).
23. Tomley, F. M. & Shirley, M. W. Livestock infectious diseases and zoonoses. *Philos. Trans. R. Soc. B Biol. Sci.* **364**, 2637–2642 (2009).
24. Hoelzer, K. *et al.* Antimicrobial drug use in food-producing animals and associated human health risks: what, and how strong, is the evidence? *BMC Vet. Res.* **13**, 211 (2017).
25. Tuomisto, H. L. Challenges of assessing the environmental sustainability of cellular agriculture. *Nat. Food* **3**, 801–803 (2022).
26. Boler, D. D. & Woerner, D. R. What is meat? A perspective from the American Meat Science Association. *Anim. Front.* **7**, 8–11 (2017).
27. Specht, E. A., Welch, D. R., Rees Clayton, E. M. & Lagally, C. D. Opportunities for applying biomedical production and manufacturing methods to the development of the clean meat industry. *Biochem. Eng. J.* **132**, 161–168 (2018).
28. Melzener, L., Verzijden, K. E., Buijs, A. J., Post, M. J. & Flack, J. E. Cultured beef: from small biopsy to substantial quantity. *J. Sci. Food Agric.* **101**, 7–14 (2021).
29. Hubalek, S., Post, M. J. & Moutsatsou, P. Towards resource-efficient and cost-efficient cultured meat. *Curr. Opin. Food Sci.* **47**, 100885 (2022).
30. Bomkamp, C. *et al.* Scaffolding Biomaterials for 3D Cultivated Meat: Prospects and Challenges. *Adv. Sci.* **9**, 2102908 (2022).
31. Ben-Arye, T. *et al.* Textured soy protein scaffolds enable the generation of three-dimensional bovine skeletal muscle tissue for cell-based meat. *Nat. Food* **1**, 210–220 (2020).
32. Furuhashi, M. *et al.* Formation of contractile 3D bovine muscle tissue for construction of millimetre-thick cultured steak. *Npj Sci. Food* **5**, 6 (2021).
33. Jones, J. D., Rebello, A. S. & Gaudette, G. R. Decellularized spinach: An edible scaffold for laboratory-grown meat. *Food Biosci.* **41**, 100986 (2021).
34. Martins, J. G. *et al.* Pectin-chitosan membrane scaffold imparts controlled stem cell adhesion and proliferation. *Carbohydr. Polym.* **197**, 47–56 (2018).
35. Zhu, H. *et al.* Production of cultured meat from pig muscle stem cells. *Biomaterials* **287**, 121650 (2022).
36. Dohmen, R. G. J. *et al.* Muscle-derived fibro-adipogenic progenitor cells for production of cultured bovine adipose tissue. *Npj Sci. Food* **6**, 6 (2022).
37. Zagury, Y., Ianovici, I., Landau, S., Lavon, N. & Levenberg, S. Engineered marble-like bovine fat tissue for cultured meat. *Commun. Biol.* **5**, 1–12 (2022).
38. Ye, Y., Zhou, J., Guan, X. & Sun, X. Commercialization of cultured meat products: Current status, challenges, and strategic prospects. *Future Foods* **6**, 100177 (2022).
39. Bryant, C. & Barnett, J. Consumer acceptance of cultured meat: A systematic review. *Meat Sci.* **143**, 8–17 (2018).
40. Verma, A., Verma, M. & Singh, A. Animal tissue culture principles and applications. *Anim. Biotechnol.* 269–293, (2020).

41. Rous, P. & Jones, F. S. A METHOD FOR OBTAINING SUSPENSIONS OF LIVING CELLS FROM THE FIXED TISSUES, AND FOR THE PLATING OUT OF INDIVIDUAL CELLS. *J. Exp. Med.* **23**, 549–555 (1916).
42. Puck, T. T., Cieciura, S. J. & Robinson, A. GENETICS OF SOMATIC MAMMALIAN CELLS : III. LONG-TERM CULTIVATION OF EUPLOID CELLS FROM HUMAN AND ANIMAL SUBJECTS. *J. Exp. Med.* **108**, 945–956 (1958).
43. Jochems, C. E. A., van der Valk, J. B. F., Stafleu, F. R. & Baumans, V. The use of fetal bovine serum: ethical or scientific problem? *Altern. Lab. Anim. ATLA* **30**, 219–227 (2002).
44. Pirkmajer, S. & Chibalin, A. V. Serum starvation: caveat emptor. *Am. J. Physiol. Cell Physiol.* **301**, C272-279 (2011).
45. Post, M. *et al.* Scientific, sustainability and regulatory challenges of cultured meat. *Nat. Food* **1**, 403–415 (2020).
46. Zhang, J. Mammalian Cell Culture for Biopharmaceutical Production. in *Manual of Industrial Microbiology and Biotechnology* 157–178 (John Wiley & Sons, Ltd, 2010).
47. Humbird, D. Scale-Up Economics for Cultured Meat: Techno-Economic Analysis and Due Diligence (2020).
48. Risner, D. *et al.* Preliminary Techno-Economic Assessment of Animal Cell-Based Meat. *Foods* **10**, 3 (2021).
49. TEA of cultivated meat. Future projections for different scenarios. *CE Delft - EN* https://cedelft.eu/publications/tea-of-cultivated-meat/.
50. Hanga, M. P. *et al.* Bioprocess development for scalable production of cultivated meat. *Biotechnol. Bioeng.* **117**, 3029–3039 (2020).
51. Ben-Arye, T. & Levenberg, S. Tissue Engineering for Clean Meat Production. *Front. Sustain. Food Syst.* **3**, (2019).
52. Stout, A. J., Kaplan, D. L. & Flack, J. E. Cultured meat: creative solutions for a cell biological problem. *Trends Cell Biol,* (2022).
53. Rivera, T., Zhao, Y., Ni, Y. & Wang, J. Human-Induced Pluripotent Stem Cell Culture Methods Under cGMP Conditions. *Curr. Protoc. Stem Cell Biol.* **54**, e117 (2020).
54. Soice, E. & Johnston, J. Immortalizing Cells for Human Consumption. *Int. J. Mol. Sci.* **22**, 11660 (2021).
55. Gao, Y. *et al.* Optimization of Culture Conditions for Maintaining Porcine Induced Pluripotent Stem Cells. *DNA Cell Biol.* **33**, 1–11 (2014).
56. Jiwlawat, S. *et al.* Differentiation and sarcomere formation in skeletal myocytes directly prepared from human induced pluripotent stem cells using a sphere-based culture. *Differentiation* **96**, 70–81 (2017).
57. García-Prat, L., Sousa-Victor, P. & Muñoz-Cánoves, P. Functional dysregulation of stem cells during aging: a focus on skeletal muscle stem cells. *FEBS J.* **280**, 4051–4062 (2013).
58. Bar-Nur, O. *et al.* Direct Reprogramming of Mouse Fibroblasts into Functional Skeletal Muscle Progenitors. *Stem Cell Rep.* **10**, 1505–1521 (2018).
59. KRIEGER, J. & WELSHHANS, K. Animal cell lines for foods containing cultured animal cells. (2020).
60. Genovese, N., DESMET, D. N. & Schulze, E. Methods for extending the replicative capacity of somatic cells during an ex vivo cultivation process. (2017).

61. Yoshimatsu, S. *et al.* Non-viral Induction of Transgene-free iPSCs from Somatic Fibroblasts of Multiple Mammalian Species. *Stem Cell Rep.* **16**, 754–770 (2021).
62. Low, M., Eisner, C. & Rossi, F. Fibro/Adipogenic Progenitors (FAPs): Isolation by FACS and Culture. in *Muscle Stem Cells: Methods and Protocols* (eds. Perdiguero, E. & Cornelison, D.) 179–189 (Springer, 2017).
63. Benedetti, A. *et al.* A novel approach for the isolation and long-term expansion of pure satellite cells based on ice-cold treatment. *Skelet. Muscle* **11**, 7 (2021).
64. Syverud, B. C., Lee, J. D., VanDusen, K. W. & Larkin, L. M. Isolation and Purification of Satellite Cells for Skeletal Muscle Tissue Engineering. *J. Regen. Med.* **3**, 117 (2014).
65. Melzener, L. *et al.* Comparative analysis of cattle breeds as satellite cell donors for cultured beef. 2022.01.14.476358, (2022).
66. Meneghel, J., Kilbride, P. & Morris, G. J. Cryopreservation as a Key Element in the Successful Delivery of Cell-Based Therapies—A Review. *Front. Med.* **7**, (2020).
67. Sambasivan, R. *et al.* Pax7-expressing satellite cells are indispensable for adult skeletal muscle regeneration. *Dev. Camb. Engl.* **138**, 3647–3656 (2011).
68. Stout, A. J. *et al.* Simple and effective serum-free medium for sustained expansion of bovine satellite cells for cell cultured meat. *Commun. Biol.* **5**, 1–13 (2022).
69. Kolkmann, A., Essen, A., Post, M. & Moutsatsou, P. Development of a Chemically Defined Medium for in vitro Expansion of Primary Bovine Satellite Cells. *Front. Bioeng. Biotechnol.* **10**, (2022).
70. Wilschut, K. J., Haagsman, H. P. & Roelen, B. A. J. Extracellular matrix components direct porcine muscle stem cell behavior. *Exp. Cell Res.* **316**, 341–352 (2010).
71. Gilbert, P. *et al.* Substrate elasticity regulates skeletal muscle stem cell self-renewal in culture. *Science* **329**, 1078–1081 (2010).
72. Harding, R. L., Halevy, O., Yahav, S. & Velleman, S. G. The effect of temperature on proliferation and differentiation of chicken skeletal muscle satellite cells isolated from different muscle types. *Physiol. Rep.* **4**, e12770 (2016).
73. Park, S. *et al.* Effects of Hypoxia on Proliferation and Differentiation in Belgian Blue and Hanwoo Muscle Satellite Cells for the Development of Cultured Meat. *Biomolecules* **12**, 838 (2022).
74. Bellani, C. F. *et al.* Scale-Up Technologies for the Manufacture of Adherent Cells. *Front. Nutr.* **7**, (2020).
75. Ahmed, A. S. I., Sheng, M. H., Wasnik, S., Baylink, D. J. & Lau, K.-H. W. Effect of aging on stem cells. *World J. Exp. Med.* **7**, 1–10 (2017).
76. Allan, S. J., De Bank, P. A. & Ellis, M. J. Bioprocess Design Considerations for Cultured Meat Production With a Focus on the Expansion Bioreactor. *Front. Sustain. Food Syst.* **3**, (2019).
77. Bodiou, V., Moutsatsou, P. & Post, M. J. Microcarriers for Upscaling Cultured Meat Production. *Front. Nutr.* **7**, (2020).
78. Khan, M. Bioreactor for mammalian cell culture. (2021).
79. Specht, L. An analysis of culture medium costs and production volumes for cultivated meat. (2020).
80. Guo, X. *et al.* In vitro Differentiation of Functional Human Skeletal Myotubes in a Defined System. *Biomater. Sci.* **2**, 131–138 (2014).

81. Eigler, T. *et al.* ERK1/2 inhibition promotes robust myotube growth via CaMKII activation resulting in myoblast-to-myotube fusion. *Dev. Cell* **56**, 3349-3363.e6 (2021).
82. LAVON, N., AVIV, M., ROTH, Y. & Toubia, D. Cultivation systems and methods for large-scale production of cultured food. (2020).
83. TANDIKUL, N. & Genovese, N. J. Systems and methods for cultivating tissue on porous substrates. (2022).
84. Mao, H. *et al.* Recent advances and challenges in materials for 3D bioprinting. *Prog. Nat. Sci. Mater. Int.* **30**, 618–634 (2020).
85. Kang, D.-H. *et al.* Engineered whole cut meat-like tissue by the assembly of cell fibers using tendon-gel integrated bioprinting. *Nat. Commun.* **12**, 5059 (2021).
86. Newton, P. & Blaustein-Rejto, D. Social and Economic Opportunities and Challenges of Plant-Based and Cultured Meat for Rural Producers in the US. *Front. Sustain. Food Syst.* **5**, (2021).
87. Zuo, H. *et al.* Metabolites Analysis on Water-Holding Capacity in Beef Longissimus lumborum Muscle during Postmortem Aging. *Metabolites* **12**, 242 (2022).
88. Dashdorj, D., Tripathi, V. K., Cho, S., Kim, Y. & Hwang, I. Dry aging of beef; Review. *J. Anim. Sci. Technol.* **58**, 20 (2016).
89. VERSTRATE, P. Packaging of cultured tissue. (2021).
90. Yin, H., Price, F. & Rudnicki, M. A. Satellite Cells and the Muscle Stem Cell Niche. *Physiol. Rev.* **93**, 23–67 (2013).
91. Relaix, F. *et al.* Perspectives on skeletal muscle stem cells. *Nat. Commun.* **12**, 692 (2021).
92. De Micheli, A. J. *et al.* Single-Cell Analysis of the Muscle Stem Cell Hierarchy Identifies Heterotypic Communication Signals Involved in Skeletal Muscle Regeneration. *Cell Rep.* **30**, 3583-3595.e5 (2020).
93. Giordani, L. *et al.* High-Dimensional Single-Cell Cartography Reveals Novel Skeletal Muscle-Resident Cell Populations. *Mol. Cell* **74**, 609-621.e6 (2019).
94. Bjornson, C. R. R. *et al.* Notch signaling is necessary to maintain quiescence in adult muscle stem cells. *Stem Cells Dayt. Ohio* **30**, 232–242 (2012).
95. Le Grand, F., Jones, A. E., Seale, V., Scimè, A. & Rudnicki, M. A. Wnt7a Activates the Planar Cell Polarity Pathway to Drive the Symmetric Expansion of Satellite Stem Cells. *Cell Stem Cell* **4**, 535–547 (2009).
96. Urciuolo, A. *et al.* Collagen VI regulates satellite cell self-renewal and muscle regeneration. *Nat. Commun.* **4**, 1964 (2013).
97. Quarta, M. *et al.* An artificial niche preserves the quiescence of muscle stem cells and enhances their therapeutic efficacy. *Nat. Biotechnol.* **34**, 752–759 (2016).
98. Holmberg, J. & Durbeej, M. Laminin-211 in skeletal muscle function. *Cell Adhes. Migr.* **7**, 111–121 (2013).
99. Mourikis, P., Gopalakrishnan, S., Sambasivan, R. & Tajbakhsh, S. Cell-autonomous Notch activity maintains the temporal specification potential of skeletal muscle stem cells. *Dev. Camb. Engl.* **139**, 4536–4548 (2012).
100. Brun, C. E., Chevalier, F. P., Dumont, N. A. & Rudnicki, M. A. Chapter 10 - The Satellite Cell Niche in Skeletal Muscle. in *Biology and Engineering of Stem Cell Niches* (eds. Vishwakarma, A. & Karp, J. M.) 145–166 (Academic Press, 2017).
101. Cheung, T. H. & Rando, T. A. Molecular regulation of stem cell quiescence. *Nat. Rev. Mol. Cell Biol.* **14**, 329–340 (2013).

102. Boonen, K. J. M., Rosaria-Chak, K. Y., Baaijens, F. P. T., van der Schaft, D. W. J. & Post, M. J. Essential environmental cues from the satellite cell niche: optimizing proliferation and differentiation. *Am. J. Physiol. Cell Physiol.* **296**, C1338-1345 (2009).
103. Rubenstein, A. B. *et al.* Single-cell transcriptional profiles in human skeletal muscle. *Sci. Rep.* **10**, 229 (2020).
104. Williams, K., Yokomori, K. & Mortazavi, A. Heterogeneous Skeletal Muscle Cell and Nucleus Populations Identified by Single-Cell and Single-Nucleus Resolution Transcriptome Assays. *Front. Genet.* **13**, (2022).
105. Bischoff, R. Proliferation of muscle satellite cells on intact myofibres in culture. *Dev. Biol.* **115**, 129–139 (1986).
106. Seale, P. *et al.* Pax7 is required for the specification of myogenic satellite cells. *Cell* **102**, 777–786 (2000).
107. Bentzinger, C. F., Wang, Y. X. & Rudnicki, M. A. Building Muscle: Molecular Regulation of Myogenesis. *Cold Spring Harb. Perspect. Biol.* **4**, a008342 (2012).
108. Schultz, E. Satellite cell proliferative compartments in growing skeletal muscles. *Dev. Biol.* **175**, 84–94 (1996).
109. Schmalbruch, H. & Lewis, D. M. Dynamics of nuclei of muscle fibers and connective tissue cells in normal and denervated rat muscles. *Muscle Nerve* **23**, 617–626 (2000).
110. Mashinchian, O., Pisconti, A., Le Moal, E. & Bentzinger, C. F. Chapter Two - The Muscle Stem Cell Niche in Health and Disease. in *Current Topics in Developmental Biology* (ed. Sassoon, D.) vol. 126 23–65 (Academic Press, 2018).
111. Montarras, D., L honoré, A. & Buckingham, M. Lying low but ready for action: the quiescent muscle satellite cell. *FEBS J.* **280**, 4036–4050 (2013).
112. Shea, K. L. *et al.* Sprouty1 Regulates Reversible Quiescence of a Self-Renewing Adult Muscle Stem Cell Pool during Regeneration. *Cell Stem Cell* **6**, 117–129 (2010).
113. Pallafacchina, G. *et al.* An adult tissue-specific stem cell in its niche: a gene profiling analysis of in vivo quiescent and activated muscle satellite cells. *Stem Cell Res.* **4**, 77–91 (2010).
114. Crist, C. G., Montarras, D. & Buckingham, M. Muscle satellite cells are primed for myogenesis but maintain quiescence with sequestration of Myf5 mRNA targeted by microRNA-31 in mRNP granules. *Cell Stem Cell* **11**, 118–126 (2012).
115. Chen, J.-F. *et al.* microRNA-1 and microRNA-206 regulate skeletal muscle satellite cell proliferation and differentiation by repressing Pax7. *J. Cell Biol.* **190**, 867–879 (2010).
116. Cheung, T. H. *et al.* Maintenance of muscle stem-cell quiescence by microRNA-489. *Nature* **482**, 524–528 (2012).
117. Scaramozza, A. *et al.* Lineage Tracing Reveals a Subset of Reserve Muscle Stem Cells Capable of Clonal Expansion under Stress. *Cell Stem Cell* **24**, 944-957.e5 (2019).
118. Monge, C. *et al.* Quiescence of human muscle stem cells is favored by culture on natural biopolymeric films. *Stem Cell Res. Ther.* **8**, 104 (2017).
119. Rocheteau, P., Gayraud-Morel, B., Siegl-Cachedenier, I., Blasco, M. A. & Tajbakhsh, S. A subpopulation of adult skeletal muscle stem cells retains all template DNA strands after cell division. *Cell* **148**, 112–125 (2012).
120. Rodgers, J. T. *et al.* mTORC1 controls the adaptive transition of quiescent stem cells from G0 to G(Alert). *Nature* **510**, 393–396 (2014).

121. Sousa-Victor, P., García-Prat, L. & Muñoz-Cánoves, P. Control of satellite cell function in muscle regeneration and its disruption in ageing. *Nat. Rev. Mol. Cell Biol.* **23**, 204–226 (2022).
122. Pietsch, P. The effects of colchicine on regeneration of mouse skeletal muscle. *Anat. Rec.* **139**, 167–172 (1961).
123. Bjornson, C. R. R. *et al.* Notch Signaling Is Necessary to Maintain Quiescence in Adult Muscle Stem Cells. *Stem Cells Dayt. Ohio* **30**, 232–242 (2012).
124. Kuang, S., Kuroda, K., Le Grand, F. & Rudnicki, M. A. Asymmetric self-renewal and commitment of satellite stem cells in muscle. *Cell* **129**, 999–1010 (2007).
125. Ishibashi, J., Perry, R. L., Asakura, A. & Rudnicki, M. A. MyoD induces myogenic differentiation through cooperation of its NH2- and COOH-terminal regions. *J. Cell Biol.* **171**, 471–482 (2005).
126. Millay, D. P. *et al.* Myomaker is a membrane activator of myoblast fusion and muscle formation. *Nature* **499**, 301–305 (2013).
127. Quinn, M. E. *et al.* Myomerger induces fusion of non-fusogenic cells and is required for skeletal muscle development. *Nat. Commun.* **8**, 15665 (2017).
128. Lepper, C., Partridge, T. A. & Fan, C.-M. An absolute requirement for Pax7-positive satellite cells in acute injury-induced skeletal muscle regeneration. *Dev. Camb. Engl.* **138**, 3639–3646 (2011).
129. McCormick, R. & Vasilaki, A. Age-related changes in skeletal muscle: changes to life-style as a therapy. *Biogerontology* **19**, 519–536 (2018).
130. Huo, F., Liu, Q. & Liu, H. Contribution of muscle satellite cells to sarcopenia. *Front. Physiol.* **13**, 892749 (2022).
131. Shefer, G., Van de Mark, D. P., Richardson, J. B. & Yablonka-Reuveni, Z. Satellite-cell pool size does matter: defining the myogenic potency of aging skeletal muscle. *Dev. Biol.* **294**, 50–66 (2006).
132. Sousa-Victor, P. *et al.* Geriatric muscle stem cells switch reversible quiescence into senescence. *Nature* **506**, 316–321 (2014).
133. Day, K., Shefer, G., Shearer, A. & Yablonka-Reuveni, Z. The depletion of skeletal muscle satellite cells with age is concomitant with reduced capacity of single progenitors to produce reserve progeny. *Dev. Biol.* **340**, 330–343 (2010).
134. Verdijk, L. B. *et al.* Satellite cells in human skeletal muscle; from birth to old age. *Age Dordr. Neth.* **36**, 545–547 (2014).
135. Lavasani, M. *et al.* Muscle-derived stem/progenitor cell dysfunction limits healthspan and lifespan in a murine progeria model. *Nat. Commun.* **3**, 608 (2012).
136. Cosgrove, B. D. *et al.* Rejuvenation of the muscle stem cell population restores strength to injured aged muscles. *Nat. Med.* **20**, 255–264 (2014).
137. Novak, J. S. *et al.* Human muscle stem cells are refractory to aging. *Aging Cell* **20**, e13411 (2021).
138. Conboy, I. M. *et al.* Rejuvenation of aged progenitor cells by exposure to a young systemic environment. *Nature* **433**, 760–764 (2005).
139. Carlson, M. E. *et al.* Relative roles of TGF-β1 and Wnt in the systemic regulation and aging of satellite cell responses. *Aging Cell* **8**, 676–689 (2009).
140. Léger, B., Derave, W., De Bock, K., Hespel, P. & Russell, A. P. Human sarcopenia reveals an increase in SOCS-3 and myostatin and a reduced efficiency of Akt phosphorylation. *Rejuvenation Res.* **11**, 163-175B (2008).

141. Conboy, I. M., Conboy, M. J., Smythe, G. M. & Rando, T. A. Notch-mediated restoration of regenerative potential to aged muscle. *Science* **302**, 1575–1577 (2003).
142. Carlson, M. E., Hsu, M. & Conboy, I. M. Imbalance between pSmad3 and Notch induces CDK inhibitors in old muscle stem cells. *Nature* **454**, 528–532 (2008).
143. Belizário, J. E., Fontes-Oliveira, C. C., Borges, J. P., Kashiabara, J. A. & Vannier, E. Skeletal muscle wasting and renewal: a pivotal role of myokine IL-6. *SpringerPlus* **5**, 619 (2016).
144. Price, F. D. *et al.* Inhibition of JAK/STAT signaling stimulates adult satellite cell function. *Nat. Med.* **20**, 1174–1181 (2014).
145. Ghadiali, R. S., Guimond, S. E., Turnbull, J. E. & Pisconti, A. Dynamic changes in heparan sulfate during muscle differentiation and ageing regulate myoblast cell fate and FGF2 signalling. *Matrix Biol.* **59**, 54–68 (2017).
146. da Silva, P. F. L. & Schumacher, B. DNA damage responses in ageing. *Open Biol.* **9**, 190168 (2019).
147. Decary, S. *et al.* Replicative potential and telomere length in human skeletal muscle: implications for satellite cell-mediated gene therapy. *Hum. Gene Ther.* **8**, 1429–1438 (1997).
148. Hernando-Herraez, I. *et al.* Ageing affects DNA methylation drift and transcriptional cell-to-cell variability in mouse muscle stem cells. *Nat. Commun.* **10**, 4361 (2019).
149. Bigot, A. *et al.* Age-Associated Methylation Suppresses SPRY1, Leading to a Failure of Re-quiescence and Loss of the Reserve Stem Cell Pool in Elderly Muscle. *Cell Rep.* **13**, 1172–1182 (2015).
150. Turner, D. C. *et al.* DNA methylation across the genome in aged human skeletal muscle tissue and muscle-derived cells: the role of HOX genes and physical activity. *Sci. Rep.* **10**, 15360 (2020).
151. Masiero, E. *et al.* Autophagy is required to maintain muscle mass. *Cell Metab.* **10**, 507–515 (2009).
152. Alsharidah, M. *et al.* Primary human muscle precursor cells obtained from young and old donors produce similar proliferative, differentiation and senescent profiles in culture. *Aging Cell* **12**, 333–344 (2013).
153. Ogrodnik, M. Cellular aging beyond cellular senescence: Markers of senescence prior to cell cycle arrest in vitro and in vivo. *Aging Cell* **20**, e13338 (2021).
154. Nassrally, M. S. *et al.* Cell cycle arrest in replicative senescence is not an immediate consequence of telomere dysfunction. *Mech. Ageing Dev.* **179**, 11–22 (2019).
155. Kim, Y.-M. *et al.* Implications of time-series gene expression profiles of replicative senescence. *Aging Cell* **12**, 622–634 (2013).
156. d'Adda di Fagagna, F. *et al.* A DNA damage checkpoint response in telomere-initiated senescence. *Nature* **426**, 194–198 (2003).
157. Lian, S. *et al.* PRL-3 activates NF-κB signaling pathway by interacting with RAP1. *Biochem. Biophys. Res. Commun.* **430**, 196–201 (2013).
158. Caliri, A. W., Tommasi, S., Bates, S. E. & Besaratinia, A. Spontaneous and photosensitization-induced mutations in primary mouse cells transitioning through senescence and immortalization. *J. Biol. Chem.* **295**, 9974–9985 (2020).
159. Ogrodnik, M., Salmonowicz, H. & Gladyshev, V. N. Integrating cellular senescence with the concept of damage accumulation in aging: Relevance for clearance of senescent cells. *Aging Cell* **18**, e12841 (2019).

160. O'Connor, M. S., Carlson, M. E. & Conboy, I. M. Differentiation rather than aging of muscle stem cells abolishes their telomerase activity. *Biotechnol. Prog.* **25**, 1130–1137 (2009).

161. Neurohr, G. E. *et al.* Excessive Cell Growth Causes Cytoplasm Dilution And Contributes to Senescence. *Cell* **176**, 1083-1097.e18 (2019).

162. Yuan, R. *et al.* Altered growth characteristics of skin fibroblasts from wild-derived mice, and genetic loci regulating fibroblast clone size. *Aging Cell* **5**, 203–212 (2006).

163. Unterluggauer, H. *et al.* Premature senescence of human endothelial cells induced by inhibition of glutaminase. *Biogerontology* **9**, 247–259 (2008).

164. Yi, S. *et al.* NMR-based metabonomic analysis of HUVEC cells during replicative senescence. *Aging* **12**, 3626–3646 (2020).

165. Konigsberg, I. R. Clonal Analysis of Myogenesis. *Science* **140**, 1273–1284 (1963).

166. Ding, S. *et al.* Maintaining bovine satellite cells stemness through p38 pathway. *Sci. Rep.* **8**, 10808 (2018).

167. Rubin, H. Cell aging in vivo and in vitro. *Mech. Ageing Dev.* **98**, 1–35 (1997).

168. Ishii, K. *et al.* Recapitulation of Extracellular LAMININ Environment Maintains Stemness of Satellite Cells In Vitro. *Stem Cell Rep.* **10**, 568–582 (2018).

169. Nelson, G. *et al.* A senescent cell bystander effect: senescence-induced senescence. *Aging Cell* **11**, 345–349 (2012).

170. Penton, C. M. *et al.* Laminin 521 maintains differentiation potential of mouse and human satellite cell-derived myoblasts during long-term culture expansion. *Skelet. Muscle* **6**, 44 (2016).

171. Slatko, B. E., Gardner, A. F. & Ausubel, F. M. Overview of Next Generation Sequencing Technologies. *Curr. Protoc. Mol. Biol.* **122**, e59 (2018).

172. Mortazavi, A., Williams, B. A., McCue, K., Schaeffer, L. & Wold, B. Mapping and quantifying mammalian transcriptomes by RNA-Seq. *Nat. Methods* **5**, 621–628 (2008).

173. Stark, R., Grzelak, M. & Hadfield, J. RNA sequencing: the teenage years. *Nat. Rev. Genet.* **20**, 631–656 (2019).

174. Fedurco, M., Romieu, A., Williams, S., Lawrence, I. & Turcatti, G. BTA, a novel reagent for DNA attachment on glass and efficient generation of solid-phase amplified DNA colonies. *Nucleic Acids Res.* **34**, e22 (2006).

175. Anders, S. & Huber, W. Differential expression analysis for sequence count data. *Genome Biol.* **11**, R106 (2010).

176. Tang, F. *et al.* mRNA-Seq whole-transcriptome analysis of a single cell. *Nat. Methods* **6**, 377–382 (2009).

177. Zheng, G. X. Y. *et al.* Massively parallel digital transcriptional profiling of single cells. *Nat. Commun.* **8**, 14049 (2017).

178. Griffiths, W. J. & Wang, Y. Mass spectrometry: from proteomics to metabolomics and lipidomics. *Chem. Soc. Rev.* **38**, 1882–1896 (2009).

179. Griffith, M., Walker, J. R., Spies, N. C., Ainscough, B. J. & Griffith, O. L. Informatics for RNA Sequencing: A Web Resource for Analysis on the Cloud. *PLoS Comput. Biol.* **11**, e1004393 (2015).

Chapter 2

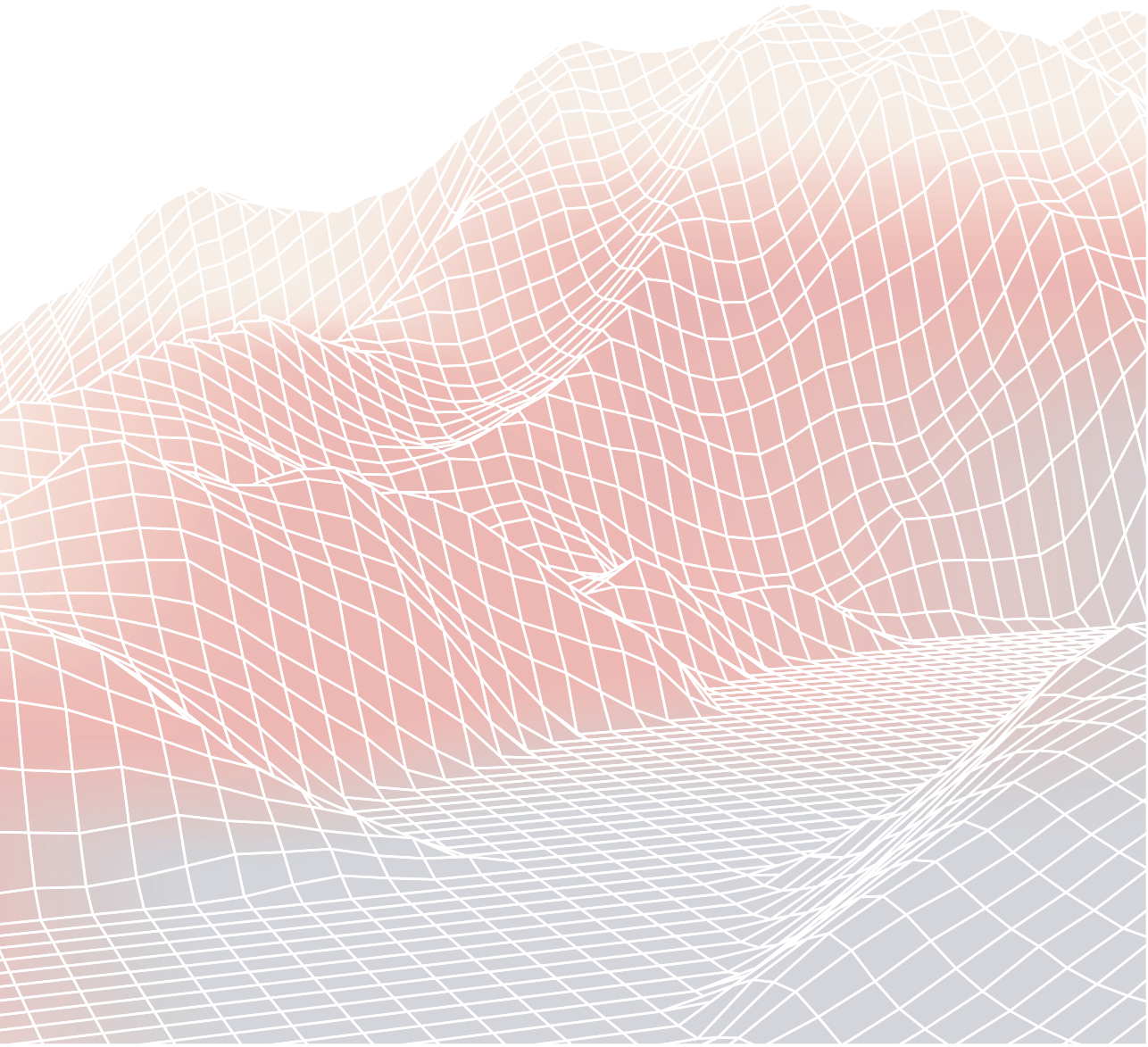

A SERUM-FREE MEDIA FORMULATION FOR CULTURED MEAT PRODUCTION SUPPORTS BOVINE SATELLITE CELL DIFFERENTIATION IN THE ABSENCE OF SERUM STARVATION

Tobias Meßmer
Iva Klevernic
Carolina Furquim
Ekaterina Ovchinnikova
Arın Doğan
Helder Cruz
Mark J Post
Joshua Flack

Nat Food **3**, 74–85 (2022)

2.1 ABSTRACT

Cultured meat production requires the robust differentiation of satellite cells into mature muscle fibres without the use of animal-derived components. Current protocols induce myogenic differentiation in vitro through serum starvation, an abrupt reduction in serum concentration. Here, we used RNA sequencing to investigate the transcriptomic remodelling of bovine satellite cells during myogenic differentiation induced by serum starvation. We characterised canonical myogenic gene expression, and identified surface receptors upregulated during the early phase of differentiation, including IGF1R, TFRC and LPAR1. Supplementation of ligands to these receptors enabled the formulation of a chemically defined media that induced differentiation in the absence of serum starvation and/or transgene expression. Serum-free myogenic differentiation was of similar extent to that induced by serum starvation, as evaluated by transcriptome analysis, protein expression and the presence of a functional contractile apparatus. Moreover, the serum-free differentiation media supported the fabrication of 3D bioartificial muscle constructs, demonstrating its suitability for cultured beef production.

2.2 INTRODUCTION

'Cultured' or 'cultivated' meat is an emerging technology based on the proliferation and differentiation of stem cells *in vitro* to produce edible tissues for human consumption. Its development is motivated primarily by sustainability issues associated with traditional meat production, including greenhouse gas emissions, resource consumption, animal welfare and food safety.[1,2]

Cultured meat is composed primarily of skeletal muscle tissue, which can be grown from adult stem cells known as muscle satellite cells (SCs), as well as several other cell types.[3,4] Previous work has described the isolation and proliferation of SCs from skeletal muscle, and their myogenic differentiation in hydrogels or scaffolds to form 3D bioartificial muscles (BAMs) through the use of tissue engineering techniques.[5,6]

However, in order to become commercially viable, cultured meat technologies must overcome a critical dependence on animal-derived components.[2] Standard protocols for SC proliferation require foetal bovine serum (FBS) at concentrations up to 20%, which affords efficient growth rates, and enables myogenic differentiation through an abrupt reduction in serum concentration, a process referred to as 'serum starvation'.[7] Scientific concerns (including batch-to-batch variation), cost, and ethical and consumer acceptance anxieties necessitate the replacement of FBS-supplemented culture media with chemically-defined, animal-free alternatives for cultured meat production in the absence of transgene expression. Whilst chemically-defined media have now been developed that support the differentiation of muscle cell lines such as C2C12, induced pluripotent stem cells (iPSCs), embryonic stem cells (ESCs) and SCs, all rely on serum starvation and/or transgene overexpression to induce differentiation.[8–11]

Differentiation of SCs into mature muscle fibres requires extensive transcriptional remodelling, including the downregulation of cell cycle-related genes, upregulation of myogenic transcription factors and membrane fusogens, and the production of a functional contractile apparatus upon terminal differentiation.[12,13] Activation of master transcriptional regulators occurs early in this process, but the mechanisms whereby serum starvation induce these changes remain poorly understood.[7,14] Whilst previous studies have focussed on myogenesis during embryonic development in cattle and other species,[15-18] the transcriptional landscape of adult bovine myogenic differentiation *in vitro* has not been studied in a detailed chronological fashion.

Here, we use bulk mRNA sequencing (RNA-seq) to study gene expression profiles during muscle differentiation upon serum starvation. By supplementing agonists to upregulated surface receptors, we develop a chemically-defined medium that can drive robust myogenic differentiation in the absence of serum starvation and/or transgene expression.

2.3 RESULTS

2.3.1 Serum starvation triggers extensive transcriptome remodelling

We induced myogenic differentiation of bovine satellite cells through withdrawal of serum (from 20% in growth medium (GM), to 2% in differentiation medium (DM); henceforth referred to as 'serum starvation'), and studied the resulting transcriptomic and proteomic profiles (Figs. 1a, b). After 96 hours, fusion index (percentage of nuclei within multinucleated myotubes)[19] increased from 1.0 to 38.3% (Fig. 1c), whilst nuclei counts did not show a specific trend (Fig. 1d). Performing principal component analysis (PCA; based on the 500 most variably expressed genes), samples clustered by timepoint, independent of batch, indicating that day of differentiation explained the majority of variation (Fig. 1e). The greater euclidean distance between 0 and 48 h, compared to that between 48 and 96 h, suggests that the majority of transcriptional remodelling occurs within the first two days.

We used the RNA-seq dataset to assess gene expression of prominent myogenic transcription factors and canonical differentiation markers, and found them to be consistently upregulated over the course of differentiation (Fig. 1f; Supplementary Fig. 1a).[20,21] Myogenic regulator *MYF5* was most highly expressed 24 h following serum starvation, whilst expression of stem cell marker *PAX7* increased during the first 24 h, before being downregulated (as previously shown in mouse).[22] Expression patterns of these genes were confirmed via RT-qPCR (Fig. 1g; Supplementary Fig. 1b), and by assessing protein levels via western blot (Fig. 1h). Moreover, we also observed increased expression of skeletal muscle-specific myosins[23] and myoblast fusogens[13] over time, whilst expression of satellite cell markers, cell adhesion-related and cell cycle maintenance genes decreased concomitantly (Supplementary Figs. 1c, d).

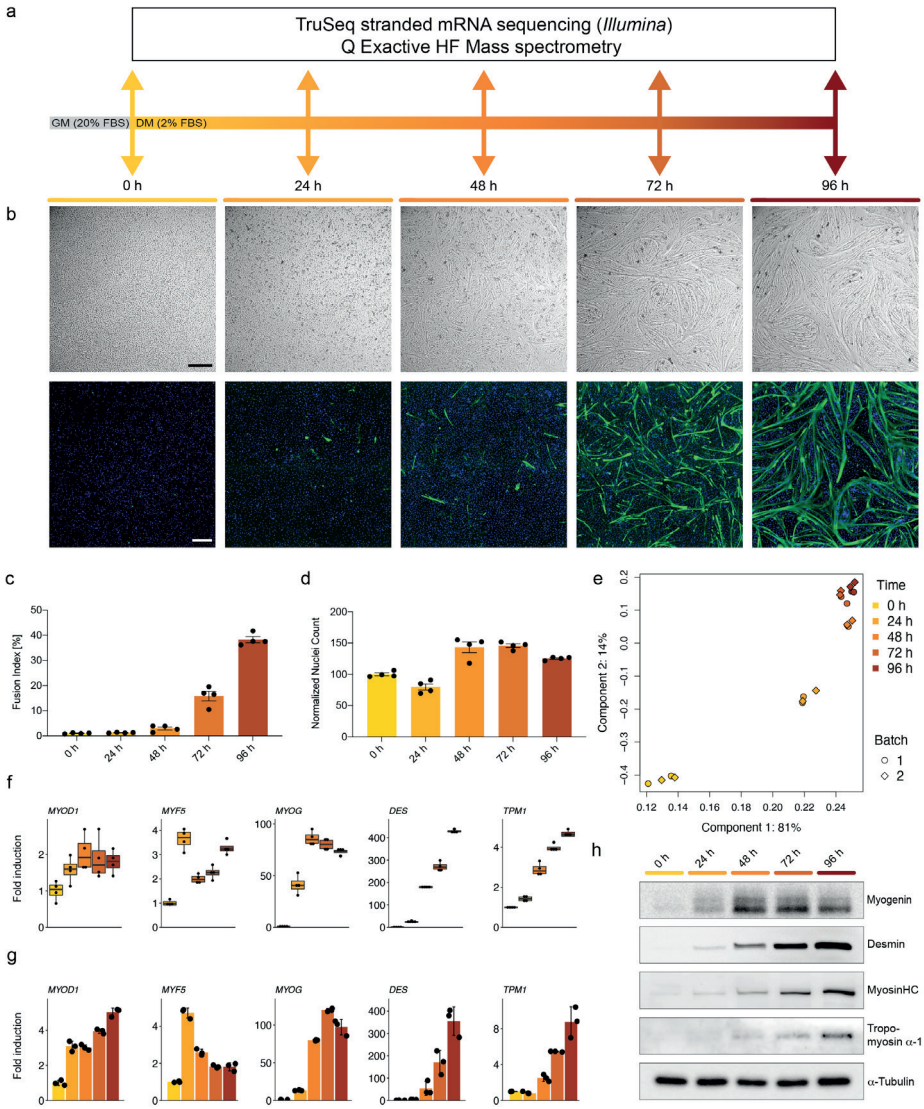

Figure 1: Bovine SCs undergo extensive transcriptomic changes upon serum starvation. a) Experimental design for the transcriptomic and proteomic characterisation of differentiating bovine SCs at 0 h, 24 h, 48 h, 72 h and 96 h following serum starvation; b) Representative brightfield (top row) and fluorescence (bottom row) images corresponding to timepoints in a); green = desmin, blue = Hoechst; scale bars = 500 µm; c) Mean quantified fusion indices of images in b); error bars indicate standard deviation (*SD*); d) Normalised nuclei count of b) as percentage of mean count at 0 h, error bars indicate *SD*; e) Principal component analysis of 500 most variably expressed genes in differentiating SCs from 0 h to 96 h. Colours indicate time after serum starvation; f) Median fold expression changes of muscle-related genes compared to 0 h as determined by RNA sequencing during the timecourse of serum starvation; box indicates IQR, whiskers show 1.5 IQR; g) Mean fold expression changes of genes shown in f), determined by RT-qPCR; error bars indicate *SD*, n = 4; h) Muscle-related protein expression during timecourse of serum starvation, as measured by western blot.

2.3.2 Surface receptors upregulated upon serum starvation

We performed differential expression analysis to identify genes up- and downregulated during differentiation (Fig. 2a). In total, 2984 of 14729 genes were significantly upregulated between 0 and 96 h (log2-FC > 1, FDR < 0.05), whilst 2438 were significantly downregulated (log2-FC < -1, FDR < 0.05; Supplementary Fig. 2a). Upregulated genes between 0 and 96 h predominantly encode proteins related to muscle development and function, protein folding, cell cycle inhibitors, and cadherins. GO terms associated with these genes relate to muscle processes or muscle development (upregulation) and to cell cycle regulation (downregulation; Fig. 2b), suggesting that serum starvation induces differentiation through cell cycle arrest, as previously described.[7,24] We noted that transcriptional remodelling upon serum starvation is largely conserved between bovine and mouse (R = 0.65; Supplementary Fig. 2b) when comparing the gene expression changes between 0 h and 96 h with those previously observed between 0 and 120 h for C2C12 cells.[25]

We subsequently compared observed changes in gene expression with changes in protein levels. Our mass spectrometry analysis identified 719 proteins for which the corresponding gene was present in the RNA-seq dataset. We determined significantly up- and downregulated proteins over the course of differentiation, which included muscle-specific markers such as desmin, myosin and tropomyosin-**α**1. These proteins showed similar expression profiles to those previously observed via western blot (Supplementary Fig. 2c; Fig. 1h). We then compared the log2-FC in protein levels identified via mass spectrometry with log2-FC in gene expression quantified by RNA-seq, between the earliest and the latest timepoints of differentiation analysed. The strong correlation (R = 0.78; Supplementary Fig. 2d) observed implies that transcriptomic changes during myogenic differentiation generally translate into corresponding changes in protein levels.

Reasoning that activation of cell-surface receptors upregulated during early differentiation might promote initiation of myogenic differentiation *in vitro* in the absence of serum starvation, we identified genes encoding surface receptors that were upregulated between 0 and 48 h (LFC > 1, FDR < 0.05). Amongst these were *IGF1R* and *IGF2R*, encoding receptors mediating signalling of insulin, IGF1 and IGF2[26], as well as the genes for transferrin (*TFRC*), lysophosphatidic acid (LPA; *LPAR1*), oxytocin (*OXTR*), glucagon (*GCGR*) and acetylcholine (*CHRNA1*) receptors (Figs. 2c, d). We confirmed upregulation of each of these receptors during differentiation by RT-qPCR (Supplementary Fig. 2e).

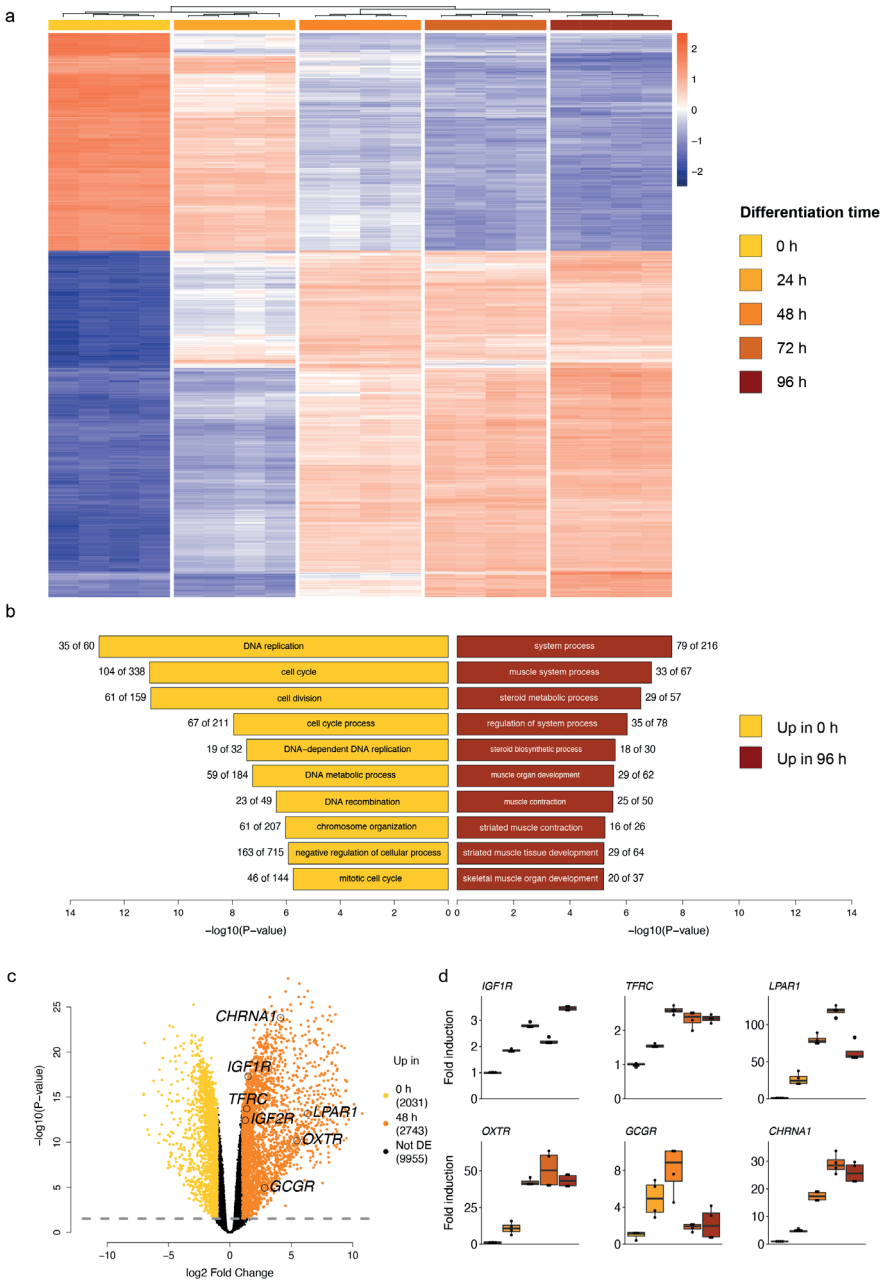

Figure 2: Differential expression analysis identifies surface receptors upregulated upon serum starvation.
a) Heatmap showing z-values of 1000 most differentially expressed genes between 0 h and 96 h after serum starvation. Genes (rows) and samples (columns) were clustered via Ward's method and z-values bound at -2.5 and 2.5; colours above samples indicate time after serum

starvation; b) Bar plot indicating GO terms (biological processes) corresponding to genes differentially expressed between 0 h (yellow) and 96 h (red). Proportion of significantly up/downregulated genes of total genes per GO term is indicated; c) Volcano plot showing differentially expressed genes between 0 h (yellow) and 48 h (orange). Genes corresponding to selected differentially expressed surface receptors are highlighted; dashed line indicates p-value at FDR = 0.05; d) Median fold changes from 0 h to 96 h post serum starvation, normalised against 0 h, for selected significantly upregulated surface receptors, determined via RNA sequencing. Box indicates IQR, whiskers show 1.5 IQR.

2.3.3 Ligands of upregulated receptors induce differentiation

To induce differentiation in the absence of serum starvation, we supplied activatory ligands to the surface receptors previously identified as upregulated during the early phase of differentiation, and investigated the effect on myogenic differentiation (Fig. 3). We initially supplemented basal DMEM/F-12 with $NaHCO_3$, L-ascorbic acid 2-phosphate, EGF1, MEM amino acids and serum albumin based on serum-free media formulations for iPSCs and SCs.[27,28] This formulation (subsequently referred to as serum-free base; 'SFB') increased nuclei count by 76% relative to DMEM/F-12, indicating increased cell survival, but did not significantly increase fusion index (Figs. 3a, b).

As transferrin receptor (TfR1) and IGF1R were amongst the most significantly upregulated surface receptors (and since ligands for these are widely used components of culture media),[26] we next supplemented SFB with transferrin and insulin. Supplementation with transferrin (T, 135 nM) alone did not have a significant effect on fusion index, whilst insulin (I, 1.8 µM) increased fusion from 7.4% (*SD* = 1.8) to 12.3% (*SD* = 1.3; $p < 0.001$, n = 4; Fig. 3c). A synergistic effect was observed upon addition of both components, resulting in an increased fusion index of 30.8% (*SD* = 1.8; $p < 0.001$, n = 4), though still less than the 39.0% (*SD* = 0.7) observed in serum starvation.

To approach the extent of differentiation induced by serum starvation, we then supplemented transferrin- and insulin-containing SFB with additional ligands to other upregulated receptors, in varying concentrations (Figs. 3d, e). Fusion index increased significantly from 30.7% (*SD* = 2.6) to 38.1% (*SD* = 2.0; $p = 0.022$, n = 4) and 41.0% (*SD* = 2.7; $p < 0.001$, n = 4) upon addition of 1 and 10 µM LPA respectively, and to 38.2% (*SD* = 2.6; $p = 0.019$, n = 4) on addition of 1 µM glucagon, whilst the effect of oxytocin or acetylcholine (ACh) supplementation was not statistically significant (Fig. 3f).

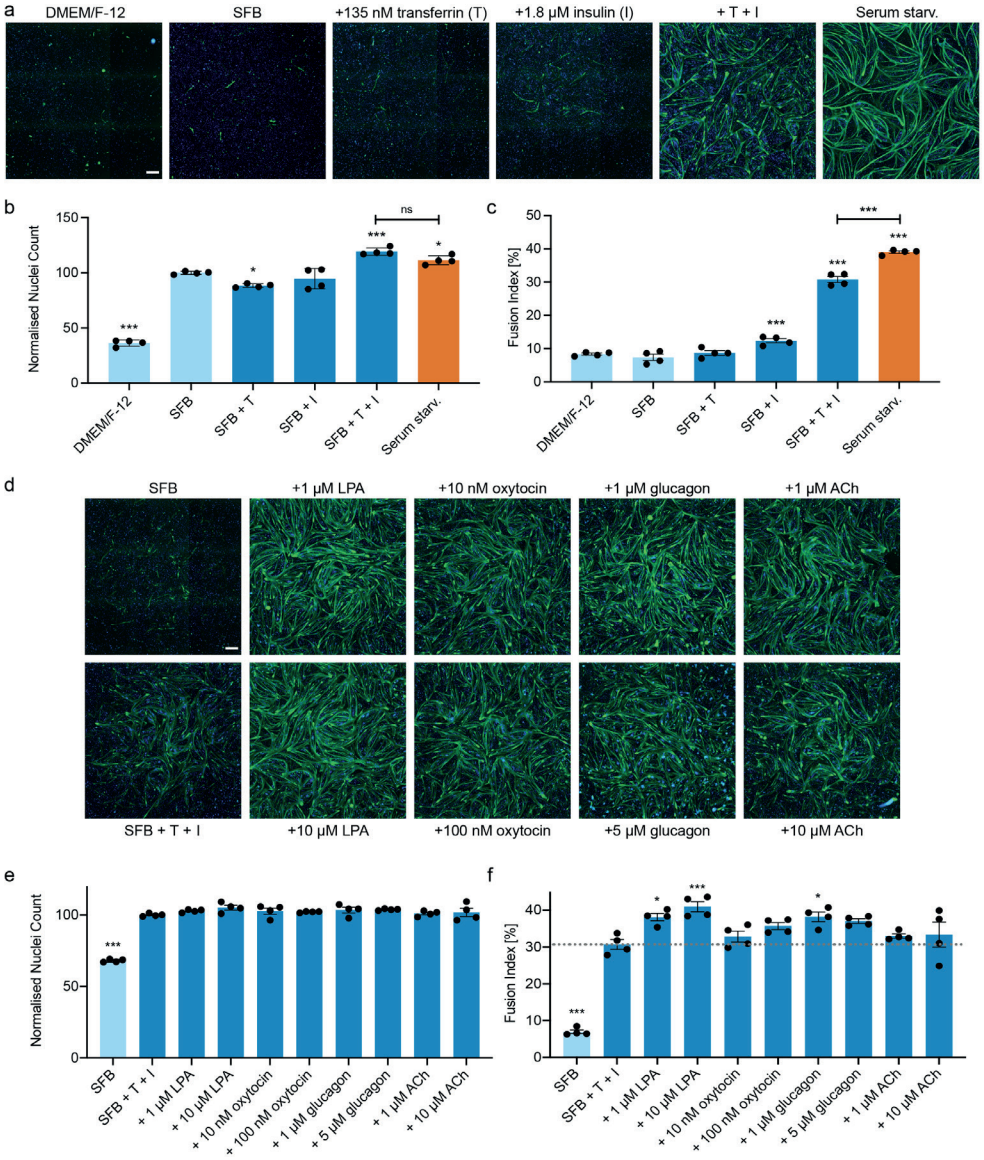

Figure 3: Serum-free differentiation is induced by supplementation of ligands to upregulated receptors.
a) Representative fluorescence images of SCs after 72 h in serum-free base media (SFB) with (blue) and without (light blue) supplementation of insulin (I, 1.8 µM), transferrin (T, 135 nM), and both; with basal DMEM/F-12 and serum starvation as reference controls; green = desmin, blue = Hoechst, scale bar = 500 µm; b) Nuclei counts derived from images in a) and three additional replicates as percentage against serum-free base media (SFB); error bars indicate *SD*, n = 4; c) Mean fusion indices derived from images in a) and three additional replicates, calculated by the percentage of nuclei within desmin-positive areas of total nuclei; statistical significance is indicated for each condition against SFB as well as between SFB

+ T + I and serum starvation; error bars indicate *SD*, n = 4; d) Representative fluorescence images of SCs after 72 h in SFB + T + I with additional supplementation of lysophosphatidic acid (LPA), oxytocin, glucagon and acetylcholine (ACh). Green = desmin, blue = Hoechst, scale bar = 500 µm; e) Nuclei counts derived from images in d) and three additional replicates as a percentage of SFB + T + I; statistical significance is indicated for each condition against SFB + T + I, error bars indicate *SD*, n = 4; f) Mean fusion indices derived from images in d) and three additional replicates; statistical significance is indicated for each condition against SFB + T + I; error bars indicate *SD*, n = 4; p-values: * < 0.05, ** < 0.005, *** < 0.001.

2.3.4 Serum-free differentiation mimics serum starvation

Supplementation of SFB with transferrin, insulin and LPA (a formulation henceforth referred to as serum-free differentiation medium; 'SFDM') resulted in fusion indices comparable to those of serum starvation controls. We characterised the extent of differentiation induced by SFDM more thoroughly, by assessing gene expression of canonical myogenic markers (Fig. 4a). *MYOD1*, *MYOG*, *DES* and *TPM1* showed significantly greater induction (between 0 and 72 h) for both SFDM and serum starvation conditions when compared to SFB. The same trend was observed for protein expression levels (Fig. 4b), indicating that SFDM induces a myogenic phenotype similar to serum starvation. For some genes (*MYOG* and *DES*) and proteins (e.g. myosin heavy chain), induction in SFDM was lower than in serum starvation.

To confirm that serum-free differentiation was not dependent on surface coating, we tested SFB, SFDM and serum starvation on a selection of extracellular matrix protein coatings (Fig. 4c). Compared with Matrigel, there was no significant difference in fusion index on any coating, with the exception of Laminin-111. Nuclei count and myotube morphology were variable throughout the conditions, although similar trends were observed for serum starvation controls (Fig. 4d; Supplementary Fig. 3a). We next studied the performance of SFDM and serum starvation with respect to fusion index as a function of number of population doublings (PDs) prior to differentiation. At early passage, serum starvation controls performed slightly better than SFDM, but at higher PDs SFDM and serum starvation showed similar fusion index (Fig. 4e; Supplementary Figs. 3b, c), indicating that SFDM might show improved performance in aged cells. We also compared the extent and variability of myogenic differentiation across SCs from additional donor animals, and found that fusion indices in SFDM were largely comparable to serum starvation (although for several donor animals, serum starvation did show a minor but statistically significant increase; Supplementary Fig. 4).

During longer timecourses (up to 10 days) of differentiation, we occasionally observed spontaneous contraction of myotubes. We therefore studied functional

differentiation by performing electrical pulse stimulation (EPS) after 192 h of serum-free differentiation.[29] EPS at 0.5 and 1 Hz resulted in rhythmic myotube contractions, indicating formation of a functional contractile apparatus sensitive to membrane depolarisation (Fig. 4f). Tetanic contraction was observed upon EPS at 5 Hz, or upon addition of 100 µM ACh.

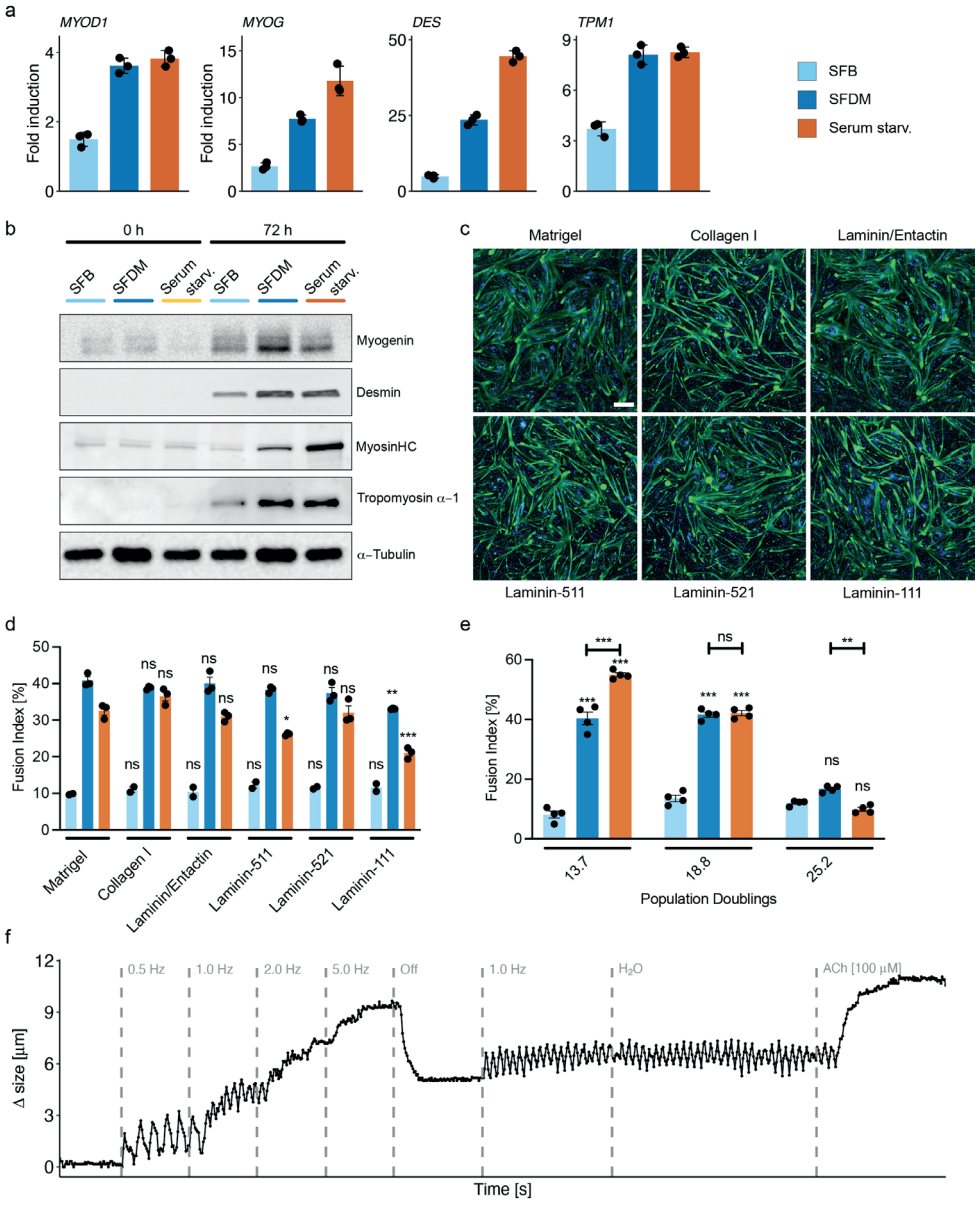

► **Figure 4: Serum-free differentiation is of comparable extent to serum starvation.**
a) Mean gene expression fold changes for SFB (light blue), SFDM (blue) and serum starvation (orange) 72 h post-induction of differentiation, normalised to respective conditions at 0 h (not shown), as determined by RT-qPCR; error bars indicate *SD*, n = 3; b) Muscle-related protein expression after 0 and 72 h in SFB, SFDM and serum control, as measured by western blot; c) Representative fluorescence images of differentiating SCs after 72 h in SFDM on indicated coatings; green = desmin, blue = Hoechst, scale bar = 500 µm; d) Fusion index corresponding to c) with SFB and serum starvation control; significance was determined for each condition separately against the respective Matrigel control; error bars indicate *SD*, n = 3; e) Fusion indices after 72 h in SFB, SFDM or upon serum starvation of SCs corresponding to early (left), medium (centre) and late (right) passages with indicated population doublings (PDs); significance was determined against SFB and between SFDM and serum starvation for each timepoint; error bars indicate *SD*, n = 4; f) Relative size change of a myotube during electrical pulse stimulation (EPS) over time with varying frequencies, and on addition of H_2O or acetylcholine (ACh); each point represents a measurement of relative distance of 2 fixed points in a 60 fps video; dashed lines delineate indicated parameter changes; p-values: * < 0.05, ** < 0.005, *** < 0.001.

2.3.5 Transcriptomic profiling of serum-free differentiation

Given that our serum-free conditions induced myogenic differentiation to a similar extent to serum starvation, we next characterised and compared the underlying transcriptional changes in depth, by performing RNA-seq prior to and after 72 h of treatment with SFB, SFDM, and serum starvation (Fig. 5). Dimensionality reduction showed that samples were most clearly separated between 0 h (GM, SFGM) and 72 h (SFB, SFDM, DM; Fig. 5a), suggesting that the three 72 h timepoints share an extensive set of differentially regulated genes.

To assess the overall similarity of gene expression changes, we determined differentially expressed genes during serum-free and serum starvation-induced differentiation, and compared the respective log2-FCs between 0 h and 72 h (Fig. 5b). Whilst slightly more genes were significantly up- and downregulated during serum starvation, the strong correlation observed (R = 0.73) suggests that the general transcriptomic changes induced are very similar, indicating that the same underlying biological mechanisms are being activated. To examine this trend more specifically, we interrogated the dataset for expression of certain myogenic regulators and muscle markers (Fig. 5c). Induction of expression of *MYOD1*, *MYOG* and *DES* was similar during serum-free and serum starvation-induced differentiation, whilst SFB also led to a small increase in expression of these genes, as previously observed (Fig. 4a). However, genes associated with late-stage differentiation, such as *MYH2,* showed significantly higher expression in serum starvation, indicating that terminal differentiation may be more pronounced after 72 h of serum starvation than the same period of serum-free differentiation. Indeed, the increased Euclidean distance between DM and the undifferentiated samples, relative to that for SFDM (Fig. 5a), suggests that serum starvation triggers myogenic gene expression programs in a faster or more pronounced fashion than serum-free differentiation.

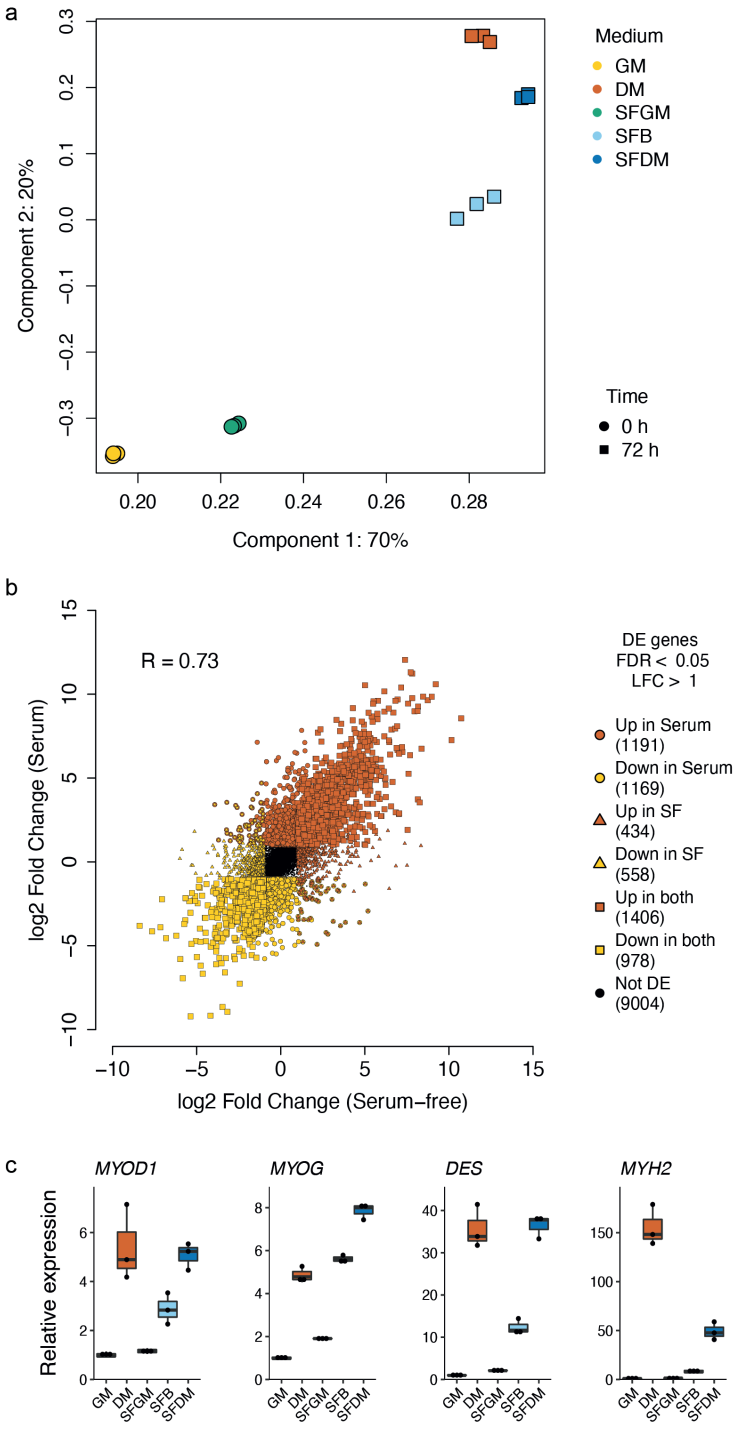
a
Component 2: 20%
0.3
0.2
0.1
0.0
−0.1
−0.2
−0.3
0.20
0.22
0.24
0.26
0.28
Component 1: 70%
Medium
GM
DM
SFGM
SFB
SFDM
Time
0 h
72 h
b
R = 0.73
log2 Fold Change (Serum)
15
10
5
0
−5
−10
log2 Fold Change (Serum−free)
DE genes
FDR < 0.05
LFC > 1
Up in Serum (1191)
Down in Serum (1169)
Up in SF (434)
Down in SF (558)
Up in both (1406)
Down in both (978)
Not DE (9004)
c
MYOD1
MYOG
DES
MYH2
Relative expression
GM
DM
SFGM
SFB
SFDM

► **Figure 5: Transcriptional remodelling during serum-free differentiation is similar to serum starvation.**
a) RNA-sequencing-derived principal component analysis of 500 most variably expressed genes before and after switching from growth media (GM, 0 h) and serum-free growth media (SFGM, 0 h) to serum starvation (DM) or SFB/SFDM respectively for 72 h; b) Scatter plot of log2-fold changes between SFGM and SFDM (x-axis) against those between GM and DM (y-axis) with Pearson correlation coefficient (R) as indicated. Data points represent genes differentially expressed as indicated, with respective counts shown; c) Median fold expression changes for selected genes upon serum starvation and serum-free differentiation, each normalised to GM, determined via RNA sequencing; box indicates IQR, whiskers show 1.5 IQR.

2.3.6 SFDM supports cultivation of differentiated BAMs

Most concepts for production of cultured meat require the cultivation of 3D muscle constructs. We therefore assessed the potential of SFDM for promoting the formation and maturation of myotubes during the fabrication of bioartificial muscles (BAMs). We embedded differentiating SCs in collagen/Matrigel hydrogels for 192 h in serum-free differentiation and serum starvation conditions (Fig. 6a), and assessed the structure and differentiation of the resulting BAMs via confocal microscopy, western blot and scanning electron microscopy (SEM).

During pilot studies, we noted that different basal media appeared to affect the overall morphology of BAM constructs. We confirmed that the supplements present in SFDM result in pronounced 2D myogenic differentiation in both DMEM/F-12 and DMEM basal media (Supplementary Fig. 5). Neither nuclei number nor fusion index differed significantly between DMEM/F-12- and DMEM-based serum-free differentiation (Supplementary Figs. 6b, c). In addition, we observed a strong correlation in transcriptional changes induced in DMEM/F-12- and DMEM-based SFDM as measured by RNA-seq (R = 0.83, Supplementary Fig. 5d). We thus tested both formulations in BAM fabrication.

All conditions resulted in the formation of viable constructs after 8 days culture (Supplementary Fig. 6a). Cell density and alignment, as well as actin and myosin expression, were visibly more pronounced in SFDM and DM when compared to SFB (Fig. 6b), suggesting a more differentiated myogenic phenotype. Furthermore, we identified desmin expression exclusively in DMEM-based SFDM and serum starvation control BAMs, which was increased further by addition of ACh after 96 h (Supplementary Fig. 6b). The presence of large myotubes at the surface of constructs (Fig. 6c; Supplementary Fig. 6c) suggests that DMEM-based SFDM supplemented with ACh was the best serum-free media formulation, supporting myotube formation in BAMs comparable to serum starvation. Protein expression

of canonical muscle differentiation markers was strongly induced (and to a similar extent) in both DMEM/F-12- and DMEM-based serum-free BAMs, although to a lesser extent than in serum starvation (Fig. 6d).

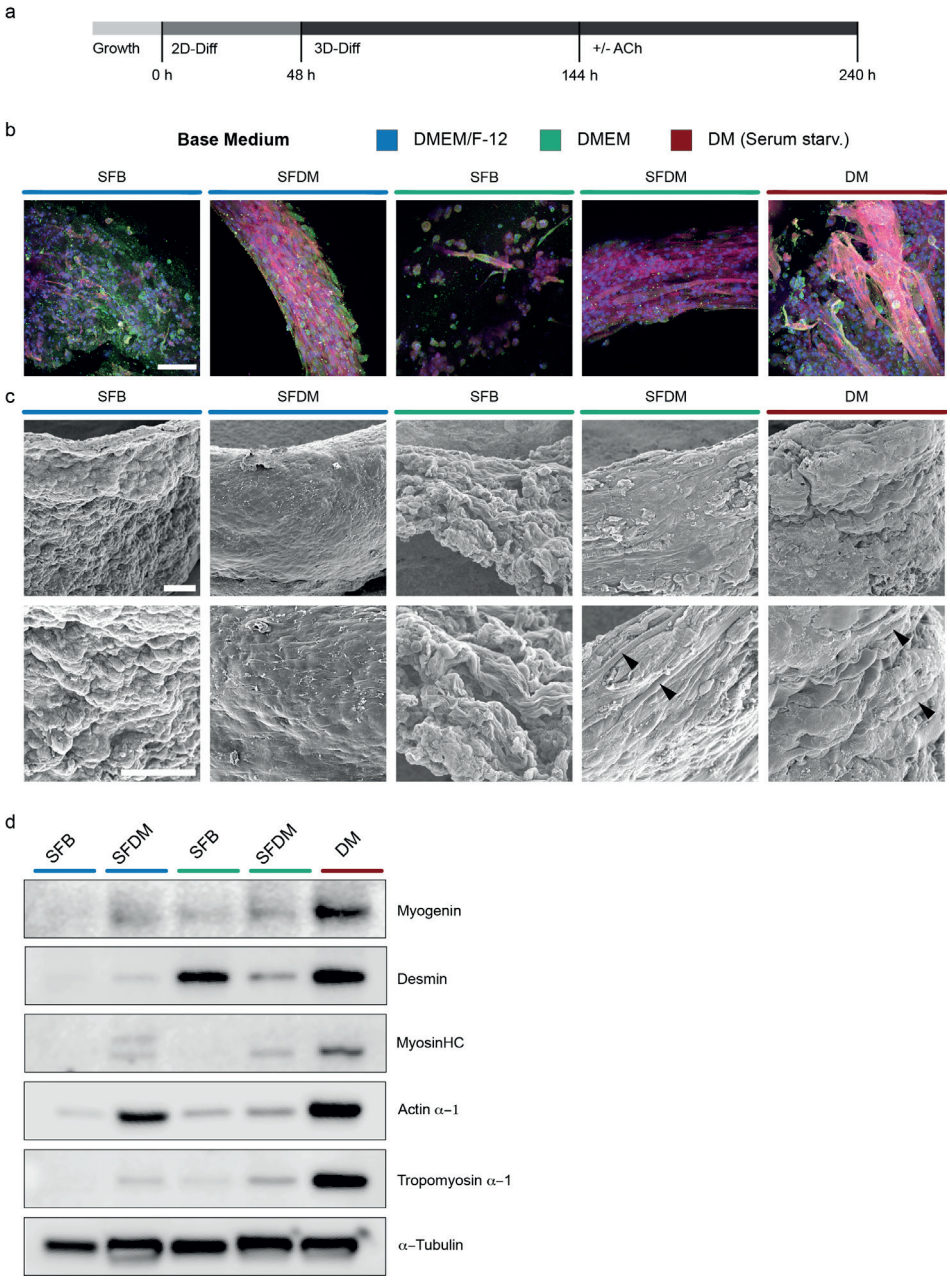

► **Figure 6: Serum-free differentiation medium enables fabrication of bioartificial muscles.** a) Experimental setup for bioartificial muscle (BAM) fabrication in collagen-Matrigel hydrogels; b) Maximum intensity projection confocal microscope images of BAMs after 192 h in SFB and SFDM (DMEM/F-12 and DMEM based) or DM; pink = desmin, red = α-actin, green = myosinHC, blue = Hoechst; scale bar = 100 µm; c) Wide (top) and close-up (bottom) scanning electron microscopy images of BAMs after 192 h in SFB and SFDM (DMEM/F-12 and DMEM based), or DM; arrowheads indicate myotube formation; scale bars = 100 µm; d) Canonical muscle protein expression in BAMs after 192 h in SFB, SFDM or upon serum starvation, as measured by western blot.

2.4 DISCUSSION

Production of cultured meat requires robust differentiation of stem cells into mature muscle fibres, without the use of serum or other animal-derived components. Chemically-defined media have previously been developed that support the myogenic differentiation of primary SCs from mouse,[8,30] human,[9] and other species,[31] as well as for cell lines, iPSCs[26] and ESCs[10]. However, these protocols invariably rely on use of serum during the proliferation phase to induce differentiation through serum starvation, and/or on transgenic overexpression of transcription factors such as MyoD.[11,32] We aimed to solve this issue by developing a chemically-defined medium that can drive robust differentiation in the absence of both serum starvation and transgene expression.

We characterised the transcriptomic and proteomic changes that occur during differentiation of bovine satellite cells upon serum starvation in high-resolution. Changes in mRNA expression observed during myogenic differentiation correlated well with changes in protein levels. In addition, they exhibited similar patterns to those previously found in cattle and other species,[17,25,33] indicating that transcriptional remodelling processes occurring during muscle differentiation are well conserved. Interestingly, switching from SFGM to a minimal medium formulation (SFB) induced transcriptional changes that somewhat resembled serum starvation, suggesting that withdrawal of growth factors and other components partially reproduces the effects of serum starvation, and that reduction in the activity of pro-mitotic signalling pathways (such as those stimulated by FGF2) contributes to induction of differentiation. Additionally, our transcriptomic analysis identified several cell-surface receptors upregulated during the early phase of differentiation. By supplementing the minimal medium with ligands to these receptors, we developed a chemically-defined medium that afforded robust myogenic differentiation in 2D and 3D assays, and which induced transcriptional and phenotypic changes with strong similarities to serum starvation.

Several of the pathways we stimulated have been related to myogenic differentiation. Insulin and transferrin have previously been identified as myotrophic factors both individually and synergistically.[34–36] These effects have been linked to increased glucose uptake and improved iron homeostasis, although no clear mechanism of action connecting both pathways has been described[34,35]. We also found that activation of the glucagon receptor, a class B GPCR, had a mild pro-myogenic effect, despite previous observations that it is not expressed at high levels in skeletal muscle *in vivo*.[37,38] Taken together, these data suggest a complex role for the insulin and glucagon signaling pathways, likely linked to glucose metabolism *in vitro*, and offer a potential avenue to further improve our SFDM formulation through the tuning of glucose levels and other metabolites. Use of metabolomic approaches to assess stabilities and consumption rates of other medium components, such as amino acids, will enable further optimisation of feeding strategies during myogenic differentiation.

LPAR1-mediated signalling has been reported to facilitate migration of activated satellite cells, through stimulation of the sphingosine kinase and sphingosine 1-phosphate pathways.[39] Interestingly, we observed that LPA supplementation at concentrations up to 10 µM yielded a pro-myogenic effect, whereas previous studies have linked higher concentrations to inhibition of differentiation in C2C12 cells.[40] Conversely, neither oxytocin nor acetylcholine significantly affected differentiation in our 2D differentiation assays, despite indications from past studies to the contrary.[27,41] However, supplementation of SFDM with ACh did promote formation of myotubes in BAMs, suggesting that myotube detachment from 2D surfaces may conceal the effects of ligands which promote the later stages of differentiation[42]. Addition of such 'maturation factors' could help promote expression of terminal differentiation-related genes, such as *MYH2*, which were not induced as strongly in SFDM.

Our SFDM formulation is the first, to our knowledge, to support the myogenic differentiation of a 3D muscle organoid in the absence of serum starvation and/or transgene expression. Various animal-free models have previously been proposed for the fabrication of cultured meat, including plant-based scaffolds and polymeric hydrogels.[43,44] While the hydrogels used in this study were not fully animal-component free, we observed robust 2D differentiation on several recombinant ECM components, and we expect that these findings will be reproduced in fully animal-free organoid cultures. Further modifications are likely to positively impact the extent of differentiation achieved in 3D, and to reduce costs. Refining the composition

and directionality of extracellular matrix proteins can enhance SC motility and alignment, leading to more pronounced myofibril development.[45] Similarly, EPS of muscle organoids has been shown to improve force generation, leading to increased expression of myoglobin and other mature muscle markers.[29,46] Finally, expanding the 3D model to include co-culture with other cell types, such as endothelial cells or fibroblasts, could promote myogenic differentiation through juxtacrine or paracrine interactions.[6,9] In this way, increased tissue complexity might narrow the disparity between current cultured meat models and traditional meat.

Other scientific challenges remain crucial hurdles to widespread success of cultured meat technologies. Significant proliferation is required to produce substantial amounts of cultured meat from a small number of starting cells.[47] Whilst serum-free differentiation outperformed serum starvation at high PDs, neither showed evidence of substantial myotube formation. This is likely attributable to a loss of SC stemness independent of differentiation conditions, and can be addressed by mitigating cellular ageing effects using small molecules or growth factors to inhibit specific signalling pathways (such as p38/MAPK).[48] Furthermore, cultured meat production will require reproducibility over a broad range of donor animals, breeds and (ideally) species. We tested SCs from eight Belgian Blue cattle, all of which demonstrated myogenic differentiation, but to a variable extent when compared to serum starvation. Further research is needed to clarify and mitigate sources of donor-to-donor variability. Nevertheless, the development of culture conditions that permit myogenic differentiation in the absence of serum starvation and transgene expression is an important step towards the realisation of cultured meat.

2.5 MATERIAL & METHODS

2.5.1 Satellite cell isolation and culture

Bovine satellite cells (SCs) were isolated and purified as previously described.[48] Briefly, freshly obtained semitendinosus muscle from slaughtered Belgian Blue cattle (both male and female, aged from 1 to 7 years) was minced, digested with collagenase (CLSAFA, Worthington) for 1 h at 37 °C prior to filtration with 100 µm nylon cell strainers. Red blood cells were lysed with Ammonium-Chloride-Potassium lysis buffer, filtered with 40 µm strainers and cultured for 72 h in serum-free growth medium (SFGM). SCs were purified by fluorescence-activated cell sorting (FACS) on a FACSAria Fusion Cell Sorter (BD Biosciences). Cells were stained

with NCAM1-PE-Cy7 (335826, BD Biosciences), CD29-APC (B247653, BioLegend), CD31-FITC (MCA1097F, Bio-Rad) and CD45-FITC (MCA2220F, Bio-Rad) and SCs sorted by gating for the CD31/CD45-, CD29+/NCAM1+ population.

SCs were cultured on flasks coated with Collagen Type-I solution (Collagen from Bovine Skin, Merck) in either growth medium (GM) or SFGM (Supplementary Table 1). Cells were passaged every 4-5 days upon approaching confluency.

2.5.2 Myogenic differentiation

SCs were differentiated on 0.5% Matrigel-coated plates (except where noted) by seeding 5 x 10^4 cells cm^{-2} in either GM (for serum starvation) or SFGM (for serum-free differentiation). Differentiation was induced by changing to DM after 24 h (for serum starvation), or by exchanging SFGM for serum-free differentiation medium (SFDM) or the media composition as indicated.

2.5.3 Immunofluorescent staining

Cells were fixed with 4% PFA, permeabilised with 0.5% Triton X-100, and blocked in 5% bovine serum albumin (BSA). Fixed cells were stained with **α**-desmin antibody (D1033, Sigma Aldrich) and Hoechst 33342 (Thermo Fisher Scientific), and imaged using an ImageXpress Pico Automated Cell Imaging System (Molecular Devices).

Nuclei counts were determined by quantifying Hoechst staining using MetaXPress software, and normalised against respective controls. Fusion index was determined by quantifying nuclei within desmin-stained myofibres as a proportion of total nuclei and multiplying by 100.[33,34]

2.5.4 RT-qPCR

Cell lysates were harvested by adding TRK lysis buffer (Omega Bio-tek) to tissue culture samples after removing culture media and washing with PBS. RNA was purified using the Omega MicroElute Total RNA Kit (Omega Bio-tek). RNA concentrations were determined by spectrophotometry and reverse-transcribed using the iScript cDNA synthesis kit (Bio-Rad). Quantitative real-time PCR (RT-qPCR) was performed using iQ SYBR Green Supermix (Bio-Rad) with primer pairs shown in Supplementary Table 2. Resulting CT values were averaged across 3 technical replicates, ΔCTs were calculated and $2^{\Delta CT}$ of genes of interest were normalised

against 'housekeeping' genes (*B2M* and *RPL19*). Statistical significance between respective fold-changes was evaluated using Dunnett's multiple comparison test against respective controls.

2.5.5 RNA sequencing

Library preparation and sequencing

Sequencing libraries were prepared from harvested RNA samples using the TruSeq stranded mRNA kit (Illumina) and sequenced on a high-output 75bp NextSeq 500 (Illumina). For GSE173198 (Fig. 1) and GSE173196 (Fig. 5), 37.0 x 10^6 (*SD* = 7.3 x 10^6) and 31.0 x 10^6 (*SD* = 3.6 x 10^6) aligned reads were obtained per sample on average, respectively.

2.5.5.1 Read alignment and quantification

STAR aligner 2.7 was used to align single-end reads to the reference genome bosTau9 (ARS UCD1.2.98). Subsequent analysis was performed in R 4.1.0. Gene counts based on the aligned reads were quantified using the FeatureCounts function of the Rsubread package.[49] For GSE173198, 78.86% (*SD* = 1.04) and for GSE173196, 80.39% (*SD* = 1.77) of reads were uniquely assigned to genes respectively.

2.5.5.2 Quality control and normalisation

DGEList-object was created using the obtained count matrix and gene meta information from the Btaurus_gene_ensembl data set.[50] Low-abundance genes (below a count of 10 for every individual sample, below a minimum count of 15 when summed over all samples, or not expressed in at least two replicates for every condition) were removed, and normalisation factors were calculated using trimmed-mean of M-values (TMM) method in the NormFactor function of edgeR.[51] Counts per million (CPM) and reads-per-kilobase per million (RPKM) were computed based on normalised library sizes.

2.5.5.3 Dimensionality reduction and differential expression analysis

Principal component analyses were performed using the 500 most variable genes based on the variance of RPKMs. Differential expression analysis was performed for each gene between all conditions using the limma package according to its suggested workflow at default parameters, i.e. by transforming the counts into

log2-CPMs, estimating mean-variance and computing observation-based weights (voom function), fitting a linear model (lmFit function), computing estimated coefficients (contrasts.fit function), and performing empirical eBayes moderation (eBayes function) towards a common value with a log2 fold change (log2-FC) threshold of 1.2.[52] Genes were considered differentially expressed above a log2-FC cutoff of 1 and a false-discovery rate (FDR) below 0.05, and visualised in volcano plots. A heatmap showing the z-values of the 1000 most differentially expressed genes between 0 h and 96 h was constructed in which genes and samples were clustered using Ward's minimum variance method with euclidean distances. Overrepresented gene ontology (GO) terms were computed for both upregulated and downregulated genes.[53]

2.5.6 Western blotting

Cells were lysed on ice using the RIPA Lysis Buffer System (Santa Cruz Biotechnology). Protein samples were boiled in Laemmli buffer for 5 min, separated by SDS-PAGE on 4-20% Mini-Protean TGX Gels (Bio-Rad), and transferred to PVDF membranes by electroblotting. Membranes were stained with primary antibodies against desmin (D1033, Sigma Aldrich), myogenin (sc-52903, Santa Cruz Biotechnology), tropomyosin-α1 (ab133292, Abcam), myosin heavy chain beta (myosinHC) (M8421, Sigma Aldrich), α-actin (ab97373, Abcam), and α-tubulin (ab4074, Abcam) and respective secondary antibodies α-mouse-HRP (ab6721, Abcam) and α-rabbit-HRP (P0447, Dako). Protein bands were detected with SuperSignal West Femto Maximum Sensitivity Substrate (Thermo Fisher Scientific) and visualised on an Azure 600 chemiluminescence imager (Azure Biosystems).

2.5.7 Mass Spectrometry

2.5.7.1 Sample preparation

Protein samples were collected as triplicates in 5 M urea, 50 mM ammonium bicarbonate and lysed by three freeze-thaw cycles. Samples were reduced with 20 mM dithiothreitol (DTT) and alkylated with 40 mM iodoacetamide (IAM). Alkylation was terminated by addition of 30 mM DTT to consume excess IAM. Digestion was performed for 2 h at 37°C in a thermoshaker (Grant Instruments) with Lys-C/trypsin mix (Promega, V5073), which was added at a ratio of 1:25 (enzyme to protein). Lysates were diluted with 50 mM ABC to 1 M urea for overnight digestion, which was terminated by addition of formic acid to a total of 1%.

2.5.7.2 Liquid chromatography

Peptide separation was performed on a Dionex Ultimate 3000 Rapid Separation UHPLC system (Thermo Fisher Scientific), equipped with a PepSep C18 analytical column (15 cm, ID 75 µm, 1,9 µm Reprosil, 120 Å). Peptide samples were first desalted on an online installed C18 trapping column. After desalting peptides were separated on the analytical column with a 90 min linear gradient from 5% to 35% acetonitrile with 0.1% FA at 300 nL min^{-1} flow rate. UHPLC system was coupled to a Q Exactive HF mass spectrometer (Thermo Fisher Scientific). DDA settings were as follows: Full MS scan between 250 – 1,250 m z^{-1} at resolution of 120,000 followed by MS/MS scans of the top 15 most intense ions at a resolution of 15,000.

2.5.7.3 Mass spectrometric raw data analysis

For protein identification and quantitation, DDA spectra were analysed with MaxQuant (Max Planck Institute). The Andromeda search engine was used with the SwissProt Bovine database (SwissProt TaxID = 9913). Dynamic modifications of methionine oxidation and protein N-terminus acetylation and static modification of cysteine carbamidomethylation were taken into account.

2.5.7.4 Quality control and data processing

Data was processed and analysed using the DEP package in R.[54] First, a summarised-experiment object was created based on label-free quantitation (LFQ) intensities from the MaxQuant output. A total of 1169 proteins were identified after filtering for proteins that were present in all replicates of at least one condition; with an average of 659.8 (*SD* = 84.3) proteins per sample and 381 proteins present in all samples. Data was normalised by variance stabilisation transformation resulting in logLFQ intensities before imputation by assuming missing-not-at-random (MNAR) values and using the MiniProb method.

2.5.7.5 Differential expression analysis and Pearson correlation

Differential protein expression between samples was determined through logLF-Q intensities using empirical eBayes moderation. The most significantly differentially enriched proteins between 0 h and 72 h were computed (FDR < 0.05, log2-FC > 1) and a Pearson correlation coefficient was calculated against the transcriptional log2-FCs between 0 h and 96 h.

2.5.8 Electrical Pulse Stimulation

Cells were differentiated as previously described in SFDM for 192 h in 6-well plates. Electrical Pulse Stimulation (EPS) was applied to cells using a C-PACE EP stimulator (IonOptix) with 6-well electrodes at 12.0 V and 1.0 ms pulse width. Contraction of myotubes was recorded at 60 fps with an Evos FL5000 microscope (Thermo Fisher Scientific). Size changes were quantified by measuring pixel distance between two fixed points on the myotubes in every fifth frame using ImageJ. Sizes were converted to nanometers (using microscope scale bar for reference) and plotted against time.

2.5.9 BAM Fabrication

Cells were cultured for one passage in either SFGM or GM on Matrigel-coated flasks until reaching confluence. Differentiation was induced by switching from SFGM to SFB or SFDM as indicated, or from GM to DM. After 48 h in SFB, SFDM or DM, cells were harvested and filtered with a 70 µm nylon strainer. Bioartificial muscles (BAMs) were fabricated by modifying a previously described method[5]. Briefly, 5.9 x 10^6 cells ml^{-1} in respective media were mixed with 1.5 mg ml^{-1} ice-cold Collagen Type-I solution (Merck) and neutralised with 0.5 N NaOH (Sigma) solution by mixing on ice. Matrigel (Corning) was mixed within the gel to a final percentage of 7%, and 70 µL plated around a stainless steel pillar (2 mm in diameter). After allowing hydrogel to compact for 2 h, respective differentiation media were added. Media changes were performed after 96 h (Ach was included in the medium at a final concentration of 10 µM where indicated) and BAMs were harvested a total of 192 h after fabrication.

2.5.10 Confocal Microscopy

BAMs were washed in ice-cold PBS, fixed in 4% PFA and harvested by careful removal from pillars. Fixed structures were stained with primary antibodies against desmin (D1033, Sigma Aldrich) and myosinHC (M8421, Sigma Aldrich) and subsequently with secondary antibodies α-rabbit-Alexa488 (A21206,Thermo Fisher Scientific) and α-mouse-Alexa633 (A21050, Thermo Fisher Scientific), and with Phalloidin-490LS (14479, Sigma-Aldrich) and Hoechst 33342 (Thermo Fisher Scientific). Images of stained BAM constructs were captured using a TCS SP8 MP confocal microscope (Leica Microsystems), and are presented as single slices or maximum intensity projections as indicated.

2.5.11 Scanning Electron Microscopy

BAM constructs were transferred to Karnovsky fixative at RT (2% PFA, 2.5% glutaraldehyde in 0.1 M NaH_2PO_4, C0250, Sigma Aldrich). BAMs were washed in 0.1M NaH_2PO_4 and post-fixed for 1 h with 1% OsO4, 1.5% ferrocyanide in 0.1 M cacodylate. After post-fixative was removed, BAMs were washed, dehydrated by critical point drying and sputter-coated with a thin gold layer using a SC7620 Mini Sputter Coater (Quorum Technologies). The prepared samples were imaged on a JSM-IT200 InTouchScope Scanning Electron Microscope (JEOL).

2.5.12 Statistical analyses

Statistical significance for nuclei counts and fusion indices was assessed using Prism 9.1.2 (GraphPad). In the case of one dependent variable, one-way analysis of variance (ANOVA) was performed to determine statistical significance, followed by Dunnett's multiple comparison test against indicated controls (Fig. 3, Supplementary Fig. 5). In the case of two independent variables, two-way ANOVA was performed, followed by Tukey's multiple comparison test (Fig. 4, Supplementary Figs. 3, 4). Sample replicates consisted of cells from the same donor animal, cultured in separate vessels. No statistical methods were used to pre-determine sample sizes, but sample sizes are similar to those previously reported.[48] For nuclei counts and fusion indices, the data distribution was assumed to be normal though this was not formally tested.

2.5.13 Data Availability

RNA-seq data has been deposited to the GEO (accession number GSE173199). Uncropped versions of western blots are available as source data. Further data supporting the findings of this study are available from the authors upon request.

2.6 ACKNOWLEDGEMENTS

We thank Kasper Derks and Demis Tserpelis (Genome Services Maastricht UMC+) for their support in the acquisition and analysis of RNA-seq data, Ronny Mohren (Imaging Mass Spectrometry, M4I, Maastricht University) for proteomics data, and Hans Duimel and Carmen López Iglesia (Microscopy CORE Lab, M4I, Maastricht University) for SEM. We would also like to acknowledge Johanna Melke and Dirk Remmers (Mosa Meat B.V.) for their assistance with confocal microscopy.

2.7 BIBLIOGRAPHY

1. Parodi, A. *et al.* The potential of future foods for sustainable and healthy diets. *Nat. Sustain.* **1**, 782–789 (2018).
2. Post, M. J. *et al.* Scientific, sustainability and regulatory challenges of cultured meat. *Nat. Food* **1**, 403–415 (2020).
3. Bischoff, R. Regeneration of single skeletal muscle fibers in vitro. *Anat. Rec.* **182**, 215–235 (1975).
4. Collins, C. A. *et al.* Stem cell function, self-renewal, and behavioral heterogeneity of cells from the adult muscle satellite cell niche. *Cell* **122**, 289–301 (2005).
5. Vandenburgh, H. *et al.* Tissue-engineered skeletal muscle organoids for reversible gene therapy. *Hum. Gene Ther.* **7**, 2195–2200 (1996).
6. Ben-Arye, T. *et al.* Textured soy protein scaffolds enable the generation of three-dimensional bovine skeletal muscle tissue for cell-based meat. *Nat. Food* 1–11 (2020) doi:10.1038/s43016-020-0046-5.
7. Pirkmajer, S. & Chibalin, A. V. Serum starvation: caveat emptor. *Am. J. Physiol.-Cell Physiol.* **301**, C272–C279 (2011).
8. Das, M. *et al.* Developing a Novel Serum-Free Cell Culture Model of Skeletal Muscle Differentiation by Systematically Studying the Role of Different Growth Factors in Myotube Formation. *In Vitro Cell. Dev. Biol. Anim.* **45**, 378–387 (2009).
9. Guo, X. *et al.* In vitro Differentiation of Functional Human Skeletal Myotubes in a Defined System. *Biomater. Sci.* **2**, 131–138 (2014).
10. Chal, J. *et al.* Differentiation of pluripotent stem cells to muscle fiber to model Duchenne muscular dystrophy. *Nat. Biotechnol.* **33**, 962–969 (2015).
11. Akiyama, T. *et al.* Efficient differentiation of human pluripotent stem cells into skeletal muscle cells by combining RNA-based MYOD1-expression and POU5F1-silencing. *Sci. Rep.* **8**, 1189 (2018).
12. Chal, J. & Pourquié, O. Making muscle: skeletal myogenesis in vivo and in vitro. *Dev. Camb. Engl.* **144**, 2104–2122 (2017).
13. Millay, D. P. *et al.* Myomaker: A membrane activator of myoblast fusion and muscle formation. *Nature* **499**, 301–305 (2013).
14. Bryson-Richardson, R. J. & Currie, P. D. The genetics of vertebrate myogenesis. *Nat. Rev. Genet.* **9**, 632–646 (2008).
15. Tsumagari, K. *et al.* Gene expression during normal and FSHD myogenesis. *BMC Med. Genomics* **4**, 67 (2011).
16. He, H. & Liu, X. Characterization of transcriptional complexity during longissimus muscle development in bovines using high-throughput sequencing. *PloS One* **8**, e64356 (2013).
17. Tripathi, A. K. *et al.* Transcriptomic dissection of myogenic differentiation signature in caprine by RNA-Seq. *Mech. Dev.* **132**, 79–92 (2014).
18. Lee, E. J. *et al.* Identification of Genes Differentially Expressed in Myogenin Knock-Down Bovine Muscle Satellite Cells during Differentiation through RNA Sequencing Analysis. *PLoS ONE* **9**, (2014).
19. Nishiyama, T., Kii, I. & Kudo, A. Inactivation of Rho/ROCK signaling is crucial for the nuclear accumulation of FKHR and myoblast fusion. *J. Biol. Chem.* **279**, 47311–47319 (2004).

20. Capkovic, K. L., Stevenson, S., Johnson, M. C., Thelen, J. J. & Cornelison, D. Neural cell adhesion molecule (NCAM) marks adult myogenic cells committed to differentiation. *Exp. Cell Res.* **314**, 1553–1565 (2008).
21. Tang, Z. *et al.* Molecular Cloning of Caveolin-3, a Novel Member of the Caveolin Gene Family Expressed Predominantly in Muscle. *J. Biol. Chem.* **271**, 2255–2261 (1996).
22. Seale, P. *et al.* Pax7 is required for the specification of myogenic satellite cells. *Cell* **102**, 777–786 (2000).
23. Weiss, A. & Leinwand, L. A. The mammalian myosin heavy chain gene family. *Annu. Rev. Cell Dev. Biol.* **12**, 417–439 (1996).
24. Pardee, A. B. A restriction point for control of normal animal cell proliferation. *Proc. Natl. Acad. Sci. U. S. A.* **71**, 1286–1290 (1974).
25. He, K. *et al.* A transcriptomic study of myogenic differentiation under the overexpression of PPARγ by RNA-Seq. *Sci. Rep.* **7**, 15308 (2017).
26. Massoner, P., Ladurner-Rennau, M., Eder, I. E. & Klocker, H. Insulin-like growth factors and insulin control a multifunctional signalling network of significant importance in cancer. *Br. J. Cancer* **103**, 1479–1484 (2010).
27. Chen, G. *et al.* Chemically defined conditions for human iPSC derivation and culture. *Nat. Methods* **8**, 424–429 (2011).
28. Breton, C. *et al.* Presence of Functional Oxytocin Receptors in Cultured Human Myoblasts. *J. Clin. Endocrinol. Metab.* **87**, 1415–1418 (2002).
29. Nikolić, N. *et al.* Electrical pulse stimulation of cultured skeletal muscle cells as a model for in vitro exercise – possibilities and limitations. *Acta Physiol.* **220**, 310–331 (2017).
30. Gawlitta, D., Boonen, K. J. M., Oomens, C. W. J., Baaijens, F. P. T. & Bouten, C. V. C. The influence of serum-free culture conditions on skeletal muscle differentiation in a tissue-engineered model. *Tissue Eng. Part A* **14**, 161–171 (2008).
31. Lawson, M. A. & Purslow, P. P. Differentiation of Myoblasts in Serum-Free Media: Effects of Modified Media Are Cell Line-Specific. *Cells Tissues Organs* **167**, 130–137 (2000).
32. Shoji, E., Woltjen, K. & Sakurai, H. Directed Myogenic Differentiation of Human Induced Pluripotent Stem Cells. *Methods Mol. Biol. Clifton NJ* **1353**, 89–99 (2016).
33. Tong, H. L. *et al.* Transcriptional profiling of bovine muscle-derived satellite cells during differentiation in vitro by high throughput RNA sequencing. *Cell. Mol. Biol. Lett.* **20**, 351–373 (2015).
34. Brunetti, A., Maddux, B. A., Wong, K. Y. & Goldfine, I. D. Muscle cell differentiation is associated with increased insulin receptor biosynthesis and messenger RNA levels. *J. Clin. Invest.* **83**, 192–198 (1989).
35. Ozawa, E. Transferrin as a muscle trophic factor. *Rev. Physiol. Biochem. Pharmacol.* **113**, 89–141 (1989).
36. Cox, R. D., Garner, I. & Buckingham, M. E. Transcriptional regulation of actin and myosin genes during differentiation of a mouse muscle cell line. *Differ. Res. Biol. Divers.* **43**, 183–191 (1990).
37. Hansen, L. H., Abrahamsen, N. & Nishimura, E. Glucagon receptor mRNA distribution in rat tissues. *Peptides* **16**, 1163–1166 (1995).
38. Uhlén, M. *et al.* Proteomics. Tissue-based map of the human proteome. *Science* **347**, 1260419 (2015).

39. Cencetti, F. *et al.* Lysophosphatidic acid stimulates cell migration of satellite cells. A role for the sphingosine kinase/sphingosine 1-phosphate axis. *FEBS J.* **281**, 4467–4478 (2014).
40. Yoshida, S., Fujisawa-Sehara, A., Taki, T., Arai, K. & Nabeshima, Y. Lysophosphatidic acid and bFGF control different modes in proliferating myoblasts. *J. Cell Biol.* **132**, 181–193 (1996).
41. Zhang, Z. *et al.* Oxytocin is involved in steroid hormone-stimulated bovine satellite cell proliferation and differentiation in vitro. *Domest. Anim. Endocrinol.* **66**, 1–13 (2019).
42. Denes, L. T. *et al.* Culturing C2C12 myotubes on micromolded gelatin hydrogels accelerates myotube maturation. *Skelet. Muscle* **9**, 17 (2019).
43. Stephens, N. *et al.* Bringing cultured meat to market: Technical, socio-political, and regulatory challenges in cellular agriculture. *Trends Food Sci. Technol.* **78**, 155–166 (2018).
44. Furuhashi, M. *et al.* Formation of contractile 3D bovine muscle tissue for construction of millimetre-thick cultured steak. *Npj Sci. Food* **5**, 6 (2021).
45. Costantini, M. *et al.* Microfluidic-enhanced 3D bioprinting of aligned myoblast-laden hydrogels leads to functionally organized myofibers in vitro and in vivo. *Biomaterials* **131**, 98–110 (2017).
46. Lk, L. *et al.* A Pilot Study on Pain and the Upregulation of Myoglobin through Low-frequency and High-amplitude Electrical Stimulation-induced Muscle Contraction. *J. Phys. Ther. Sci.* **26**, 985–988 (2014).
47. Melzener, L., Verzijden, K., Buijs, A., Post, M. & Flack, J. Cultured Beef: from small biopsy to substantial quantity. *J. Sci. Food Agric.* (2020) doi:10.1002/jsfa.10663.
48. Ding, S. *et al.* Maintaining bovine satellite cells stemness through p38 pathway. *Sci. Rep.* **8**, 1–12 (2018).
49. Liao, Y., Smyth, G. K. & Shi, W. featureCounts: an efficient general purpose program for assigning sequence reads to genomic features. *Bioinforma. Oxf. Engl.* **30**, 923–930 (2014).
50. Yates, A. D. *et al.* Ensembl 2020. *Nucleic Acids Res.* **48**, D682–D688 (2020).
51. Anders, S. & Huber, W. Differential expression analysis for sequence count data. *Genome Biol.* **11**, R106 (2010).
52. Ritchie, M. E. *et al.* limma powers differential expression analyses for RNA-sequencing and microarray studies. *Nucleic Acids Res.* **43**, e47 (2015).
53. The Gene Ontology Consortium. The Gene Ontology Resource: 20 years and still GOing strong. *Nucleic Acids Res.* **47**, D330–D338 (2019).
54. Zhang, X. *et al.* Proteome-wide identification of ubiquitin interactions using UbIA-MS. *Nat. Protoc.* **13**, 530–550 (2018).

2.8 SUPPLEMENTARY INFORMATION

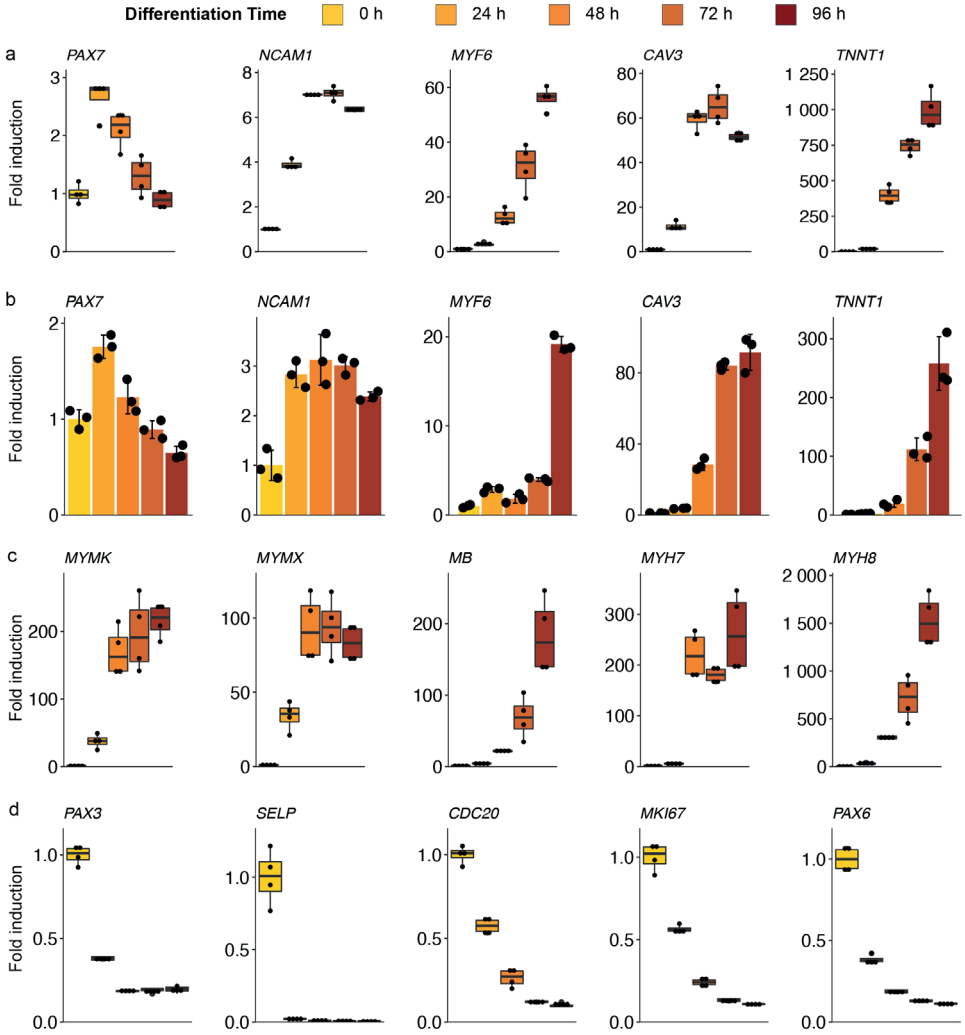

Supplementary Figure 1: Gene expression during myogenic differentiation induced by serum starvation (related to Fig. 1).
a) RNA sequencing-derived median fold changes of selected muscle-related genes during serum starvation compared to 0 h; box indicates IQR, whiskers show 1.5 IQR; b) Mean fold changes of genes shown in a), determined via RT-qPCR; error bars indicate *SD,* n = 3; c) Median fold changes of selected strongly upregulated myogenic genes compared to 0 h, determined via RNA sequencing; box indicates IQR, whiskers show 1.5 IQR; d) Median fold changes of selected downregulated genes compared to 0 h, determined via RNA sequencing; box indicates IQR, whiskers show 1.5 IQR.

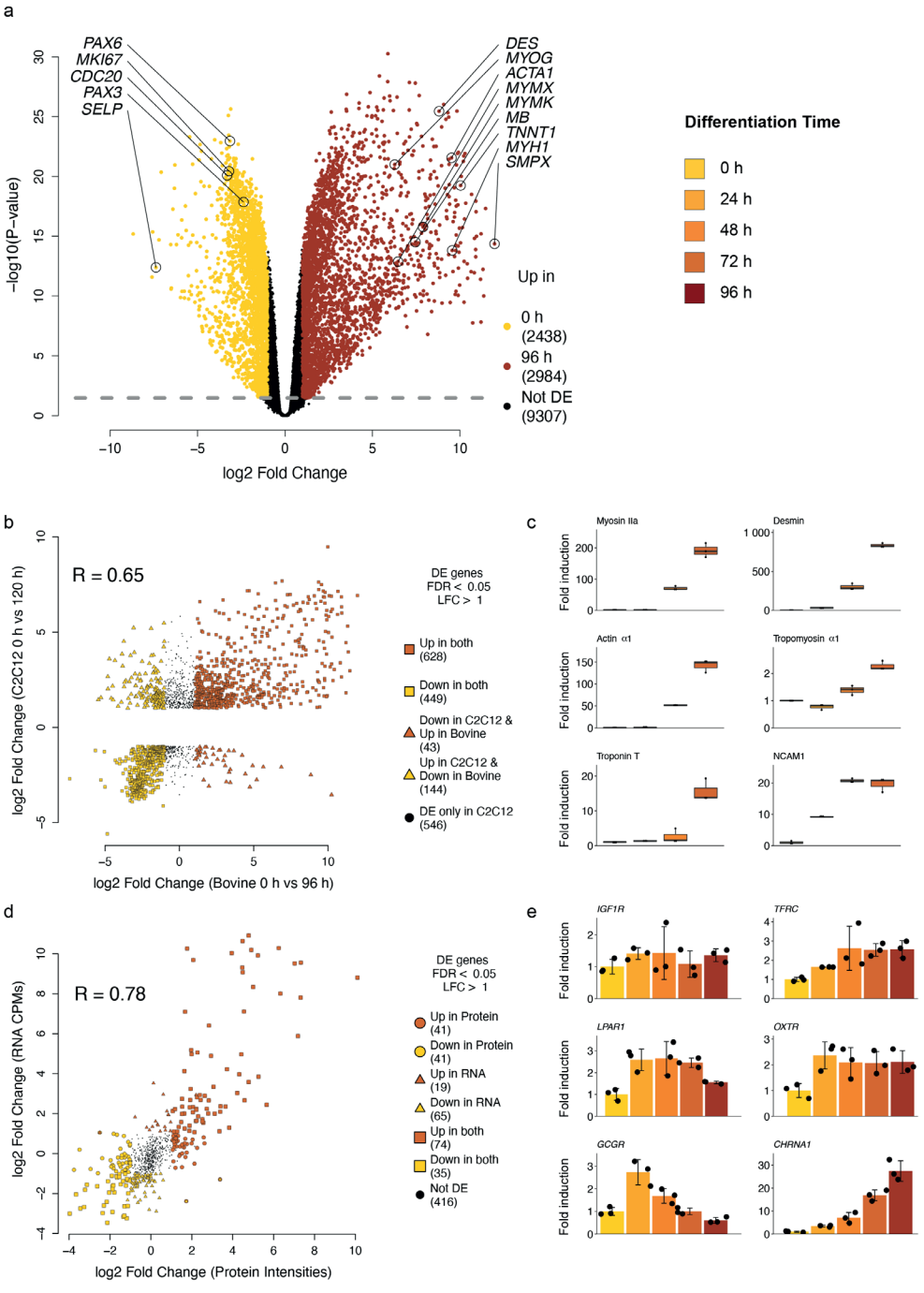
a
PAX6
MKI67
CDC20
PAX3
SELP
DES
MYOG
ACTA1
MYMX
MYMK
MB
TNNT1
MYH1
SMPX
−log10(P−value)
log2 Fold Change
Differentiation Time
0 h
24 h
48 h
72 h
96 h
Up in
0 h (2438)
96 h (2984)
Not DE (9307)
b
R = 0.65
log2 Fold Change (C2C12 0 h vs 120 h)
log2 Fold Change (Bovine 0 h vs 96 h)
DE genes FDR < 0.05 LFC > 1
Up in both (628)
Down in both (449)
Down in C2C12 & Up in Bovine (43)
Up in C2C12 & Down in Bovine (144)
DE only in C2C12 (546)
c
Myosin IIa
Desmin
Actin α1
Tropomyosin α1
Troponin T
NCAM1
Fold induction
d
R = 0.78
log2 Fold Change (RNA CPMs)
log2 Fold Change (Protein Intensities)
DE genes FDR < 0.05 LFC > 1
Up in Protein (41)
Down in Protein (41)
Up in RNA (19)
Down in RNA (65)
Up in both (74)
Down in both (35)
Not DE (416)
e
IGF1R
TFRC
LPAR1
OXTR
GCGR
CHRNA1
Fold induction

► **Supplementary Figure 2: Transcriptomic and proteomic characterisation of serum starvation (related to Fig. 2)**.
a) Volcano plot showing differentially expressed genes between 0 h (yellow) and 96 h (red) of serum starvation. Selected differentially expressed muscle, stem cell or cell cycle-related genes are indicated;
b) Scatter plot showing correlation of log2-fold changes of overlapping genes from bovine (x-axis) with C2C12 (y-axis) with indicated Pearson correlation coefficient (R). Colours indicate upregulation (red) or downregulation (yellow) in bovine gene expression, shapes indicate whether differentially expressed genes are simultaneously up/down-regulated in both species (squares) or significantly up/down-regulated in one species while inversely regulated in the other (triangles);
c) Median fold changes of muscle-related protein levels from 0 h to 72 h post serum starvation, normalised against 0 h; box indicates IQR, whiskers show 1.5 IQR;
d) Scatter plot showing the Pearson correlation of log2-fold changes of genes from RNA sequencing (y-axis) and corresponding proteins from mass spectrometry (x-axis) upon serum starvation with indicated correlation coefficient (R). Colours indicate upregulation (red) or downregulation (yellow) while shapes indicate significantly regulated proteins (points), genes (triangles), or both (squares);
e) Mean fold gene expression changes of differentially regulated surface receptors, determined by RT-qPCR; error bars indicate *SD*, n = 3.

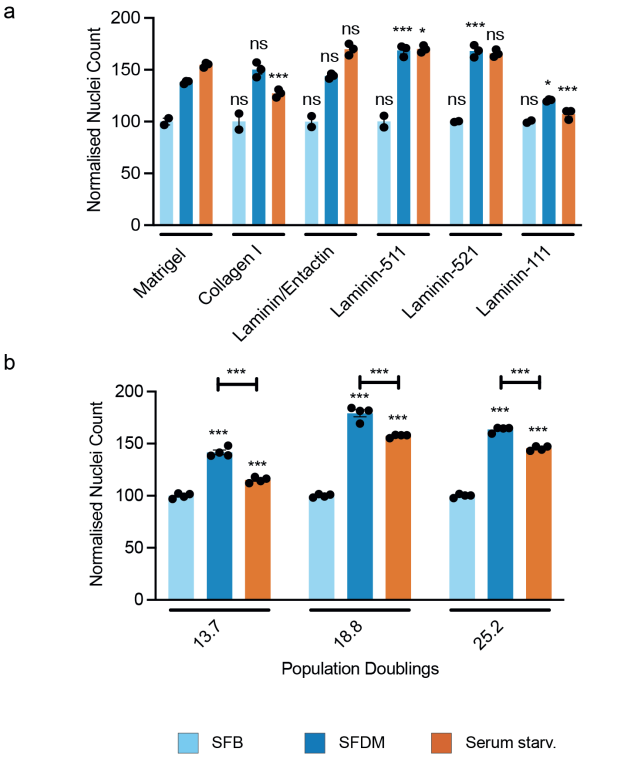
a
Normalised Nuclei Count
200
150
100
50
0
ns
***
*
Matrigel
Collagen I
Laminin/Entactin
Laminin-511
Laminin-521
Laminin-111
b
Normalised Nuclei Count
13.7
18.8
25.2
Population Doublings
SFB
SFDM
Serum starv.

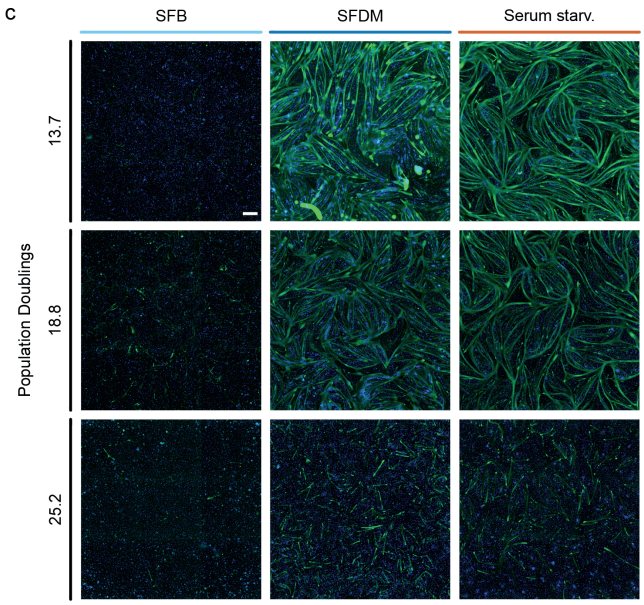
c
SFB
SFDM
Serum starv.
Population Doublings
13.7
18.8
25.2

► Supplementary Figure 3: Serum-free differentiation and serum starvation are similar with respect to cell age and coating (related to Fig. 4).
a) Normalised nuclei counts of SCs differentiating on indicated coatings after 72 h in SFB, SFDM and serum starvation as percentage against SFB; statistical significance is indicated for each media against respective Matrigel control, error bars indicate *SD*, n = 3;
b) Normalised nuclei counts of SCs after 72 h of SFB, SFDM or serum starvation at early (left), medium (centre), and late (right) passages with indicated PDs, as percentage of low PDs in SFB; asterisks directly above bars indicate statistical significance against SFB; error bars indicate *SD*, n = 4; c) Representative fluorescence images of differentiating SCs at early (top), medium (middle) or late (bottom row) passages after 72 h in SFB (left), SFDM (centre) or serum starvation (right), corresponding to Fig. 4e, Fig. S3b; green = desmin, blue = Hoechst, scale bar = 500 µm; p-values: * < 0.05, ** < 0.005, *** < 0.001.

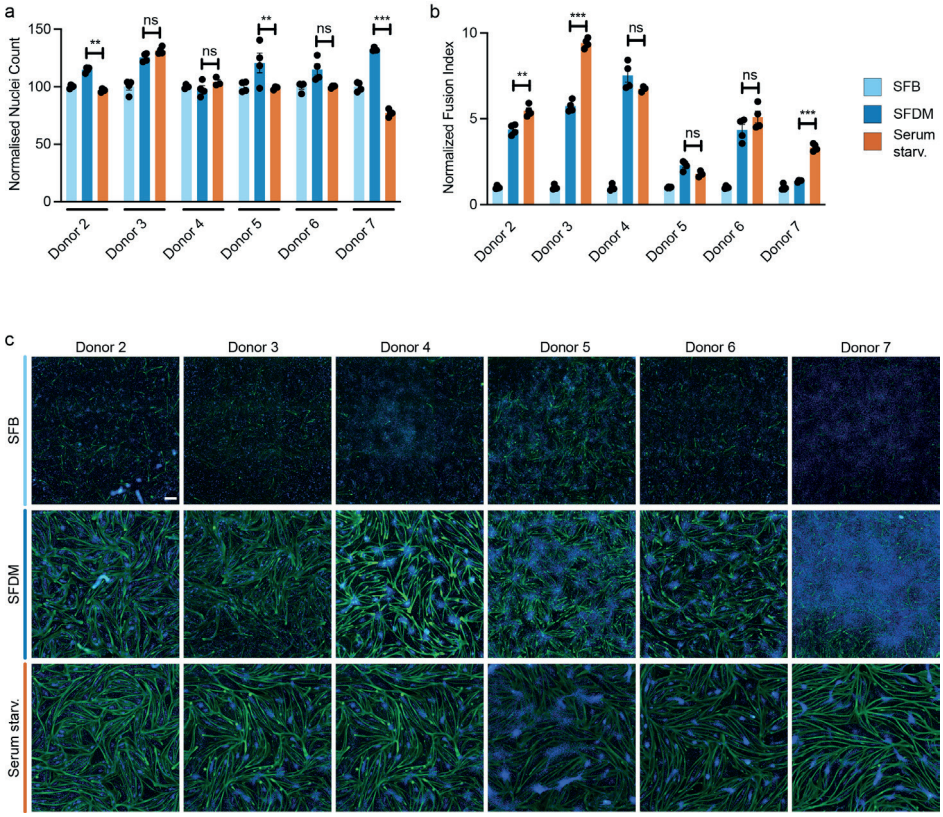

Supplementary Figure 4: Extent of serum-free differentiation varies between donor animals (related to Fig. 4).
a) Normalised nuclei counts of SCs from different donor animals after 72 h of myogenic differentiation as percentage of SFB with statistical significance indicated between SFDM and serum starvation respectively for each donor; error bars indicate *SD*, n = 4; b) Mean fusion indices of SCs from different donor animals after 72 h of serum-free or serum starvation induced differentiation, normalised against respective SFB condition. Statistical significance is indicated between SFDM and serum starvation respectively for each donor; error bars indicate *SD*, n = 4; c) Representative fluorescence images of myogenic differentiation of SCs from different donor animals after 72 h in SFB (top), SFDM (middle) and serum starvation (bottom row); green = desmin, blue = Hoechst, scale bar = 500 µm; p-values: * < 0.05, ** < 0.005, *** < 0.001.

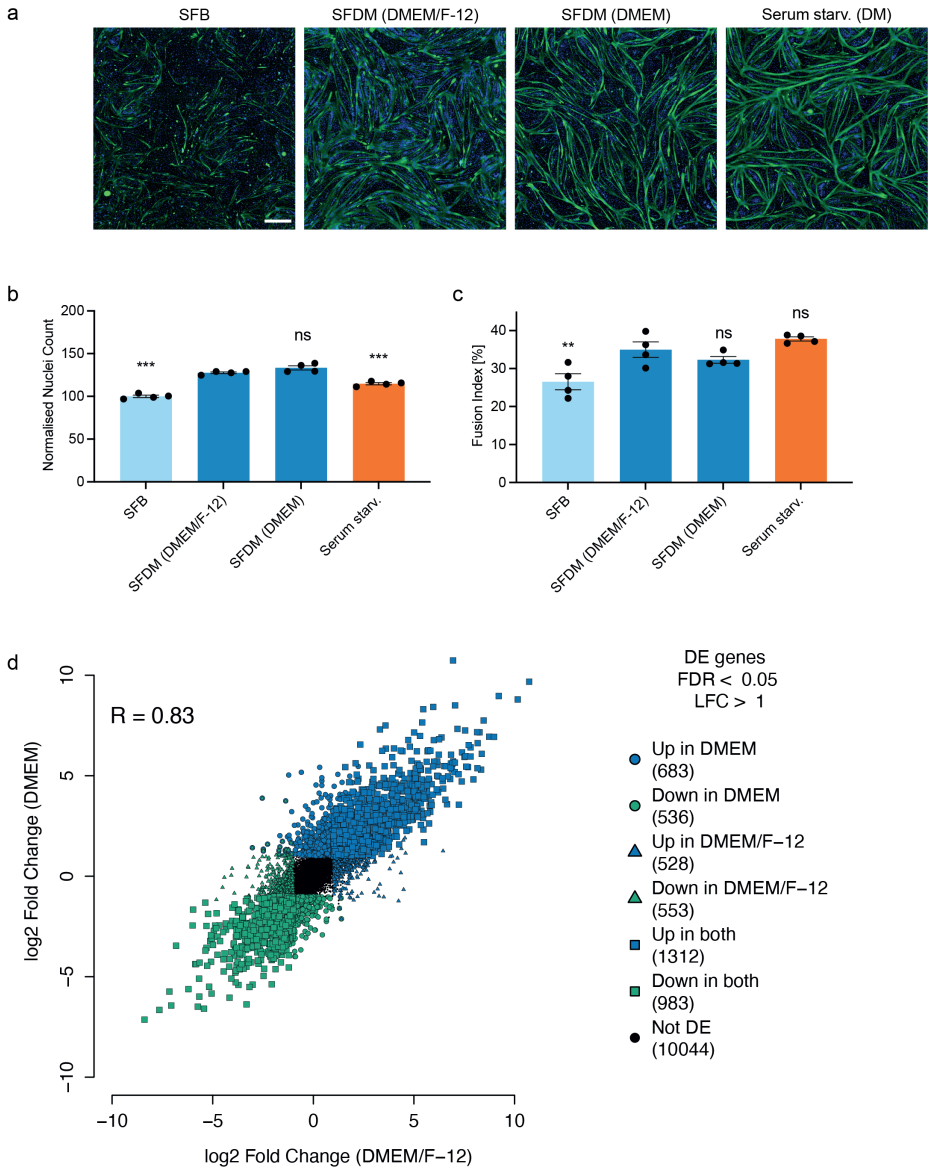

Supplementary Figure 5: 2D serum-free differentiation can be achieved with different basal media (related to Fig. 6).
a) Representative fluorescence images of SCs after 72 h in SFB, SFDM with DMEM/F-12 and DMEM base, and upon serum starvation; green = desmin, blue = Hoechst, scale bar = 500 µM; b) Normalised nuclei counts from a) as percentage of SFB with statistical significance indicated against SFDM (DMEM/F-12); error bars indicate *SD*, n = 4; c) Mean fusion indices derived from a) with statistical significance performed against SFDM (DMEM/F-12); error bars indicate *SD*, n = 4; d) Scatter plot indicating correlation of log2-fold changes between SFGM and DMEM/F-12-based SFDM (x-axis) against log2-fold changes between SFGM and DMEM-based SFDM (y-axis) with Pearson correlation coefficient indicated; p-values: * < 0.05, ** < 0.005, *** < 0.001.

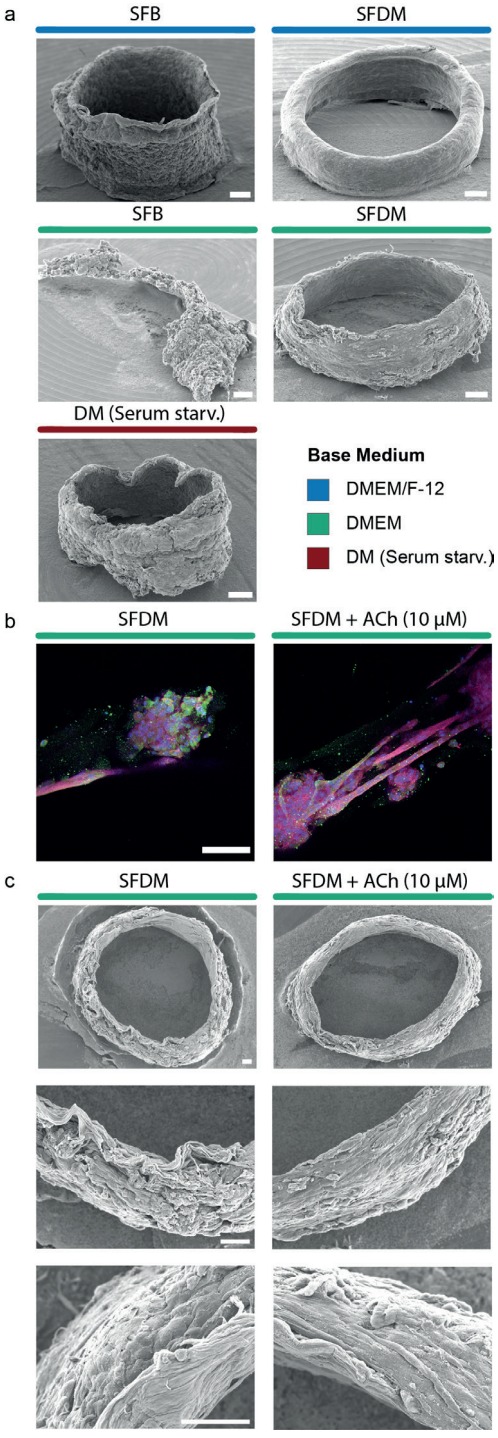
a
SFB
SFDM
SFB
SFDM
DM (Serum starv.)
Base Medium
DMEM/F-12
DMEM
DM (Serum starv.)
b
SFDM
SFDM + ACh (10 µM)
c
SFDM
SFDM + ACh (10 µM)

► Supplementary Figure 6: Acetylcholine supplementation improves myogenic fusion in bioartificial muscles (related to Fig. 6).
a) Ultrastructure of BAMs after 192 h in SFB or SFDM (with DMEM/F-12 or DMEM basal media) or serum starvation; scale bar = 100 µm; b) Representative fluorescence images of BAMs after 192 h in DMEM-based SFDM without (left) and with (right) 10 µM acetylcholine (ACh); pink = desmin, red = α-actin, green = myosinHC, blue = Hoechst; scale bars = 100 µm; c) Ultrastructure (top), wide (middle) and close-up (bottom) scanning electron microscopy images of BAMs after 192 h in DMEM-based SFDM with (right) and without (left) 10 µM acetylcholine; scale bars = 100 µm.

Supplementary Table 1: Media formulations.

#	Component	Reference	Concentration
Growth medium (GM)			
1	Ham's F-10 Nutrient Mix +	31550-023, Gibco	
2	Fetal Bovine Serum, heat inactivated (FBS)	10500064, Gibco	20%
3	FGF-2	100-18B, Peprotech	5 ng ml^{-1}
4	Penicillin/Streptomycin/Amphotericin (PSA)	17-745E, Lonza	5.0 mg ml^{-1}
Differentiation medium (DM)			
1	DMEM	22320-022, Gibco	
2	FBS	10500064, Gibco	2%
3	Penicillin/Streptomycin/ Amphotericin (PSA)	17-745E, Lonza	1%
Serum-free growth medium (SFGM)			
1	DMEM/F-12	21331-020, Gibco	
2	α-linolenic acid	L2376, Sigma Aldrich	1.0 µg ml^{-1}
3	FGF-2	100-18B, Peprotech	10 ng ml^{-1}
4	Human Serum Albumin	Rc HA NW20, Richcore Lifesciences	5.0 mg ml^{-1}
5	HGF	100-39H, Peprotech	50 ng ml^{-1}
6	Hydrocortisone	H0135, Sigma Aldrich	36 ng ml^{-1}
7	ITSE	00-101, biogems	1%
8	GlutaMax	35050-061, Gibco	1%
9	Glucose	G7021, Sigma Aldrich	17.7 mM
10	L-ascorbic acid 2-phosphate (Vitamin C)	A8960, Sigma Aldrich	155 µM
11	PSA	17-745E, Lonza	1%
12	Triiodothyronine	T6397, Sigma Aldrich	30 nM
Serum-free base medium (SFB)			
1	DMEM/F-12 (or DMEM, where indicated) +	21311-020, Gibco	
2	EGF-1	AF-100-15, Peprotech	10 ng ml^{-1}
3	Human Serum Albumin	Rc HA NW20, Richcore Lifesciences	0.5 mg ml^{-1}
4	L-ascorbic acid 2-phosphate (Vitamin C)	A8960, Sigma Aldrich	40 µM
5	MEM Amino Acids Solution	11130-051, ThermoFisher	0.50%
6	$NaHCO_3$	P2256, Sigma Aldrich	6.5 mM
7	Selenium	5261, Sigma Aldrich	80 nM
8	PSA	17-745E, Lonza	1%
Serum-free differentiation medium (SFDM)			
1	SFB +		
2	Insulin	10-365, biogems	1.8 µM
3	Lysophosphatidic acid (LPA)	L7260, Sigma Aldrich	1 µM
4	Transferrin	10-366, biogems	135 nM
5	ACh (for BAM fabrication after 96 h)	S1805, Selleck Chem	10 µM

Supplementary Table 2: RT-qPCR primers.

Gene		*Primer Sequence*
B2M	*Fwd:*	*5'-TGGAGGTGCTGGCATCTTAG*
	Rev:	*5'-ATGCAGAAGACACCCAGATGTT*
CAV3	*Fwd:*	*5'-GATCGATCTGGTGAACCGGG*
	Rev:	*5'-TGTAGCTCACCTTCCACACG*
CHRNA1	*Fwd:*	*5'-ACTTCATGGAGAGCGGAGAA*
	Rev:	*5'-AACACTAGGCCGGTCAAGAA*
DES	*Fwd:*	*5'-GGAAGCCGAGGAATGGTACA*
	Rev:	*5'-TCGATCTCGCAGGTGTAGGA*
GCGR	*Fwd:*	*5'-CGGAGGCTAGAGTGTGGAAG*
	Rev:	*5'-GAATGTGGACACGCTGACAC*
IGF1R	*Fwd:*	*5'-CCTCCACATCCTGCTCATTT*
	Rev:	*5'-GATGACCAGGGCGTAGTTGT*
LPAR1	*Fwd:*	*5'-CCGCAGTGCTTCTACAATGA*
	Rev:	*5'-GCCAGATTCGCCATAAGGTA*
MYOD1	*Fwd:*	*5'-CGACGGCATGATGGACTACA*
	Rev:	*5'-GTAAGTGCGGTCGTAGCAGT*
MYF5	*Fwd:*	*5'-TCTATCTCTCTGCTGTCCAGGC*
	Rev:	*5'-AACTCGTCCCCGAACTCAC*
MYF6	*Fwd:*	*5'-GCGAGAGGCGGCGGCTCAAGAAAATCAACG*
	Rev:	*5'-TGGAATGATCCGAAACACTTGGCCACTG*
NCAM1	*Fwd:*	*5'-CCGAGAAGGGTCCCGTAGA*
	Rev:	*5'-ATTTGTGTGGCATCGTTGGG*
OXTR	*Fwd:*	*5'-TCCACGCTGTGACTGATAGG*
	Rev:	*5'-GCTTGGTTTGATGGTGGAGT*
PAX7	*Fwd:*	*5'-CTCCCTCTGAAGCGTAAGCA*
	Rev:	*5'-GGGTAGTGGGTCCTCTCGAA*
RPL19	*Fwd:*	*5'-TCGAATGCCCGAGAAGGTAAC*
	Rev:	*5'-CTGTGATACATGTGGCGGTC*
TFRC	*Fwd:*	*5'-GGCTCTGGCTCTCACACTCT*
	Rev:	*5'-TTCGTTGTCAATGTCCCAAA*
TNNT1	*Fwd:*	*5'-CCTCTGATCCCGCCAAAGAT*
	Rev:	*5'-GGTCCTTTTCCATGCGCTTC*
TPM1	*Fwd:*	*5'-GAGTTGAAAACTGTGACGAACAAC*
	Rev:	*5'-ACCTCTCCGCAAACTCAGC*

Chapter 3

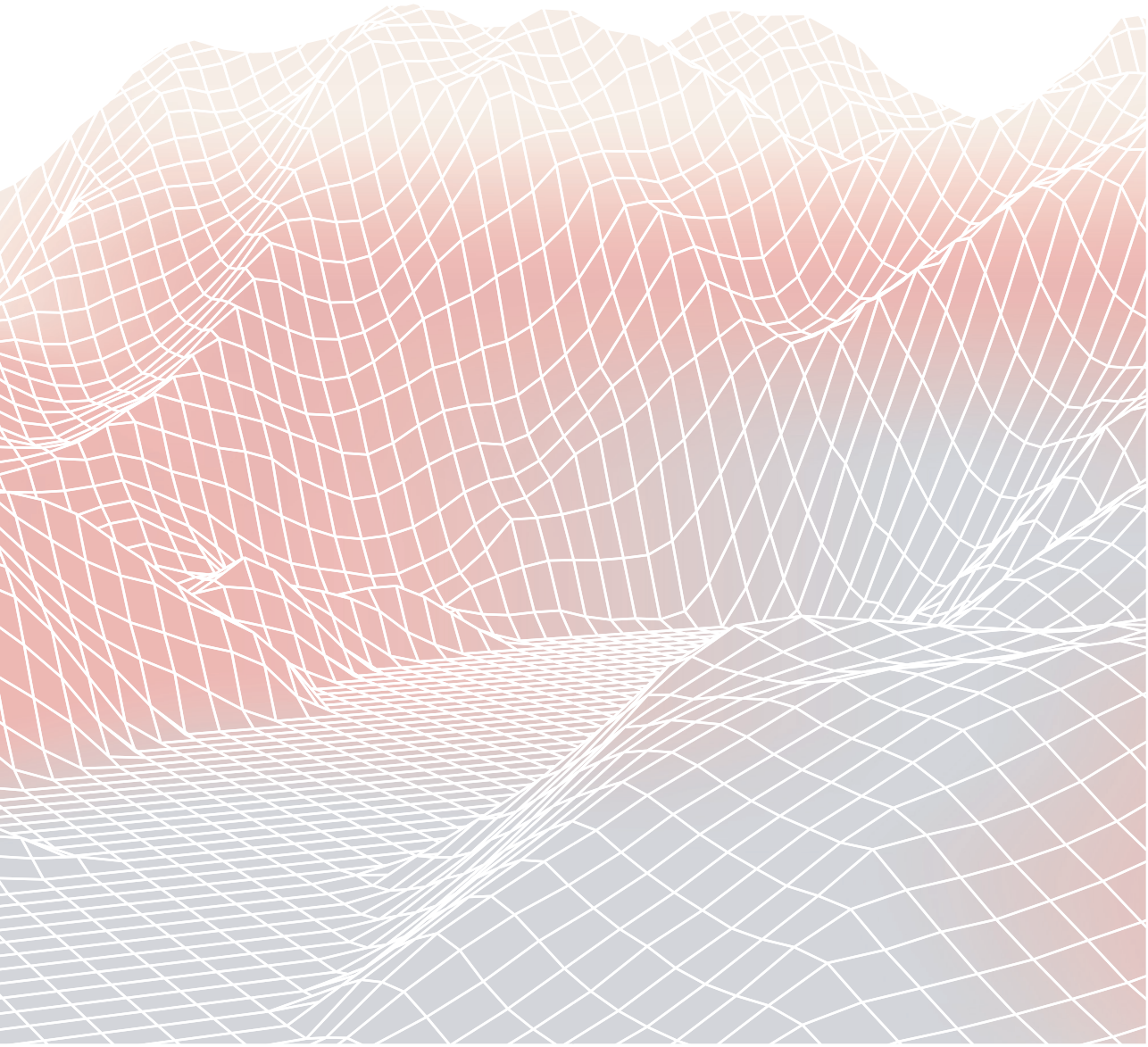

SINGLE-CELL ANALYSIS OF BOVINE MUSCLE-DERIVED CELL TYPES FOR CULTURED MEAT PRODUCTION

Tobias Meßmer
Richard GJ Dohmen
Lieke Schaeken
Lea Melzener
Rui Hüber
Mary Godec
Mark J Post
Joshua Flack

Submitted for publication

3.1 ABSTRACT

'Cultured' meat technologies leverage the proliferation and differentiation of animal-derived stem cells ex vivo to produce edible tissues for human consumption in a sustainable fashion. However, skeletal muscle is a dynamic and highly complex tissue, involving the interplay of numerous mono- and multinucleated cells, including muscle fibres, satellite cells (SCs) and fibro-adipogenic progenitors (FAPs), and recreation of the tissue in vitro thus requires the characterisation and manipulation of a broad range of cell types. Here, we use a single-cell RNA sequencing approach to characterise cellular heterogeneity within bovine muscle and muscle-derived cell cultures over time. Using this data, we identify numerous distinct cell type, and develop robust protocols for the easy purification and proliferation of several of these populations. We note overgrowth of undesirable cell types within heterogeneous proliferative cultures as a barrier to efficient cultured meat production, and use transcriptomics to identify conditions that favour the growth of SCs in the context of serum-free medium. Combining RNA velocities computed in silico with time-resolved flow cytometric analysis, we characterise dynamic subpopulations and transitions between active, quiescent, and committed states of SCs, and demonstrate methods for modulation of these states during long-term proliferative cultures. This work provides an important reference for advancing our knowledge of bovine skeletal muscle biology, and its application in the development of cultured meat technologies.

3.2 INTRODUCTION

'Cultured' or 'cultivated' meat is an emergent technology that leverages in vitro proliferation and differentiation of stem cells to produce edible tissues that mimic conventional meat.[1,2] Whilst there are numerous potential advantages to this technology, including reduced greenhouse gas emissions and improved animal welfare,[3] many technical challenges remain, such as the removal of animal-derived components, scaling of culture volumes, and cost reduction.[4,5] Moreover, consumer acceptance will be reliant on the taste and texture of cultured meat products closely replicating those of the conventionally-reared equivalent.[6,7]

Meat is composed primarily of skeletal muscle, a complex tissue whose function requires the interplay of numerous mono- and multinucleated cell types, including muscle fibres, satellite cells (SCs) and fibro-adipogenic progenitors (FAPs), as well as vascular, nervous and connective tissue.[8,9] Whilst most cultured meat products currently being pursued consist of unstructured muscle fibres, with or without fat tissue, accurate recreation of the entire tissue requires the identification, purification, proliferation and characterisation of a broad range of cell types.[10,11] Descriptions of the composition of human and murine skeletal muscle at the cellular level are now available,[12–16] but a similarly detailed understanding of muscle biology in agriculturally relevant species, such as cattle, is currently lacking. Furthermore, the extent to which complex muscle-derived cell behaviours and interactions are recapitulated during in vitro culture is unclear, limiting the progress of cultured meat development.[17,18]

Here, we used droplet-based single-cell RNA sequencing (scRNA-seq) to profile bovine skeletal muscle, and muscle-derived cell cultures, in a time-resolved fashion across the process of cultured meat production. We use the resultant dataset to gain insight into transcriptional heterogeneity between and within cell types, and to inform various steps of cultured meat bioprocess design.

3.3 RESULTS

3.3.1 scRNA-seq identifies 11 distinct cell types in bovine muscle

In order to investigate heterogeneity between and within bovine muscle-derived cell types, we used the 10x Chromium platform for scRNA-seq to study gene expression at five timepoints in a primary adult stem cell-based cultured meat production process (Fig. 1a, Supplementary Table 1). A total of 36129 single-cell transcriptomes, with an average expression of 3815 genes and 21131 transcripts per cell, were analysed across 10 donor cattle and assembled into a single dataset (Supplementary Fig. 1). Using UMAP dimensionality reduction, based on the first 30 principal components (Fig. 1b), cells from Timepoints 1 (muscle tissue) and 2 (passage 0, after 72 h in vitro culture) clustered separately from each other, and from Timepoints 3 to 5 (after passages 2, 5 and 8 respectively), indicating significant transcriptomic changes between timepoints and within cell types during the proliferative process.

Within enzymatically digested bovine muscle tissue (Timepoint 1), we identified 11 defined populations of mononuclear cells with distinct gene expression profiles (Fig. 1c), which were present in varying proportions in all donor animals (Supplementary Fig. 2a). Based on differential gene expression, these clusters were assigned to cell types previously characterised in other species,[12,13,19] namely fibro-adipogenic progenitors (FAPs), satellite cells (SCs), vascular and lymphatic endothelial cells (ECs; vascular, VECs; lymphatic, LECs, Supplementary Fig. 2b), smooth muscle and mesenchymal cells (SMMCs), monocytes/macrophages (MΦ), neutrophils, lymphocytes (B/T/NK cells), glial cells, tenocytes and myocytes (Fig. 1d, Supplemental Fig. 2d). The expression of canonical genes in each of these populations in analogous studies indicated their conservation between mouse and cattle (Fig. 1e, Supplemental Fig. 2e).[14]

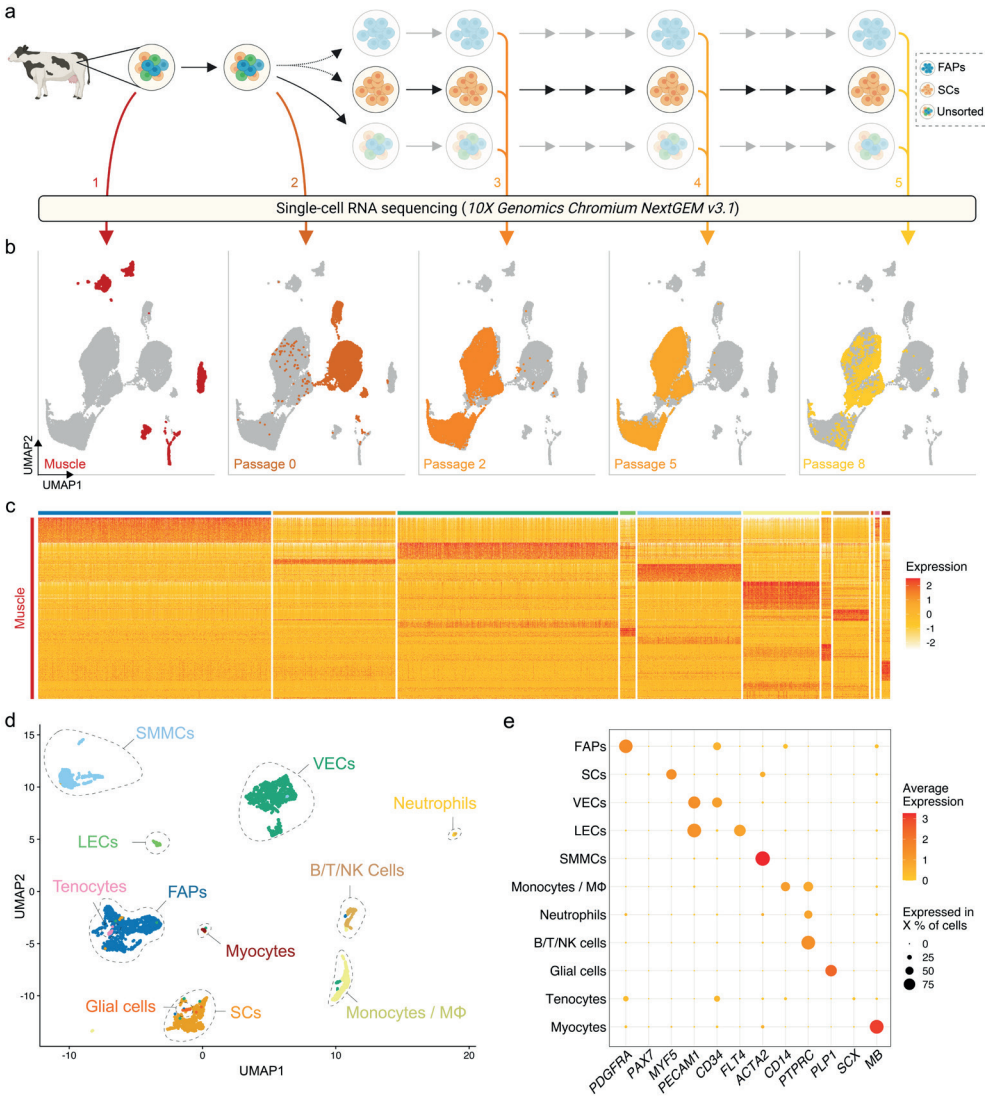

Figure 1: Single-cell RNA sequencing of bovine muscle and muscle-derived cell cultures. a) Overview of experimental design; coloured arrows and numerals indicate timepoints of RNA sequencing of single cells isolated from bovine muscle (Timepoint 1), at passage 0 after 72 h in serum-free growth medium (2) and at passages 2, 5 and 8 (3, 4 and 5 respectively); solid arrows indicate passaging, dotted arrows indicate FACS sorting; b) Combined UMAP plots showing single cells (individual points) from all five experimental timepoints; clustering is based on first 30 principal components, cells from each timepoint are coloured in each respective plot; c) Heatmap displaying normalised expression of significantly upregulated genes in each cluster identified in Timepoint 1. d) UMAP of Timepoint 1; cells are coloured and clusters labelled for their assigned cell types; e) Dotplot showing normalised expression of cell-type specific genes, averaged within each population; dot size indicates percentage of cells expressing the respective gene with at least 1 count.

3.3.2 Cell types can be identified in vitro by unique surface marker expression

In order to identify proliferative muscle tissue-derived cell types that might be used for cultured meat production, we analysed the adherent cell fraction after 72 h (Timepoint 2) culture in serum-free growth medium (SFGM, Supplementary Table 2). We discerned 7 populations present in these cultures, which were separated from the same populations in Timepoint 1 by UMAP, indicating stark transcriptional changes during the transition to in vitro culture (Fig. 2a). GO terms corresponding to differentially expressed genes (independent of cell type) between Timepoints 1 and 2 (Fig. 2b) suggest that these transcriptional switches relate to decreased interaction with the extracellular matrix (ECM) and increased protein production, concomitant with increased cellular proliferation in the in vitro environment.

Comparison of Timepoints 1 and 2 enabled the assigning of cell identities to individual clusters (Fig. 2c), indicating that of the 11 populations identified in Timepoint 1, only myocytes, tenocytes, neutrophils and lymphocytes did not persist in short-term serum-free culture. Conversely, FAPs, SCs, SMMCs, ECs, glial cells and monocytes/macrophages remained present in cultures from all genotypes (donor animals) sequenced (Supplementary Figs. 3a, b). These same cell types were identified when culturing cells in growth medium (GM) containing 20% foetal bovine serum (FBS; Supplementary Fig. 3c, Supplementary Table 2), indicating that our SFGM formulation was able to support culture of muscle-derived cells as robustly as traditional serum-containing media.

Analysis of differentially expressed genes yielded highly and exclusively expressed markers for each population (Fig. 2d)[10,20] that have previously been described in mouse and human.[12–14,21] Filtering these lists for genes encoding plasma membrane-localised proteins facilitated the identification of candidate cell surface markers for separation of populations by flow cytometry (Fig. 2e). Staining of muscle tissue-derived cells 72 h post-isolation for JAM-1 (*F11R*), CD45 (*PTPRC*), ITGA7 and ITGA5 confirmed the suitability of this quartet of markers as a FACS panel (Fig. 2f, Supplementary Fig. 3d).

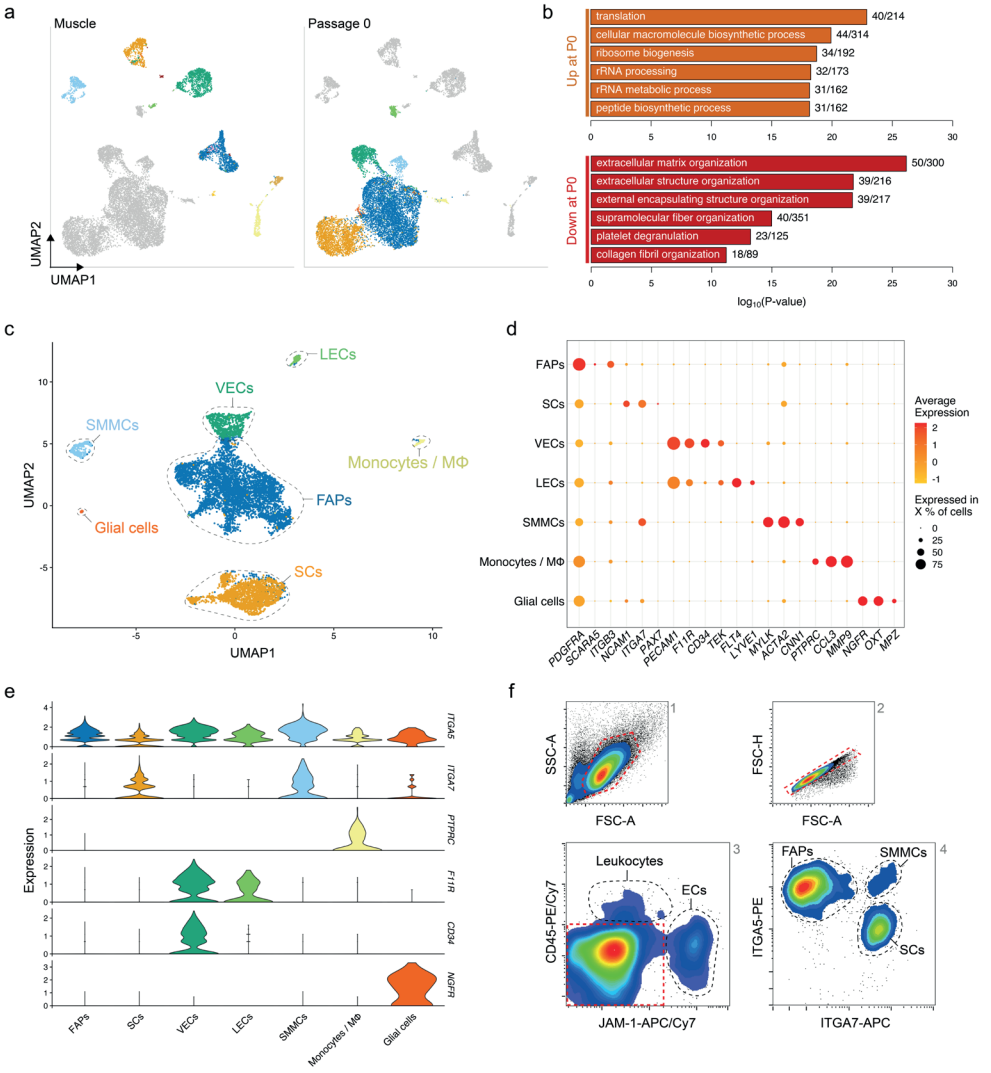

Figure 2: Transcriptomic analysis defines adherent cell types with distinct immunosurface phenotypes.
a) Combined UMAP of Timepoints 1 and 2, coloured for populations in Timepoint 1 (left) or 2 (right), respectively; b) Top five most significantly enriched GO terms corresponding to differentially expressed genes up- (top) or downregulated (bottom) between Timepoints 1 and 2, after regressing out the effect of cell type; c) UMAP of Timepoint 2; cells are coloured and clusters labelled for their assigned cell types; d) Normalised gene expression of canonical markers in each population at Timepoint 2; e) Violin plots showing expression of surface markers in different cell types at Timepoint 2; f) Representative flow cytometry contour plots showing gating strategy for purification of cell types; red dashed lines indicate gates for the subsequent plot (from 1 to 4); black dashed lines indicate sorting gates for the labelled populations.

3.3.3 Four principal muscle-derived cell types can be proliferated in vitro

In order to characterise their in vitro phenotypes in more detail, we sorted muscle-derived cells into FAPs, SCs, ECs and SMMCs using the FACS panel previously described (Fig. 2). The purified populations exhibited markedly different morphologies; whilst FAPs had a spindle-like morphology and SCs were more spherical, ECs and SMMCs appeared flatter and larger (Fig. 3a). Flow cytometric analysis post-FACS using the same antibody panel confirmed high sorting purities for all populations (Fig. 3b). In addition, immunofluorescent staining for canonical markers PDGFRα, Pax7, TEK (also known as Tie2), and Calponin-1 (CNN1) further verified the identity of FAPs, SCs, ECs, and SMMCs respectively (Fig. 3c).

Long-term proliferation of each of these populations was supported in SFGM (FAPs, SCs) or BioAMF-3 medium (ECs, SMMCs), with each culture undergoing at least 15 population doublings (PDs) over a period of at least 6 passages (Fig. 3d). Proliferation rates varied between cell types (for example, from 0.46 (ECs) to 1.0 PDs/day (SMMCs) at early passage), and tended to decrease over time (Fig. 3e).

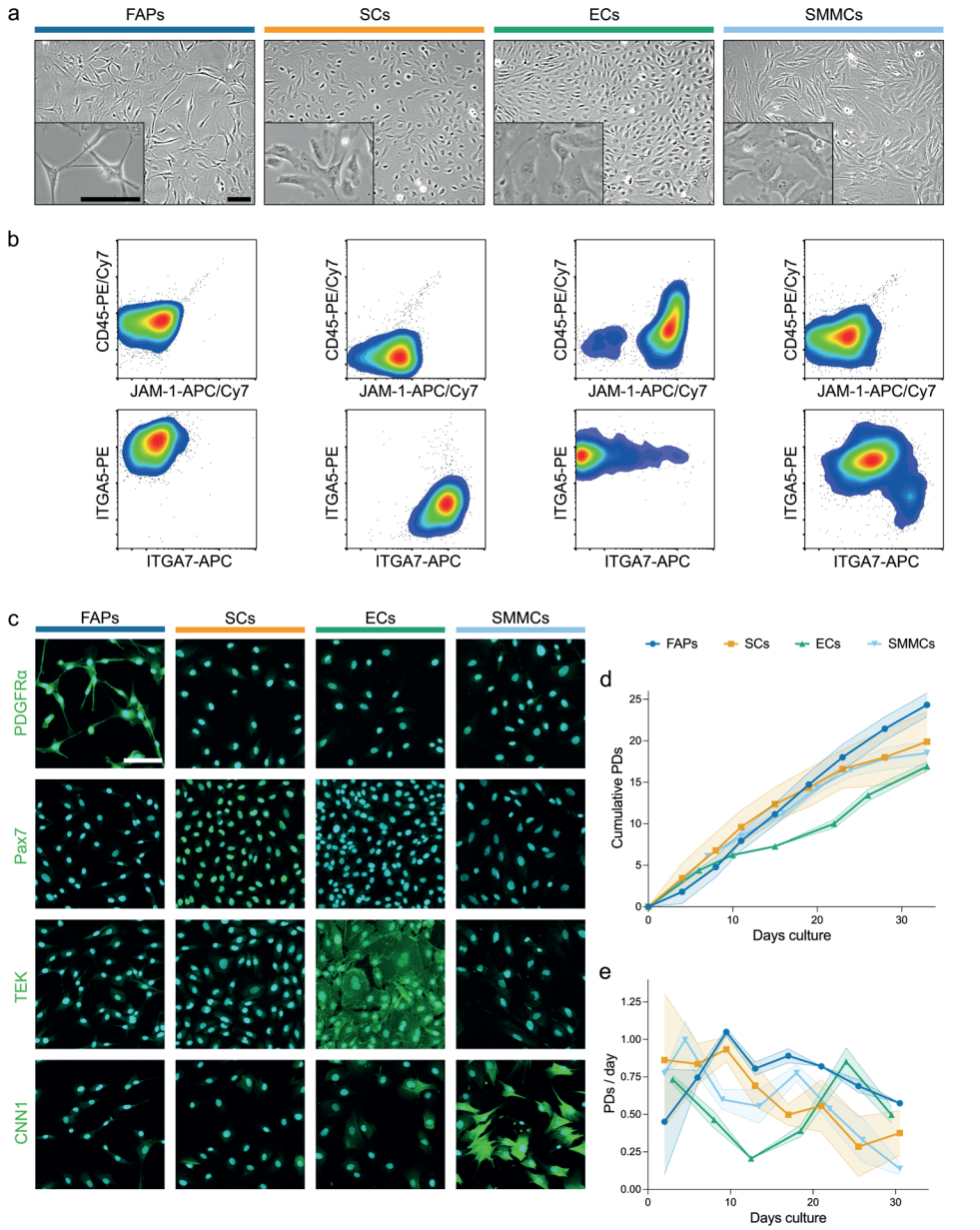

Figure 3: Four muscle-derived cell types can be purified and expanded in long-term culture. a) Brightfield microscopy images of purified FAPs (blue), SCs (orange), ECs (green) and SMMCs (light blue) in vitro; scale bars = 100 µm; b) Flow cytometry plots of purified cell types stained for CD45/JAM-1 (top) and ITGA5/ITGA7 (bottom); c) Immunofluorescent staining for PDGFRα, Pax7, TEK and CNN1 (green) in purified cell types; nuclei stained with Hoechst (cyan); scale bar = 100 µm; d) Long-term growth curves of purified cell types in vitro, shown as cumulative population doublings (PDs); shaded areas indicate standard deviation (*SD*), n = 3; e) Growth rates for long-term growth experiments shown in d), shown as PDs per day, n = 3.

3.3.4 Optimised culture conditions prevent SC overgrowth by FAPs

We next aimed to understand heterogeneity within FACS-purified SC cultures during long-term proliferation. Surprisingly, we found that cells in these cultures clustered into two distinct populations, marked by differential expression of *ITGA7* (Fig. 4a). *ITGA7*- cells expressed FAP marker genes such as *ITGA5* (Supplemental Fig. 4a, Fig. 2), suggesting that these cells were FAPs that were inaccurately sorted into, and remained prevalent within, SC cultures. Quantification of these cell types showed that the proportion of FAPs increased over time, indicating that our standard culture conditions favoured long-term proliferation of FAPs over SCs (Fig. 4b, Supplemental Fig. 4b). The percentage of contaminating FAPs correlated negatively with myogenic differentiation, as determined by fusion index (Figs. 4c, d), emphasising the importance of eliminating overgrowth by non-SCs for cultured muscle production.

We therefore sought to adapt the long-term culture conditions, with the aim of preventing FAPs from overgrowing SCs. To inform our approach, we filtered the scRNA-seq data for differentially expressed genes between SCs and FAPs encoding receptors that interact with proteins commonly used as surface coatings or growth factors, revealing a number of interesting candidates (Fig. 4e, f). Sorting SCs using an ITGA7+/ITGA5- strategy significantly decreased FAP contamination as compared to a CD29+/NCAM1+ sorting strategy (used in previous studies[22]), reducing FAP overgrowth after multiple passages (Figs. 4g, h). Culturing SCs contaminated with FAPs on different coatings, we observed that within 3 passages, SC purity was reduced on collagen I and fibronectin (FN; interacting with ITGA5) but remained high on laminin-521 (LN-521; interacting with ITGA7; Fig. 4i). We further adapted SFGM by adding triiodothyronine (T3, 30 nM, ligand for THRA), increasing the concentration of HGF (ligand for c-Met) and removing PDGF-BB (ligand for PDGFRα; Fig. 4j). Each individual adaptation reduced FAP overgrowth over 3 passages, whilst the combination of all three showed no significant reduction in SC proportion over the course of the experiment, and was thus labelled ‘improved SFGM’ (i-SFGM).

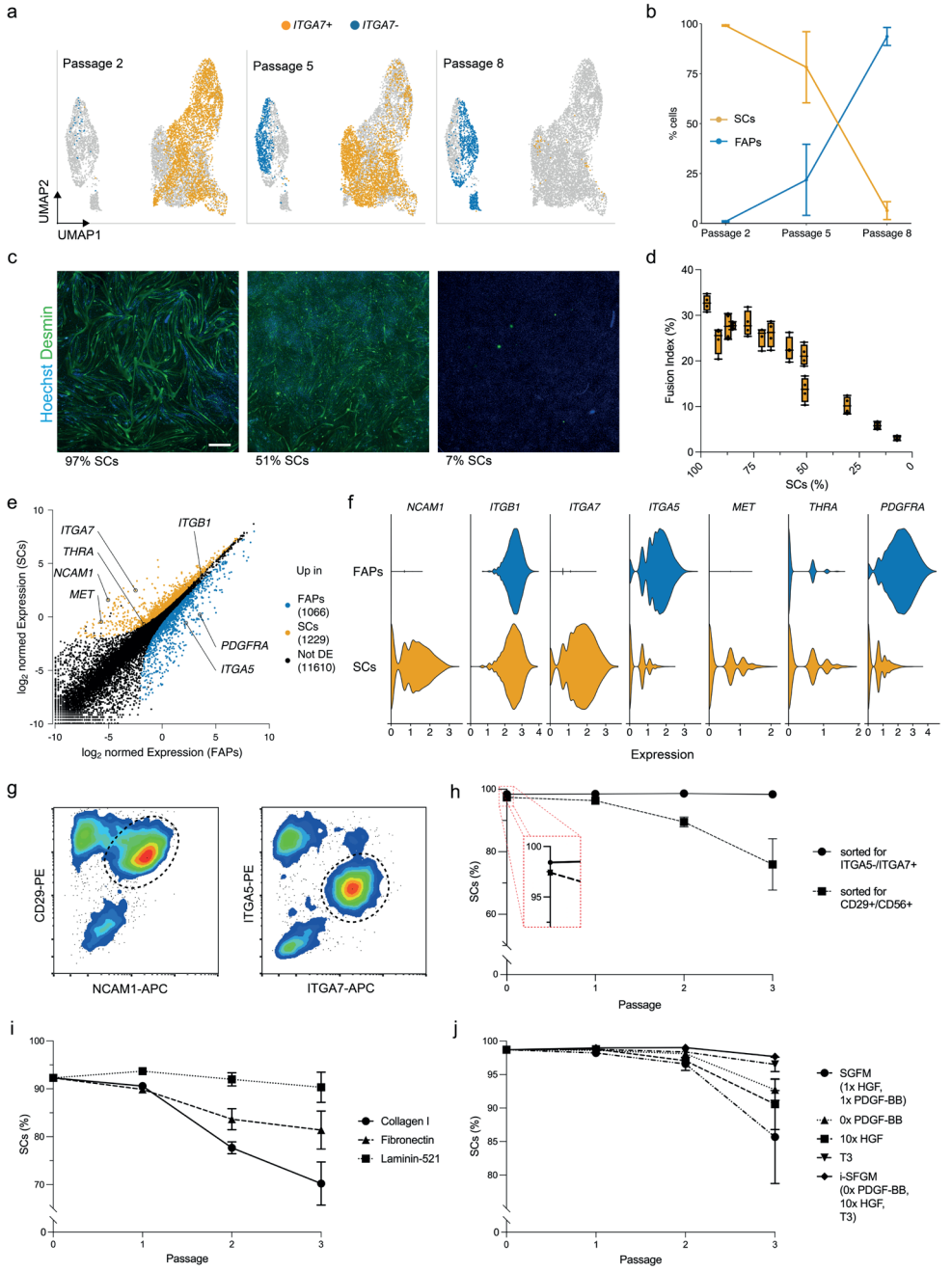

Figure 4: Optimised culture conditions prevent overgrowth of SCs.
a) Combined UMAPs of sorted SCs at passages 2 (Timepoint 3, left), 5 (Timepoint 4, centre) and 8 (Timepoint 5, right); clusters in respective passages are coloured for *ITGA7* expression; b) Proportion of SCs (*ITGA7*+) during long-term culture; error bars indicate *SD*, n = 3; c)

Immunofluorescent staining of cultures with varying proportions of SCs for desmin (green) and Hoechst (blue) after 72 h in serum-free myogenic differentiation media; scale bar = 100 µm; d) Fusion indices (nuclei within desmin-stained areas as a proportion of total nuclei) corresponding to c), shown as box plots, n = 4; e) Normalised gene expression in SCs and FAPs at passage 2 (Timepoint 3). Points represent genes, which are coloured if significantly (FDR < 0.05, log-FC > 1) upregulated in FAPs (blue) or SCs (orange). Selected genes are annotated. f) Violin plots showing expression of differentially expressed receptors in SCs and FAPs at passage 2; g) Flow cytometry plots of muscle-derived cells after 72 h in SFGM stained for ITGA5/ITGA7 (left) or CD29/NCAM1 (right) prior to FACS; cells are shown after removal of doublets, CD45+ and JAM-1+ cells; dashed lines indicated gating strategy for sorting; h) Proportion of SCs purified with FACS protocols shown in g) during long-term culture, as measured by flow cytometry; error bars indicate *SD*, n = 3; i) Proportion of SCs during long-term culture on different coatings as indicated, n = 3; j) As (i), but for different media formulations as indicated, n = 3.

3.3.5 SCs transition between three dynamic states

To further investigate SC heterogeneity in vitro, we filtered out FAPs and reanalysed the remaining single-cell transcriptomes at passage 2 (Timepoint 3). Reclustering identified three subpopulations within SCs, with distinct gene expression profiles suggestive of quiescent, activated, and committed states (similar to those previously observed in murine SCs[14]; Figs. 5a, b). Genes encoding proteins related to focal adhesion and ECM organisation were upregulated in the quiescent state, cell cycle and replication in the activated state, and myogenic differentiation the committed state (Fig. 5c, Supplementary Fig. 5a). These cell states were also observed at passages 5 and 8, but in different ratios (Supplementary Figs. 5b, c), suggesting the possibility of transitioning between states.

We next established protocols to measure these states in vitro, through analysis of CD151 (upregulated in quiescent SCs[14]) and desmin (upregulated in committed SCs) via flow cytometry (Fig. 5d, Supplementary Fig. 5d). Combining this panel with EdU-staining, we confirmed increased cell cycle activity in activated as compared to quiescent SCs (Fig. 5e; Supplementary Fig. 5e). Investigating the dynamics of these subpopulations during a single passage, we found dynamic conversion between quiescent (CD151+) and activated (CD151-) states, with an initial increase in quiescent SCs followed by a rapid decline and a renewed increase as cells approach confluence (Fig. 5f). The proportion of cells in the committed state remained stable throughout the first 72 h, increasing after 96 h. Investigating over multiple passages revealed that this interchangeability decreased over time (Supplementary Fig. 5f). We observed that i-SFGM increased the proportion of activated SCs compared to SFGM, both within a single passage (Fig. 5f) and over the course of multiple passages (Supplementary Fig. 5f). In addition to transitions between cell states changing over the course of cell ageing, transcriptional changes related to increased ECM remodelling and decreased translation were also observed *within* states over time (Supplementary Fig. 6).

Finally, we performed RNA velocity analysis of SCs at passage 2, in order to investigate these cell state transitions in silico. RNA velocity averaged across all genes indicated transitions from the activated to the quiescent state or committed states (Fig. 5g), whilst an increase in expression of cell cycle genes within a subset of quiescent cells suggested they are able to return to the activated state (Fig. 5h). Taken together with in vitro data, this suggests a dynamic, reversible transition between activated and quiescent states, whilst activated cells can also differentiate towards committed myocytes as SCs become confluent (Fig. 5i).

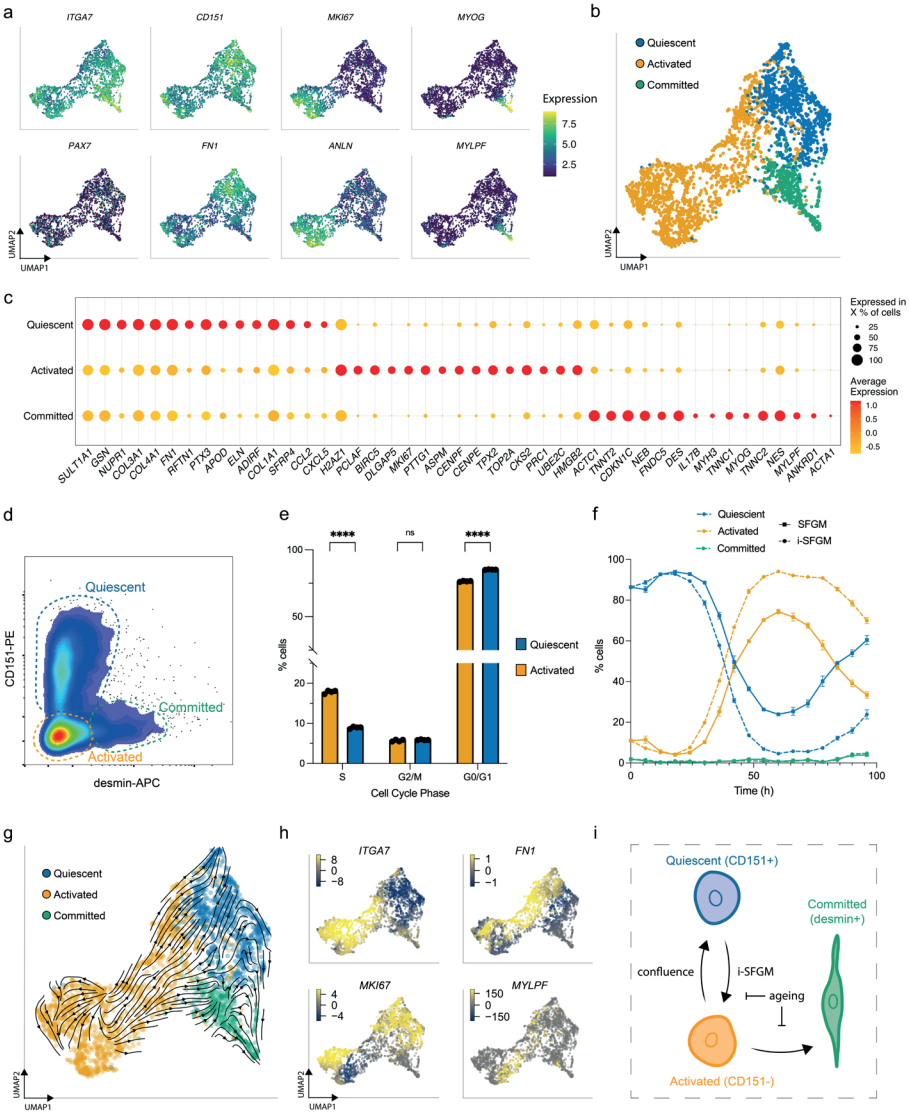

► **Figure 5: SCs switch dynamically between three cellular states in vitro.**
a) UMAPs of SCs at passage 2 (Timepoint 3), coloured by expression of indicated genes; b) UMAP as (a), but labelled according to SC state; c) Normalised expression of the 15 most upregulated genes, averaged within SCs in each state; d) Flow cytometry plot of purified SCs stained for CD151 and desmin; dashed gates indicate the respective cell states; e) Cell cycle analysis of CD151+ (blue) and CD151- cells (orange) determined via flow cytometry using the gating strategy in Supplementary Fig. 5e; f) Proportion of activated, quiescent and committed SCs over one passage in SFGM or i-SFGM media, as determined via flow cytometry; g) UMAP as (b), with averaged RNA velocity vectors embedded; h) UMAPs as (a), coloured by RNA velocities of denoted genes; i) Dynamic model of SC states in vitro; arrows indicate direction(s) of proposed transitions between states.

3.4 DISCUSSION

The complexity of muscle tissue arises from the interplay of multiple cell types.[8,9] Here, we have presented an annotated scRNA-seq dataset comprising over 36,000 muscle cellular transcriptomes, from 10 donor cattle, across five timepoints during a cultured beef production process. This dataset gives significant insight into the cellular heterogeneity present in bovine skeletal muscle for the first time, including comprehensive analysis of 11 defined cell types (Fig. 1). Our analysis showed notable similarity between bovine muscle and analogous approaches employed for more well-studied species, with expression of canonical genes for distinct cell types largely conserved between cattle, human and mouse. Comparison of bovine muscle with the corresponding cell cultures shed light on transcriptional changes that occur during the transition to in vitro culture. Notably, genes related to protein synthesis were strongly upregulated (suggesting cell activation), whilst those relating to ECM were downregulated, highlighting the pivotal role of cell-matrix interactions in the muscle niche. However, despite the absence of signalling from the microenvironment, the expression of most canonical marker genes was conserved in vitro (Fig. 2), suggesting that muscle-derived cell cultures are able to recapitulate in vivo behaviour to a large extent.

Differential expression analysis allowed us to identify surface marker panels for physical separation of multiple cell types, including SCs, FAPs, ECs and SMMCs (together representing over 80% of mononucleated cells). Notably, inclusion of ITGA5 in the panel offered significant purity improvements over previous protocols, as this integrin serves as a negative selection marker for SCs, whilst ITGB1/CD29 (previously used as a SC marker[22,23]) is highly expressed by both SCs and FAPs. Whilst we were able to proliferate each of these cell types for multiple passages (Fig. 3), further work is needed to assess the potential of ECs and SMMCs, with respect to their long-term proliferation in the absence of FBS and their capacity to

promote myogenesis or adipogenesis, for example in co-culture systems.[12,24] Other low-abundance cell types, such as macrophages, could also offer benefits in terms of tissue remodelling and angiogenesis for structured cultured meat products.[25,26]

Cultured meat production requires an extensive proliferation phase, with many PDs, to achieve required cell yields.[5] This prompts several issues, including reduced growth rates, loss of differentiation capacity, and the possibility of overgrowth of undesired cell types. Transcriptomic analysis indeed revealed that sorted SCs were rapidly overgrown by a small proportion of contaminating FAPs, indicating variable growth dynamics in our initial culture conditions that favour FAP proliferation (Fig. 4). Whilst high levels of animal-derived sera have traditionally been used to control fibroblastic overgrowth in SC cultures,[27] this phenomenon is poorly understood, and in any case is unsuited for cultured meat applications. We used differential expression analysis to inform several improvements to the SC culture conditions, including the switch to an ECM mimic that corresponds to the integrin expression profile of SCs (laminin is known to interact with ITGA7/ITGB1 dimers[28]), and the addition of growth factors, such as HGF, whose receptor expression is specific to SCs.[29,30] Our dataset will also provide insights into design of selective media for other cell types, such as ECs, which is likely complicated by their slow proliferation. Detailed metabolic profiling, which was beyond the scope of this study, could help to further inform the design of feeding strategies that afford efficient and selective growth of desired cell types.[31] It should be noted that our experiments are conducted at lab scale, and that proliferation in bioreactor systems used for upscaled cultured meat production will introduce additional stresses, that could act differentially across cell types.[32] Further cost reduction will also be required, and our dataset can assist in the replacement of growth and attachment factors with peptide alternatives with retained (or superior) cell type selectivities.

Our transcriptomic analysis also revealed remarkable heterogeneity *within* cell types, notably between distinct subpopulations of SCs, that points towards a dynamic equilibrium of quiescent, active and committed states (Fig. 5). Different SC states have previously been proposed, both from dissociated muscle samples[15,33–35] and in vitro cultures[16,36,37], although without clear consensus. We identified CD151 (previously observed in human skeletal muscle[13]) as a cell-surface marker for the 'quiescent' cluster, although the extent to which the quiescent phenotype we observed in vitro reflects physiological SC behaviour during embryonic development or wound healing remains unclear. We did not distinguish such states in our bovine

muscle samples, perhaps because the majority of cells are activated during tissue dissociation.[33] RNA velocity analysis suggests a model in which only activated SCs are able to differentiate, which is congruent with a physiological model of wound healing in which activated SCs either differentiate to form muscle fibres, or return to a quiescent state in order to preserve the ability of the tissue to respond to future regenerative stimuli. However, higher resolution velocity analysis of SCs would be informative, given that we only sampled a snapshot within each passage (when cells were approaching confluency). Indeed, the role that confluency plays in the promotion of differentiation, and the extent to which premature differentiation might negatively affect a proliferative culture, requires further study in the context of a cultured meat bioprocess design. Similarly, whilst increased culture length clearly affects the transitions of SCs between states, it is important to note that we also observed substantial transcriptomic differences between equivalent states at different timepoints (Supplementary Fig. 6), indicating that cellular ageing cannot be understood solely in terms of subpopulation ratio changes. Indeed, our data supports the hypothesis that a reduced rate of switching between states could be a characteristic of SC ageing or senescence.[38,39] Future transcriptomic experiments, including single-nuclei approaches, could illuminate the formation of cultured muscle tissues during the differentiation of SCs. Furthermore, although not specified in this study, it is likely that similar cellular heterogeneity is present in other cell types, including FAPs, where adipogenic and fibroblastic fate decisions could be critical for cultured fat production.[40,41]

In conclusion, scRNA-seq is a powerful approach to study cell heterogeneity in the context of cultured meat production. Our dataset offers a number of important insights for cell purification and proliferation steps, has led to the development of refined medium conditions, and represents a useful resource for further analysis and improvement of cultured meat bioprocesses.

3.5 MATERIAL & METHODS

3.5.1 Cell isolation

Cells were isolated from semitendinosus muscles of 10 Belgian Blue cattle (Supplementary Table 1) by collagenase digestion (CLSAFA, Worthington; 1 h; 37 °C), filtration with 100 µm cell strainers, red blood lysis using a Ammonium-Chloride-Potassium (ACK) lysis buffer, and final filtration with 40 µm cell strainers. Cells

from each donor animal were plated as separate cultures in serum-free growth medium[42] (SFGM, Supplementary Table 2) on fibronectin-coated (4 µg cm^{-2} bovine fibronectin; F1141, Sigma-Aldrich) tissue culture vessels for 72 h prior to FACS, or (where denoted) in growth medium (GM) containing 20% foetal bovine serum (heat-inactivated FBS; 10500-064, Gibco).

3.5.2 Cell culture

Tissue culture vessels were coated with fibronectin for unsorted cells, ECs, and SMMCs, laminin-521 (0.5 µg cm^{-2}, LN521-05, Biolamina) for SCs, or collagen I (0.6 µg cm^{-2}, bovine skin collagen; C2124, Sigma-Aldrich) for FAPs for 1 h prior to plating. Unsorted cells, SCs and FAPs were cultured in SFGM (except where otherwise noted), and passaged every 3-4 days upon reaching confluency. ECs and SMMCs were cultured in BioAMF-3 (01-196-1A, Sartorius).

To assess long-term proliferation, cells were cultured as described above for each cell type. Cells were harvested upon approaching confluence, counted, reseeded at 5×10^3 cm^{-2} and purity assessed at each passage via flow cytometry.

3.5.3 Single cell RNA-sequencing

3.5.3.1 Cell harvesting

Five timepoints throughout long-term in vitro culture were selected for single-cell RNA sequencing (scRNA-seq), for each of which cells from all genotypes (donor animals) were pooled in equal ratios and washed with 1% BSA in PBS prior to injection. Timepoints 1 to 5 corresponded to unsorted cells directly after isolation ('Muscle') and after 72 h ('passage 0'), and to cultured cells (unsorted cells, SCs and FAPs) at passages 2, 5, and 8 respectively (Fig. 1a, Supplementary Table 1).

3.5.3.2 Library preparation and sequencing

25000 cells were injected for each timepoint into Chromium Single Cell Controller, emulsified with bar-coded gel beads and libraries were constructed following the protocol of the Chromium NextGEM Single Cell 3' Kit V3.1 (10x Genomics). Quality control of the DNA library was performed on Qiaxcel (QIAgen) and quantified by qPCR using the KAPA SYBR Fast qPCR Master Mix (Illumina). Paired- end single cell 3' gene expression libraries were sequenced on a Novaseq 6000 System (Illumina) using a NovaSeq S1 flow-cell to a depth of at least 3.5×10^8 reads/timepoint.

3.5.3.3 Data processing and demultiplexing

Raw base call files were demultiplexed using the cellranger mkfastq function (CellRanger 6.0.1). Reads were aligned to Bos Taurus genome (build ARS-UCD1.2) with Ensembl annotations (release 101), using CellRanger count function. Default filtering parameters of CellRanger were applied to obtain a gene expression matrix. Genotypes were deconvolved and assigned to individual cells using demuxlet,[43] based on VCF files previously generated by genotyping of each donor animal with a BovineSNP50 v3 DNA Analysis BeadChip (Illumina).

3.5.3.4 Quality control and normalisation

Across the five timepoints, 36129 cells (90.8%) passed quality control (within 3 median absolute deviations of the median for expressed genes, total counts and percentage mitochondrial genes; Supplementary Fig. 1). Counts for each timepoint were normalised using the sctransform function of Seurat with default parameters,[44,45] regressing out percentage of mitochondrial genes, library size, number of genes, and cell cycle effects.

3.5.3.5 Dimensionality reduction and differential gene expression analysis

Cells were clustered using the FindNeighbors() and FindClusters() functions based on the first 50 principal components and with a resolution of 0.1 respectively. Dimensionality was reduced by uniform manifold approximation and projection (UMAP)[46] using the first 30 principal components as input, 50 neighbouring points and a minimal distance of 0.1).

Differentially expressed (DE) genes were computed for clusters identified in each timepoint by using the FindAllMarkers(), or between denoted conditions using FindMarkers(), with a $\log_2$ fold-change (log-FC) threshold of 1, a false discovery rate (FDR) of 0.05, and expressed in at least 50% of cells. For Timepoint 1, cell types were assigned to each cluster based on DE genes and on predicted phenotypes from FindTransferAnchors()[47] using analogous murine scRNA-seq data (GSE143437[14]). ECs were further characterised by their expression of signatures derived from the Descartes human genes expression atlas[19] using the AddModuleScore function. For Timepoint 2, surface markers amongst the DE genes were identified by filtering for genes coding for proteins located in the plasma membrane.[48] GO terms for biological processes (2021) were computed using enrichR.[49] For the analysis of SC cultures, Timepoints 3 to 5 were filtered for genotypes 5, 6, and 10 (Fig. 4), whilst for analysis of SC states these were further filtered by removal of *ITGA5*+ FAP clusters (Fig. 5).

3.5.3.6 RNA velocity analysis

RNA velocities were computed for SCs at Timepoint 3 by generating separate count matrices for spliced and unspliced transcripts using velocyto. The resulting loom files were analysed using scVelo in Python 3.9.12. Transcription kinetics for selected genes were computed, as well as RNA velocity vectors (based on the scVelo dynamical model) across all genes.[50,51]

3.5.4 Flow cytometry

For cell type identification, unsorted cells were stained for ITGA5, ITGA7, JAM-1 and CD45 (Fig. 3, Supplementary Table 3) for 15 min prior to analysis on a MACSQuant10 Flow Analyzer (Miltenyi Biotec). To determine proportions of SCs and FAPs (Fig. 4), cells were stained for ITGA7 and ITGA5. For analysis of SC states (Fig. 5), cells were stained for CD151 prior to fixation (PFA), permeabilisation (10% saponin), and staining for desmin. Samples were subsequently washed and stained with α-mouse-PE secondary antibodies prior to analysis.

3.5.5 Fluorescent-activated cell sorting (FACS)

Cells were purified by FACS 72 h post-isolation on a MACSQuant Tyto Cell Sorter (Miltenyi Biotec) following antibody staining as described above. SCs, FAPs, SMMCs and ECs were gated as described in Fig. 2. Where noted, cells were gated for NCAM1+/CD29+ (Fig. 4g).

3.5.6 Immunofluorescent staining

After formaldehyde fixation, cells were permeabilised (0.5% Triton X-100), blocked (2% bovine serum albumin (BSA)) and stained with PDGFRα, Pax7, TEK, and CNN1 (for phenotype confirmation; Fig. 3c) or desmin (for fusion index; Fig. 4c) primary antibodies (see Supplementary Table 3). After washing, cells were incubated with AF488-conjugated secondary antibodies and Hoechst 33342 (Thermo Fisher) prior to imaging on an ImageXpress Pico Automated Cell Imaging System (Molecular Devices).

3.5.7 Myogenic differentiation assay

Mixed cultures containing SCs and FAPs in varying proportions were seeded on 0.5% Matrigel-coated vessels at a density of 5 x 10^4 cm^{-2} in SFGM for 24 h, before switching to serum-free differentiation media (SFDM). After 72 h in SFDM, cells

were fixed with 4% formaldehyde, stained for desmin and imaged as previously described. To calculate fusion indices, number of nuclei within desmin-stained areas were divided by total nuclei.

3.5.8 Cell cycle analysis

For flow cytometric cell cycle analysis, SCs were incubated with EdU for 90 min prior to trypsinisation. Following α-CD151-APC staining, Click-iT reaction was performed using the Click-iT EdU Alexa Fluor 488 Flow Cytometry Assay Kit (C10420, Thermo Fisher) according to the supplier's protocol, followed by α-desmin staining as previously described. Finally, the cells were gated into quiescent ($DES^-/CD151^+$) and activated ($DES^-/CD151^-$) and within these, into EdU^+ (S-Phase), $DAPI^{low}/EdU^-$ (G0/1-Phase) and $DAPI^{high}/EdU^-$ (G2-Phase), as shown in Supplementary Fig. 5d.

3.5.9 Statistical analyses

Statistical analyses were performed using Prism 9 (Graphpad). Pearson correlation of fusion indices with percentages of ITGA7+ cells was computed assuming a normal distribution (Fig. 4d). For comparisons of culture conditions (Figs. 4h-j) and the analysis of cell cycle states in SCs (Fig. 5e), two-way ANOVAs were performed including post-hoc Tukey's multiple comparison test. Sample replicates consisted of cells from the same donor animal, cultured in separate vessels.

3.5.10 Data availability

scRNA-seq data is deposited in the NCBI Gene Expression Omnibus database (accession code GSE211428).

3.5.11 Code availability

Code for scRNA-seq analysis (including RNA velocity calculations) are available from the authors on request.

3.6 ACKNOWLEDGEMENTS

We would like to thank Latifa Karim, Wouter Coppieters, Alice Mayer and Manon Deckers (GIGA institute, ULiège) for support in the acquisition and analysis of scRNA-seq data, Benjamin Bouchet for advice on immunofluorescent stainings, Christoph Börlin for help with RNA velocity analysis and Dhruv Raina for critical feedback on the manuscript.

3.7 BIBLIOGRAPHY

1. Post, M. J. Cultured beef: medical technology to produce food. *J. Sci. Food Agric.* **94**, 1039–1041 (2014).
2. Datar, I. & Betti, M. Possibilities for an in vitro meat production system. *Innov. Food Sci. Emerg. Technol.* **11**, 13–22 (2010).
3. Parodi, A. *et al.* The potential of future foods for sustainable and healthy diets. *Nat. Sustain.* **1**, 782–789 (2018).
4. Post, M. *et al.* Scientific, sustainability and regulatory challenges of cultured meat. *Nat. Food* **1**, 403–415 (2020).
5. Melzener, L., Verzijden, K. E., Buijs, A. J., Post, M. J. & Flack, J. E. Cultured beef: from small biopsy to substantial quantity. *J. Sci. Food Agric.* **101**, 7–14 (2021).
6. Wilks, M., Phillips, C. J. C., Fielding, K. & Hornsey, M. J. Testing potential psychological predictors of attitudes towards cultured meat. *Appetite* **136**, 137–145 (2019).
7. Bryant, C. & Barnett, J. Consumer acceptance of cultured meat: A systematic review. *Meat Sci.* **143**, 8–17 (2018).
8. Mukund, K. & Subramaniam, S. Skeletal muscle: A review of molecular structure and function, in health and disease. *Wiley Interdiscip. Rev. Syst. Biol. Med.* **12**, e1462 (2020).
9. Forcina, L., Miano, C., Pelosi, L. & Musarò, A. An Overview about the Biology of Skeletal Muscle Satellite Cells. *Curr. Genomics* **20**, 24–37 (2019).
10. Dohmen, R. G. J. *et al.* Muscle-derived fibro-adipogenic progenitor cells for production of cultured bovine adipose tissue. *Npj Sci. Food* **6**, 6 (2022).
11. Reiss, J., Robertson, S. & Suzuki, M. Cell Sources for Cultivated Meat: Applications and Considerations throughout the Production Workflow. *Int. J. Mol. Sci.* **22**, 7513 (2021).
12. Giordani, L. *et al.* High-Dimensional Single-Cell Cartography Reveals Novel Skeletal Muscle-Resident Cell Populations. *Mol. Cell* **74**, 609-621.e6 (2019).
13. De Micheli, A. J., Spector, J. A., Elemento, O. & Cosgrove, B. D. A reference single-cell transcriptomic atlas of human skeletal muscle tissue reveals bifurcated muscle stem cell populations. *Skelet. Muscle* **10**, 19 (2020).
14. De Micheli, A. J. *et al.* Single-Cell Analysis of the Muscle Stem Cell Hierarchy Identifies Heterotypic Communication Signals Involved in Skeletal Muscle Regeneration. *Cell Rep.* **30**, 3583-3595.e5 (2020).
15. Rubenstein, A. B. *et al.* Single-cell transcriptional profiles in human skeletal muscle. *Sci. Rep.* **10**, 229 (2020).
16. Williams, K., Yokomori, K. & Mortazavi, A. Heterogeneous Skeletal Muscle Cell and Nucleus Populations Identified by Single-Cell and Single-Nucleus Resolution Transcriptome Assays. *Front. Genet.* **13**, (2022).
17. Cornelison, D. D. W. Context Matters: In Vivo and In Vitro Influences on Muscle Satellite Cell Activity. *J. Cell. Biochem.* **105**, 663–669 (2008).
18. Khodabukus, A., Prabhu, N., Wang, J. & Bursac, N. In Vitro Tissue-Engineered Skeletal Muscle Models for Studying Muscle Physiology and Disease. *Adv. Healthc. Mater.* **7**, e1701498 (2018).
19. Cao, J. *et al.* A human cell atlas of fetal gene expression. *Science* **370**, eaba7721 (2020).

20. Joe, A. W. B. *et al.* Muscle injury activates resident fibro/adipogenic progenitors that facilitate myogenesis. *Nat. Cell Biol.* **12**, 153–163 (2010).
21. Proietti, D. *et al.* Activation of skeletal muscle–resident glial cells upon nerve injury. *JCI Insight* **6**, e143469.
22. Ding, S. *et al.* Maintaining bovine satellite cells stemness through p38 pathway. *Sci. Rep.* **8**, 10808 (2018).
23. Sherwood, R. I. *et al.* Isolation of Adult Mouse Myogenic Progenitors: Functional Heterogeneity of Cells within and Engrafting Skeletal Muscle. *Cell* **119**, 543–554 (2004).
24. Ben-Arye, T. *et al.* Textured soy protein scaffolds enable the generation of three-dimensional bovine skeletal muscle tissue for cell-based meat. *Nat. Food* **1**, 210–220 (2020).
25. Wang, X. & Zhou, L. The Many Roles of Macrophages in Skeletal Muscle Injury and Repair. *Front. Cell Dev. Biol.* **10**, (2022).
26. Cantini, M. *et al.* Macrophages Regulate Proliferation and Differentiation of Satellite Cells. *Biochem. Biophys. Res. Commun.* **202**, 1688–1696 (1994).
27. Rosenblatt, J. D., Lunt, A. I., Parry, D. J. & Partridge, T. A. Culturing satellite cells from living single muscle fiber explants. *In Vitro Cell. Dev. Biol. Anim.* **31**, 773–779 (1995).
28. Barczyk, M., Carracedo, S. & Gullberg, D. Integrins. *Cell Tissue Res.* **339**, 269 (2009).
29. Gal-Levi, R., Leshem, Y., Aoki, S., Nakamura, T. & Halevy, O. Hepatocyte growth factor plays a dual role in regulating skeletal muscle satellite cell proliferation and differentiation. *Biochim. Biophys. Acta* **1402**, 39–51 (1998).
30. González, M. N. *et al.* HGF potentiates extracellular matrix-driven migration of human myoblasts: involvement of matrix metalloproteinases and MAPK/ERK pathway. *Skelet. Muscle* **7**, 20 (2017).
31. Hubalek, S., Post, M. J. & Moutsatsou, P. Towards resource-efficient and cost-efficient cultured meat. *Curr. Opin. Food Sci.* **47**, 100885 (2022).
32. Bellani, C. F. *et al.* Scale-Up Technologies for the Manufacture of Adherent Cells. *Front. Nutr.* **7**, (2020).
33. Machado, L. *et al.* Tissue damage induces a conserved stress response that initiates quiescent muscle stem cell activation. *Cell Stem Cell* **28**, 1125-1135.e7 (2021).
34. Zammit, P. S. *et al.* Muscle satellite cells adopt divergent fates: a mechanism for self-renewal? *J. Cell Biol.* **166**, 347–357 (2004).
35. Dell'Orso, S. *et al.* Single cell analysis of adult mouse skeletal muscle stem cells in homeostatic and regenerative conditions. *Dev. Camb. Engl.* **146**, dev174177 (2019).
36. Zeng, W. *et al.* Single-nucleus RNA-seq of differentiating human myoblasts reveals the extent of fate heterogeneity. *Nucleic Acids Res.* **44**, e158 (2016).
37. Trapnell, C. *et al.* The dynamics and regulators of cell fate decisions are revealed by pseudotemporal ordering of single cells. *Nat. Biotechnol.* **32**, 381–386 (2014).
38. Sousa-Victor, P. *et al.* Geriatric muscle stem cells switch reversible quiescence into senescence. *Nature* **506**, 316–321 (2014).
39. Carlson, M. E. *et al.* Molecular aging and rejuvenation of human muscle stem cells. *EMBO Mol. Med.* **1**, 381–391 (2009).
40. Fiore, D. *et al.* Pharmacological blockage of fibro/adipogenic progenitor expansion and suppression of regenerative fibrogenesis is associated with impaired skeletal muscle regeneration. *Stem Cell Res.* **17**, 161–169 (2016).

41. Uezumi, A. *et al.* Fibrosis and adipogenesis originate from a common mesenchymal progenitor in skeletal muscle. *J. Cell Sci.* **124**, 3654–3664 (2011).
42. Kolkmann, A., Essen, A., Post, M. & Moutsatsou, P. Development of a Chemically Defined Medium for in vitro Expansion of Primary Bovine Satellite Cells. *Front. Bioeng. Biotechnol.* **10**, (2022).
43. Kang, H. M. *et al.* Multiplexed droplet single-cell RNA-sequencing using natural genetic variation. *Nat. Biotechnol.* **36**, 89–94 (2018).
44. Hafemeister, C. & Satija, R. Normalization and variance stabilization of single-cell RNA-seq data using regularized negative binomial regression. *Genome Biol.* **20**, 296 (2019).
45. Hao, Y. *et al.* Integrated analysis of multimodal single-cell data. *Cell* **184**, 3573-3587.e29 (2021).
46. McInnes, L., Healy, J. & Melville, J. UMAP: Uniform Manifold Approximation and Projection for Dimension Reduction. Preprint at https://doi.org/10.48550/arXiv.1802.03426 (2020).
47. Stuart, T. *et al.* Comprehensive Integration of Single-Cell Data. *Cell* **177**, 1888-1902.e21 (2019).
48. Thul, P. J. *et al.* A subcellular map of the human proteome. *Science* **356**, eaal3321 (2017).
49. Gene Ontology Consortium. The Gene Ontology resource: enriching a GOld mine. *Nucleic Acids Res.* **49**, D325–D334 (2021).
50. La Manno, G. *et al.* RNA velocity of single cells. *Nature* **560**, 494–498 (2018).
51. Bergen, V., Lange, M., Peidli, S., Wolf, F. A. & Theis, F. J. Generalizing RNA velocity to transient cell states through dynamical modeling. *Nat. Biotechnol.* **38**, 1408–1414 (2020).

3.8 SUPPLEMENTARY INFORMATION

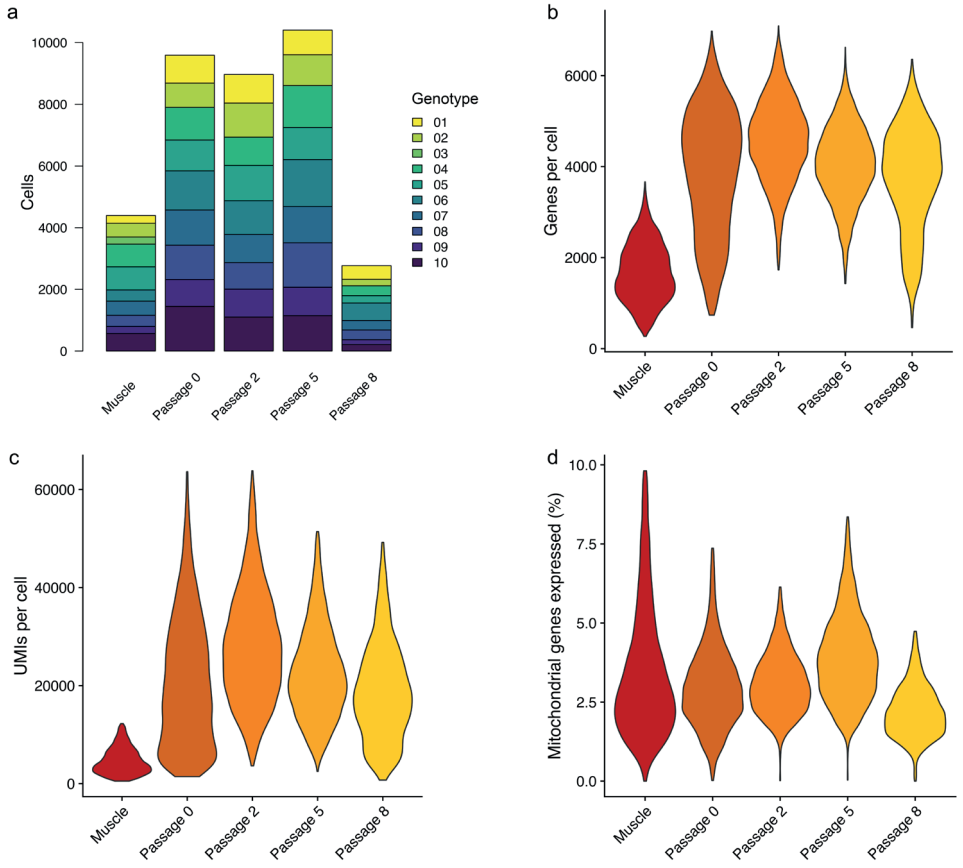

Supplementary Figure 1: Single-cell RNA-sequencing quality control (related to Figure 1) a) Number of cells at each timepoint of the scRNA-seq experiment, coloured by genotype (donor animal); b) Total number of genes per cell at each timepoint; c) Total number of unique molecular identifiers (UMIs) per cell at each timepoint; d) Percentage of reads assigned to mitochondrial genes at each timepoint.

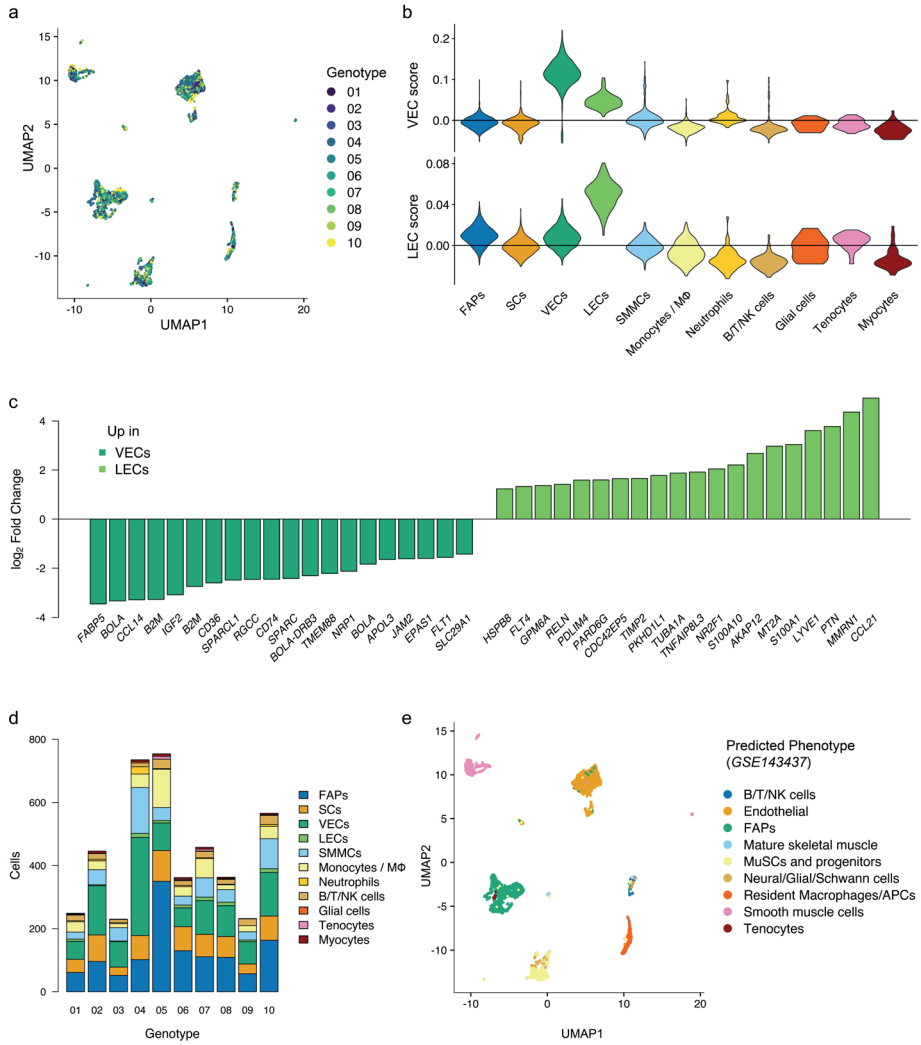

Supplementary Figure 2: Identification of cell types in the bovine muscle niche (related to Figure 1).
a) UMAP of bovine muscle cells coloured by genotype; b) Averaged expression of *Descartes'* gene signature for vascular (top) and lymphatic endothelial (bottom) marker genes per cluster; c) Fold changes of the 20 most differentially expressed genes between vascular endothelial cells (VECs, dark green) and lymphatic endothelial cells (LECs, light green); d) Number of cells per genotype at Timepoint 1, coloured by respective cell type; e) UMAP of bovine muscle cells coloured by predicted phenotype, based on gene expression profiles of murine muscle cells (from *GSE143437*).

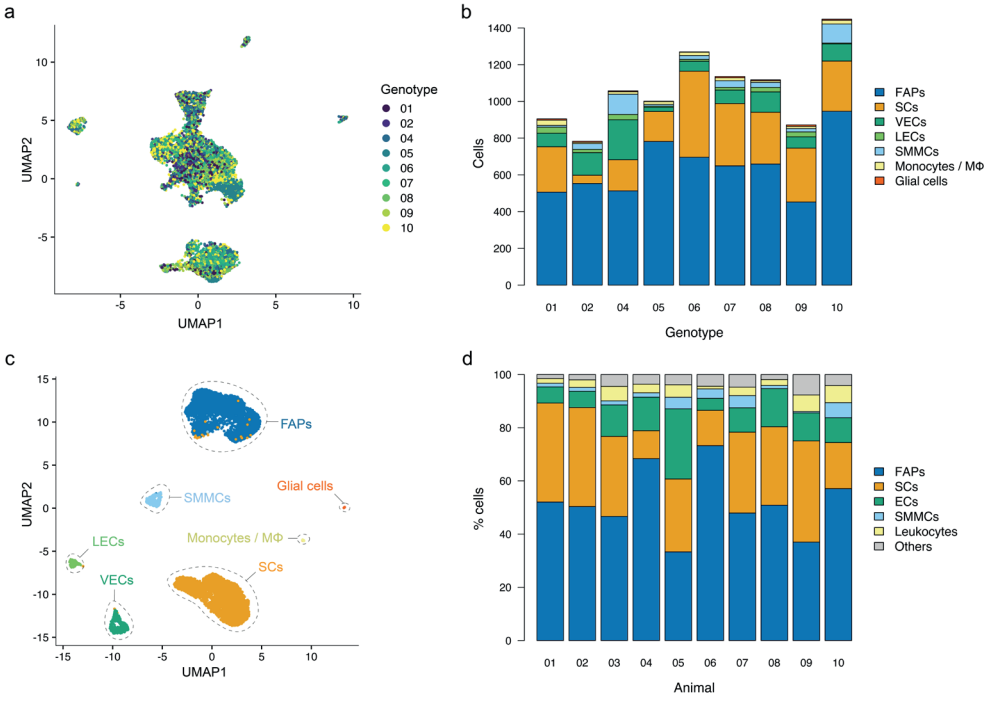

Supplementary Figure 3: Adherent cell types from bovine muscle niche after 72 h in vitro (related to Figure 2).
a) UMAP of adherent cell fraction after 72 h in SFGM, coloured by genotype; b) Number of cells per genotype at Timepoint 2, coloured by respective cell type; c) UMAP of adherent cell fraction after 72 h in serum-containing GM, coloured by respective phenotype; d) Percentage of cell types in 10 donor animals, measured via flow cytometry based on gating strategy shown in Fig. 2f.

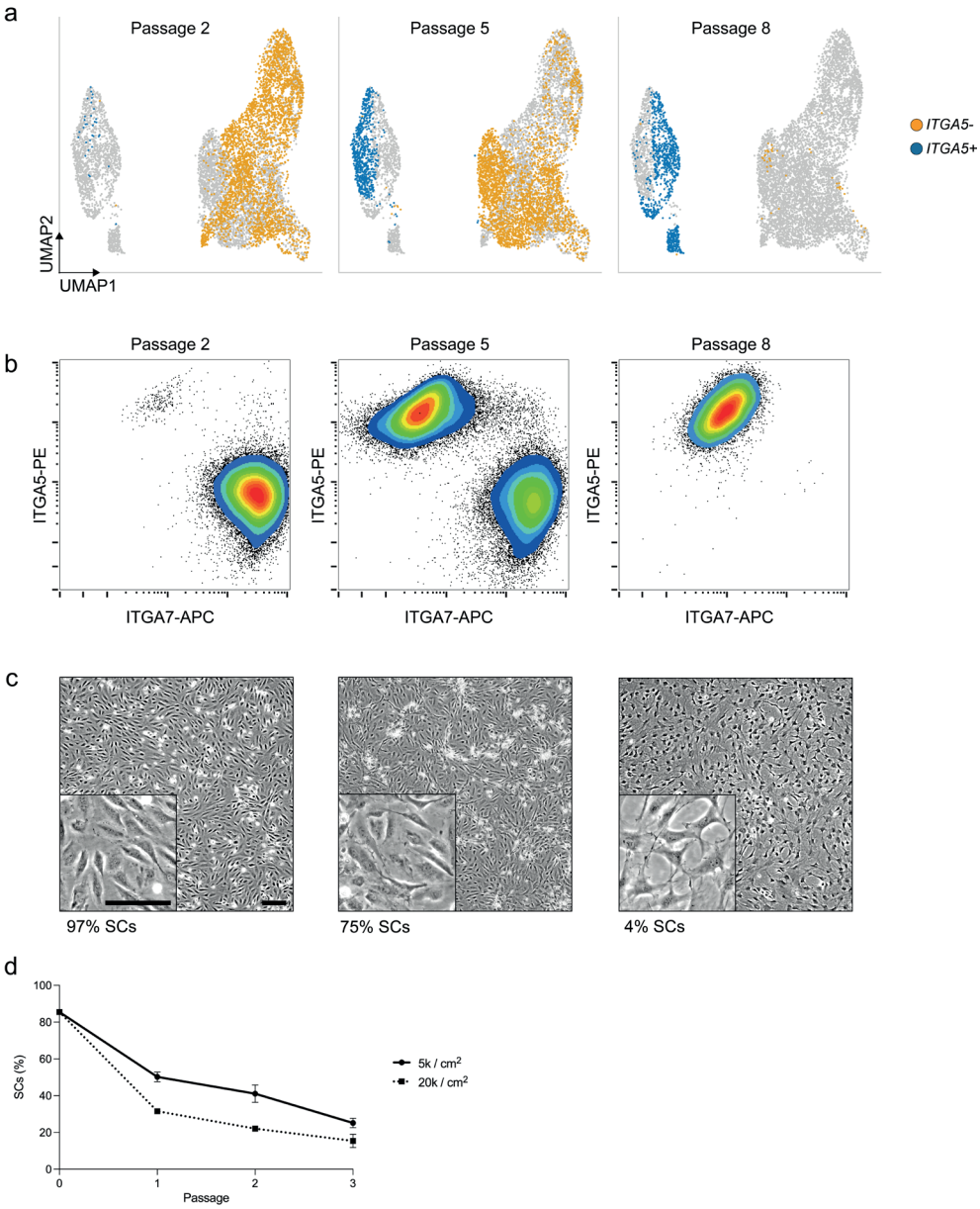

Supplementary Figure 4: Overgrowth of SCs by FAPs during long-term cultivation (related to Figure 4).
a) UMAPs of sorted SCs at passages 2 (Timepoint 3, left), 5 (Timepoint 4, centre) and 8 (Timepoint 5, right), clusters coloured for expression of *ITGA5*; b) Flow cytometry plots of sorted SCs at passages 2 (left), 5 (centre) and 8 (right); c) Brightfield images of heterogeneous cultures with denoted ITGA7+ percentages; scale bar = 100 µm; d) Proportion of SCs resulting from passaging at different seeding densities, as measured via flow cytometry; error bars indicate *SD*, n = 4.

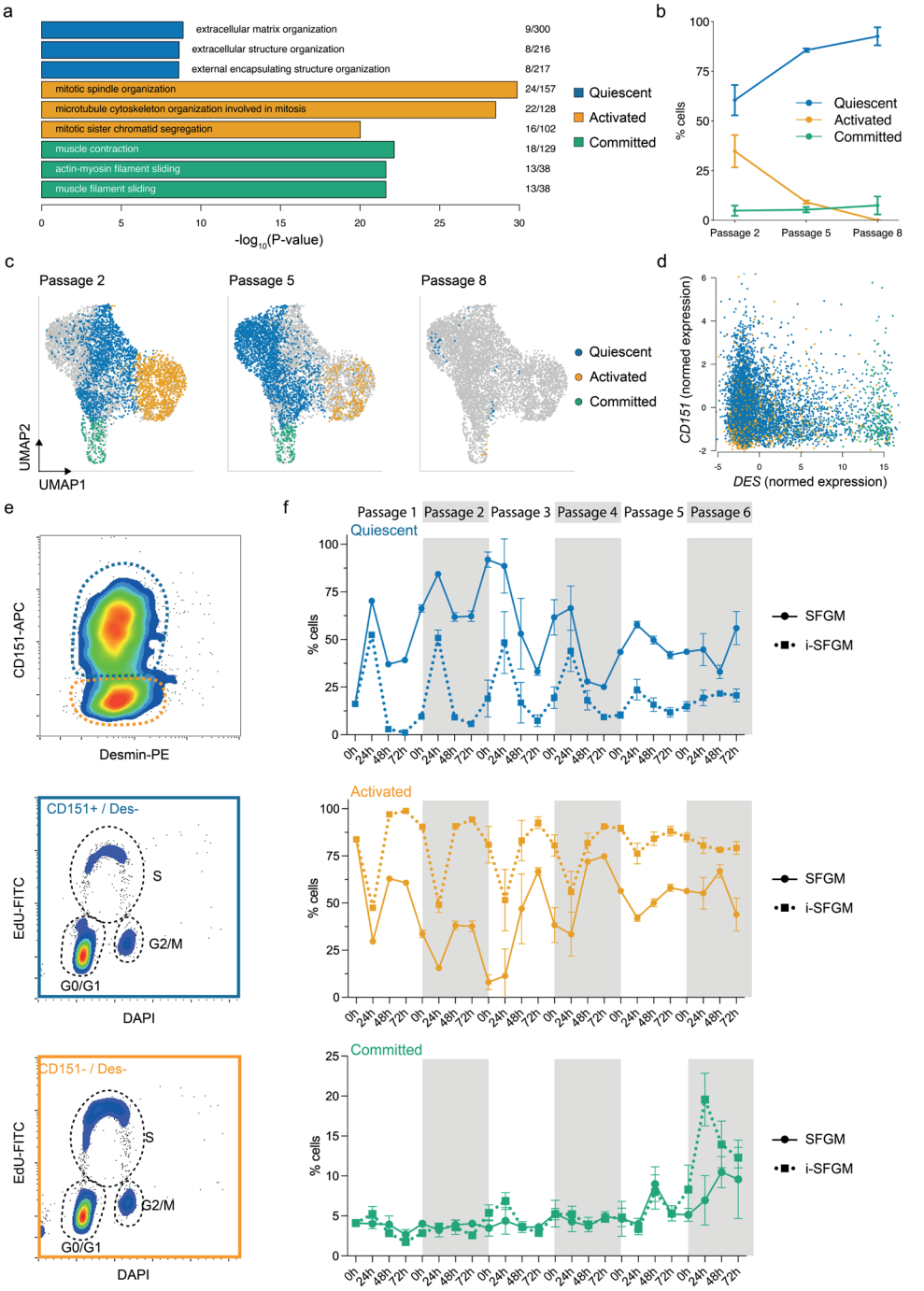
a
extracellular matrix organization
extracellular structure organization
external encapsulating structure organization
mitotic spindle organization
microtubule cytoskeleton organization involved in mitosis
mitotic sister chromatid segregation
muscle contraction
actin-myosin filament sliding
muscle filament sliding
9/300
8/216
8/217
24/157
22/128
16/102
18/129
13/38
13/38
Quiescent
Activated
Committed
-log10(P-value)
b
% cells
Passage 2
Passage 5
Passage 8
c
Passage 2
Passage 5
Passage 8
UMAP2
UMAP1
d
CD151 (normed expression)
DES (normed expression)
e
CD151-APC
Desmin-PE
CD151+ / Des-
EdU-FITC
DAPI
S
G2/M
G0/G1
CD151- / Des-
f
Passage 1
Passage 2
Passage 3
Passage 4
Passage 5
Passage 6
Quiescent
Activated
Committed
SFGM
i-SFGM

► Supplementary Figure 5: Three dynamic states identified within purified SCs (related to Figure 5).
a) Top three most significantly enriched GO terms corresponding to upregulated genes genes in quiescent, activated, and committed SCs; b) Proportions of quiescent, activated and committed SCs at passages 2, 5 and 8, as determined via scRNA-seq; c) Combined UMAPs showing SCs at passages 2 (left), 5 (centre) and 8 (right), coloured according to cell state; d) Expression of *CD151* and *DES* in SCs at passage 2; cells are coloured by state; e) Gating strategy for cell cycle analysis via flow cytometry; SCs were stained for CD151 and desmin (top); CD151+ (blue, centre) and CD151- (orange, bottom) cells were assigned to cell cycle phases as indicated by dotted gates; h) Proportion of quiescent (top), activated (centre) and committed (right) SCs in SFGM and improved SFGM media over the course of three passages, determined every 24 h via flow cytometry.

a

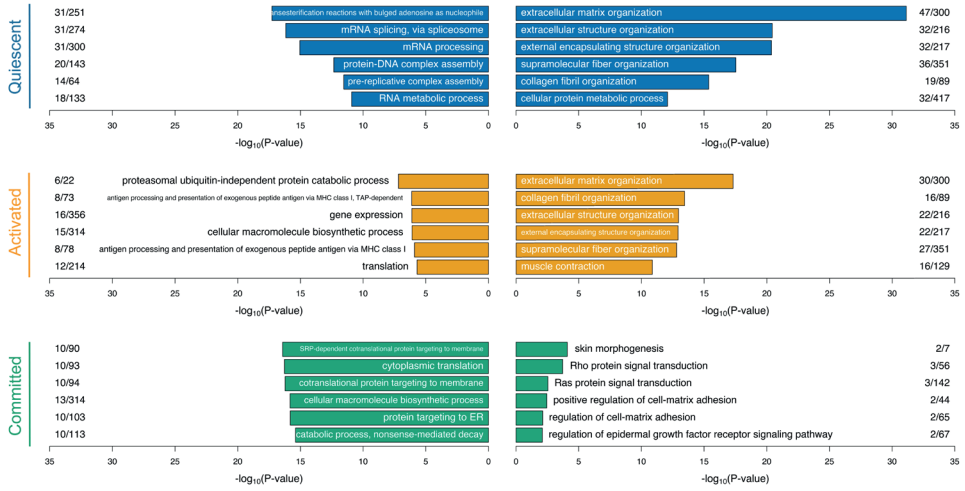
Up in P2
Up in P5
Quiescent
31/251 transesterification reactions with bulged adenosine as nucleophile
31/274 mRNA splicing, via spliceosome
31/300 mRNA processing
20/143 protein-DNA complex assembly
14/64 pre-replicative complex assembly
18/133 RNA metabolic process
extracellular matrix organization 47/300
extracellular structure organization 32/216
external encapsulating structure organization 32/217
supramolecular fiber organization 36/351
collagen fibril organization 19/89
cellular protein metabolic process 32/417
-log10(P-value)
Activated
6/22 proteasomal ubiquitin-independent protein catabolic process
8/73 antigen processing and presentation of exogenous peptide antigen via MHC class I, TAP-dependent
16/356 gene expression
15/314 cellular macromolecule biosynthetic process
8/78 antigen processing and presentation of exogenous peptide antigen via MHC class I
12/214 translation
extracellular matrix organization 30/300
collagen fibril organization 16/89
extracellular structure organization 22/216
external encapsulating structure organization 22/217
supramolecular fiber organization 27/351
muscle contraction 16/129
-log10(P-value)
Committed
10/90 SRP-dependent cotranslational protein targeting to membrane
10/93 cytoplasmic translation
10/94 cotranslational protein targeting to membrane
13/314 cellular macromolecule biosynthetic process
10/103 protein targeting to ER
10/113 catabolic process, nonsense-mediated decay
skin morphogenesis 2/7
Rho protein signal transduction 3/56
Ras protein signal transduction 3/142
positive regulation of cell-matrix adhesion 2/44
regulation of cell-matrix adhesion 2/65
regulation of epidermal growth factor receptor signaling pathway 2/67
-log10(P-value)

b

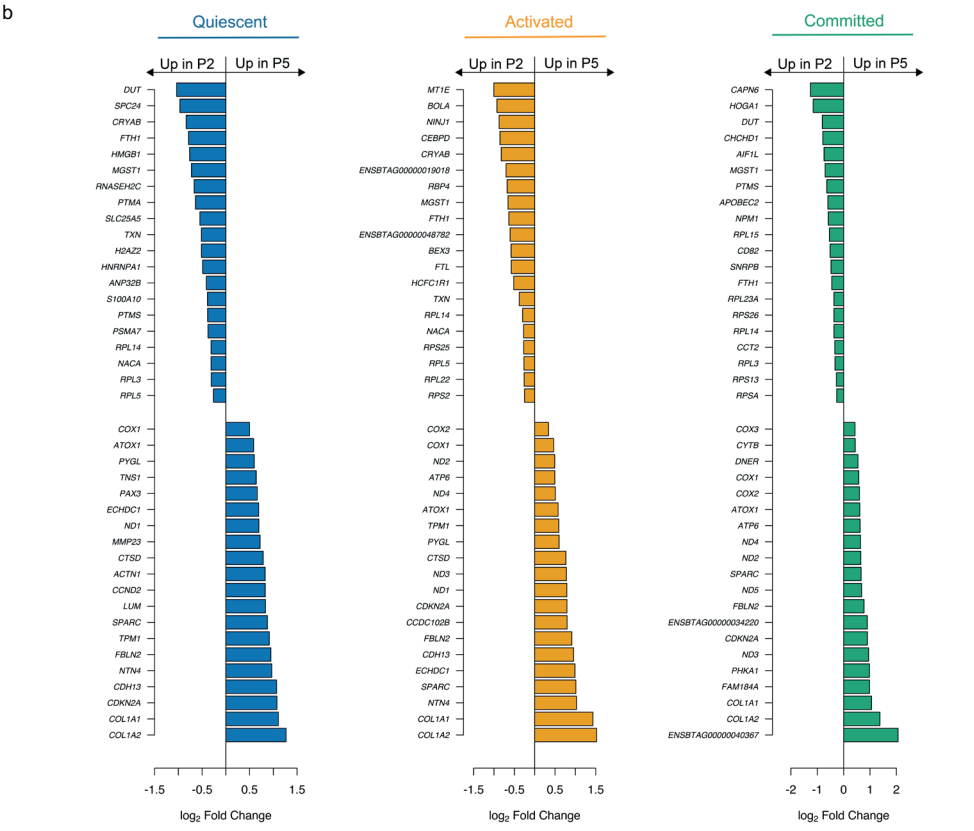
Quiescent
Activated
Committed
Up in P2
Up in P5
DUT SPC24 CRYAB FTH1 HMGB1 MGST1 RNASEH2C PTMA SLC25A5 TXN H2AZ2 HNRNPA1 ANP32B S100A10 PTMS PSMA7 RPL14 NACA RPL3 RPL5
COX1 ATOX1 PYGL TNS1 PAX3 ECHDC1 ND1 MMP23 CTSD ACTN1 CCND2 LUM SPARC TPM1 FBLN2 NTN4 CDH13 CDKN2A COL1A1 COL1A2
MT1E BOLA NINJ1 CEBPD CRYAB ENSBTAG00000019018 RBP4 MGST1 FTH1 ENSBTAG00000048782 BEX3 FTL HCFC1R1 TXN RPL14 NACA RPS25 RPL5 RPL22 RPS2
COX2 COX1 ND2 ATP6 ND4 ATOX1 TPM1 PYGL CTSD ND3 ND1 CDKN2A CCDC102B FBLN2 CDH13 ECHDC1 SPARC NTN4 COL1A1 COL1A2
CAPN6 HOGA1 DUT CHCHD1 AIF1L MGST1 PTMS APOBEC2 NPM1 RPL15 CD82 SNRPB FTH1 RPL23A RPS26 RPL14 CCT2 RPL3 RPS13 RPSA
COX3 CYTB DNER COX1 COX2 ATOX1 ATP6 ND4 ND2 SPARC ND5 FBLN2 ENSBTAG00000034220 CDKN2A ND3 PHKA1 FAM184A COL1A1 COL1A2 ENSBTAG00000040367
log2 Fold Change

► **Supplementary Figure 6: Ageing effects within SC subpopulations (related to Figure 5).** a) Most significantly enriched GO-terms corresponding to the 200 most upregulated genes between passage 2 (left) and passage 5 (right) in quiescent (blue), activated (orange), and committed (green) SCs; b) Fold changes of the 20 most up- and downregulated genes in quiescent (blue), activated (orange), and committed (green) SCs.

Supplementary Table 1: Experimental overview.

Animal	Breed	Sex	Age	Sorted population	Number of cells				
					Timepoint 1	Timepoint 2	Timepoint 3	Timepoint 4	Timepoint 5
					Muscle	P0	P2	P5	P8
1	Belgian Blue	Female	Adult	Unsorted	249	905	927	801	443
2	Belgian Blue	Female	Calf	Unsorted	446	783	1102	998	216
3	Belgian Blue	Female	Adult	N/A	230	-	-	-	-
4	Belgian Blue	Female	Calf	FAPs	735	1058	917	1355	317
5	Belgian Blue	Female	Calf	SCs	754	1001	1144	1041	239
6	Belgian Blue	Male	Adult	SCs	362	1270	1092	1522	567
7	Belgian Blue	Female	Calf	FAPs	458	1136	915	1177	307
8	Belgian Blue	Male	Adult	FAPs	363	1118	863	1442	316
9	Belgian Blue	Female	Adult	Unsorted	232	872	905	922	159
10	Belgian Blue	Male	Calf	SCs	566	1448	1101	1147	208
				Total:	**4395**	**9591**	**8966**	**10405**	**2772**
								Overall total:	**36129**

Supplementary table 2: Media formulations.

#	Component	Reference	Concentration
Pre-sorting serum-free growth medium (ps-SFGM)			
1	DMEM/F-12	21331-020, Gibco	
2	α-linolenic acid	L2376, Sigma Aldrich	1.0 µg ml^{-1}
3	FGF-2	100-18B, Peprotech	10 ng ml^{-1}
4	Human Serum Albumin	Rc HA NW20, Richcore Lifesciences	5.0 mg ml^{-1}
5	HGF	100-39H, Peprotech	5 ng ml^{-1}
6	Hydrocortisone	H0135, Sigma Aldrich	36 ng ml^{-1}
7	IGF-1	100-11, Peprotech	100 ng ml^{-1}
8	IL-6	200-06, Peprotech	20 ng ml^{-1}
9	ITSE	00-101, biogems	1%
10	GlutaMax	35050-061, Gibco	1%
11	Glucose	G7021, Sigma Aldrich	17.7 mM
12	L-ascorbic acid 2-phosphate (Vitamin C)	A8960, Sigma Aldrich	155 µM
13	PDGF-BB	100-14B, Peprotech	10 ng ml^{-1}
14	Penicillin/Streptomycin/ Amphotericin (PSA)	17-745E, Lonza	1%
15	VEGF	100-20 Peprotech	10 ng ml^{-1}
Serum-free growth medium (SFGM)			
1	DMEM/F-12	21331-020, Gibco	
2	α-linolenic acid	L2376, Sigma Aldrich	1.0 µg ml^{-1}
3	FGF-2	100-18B, Peprotech	10 ng ml^{-1}
4	Human Serum Albumin	Rc HA NW20, Richcore Lifesciences	5.0 mg ml^{-1}
5	HGF	100-39H, Peprotech	50 ng ml^{-1}
6	Hydrocortisone	H0135, Sigma Aldrich	36 ng ml^{-1}
7	ITSE	00-101, biogems	1%
8	GlutaMax	35050-061, Gibco	1%
9	Glucose	G7021, Sigma Aldrich	17.7 mM
10	L-ascorbic acid 2-phosphate (Vitamin C)	A8960, Sigma Aldrich	155 µM
11	PSA	17-745E, Lonza	1%
12	Triiodothyronine	T6397, Sigma Aldrich	30 nM
Serum-free differentiation medium (SFDM)			
1	DMEM/F-12	21311-020, Gibco	
2	EGF-1	AF-100-15, Peprotech	10 ng ml^{-1}
3	Human Serum Albumin	Rc HA NW20, Richcore Lifesciences	0.5 mg ml^{-1}
4	ITSE	00-101, biogems	2%
5	L-ascorbic acid 2-phosphate (Vitamin C)	A8960, Sigma Aldrich	40 µM
6	Lysophosphatidic acid (LPA)	L7260, Sigma Aldrich	1 µM
7	MEM Amino Acids Solution	11130-051, ThermoFisher	0.50%
8	$NaHCO_3$	P2256, Sigma Aldrich	6.5 mM
9	PSA	17-745E, Lonza	1%
10	Soy hydrolysates	58903C, Merck	1%

Supplementary table 3: Antibodies used in this study.

Target	Fluorophore	Source	Dilution	Reference	Application
Calponin-1	-	Abcam	1:400	ab46794	IF
CD151	APC	Miltenyi Biotec	1:50	130-103-664	Flow
CD29	APC	BioLegend	1:20	B247653	Flow
CD45-Ro	APC-Vio770	Miltenyi Biotec	1:50	130-114-083	Flow
Desmin	-	Sigma Aldrich	1:1000	D1033	Flow; IF
ITGA5	PE	Miltenyi Biotec	1:50	130-110-532	Flow
ITGA7	APC	Miltenyi Biotec	1:50	130-123-833	Flow
JAM-1 / F11R	PE-Vio770	Miltenyi Biotec	1:50	130-109-484	Flow
NCAM1	PE	BD Biosciences	1:20	335826	Flow
Pax7	-	Developmental Studies Hybridoma Bank	1:100	Cat# PAX7	IF
PDGFRα	-	Abcam	1:200	ab203491	IF
TEK / Tie2	-	BioLegend	1:100	334202	IF
mouse	AF488	Invitrogen	1:250	A-11029	IF
mouse	PE	Miltenyi Biotec	1:250	30-119-684	IF
rabbit	AF488	Invitrogen	1:250	A-11034	IF

Chapter 4

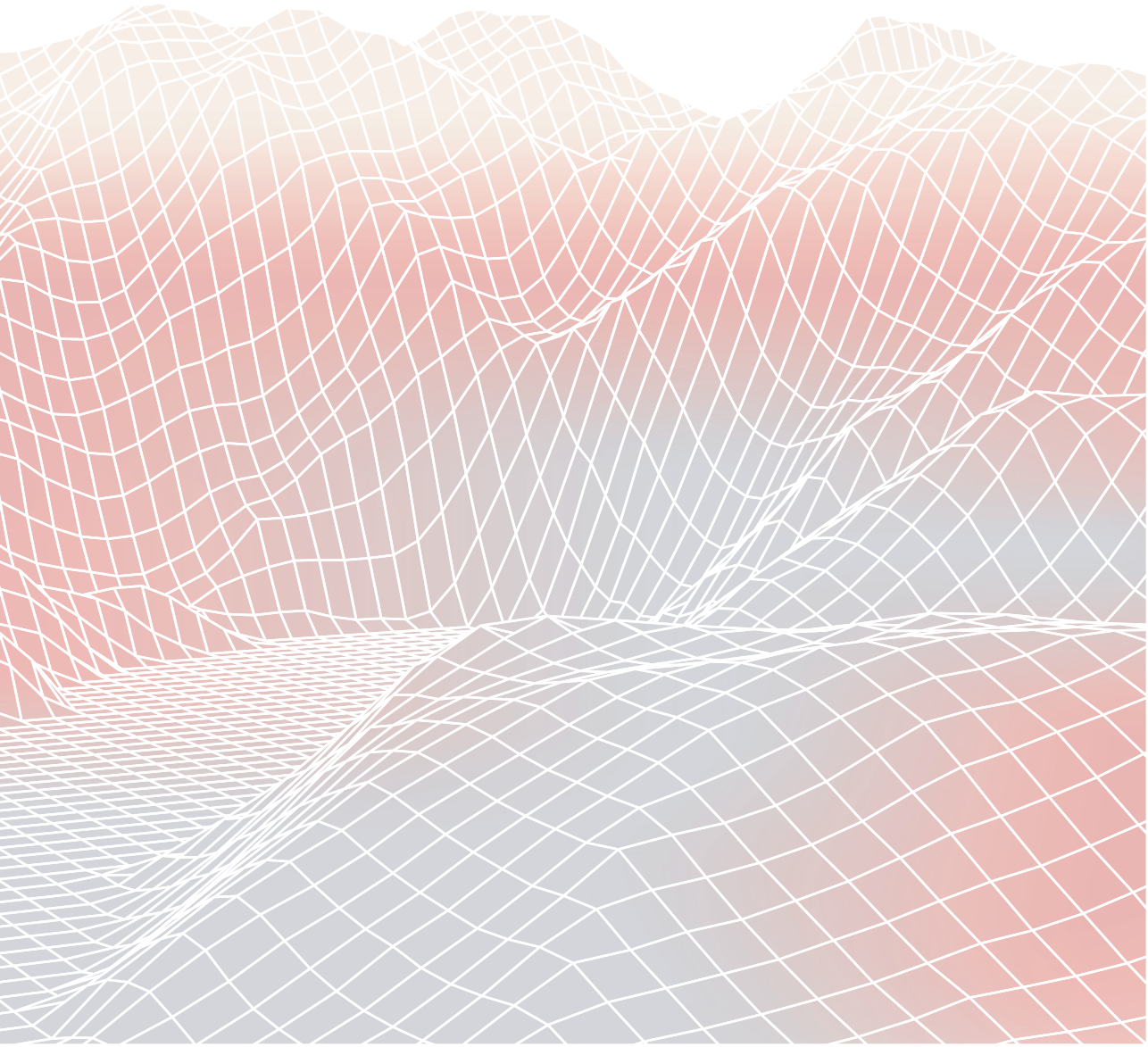

VARIABILITY IN PROLIFERATION AND DIFFERENTIATION BETWEEN SATELLITE CELL CULTURES EMERGES DURING LONG-TERM EXPANSION

Tobias Meßmer
Lieke Schaeken
Joanna Papadopoulos
Lea Melzener
Rui Hüber
Christoph Börlin
Mark Post
Joshua Flack

4.1 ABSTRACT

To advance cultured meat technology from proof of principle to commercial scale, it is necessary to develop a robust and resource-efficient bioprocess. This includes the isolation and in vitro multiplication of cells that possess the ability to differentiate towards skeletal muscle fibres, such as satellite cells (SCs). The limited in vitro lifespan of primary adult stem cells including SCs requires regular cell sourcing, which introduces cell-batch variability to the bioprocess. In order to evaluate the extent of this variability and its implications for cultured meat production, we studied the proliferation and differentiation capacity of bovine SC cultures during a multi-passage serum-free in vitro expansion. We found that for early passages, SC cultures exhibited highly similar in vitro behaviour. Pronounced differences between the cultures emerged after 20 population doublings, manifesting in three distinct outcomes: proliferative exhaustion, loss of differentiation potential during continuous proliferation, and maintenance of both proliferation and differentiation capacity. Transcriptional analysis of these phenotypes indicated the involvement of genes related to myogenic differentiation in cellular ageing. With this data, we provide a reference to gauge the efficiency of cultured meat production from primary SCs in a serum-free environment and highlight the importance of maintaining the stemness of SCs for upscaled production.

4.2 INTRODUCTION

Cultured meat technology utilises stem cells grown in vitro to produce edible skeletal muscle tissue, which promises to resolve many of the environmental, ethical, and health issues associated with conventionally grown meat.[1–3] To realise the commercialisation of this technology, cultured meat needs to advance from proof-of-principle prototypes to upscale production.[4,5] The basis for this is a robust, scalable, and resource-efficient bioprocess, which is strongly dependent on reliable behaviour of the utilised progenitor cells.

Cultured beef can be produced from a variety of bovine cell sources, including cell lines, pluripotent stem cells, and primary adult stem cells such as satellite cells (SCs)[1,6]. Immortalised cell lines and pluripotent stem cells possess near-unlimited proliferation capacity in vitro but their generation and differentiation may require complex protocols or genetic modification that are less compatible with food regulation and consumer acceptance, especially in EU countries.[7–10] In contrast, primary stem cells (including SCs) possess a limited proliferative capacity in vitro, and gradually lose their ability to efficiently differentiate into skeletal muscle; two primary hallmarks of SC stemness.[11] This process is closely linked to cellular ageing, characterised in vitro by a prolonged cell cycle, increase in cell size, metabolic shifts, DNA damage and epigenetic alterations proportional to the time in culture.[12]

Cellular ageing necessitates regular sourcing of new SC cultures from donor animals and thus inevitably introduces variability into the bioprocess.[13] However, it has not yet been studied in detail the extent to which SCs from different donor animals or in different cultures from the same donor animal vary in their in vitro behaviour. Differences in proliferation and differentiation dynamics between SCs derived from different non-human or human mammals have been observed in short-term in vitro experiments.[14–17] However, the degree to which proliferative exhaustion and loss of stemness may vary between cultures is insufficiently quantified.

The development of optimised sorting protocols and selective culture conditions enabled us to culture SCs in a serum-free environment without risk of overgrowth by contaminating cell types (Chapter 3). Therefore, we set out to investigate the variability between highly pure bovine SC cultures and assessed proliferation, differentiation, and additional bioprocess-relevant readouts in a time-resolved fashion. We further aimed to link in vitro phenotypes to changes on a transcriptomic

or DNA level in an attempt to understand underlying culture-specific differences. With this study, we want to inform both the necessity and the feasibility of regular cell sourcing of primary SCs for a robust cultured meat production process.

4.3 RESULTS

4.3.1 Proliferative differences between cultures arise after 20 population doublings

To assess variability in proliferation between SC cultures, we performed a long-term proliferation assay of SCs isolated from 14 different donor animals. In addition, three SC cultures were isolated from samples of the same animal but at different locations of the same muscle (samples A and B of animals 4, 10, and 11) and one culture was divided into three technical replicates (animal 13). On average, 2.8 ± 1.5 x 10^4 SCs were isolated per 1 g of tissue, resulting in a total of 19 parallel SC cultures that were > 98.4% positive for ITGA7 (Table 1) indicating high SC purity that was maintained throughout the experiment (Chapter 3).

Within 32 days, the cultures grew on average from 5.3 ± 0.9 population doublings (PDs) to 24.4 ± 2.3 PDs (Fig. 1a). For the first 3 passages (12 days) of this initial growth period, the proliferation rate varied between 0.7 and 1.0 PDs day^{-1}, followed by a steady decline with each additional passage (Fig. 1b). For 9 out of the 19 cultures, this decline in doubling speed led to a complete growth stop and an altered cell morphology (Fig. 1c), whereas the remaining 10 cultures equilibrated at a proliferation rate between 0.3 and 0.6 PDs day^{-1} that continued beyond 35 cumulative PDs. This showed that proliferation rates were overall similar in early SC cultures but a subset of ageing SCs exhausted their proliferative capacity.

We next studied how the proliferation behaviour compared between SC cultures isolated from the same animal. The three cultures of SCs that were separated after FACS (culture 13) showed similar proliferation rates compared to the average culture (Figs. 1d, e; left). However, the decline of proliferation that occurred between P2 and P6 led to a growth stop in replicate 13-3 but not in 13-1 and 13-2, which continued to proliferate up to 35 PDs. This indicated that the process of replicative exhaustion was at least partly dependent on changes occurring during cell culture as opposed to genotype-intrinsic properties. For the replicates that were isolated from different locations of the same muscle, both proliferation rate and the dynamics of proliferative exhaustion were highly similar within each animal (Figs. 1d, e; right).

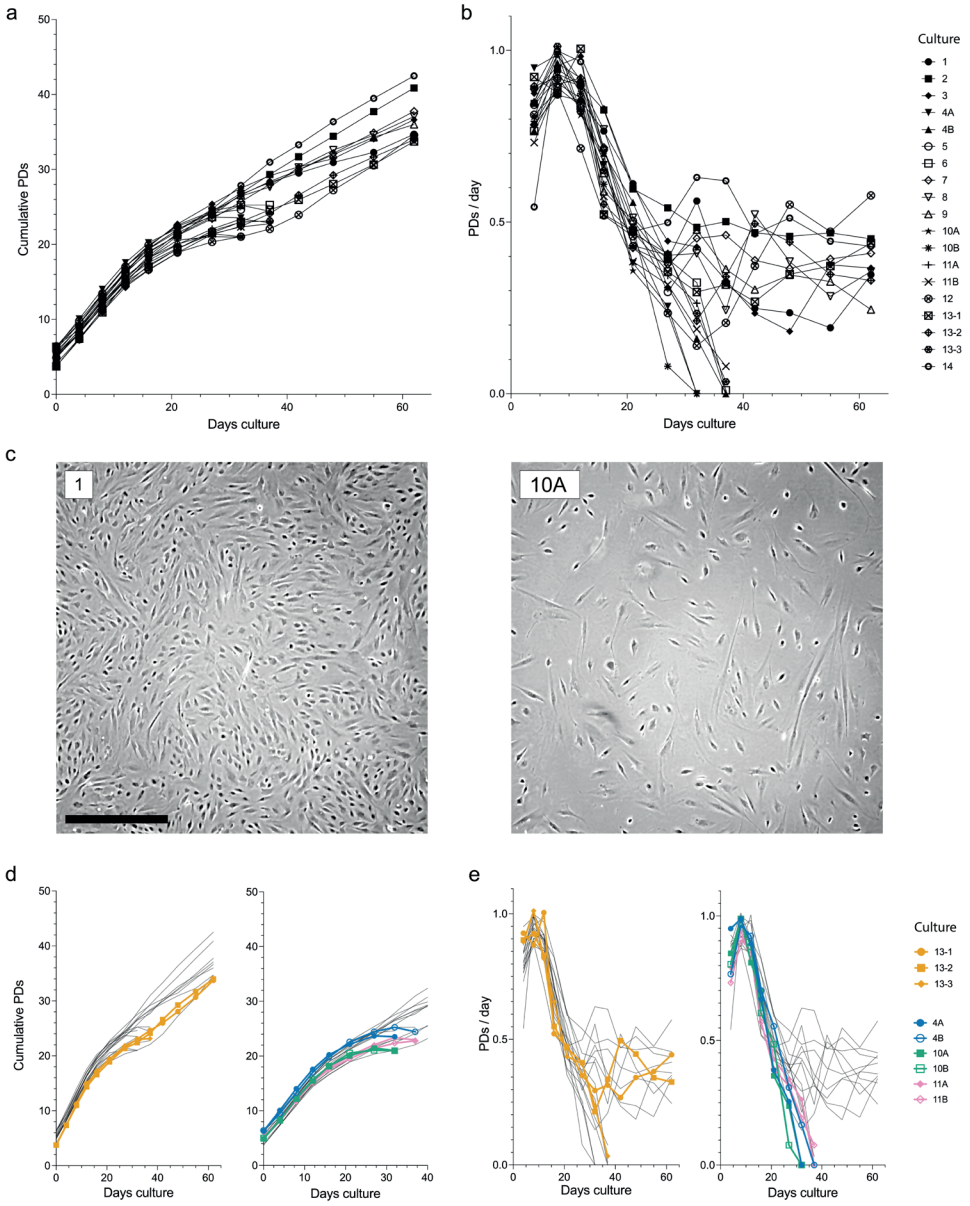

Figure 1: Proliferation rate follows a similar trend for the first 30 days of in vitro growth. a) Growth curves of SC cultures, points on curves indicate new passage, PDs = population doublings; b) Proliferation rates corresponding to (a); c) Brightfield images of SCs at the end of passage 7, numbers in top left show culture ID, scale bar = 500 µm; d) Growth curves of SC cultures, where technical replicates of culture 13 are coloured orange (left) and those derived from different locations of same animal are shown in the blue, pink or green (right); black lines indicate all remaining cultures, points indicate passaging; d) Proliferation rates corresponding to (c).

4.3.2 Loss of myogenic differentiation capacity occurs at different speeds between proliferative cultures

To create a cultured meat product that resembles skeletal muscle, cultured SCs must efficiently differentiate after undergoing multiple cycles of in vitro replication. Therefore, we next studied differences in myogenic differentiation between the cultures at subsequent time points throughout the proliferation phase to assess whether loss of differentiation capacity occurs at a similar rate.

Maximum extent of serum-free differentiation at passage 3 (~12 PDs) was similar across all cultures with a mean fusion index of 69.9 ± 3.7% after 96 h in SFDM supplemented with ERK-inhibitor SCH772984 (Fig. 2a, Supplementary Fig. 1).[18] This high similarity in differentiation capacity suggested that SC functionality did not depend on animal characteristics such as donor age, sex or breed. At passage 6 (~ 21 PDs), the maximum extent of differentiation decreased to 53.0 ± 9.0% and showed a higher variability between the cultures than at early PDs (Fig. 2b, Supplementary Fig. 2). These differences further augmented in the cultures that remained proliferative, where 4 out of 10 cultures retained pronounced differentiation at ~30 PDs while the others showed little to no myotube formation (Fig. 2c).

Similar to proliferation, this indicated that differentiation capacity was equal between SCs at early passage and that differences emerged only upon long-term culture. In addition, these results showed that the loss of stemness, indicated by a gradual loss of differentiation capacity, occurred at varying speed between the remaining proliferative cultures.

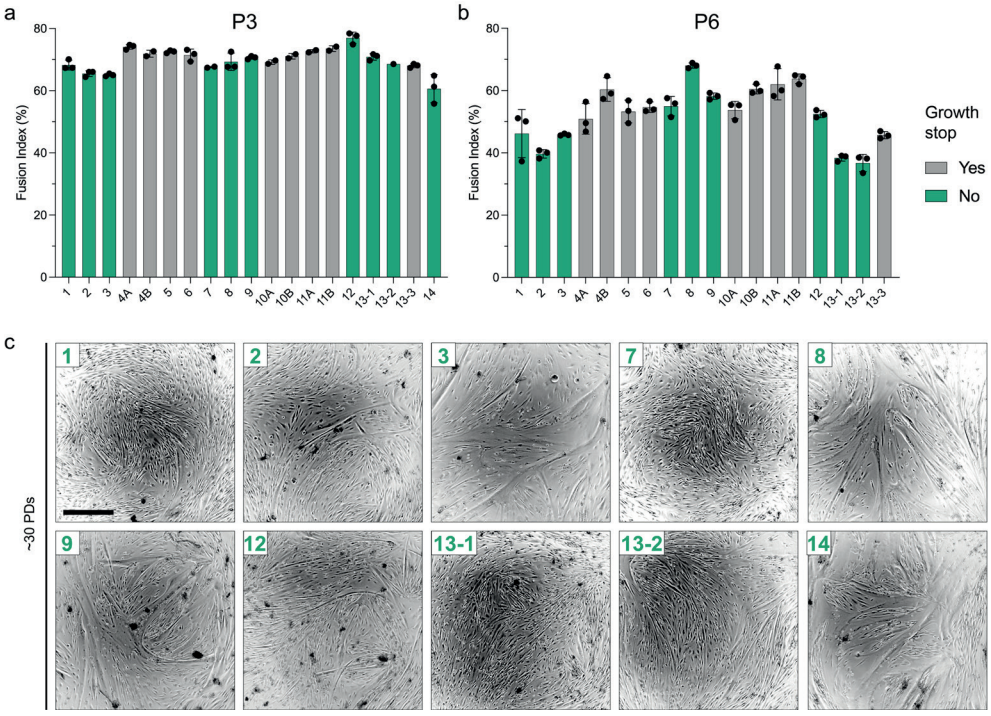

Figure 2: Differences in differentiation capacity emerge during long-term culture.
a) Fusion indices at passage 3 after 96 h in SFDM + 1 µM SCH772984, coloured green if culture continued to grow beyond 25 PDs, n = 3; b) Same as (a) but at passage 6, n = 3; c) Brightfield images of SCs at 30 ± 1 PDs at maximum extent of differentiation in SFDM, numbers in top left show culture ID, scale bar = 500 µm

4.3.3 Early in vitro readouts do not predict future phenotype

Based on these observations, we classified the cultures into three primary phenotypes: those that stopped proliferating ('Growth stop', n = 9), those that continued to proliferate but stopped differentiating at high PDs ('Stemness^{lo}', n = 6) and those that continued to proliferate and continued to differentiate ('Stemness^{hi}', n = 4). For an efficient bioprocess, the ability to determine future in vitro behaviour at an early stage may enable the exclusion of low-performance cultures. We thus sought to correlate the observed phenotypes with early culture characteristics such as proliferation rate, CD151 positivity (indicating the proportion of quiescent to activated SCs; Chapter 3) or differentiation kinetics.

Proliferation rates were similar between the three phenotypes at low PDs, as well as between Stemness^{lo} and Stemness^{hi} cultures at later PDs (Figs. 3a, b), suggesting that proliferation rate was not predictive of future behaviour. Similarly, there was no significant difference in the ratio of quiescent (CD151^{+}) to activated (CD151^{-}) SCs at the end of each passage, although the Stemness^{lo} culture showed a minor trend towards increased quiescence (Fig. 3c). The same pattern was observed for the CD151 positivity within one passage, which increased within the first 24 h before decreasing at 48 h and 72 h after plating but was similar between the three phenotypes at passage 2 (Fig. 3d) and passage 5 (Fig. 3e). At passage 7, the CD151 dynamics flattened, which was previously observed for ageing SCs (Chapter 3), but again did not differ between the phenotypes (Fig. 3f). This showed that the proportions of in vitro SC states did not correlate with late in vitro behaviour.

Finally, we studied whether differentiation dynamics would predict either Growth stop or the decline of stemness. We found that fusion indices after 72 h in SFDM (before the maximum extent of differentiation was reached) did not significantly differ between the phenotypes at passage 3 (Fig. 3g) but were significantly reduced in the Stemness^{lo} condition at passage 6 ($p = 0.03$, Fig. 3h), suggesting that the decline of differentiation occurs gradually and may be identified in culture prior to a full loss of differentiation capacity.

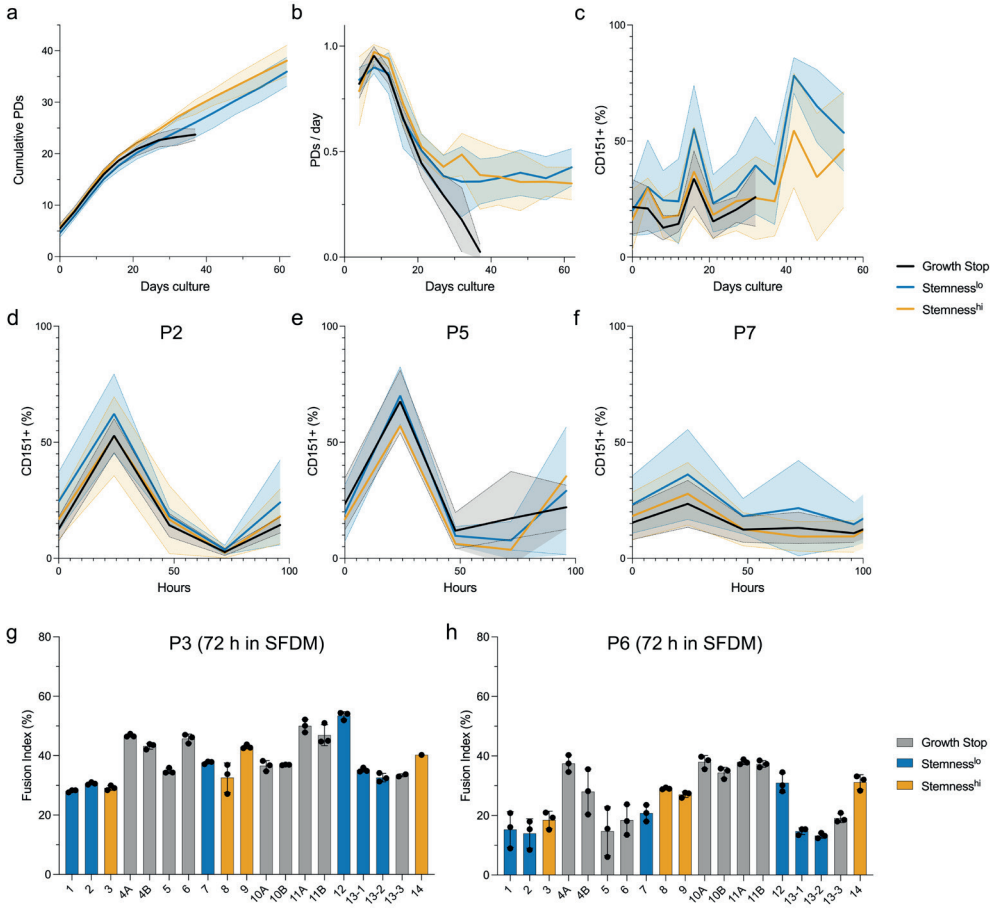

Figure 3: In vitro characterization of SC cultures categorised into three phenotypes.
a) Mean growth curves of cultures exhibiting growth stop (grey, n = 9), low stemness (blue, n = 6) or high stemness (orange, n = 4); shaded areas indicate standard deviation; b) Mean proliferation rates corresponding to (a); c) Mean percentage of quiescent (CD151⁺) SCs at the end of each passage; d) Mean percentage of quiescent (CD151⁺) SCs within passage 2, measured every 24 h; e) as (d) but at passage 5; f) as (d) but at passage 7; g) Mean fusion indices at passage 3 after 72 h in SFDM, coloured for indicated phenotype, n = 3; h) as (g) but at passage 6.

4.3.4 Phenotype differences cannot be explained by copy-number variations

Genotyping is commonly used in animal science to characterise beneficial traits of cattle to inform selective breeding and includes techniques that analyse specific single-nucleotide polymorphisms (SNPs) as well as structural variation.[19,20] We therefore assessed whether alterations on the DNA-level correlated to the differences of in vitro proliferation or differentiation capacity observed between the SC cultures. For this, we studied copy-number variation (CNV) as the most common source of genetic structural variation throughout different passages of selected cultures using a molecular karyotyping assay.[21]

In total, we found 156 CNV regions where either a gain or a loss of copy-number was detected. With these, we first constructed a hierarchical cluster tree based on the identified CNV regions using the Jaccard similarity coefficient (Fig. 4a). This consistently clustered the samples by genotype, indicating that genetic variation between animals was greater than within-animal variation acquired during in vitro proliferation. However, the samples did not cluster by in vitro phenotype, which suggested that CNV did not underlie the observed differences in proliferative exhaustion or stemness. Amongst the 156 detected CNV regions, we could not identify one region that was exclusively gained or lost in any of the three phenotypes (Fig. 4b). We therefore concluded that the observed phenotypic differences were not explainable by structural variation of a distinct genomic location.

Furthermore, we investigated whether the cultures that stopped proliferating or differentiating exhibited increased or decreased methylation of CpG islands, a common epigenetic alteration in ageing SCs. Using a global methylation assay, we measured a significant reduction in the proportion of 5-methyl cytosines in the total DNA (5-mC) in passage 2 compared to passage 6 ($p = 0.025$, Fig. 4c). This indicated a general trend towards global hypomethylation after prolonged in vitro culture, which has previously been reported for cultured fibroblasts but conflicts with global hypermethylation observed in SCs from aged donors.[22,23] Comparing global methylation changes between cultures exhibiting different phenotypes showed no significant difference, suggesting that global methylation could not explain the observed in vitro behaviour (Fig. 4d).

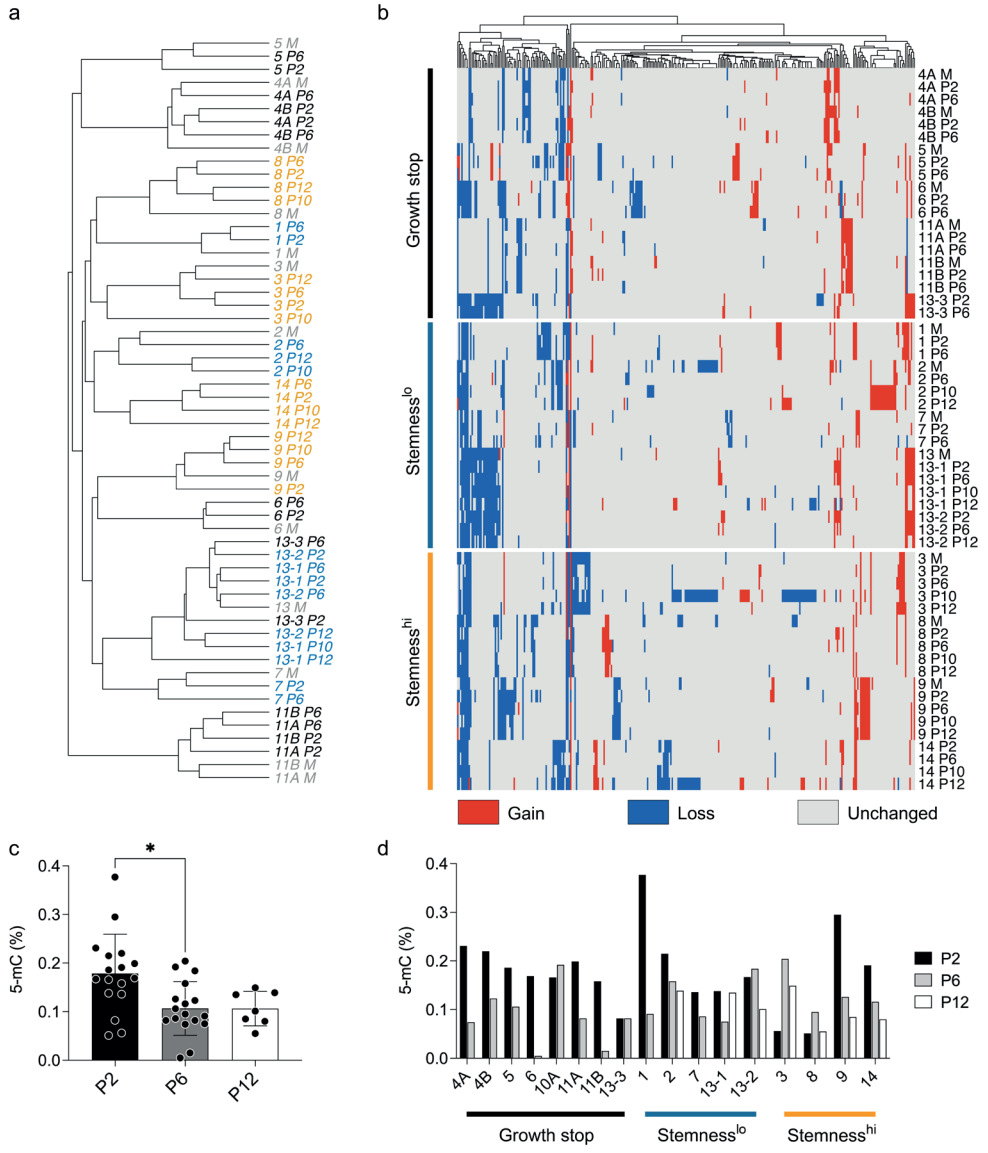

Figure 4: Structural variation and global methylation alterations of DNA from cultures with different phenotypes.
a) Hierarchical clustering of cultures at indicated passage (P) based on gain or loss of copy number variation regions, colours indicate phenotype where grey = muscle samples (M), black = Growth stop, blue = Stemness^{lo} and orange = Stemness^{hi}; b) Heatmap showing gain (red) and loss (blue) of copy-number variation regions; each column shows a region with at least two identified copy-number variations; cultures (rows) are categorised into observed phenotype; c) Percentage of 5-methyl cytosines (5-mC) grouped by passage; d) Percentage of 5-methyl cytosines of culture sorted for phenotype; p-values: * < 0.05.

4.3.5 Differentiation-related genes play a role in SC ageing

Finally, we analysed the transcriptomes of the different cultures at the end of passage 2, 6, and 10 to investigate whether the expression of specific gene signatures may explain the variability in late proliferation and differentiation.

Performing dimensionality reduction through principal component analysis (PCA) separated the samples by time point in the direction of the first principal component (Fig. 5a). Although the dataset was constructed in three batches compounding with the passage of the cultures and therefore allows only limited comparison between time points, we noted that the samples of passage 6 clustered with those of passage 10. This suggested that the gene expression of SCs changed stronger during early than during late culture, possibly an effect of the adaptation to culture conditions, as previously observed (Chapter 3). We also noted that the second principal component separated the cultures within passage 2 but were not able to link this clustering to culture differences such as in vitro phenotype, breed, age of the animal, or CD151 positivity (Supplementary Fig. 3a).

We then studied the transcriptomic profiles of the observed phenotypes by performing differential expression analysis within time points. At passage 2, we found only few genes to be differentially expressed between the Stemness^{lo} and Stemness^{hi} phenotypes (Supplementary Fig. 3b). As observed before with flow cytometry, expression of *CD151* did not correlate with in vitro behaviour (Supplementary Fig. 3c). Instead, several genes were significantly upregulated in the 'Growth stop' cultures, mostly related to differentiation or to pathways that have previously been linked to the regulation of SC proliferation such as the PDGF and the EGF receptor tyrosine kinase families (Fig. 5b).[24,25] This suggested that cultures that were more prone to differentiation during the expansion phase had an increased risk of proliferative exhaustion. Yet, we did not observe a similar trend at passage 6 (Supplementary Fig. 3d). At passage 10, we found that the cultures clustered mostly by phenotype on the first principal component (Fig. 5c). Differential expression analysis between these two conditions identified 11 genes that were significantly upregulated in cultures with high stemness (Fig. 5d). These were primarily associated with differentiation as well as with differentiation-related pathways such as p38 MAPK (*MXRA8*) or TGF-β.[26,27] Genes that were significantly upregulated in cultures with low stemness were related to matrix interaction (*LOXL3*), the Wnt pathway (*DKK3*) or SC quiescence (*TFPI2*).[28–30]

Together, these expression profiles suggest that high expression of differentiation genes at early passage may be predictive for growth arrest but that a base-level expression is necessary to maintain effective differentiation capacity (Supplementary Fig. 3e).

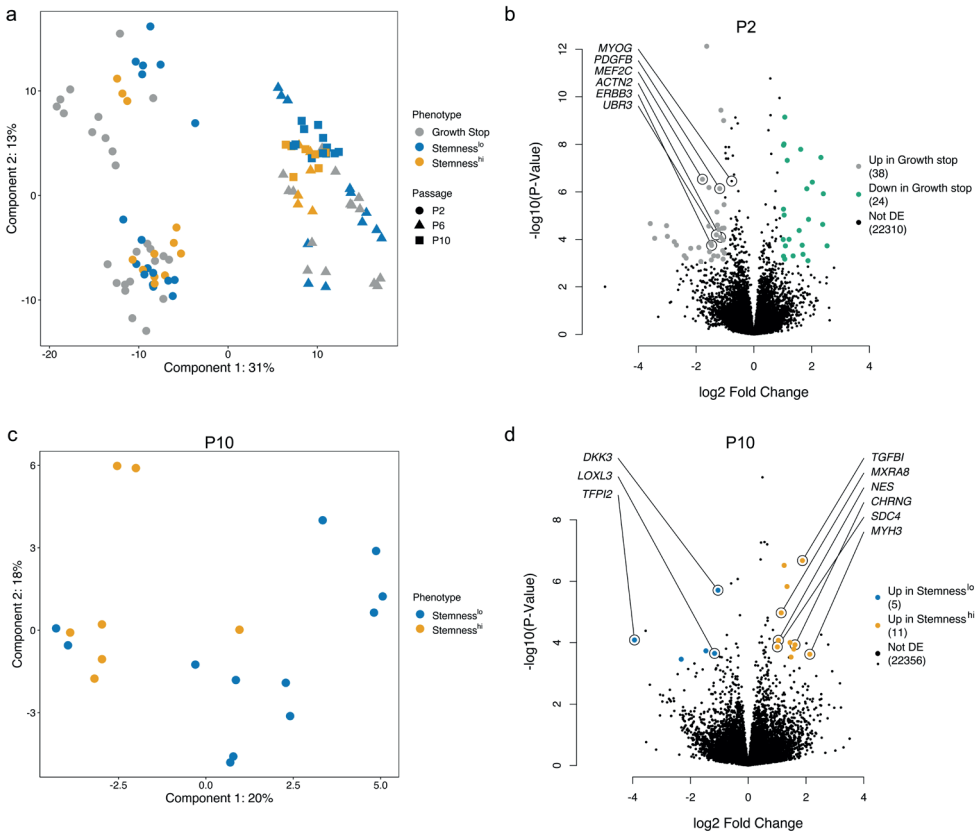

Figure 5: Transcriptional analysis of cultures at early and late passage indicate predictive power of differentiation-related genes.
a) Principal component analysis (PCA) of cultures at passage 2, 6 and 10 based on the 500 most differentially expressed genes, coloured by observed phenotype; points indicate individual samples; b) Volcano plot showing differentially expressed genes (points) at passage 2 between cultures that stop growing (grey) and those that continue (green); c) PCA of cultures at passage 10, where samples (points) are coloured by stemness; d) Volcano plot showing differential expression analysis at passage 10 between cultures with low and high stemness; DE = differentially expressed (logFC > 1, FDR < 0.05).

4.4 DISCUSSION

Adult stem cells such as SCs have scientific, regulatory, and consumer acceptance-related advantages over pluripotent stem cells or engineered cell lines, including simple protocols that enable their serum-free proliferation and differentiation (Chapters 2 & 3). However, their limited lifespan in vitro demands the necessity of regular sourcing of new cell batches to produce cultured meat on a commercial scale, introducing batch-to-batch variability that may impede the efficiency of the bioprocess. To evaluate the extent of this limitation, we characterised the differences between multiple batches of SCs during serum-free long-term culture, focusing on the two most process-relevant properties; proliferation and differentiation capacity.

We found that SC cultures exhibit a high degree of similarity within the first six passages (up to 20 PDs) of serum-free proliferation, generally supporting the possibility of regular cell sourcing of primary SCs to produce cultured meat. However, differences both in proliferation and differentiation capacity appeared as the cells aged, where we noted three main phenotypes: SCs that fully stopped proliferating between 20 and 25 PDs, SCs that continued proliferating but stopped differentiating between 25 and 30 PDs, and SCs that continued proliferating and differentiating up until 35 PDs.

Reduction of proliferation rate and loss of differentiation are two primary hallmarks of the loss of stemness in vitro.[31] Our observation that proliferation may continue while differentiation capacity decreases raises the questions to which degree these two processes are interconnected and whether they comprise the same or different phenomena. For instance, the steep decline that occurred for all cultures at the beginning of the experiment might be explained by the cells adapting to in vitro conditions, such as increased stiffness, a less complex extracellular environment compared to the muscle niche, or stress induced by cell handling,[32–35] as previously noted in Chapter 3. The growth stop that subsequently occurred in a subset of samples might thus be partly a result of failure to adapt, in addition to a manifestation of cellular ageing.[36] Whether these cells entered senescence or might be in a reversible cell cycle arrest (such as quiescence) was not assessed in this study and is subject to future investigations. Moreover, we found that cultures more prone to proliferative exhaustion had a higher base-level expression of differentiation-related genes. More research is needed to confirm this observation

and to clarify underlying biological mechanisms. For instance, studying cultures of both phenotypes by single-cell RNA sequencing may indicate whether base-level expression of myogenic genes is increased in all SCs prone to proliferative exhaustion or whether they contain a higher proportion of SCs committed to differentiation. As these cultures did not have higher fusion indices or showed significantly faster differentiation, future work needs to evaluate the potential of increased expression of differentiation markers during early proliferation as a predictive tool for lower in vitro survival.

The cultures that remained proliferative in this experiment exhibited pronounced differences in stemness, which we defined as the differentiation capacity at 30 PDs. The categorisation into two distinct phenotypes allowed the identification of differentially expressed genes, most prominently the relative increase of differentiation-related genes in the high-stemness group. However, we observed the decline of differentiation as a gradual process throughout the long-term culture, and therefore acknowledge that a binary categorization may not adequately represent the underlying biological process. As opposed to proliferative exhaustion, we did not find characteristics that could serve as a predictive tool for the decline of differentiation in proliferative cultures. Again, we hypothesise that readouts with higher resolution, such as single-cell RNA sequencing, may provide more nuanced insights into the cellular processes responsible for the observed behaviour. For instance, a subpopulation of SCs with higher myogenic potential may disappear upon long-term proliferation due to different growth rates, as previously described.[37]

In future work, alternative readouts may shed additional light on the observed phenomena of proliferative exhaustion and loss of differentiation capacity. These include investigation of epigenetic alterations with higher resolution methods than a global methylation assay (for instance by methylation or ATAC sequencing), as well as the study of metabolic shift or autophagy, which have previously been described as hallmarks of cellular ageing.[12] The cultures did not exhibit considerable CNV during long-term proliferation, nor did a specific CNV region explain either of the in vitro phenotypes. Nevertheless, assessment of DNA damage, other structural variation, as well as telomere shortening may provide further avenues for understanding the changes that SCs undergo upon prolonged culture.[38]

Finally, we observed a high similarity of proliferation and differentiation behaviour within cultures from the same animal. This suggests that the different phenotypes of in vitro ageing that manifested during long-term proliferation were (at least to

some extent) inherent to the cells already at the start of the culture, as opposed to entirely obtained throughout passaging. This might suggest that animal attributes, including specific genetic traits, can determine the course of SCs during in vitro culture. However, while the number of SCs that can be isolated from specific muscle locations or breeds may differ between animals,[14,16] we did not find a correlation between in vitro behaviour and animal characteristics such as age, breed or sex. Given the small differences between SCs especially at early PDs, we hypothesise that large sample sizes would be necessary to identify effects of animal metadata on SC in vitro behaviour. This observation is in accordance with studies in mice and humans that showed marginal or no differences in proliferation or differentiation between SCs from young and geriatric muscle,[39–42] or from different muscle groups.[43] On a DNA level, we did not find regions with CNVs that could be related to the observed in vitro phenotypes. However, this does not dismiss the hypothesis that genetic differences may at least partially determine in vitro behaviour. To fully address this question, it is necessary to follow up this initial investigation with higher-resolution methods that allow the identification of animal-specific SNPs, such as whole-genome or whole-exon sequencing.

By quantifying in vitro behaviour of cultures derived from multiple animals during long-term proliferation, this dataset provides a reference to inform the usage of primary bovine SCs to produce commercially relevant quantities of differentiated muscle tissue for cultured meat. Translation of this experimental setup to a larger scale in future studies that involve spinner-flask or bioreactor cultures would increase comparability to a commercial bioprocess. Nevertheless, the presented data highlights the importance of cellular in vitro ageing and the need for its prevention for upscaled cultured meat production.

4.5 MATERIAL & METHODS

4.5.1 Satellite cell isolation and sorting

Cells were isolated from skeletal muscle tissue of various cows (Table 1) by collagenase digestion (CLSAFA, Worthington; 1 h; 37°C), followed by filtering with 100 µm and 40 µm cell strainers to remove debris. For samples 4, 10, and 11, two separate samples were taken from the same muscle. Ammonium-Chloride-Potassium (ACK) was used to lyse red blood cells, and cells were plated in pre-sorting serum-free growth medium (ps-SFGM, Supplementary Table 1) on fibronectin-

coated (4 µg cm^{-2} bovine fibronectin; F1141, Merck/Sigma) culture flasks. After 72 h, satellite cells (SCs) were purified by harvesting the muscle tissue-derived cells, staining them for ITGA7 (APC) and ITGA5 (PE) and sorting for ITGA7+/ITGA5- SCs with fluorescence-activated cell sorting (FACS) using a MACSQuant Tyto Cell Sorter (Miltenyi). For sample 13, SCs were divided into 3 separate flasks post sorting.

Table 1: Sample overview

Culture ID	Breed	Age of cow (years)	Sex of cow	Tissue mass (g)	Number of SCs after sort (x103)	ITGA7+ cells at start (%)	PDs at start	Location
1	Belgian Blue	4.1	M	39.8	1568	99.6	5.4	Gluteus medius
2	Belgian Blue	4.0	M	42.1	764	99.4	4.1	Gluteus medius
3	Belgian Blue	4.1	M	40.6	1000	99.4	5.1	Gluteus medius
4A	Belgian Blue	~1	M	41.9	2483	99.4	6.3	Gluteus medius (left)
4B	Belgian Blue	~1	M	41.1	1770	99.3	6.4	Gluteus medius (right)
5	Belgian Blue	~1	M	38.6	327	99.3	6.4	Gluteus medius
6	Holstein-Fresian	3.8	F	40.3	330	99.1	6.4	Gluteus medius
7	Holstein-Fresian	4.9	F	42.4	428	99.3	5.8	Gluteus medius
8	Holstein-Fresian	6.7	F	40.8	2200	99.6	5.5	Gluteus medius
9	Holstein-Fresian	4.0	F	41.2	440	99.3	6.0	Gluteus medius
10A	Limousin	1.8	M	38.0	1502	99.1	4.8	Gluteus medius (left)
10B	Limousin	1.8	M	41.7	948	99.0	5.0	Gluteus medius (right)
11A	Limousin	1.7	M	42.3	1100	99.0	5.0	Gluteus medius (left)
11B	Limousin	1.7	M	39.3	887	99.3	5.3	Gluteus medius (right)
12	Holstein-Fresian	10.2	F	80.1	2417	98.4	4.9	Semitendinosus
13-1	Holstein-Fresian	7.6	F	82.4	2820	99.3	3.8	Semitendinosus
13-2	Holstein-Fresian	7.6	F	82.4	2820	99.3	3.8	Semitendinosus
13-3	Holstein-Fresian	7.6	F	82.4	2820	99.3	3.8	Semitendinosus
14	Belgian Blue	~2.5	Unk.	Unk.	Unk.	98.4	6.5	Gluteus medius

4.5.2 Cell culture

SCs were cultured in serum-free growth medium (SFGM, Supplementary Table 1) on vessels coated with laminin-521 (0.5 µg cm^{-2}, LN521-05, Biolamina) for 1 h prior to seeding. Cells were seeded at a density of 5 x 10^3 cm^{-2} and passaged every 4 days for passages 1 to 4; and seeded at a density of 7.5 x 10^3 cm^{-2} and passaged every 5-7 days for passages 5 to 12. For passages lasting 5 days and longer, SFGM was exchanged on day 3.

4.5.3 Long-term proliferation assay

SCs from 14 different animals (indicated by sample number), 3 different locations of the same animal (indicated by sample letter), or from 3 replicates of the same starting population (sample 13, indicated by appendices -1, -2, -3) were cultured as described above over the course of 64 days. Cell proliferation was estimated by counting the cells on a Countess 3 (Thermo Fisher) at the end of each passage. Samples for RNA sequencing and DNA arrays were taken from the harvested cells as described below. In addition, flow cytometry and myogenic differentiation assays were performed each passage. For selected passages (indicated in respective figures), immunofluorescent staining and flow cytometry-based assays were performed.

4.5.4 Flow cytometry

The SCs were stained for ITGA7 (APC), ITGA5 (PE) and CD151 (PE/Cy-7) and measured on a MACSQuant 10 Flow Analyzer (Miltenyi Biotec) after each passage to assess SC purity (indicated by ITGA7+ / ITGA5- cells) and SC state (indicated by the ratio of $CD151^+$ to $CD151^-$ SCs, see Chapter 3).

4.5.5 Myogenic differentiation assay

SCs were plated in SFGM at a density of 5 x 10^4 cm^{-2} on vessels coated with 0.5% Matrigel (354230, Corning) for 24 h. Differentiation was induced by first washing with PBS before switching to serum-free differentiation media (SFDM, Table 1), or SFDM supplemented with differentiation-augmenting ERK-inhibitor SCH772984 (S7101, SelleckChem) at 1 µM where indicated (Figs. 1c, d; Supplementary Figs. 1, 2).[18] The extent of differentiation was either followed over 7 days by taking Brightfield images every 24 h, or by computing fusion indices at 72 h or 96 h. For this, the SCs were fixed and stained for desmin as described below. Fusion indices were

computed by dividing nuclei within desmin-positive areas by the total amount of nuclei using the MetaXPress software.

4.5.6 Immunofluorescent staining

SCs were fixed using 4% paraformaldehyde, permeabilized in 0.5% triton X-100, and blocked with 2% bovine serum albumin (BSA). The cells were stained with primary antibodies for desmin (D1033, Sigma Aldrich) and secondary antibodies αMouse-AF488 (Sigma Aldrich). Hoechst 33342 (Thermo Fisher Scientific) was added as a nuclei stain prior to imaging on the ImageXpress Pico Automated Cell Imaging System (Molecular Devices).

4.5.7 RNA sequencing

4.5.7.1 Sample preparation

After passage 2, 6, and 10, 5 x 10^5 cm^{-2} SCs of the different cultures were pelleted and lysed in Lysis/Binding Buffer of the Dynabeads mRNA DIRECT Micro Kit (Invitrogen). The lysates were split into technical replicates and mRNA was isolated according to the protocol of the kit. The mRNA was reverse transcribed using the PCR-cDNA Barcoding Kit (SQK-PCB109, Oxford Nanopore Technologies). After barcoding, cDNA libraries of the three timepoints were sequenced separately using SpotOn flow cells and a MinION sequencer (Oxford Nanopore Technologies), resulting in three separate data sets (one per time point).

4.5.7.2 Data processing and analysis

After mapping the sequencing reads to the bosTau9 (ARS UCD1.2.98) reference genome using minimap2[44] and quantification using Salmon[45], the three data sets were combined. Gene counts were transformed to transcripts per million and normalised using the varianceStabilizingTransformation function (DESeq2).[46,47] The samples were clustered using principal component analysis (PCA) based on the 500 most variable genes, either within or including all the time points (as indicated). Differentially expressed genes were computed between indicated comparisons using Wald's significance test.

4.5.8 DNA array

To estimate copy number variation, DNA was isolated from muscle and from snap-frozen cell pellets at P2, P5, P8, P10 and P12 using the GenElute Mammalian Genomic DNA Miniprep Kit (Merck). DNA array was performed using the BovineHD Genotyping BeadChip (WG-450-1002, Illumina) and scanned on an iScan System (Illumina).[48] Copy number variation regions (CNVR) were classified as 'deletion' with a score of -1, 'amplification' with a score of 1, or 'unaltered' with a score of 0. Distances between the samples were calculated using Jaccard's Matrix. Hierarchical clustering was computed with the unweighted pair group method with arithmetic mean (UPGMA).

4.5.9 Methylation assay

The proportion of methylated cytosines in the total DNA were measured using the Global DNA Methylation Assay Kit by following the supplier's protocol (ab233486, Abcam) with the same DNA samples used for the DNA array. Colorimetric intensities were measured for each sample in duplicates at 450 nm on a Victor X-5 plate reader (Perkin Elmer). The slope of the standard curve was calculated using logarithmic regression.

4.5.10 Statistical analyses

Statistical analyses were carried out using Prism 9 (Graphpad Software). To assess the significance of differences in fusion index between the phenotypes (Figs. 2a, b; Figs. 3g, h), one-way ANOVA were performed and, if applicable, followed up with Dunnett's multiple comparison tests. Replicates consisted of SCs differentiated in separate wells. To assess the significance of differences between proportions of 5-methyl cytosines (Figs. 5c, d), a two-way ANOVA was performed, where replicates consisted of grouped cultures at each passage and phenotype.

4.6 BIBLIOGRAPHY

1. Post, M. J. Cultured beef: medical technology to produce food. *J. Sci. Food Agric.* **94**, 1039–1041 (2014).
2. Datar, I. & Betti, M. Possibilities for an in vitro meat production system. *Innov. Food Sci. Emerg. Technol.* **11**, 13–22 (2010).
3. Parodi, A. *et al.* The potential of future foods for sustainable and healthy diets. *Nat. Sustain.* **1**, 782–789 (2018).
4. Post, M. *et al.* Scientific, sustainability and regulatory challenges of cultured meat. *Nat. Food* **1**, 403–415 (2020).
5. Hubalek, S., Post, M. J. & Moutsatsou, P. Towards resource-efficient and cost-efficient cultured meat. *Curr. Opin. Food Sci.* **47**, 100885 (2022).
6. Specht, E. A., Welch, D. R., Rees Clayton, E. M. & Lagally, C. D. Opportunities for applying biomedical production and manufacturing methods to the development of the clean meat industry. *Biochem. Eng. J.* **132**, 161–168 (2018).
7. Bryant, C., van Nek, L. & Rolland, N. C. M. European Markets for Cultured Meat: A Comparison of Germany and France. *Foods* **9**, 1152 (2020).
8. Genovese, N. J., Domeier, T. L., Telugu, B. P. V. L. & Roberts, R. M. Enhanced Development of Skeletal Myotubes from Porcine Induced Pluripotent Stem Cells. *Sci. Rep.* **7**, 41833 (2017).
9. Bar-Nur, O. *et al.* Direct Reprogramming of Mouse Fibroblasts into Functional Skeletal Muscle Progenitors. *Stem Cell Rep.* **10**, 1505–1521 (2018).
10. Su, Y. *et al.* Establishment of Bovine-Induced Pluripotent Stem Cells. *Int. J. Mol. Sci.* **22**, 10489 (2021).
11. Ancel, S., Stuelsatz, P. & Feige, J. N. Muscle Stem Cell Quiescence: Controlling Stemness by Staying Asleep. *Trends Cell Biol.* **31**, 556–568 (2021).
12. Ogrodnik, M. Cellular aging beyond cellular senescence: Markers of senescence prior to cell cycle arrest in vitro and in vivo. *Aging Cell* **20**, e13338 (2021).
13. Melzener, L., Verzijden, K. E., Buijs, A. J., Post, M. J. & Flack, J. E. Cultured beef: from small biopsy to substantial quantity. *J. Sci. Food Agric.* **101**, 7–14 (2021).
14. Melzener, L. *et al.* Comparative analysis of cattle breeds as satellite cell donors for cultured beef. 2022.01.14.476358 Preprint at https://doi.org/10.1101/2022.01.14.476358 (2022).
15. Metzger, K., Tuchscherer, A., Palin, M.-F., Ponsuksili, S. & Kalbe, C. Establishment and validation of cell pools using primary muscle cells derived from satellite cells of pig skeletal muscle. *Vitro Cell. Dev. Biol. - Anim.* **56**, 193–199 (2020).
16. Riddle, E. S., Bender, E. L. & Thalacker-Mercer, A. E. Transcript profile distinguishes variability in human myogenic progenitor cell expansion capacity. *Physiol. Genomics* **50**, 817–827 (2018).
17. Stern-Straeter, J. *et al.* Characterization of human myoblast cultures for tissue engineering. *Int. J. Mol. Med.* **21**, 49–56 (2008).
18. Eigler, T. *et al.* ERK1/2 inhibition promotes robust myotube growth via CaMKII activation resulting in myoblast-to-myotube fusion. *Dev. Cell* **56**, 3349-3363.e6 (2021).
19. da Silva, J. M. *et al.* Genome-wide copy number variation (CNV) detection in Nelore cattle reveals highly frequent variants in genome regions harboring QTLs affecting production traits. *BMC Genomics* **17**, 454 (2016).

20. Hay, E. H. A. *et al.* Genomic predictions combining SNP markers and copy number variations in Nellore cattle. *BMC Genomics* **19**, 441 (2018).
21. Alkan, C., Coe, B. P. & Eichler, E. E. Genome structural variation discovery and genotyping. *Nat. Rev. Genet.* **12**, 363–376 (2011).
22. Sidler, C., Woycicki, R., Kovalchuk, I. & Kovalchuk, O. WI-38 senescence is associated with global and site-specific hypomethylation. *Aging* **6**, 564–574 (2014).
23. Turner, D. C. *et al.* DNA methylation across the genome in aged human skeletal muscle tissue and muscle-derived cells: the role of HOX genes and physical activity. *Sci. Rep.* **10**, 15360 (2020).
24. Contreras, O., Córdova-Casanova, A. & Brandan, E. PDGF-PDGFR network differentially regulates the fate, migration, proliferation, and cell cycle progression of myogenic cells. *Cell. Signal.* **84**, 110036 (2021).
25. Golding, J. P., Calderbank, E., Partridge, T. A. & Beauchamp, J. R. Skeletal muscle stem cells express anti-apoptotic ErbB receptors during activation from quiescence. *Exp. Cell Res.* **313**, 341–356 (2007).
26. Han, S.-W. *et al.* DICAM inhibits angiogenesis via suppression of AKT and p38 MAP kinase signalling. *Cardiovasc. Res.* **98**, 73–82 (2013).
27. Rathbone, C. R. *et al.* Effects of transforming growth factor-beta (TGF-β1) on satellite cell activation and survival during oxidative stress. *J. Muscle Res. Cell Motil.* **32**, 99–109 (2011).
28. Kraft-Sheleg, O. *et al.* Localized LoxL3-Dependent Fibronectin Oxidation Regulates Myofiber Stretch and Integrin-Mediated Adhesion. *Dev. Cell* **36**, 550–561 (2016).
29. Fukada, S. *et al.* Molecular Signature of Quiescent Satellite Cells in Adult Skeletal Muscle. *STEM CELLS* **25**, 2448–2459 (2007).
30. Yin, J. *et al.* Dkk3 dependent transcriptional regulation controls age related skeletal muscle atrophy. *Nat. Commun.* **9**, 1752 (2018).
31. Konigsberg, I. R. Clonal Analysis of Myogenesis. *Science* **140**, 1273–1284 (1963).
32. Engler, A. J. *et al.* Myotubes differentiate optimally on substrates with tissue-like stiffness: pathological implications for soft or stiff microenvironments. *J. Cell Biol.* **166**, 877–887 (2004).
33. Romagnoli, C., Iantomasi, T. & Brandi, M. L. Available In Vitro Models for Human Satellite Cells from Skeletal Muscle. *Int. J. Mol. Sci.* **22**, 13221 (2021).
34. Hirsch, C. & Schildknecht, S. In Vitro Research Reproducibility: Keeping Up High Standards. *Front. Pharmacol.* **10**, (2019).
35. Charville, G. W. *et al.* Ex Vivo Expansion and In Vivo Self-Renewal of Human Muscle Stem Cells. *Stem Cell Rep.* **5**, 621–632 (2015).
36. Rubin, H. Cell aging in vivo and in vitro. *Mech. Ageing Dev.* **98**, 1–35 (1997).
37. Ono, Y. *et al.* Slow-dividing satellite cells retain long-term self-renewal ability in adult muscle. *Development* **139**, e707 (2012).
38. Lai, T.-P., Wright, W. E. & Shay, J. W. Comparison of telomere length measurement methods. *Philos. Trans. R. Soc. B Biol. Sci.* **373**, 20160451 (2018).
39. García-Prat, L., Sousa-Victor, P. & Muñoz-Cánoves, P. Functional dysregulation of stem cells during aging: a focus on skeletal muscle stem cells. *FEBS J.* **280**, 4051–4062 (2013).
40. Sousa-Victor, P. *et al.* Geriatric muscle stem cells switch reversible quiescence into senescence. *Nature* **506**, 316–321 (2014).

41. Shefer, G., Van de Mark, D. P., Richardson, J. B. & Yablonka-Reuveni, Z. Satellite-cell pool size does matter: defining the myogenic potency of aging skeletal muscle. *Dev. Biol.* **294**, 50–66 (2006).
42. Alsharidah, M. *et al.* Primary human muscle precursor cells obtained from young and old donors produce similar proliferative, differentiation and senescent profiles in culture. *Aging Cell* **12**, 333–344 (2013).
43. Randolph, M. E. & Pavlath, G. K. A muscle stem cell for every muscle: variability of satellite cell biology among different muscle groups. *Front. Aging Neurosci.* **7**, (2015).
44. Li, H. Minimap2: pairwise alignment for nucleotide sequences. *Bioinformatics* **34**, 3094–3100 (2018).
45. Patro, R., Duggal, G., Love, M. I., Irizarry, R. A. & Kingsford, C. Salmon provides fast and bias-aware quantification of transcript expression. *Nat. Methods* **14**, 417–419 (2017).
46. Love, M. I., Huber, W. & Anders, S. Moderated estimation of fold change and dispersion for RNA-seq data with DESeq2. *Genome Biol.* **15**, 550 (2014).
47. Anders, S. & Huber, W. Differential expression analysis for sequence count data. *Genome Biol.* **11**, R106 (2010).
48. Rincon, G., Weber, K. L., Van Eenennaam, A. L., Golden, B. L. & Medrano, J. F. Hot topic: Performance of bovine high-density genotyping platforms in Holsteins and Jerseys. *J. Dairy Sci.* **94**, 6116–6121 (2011).

4.7 SUPPLEMENTARY INFORMATION

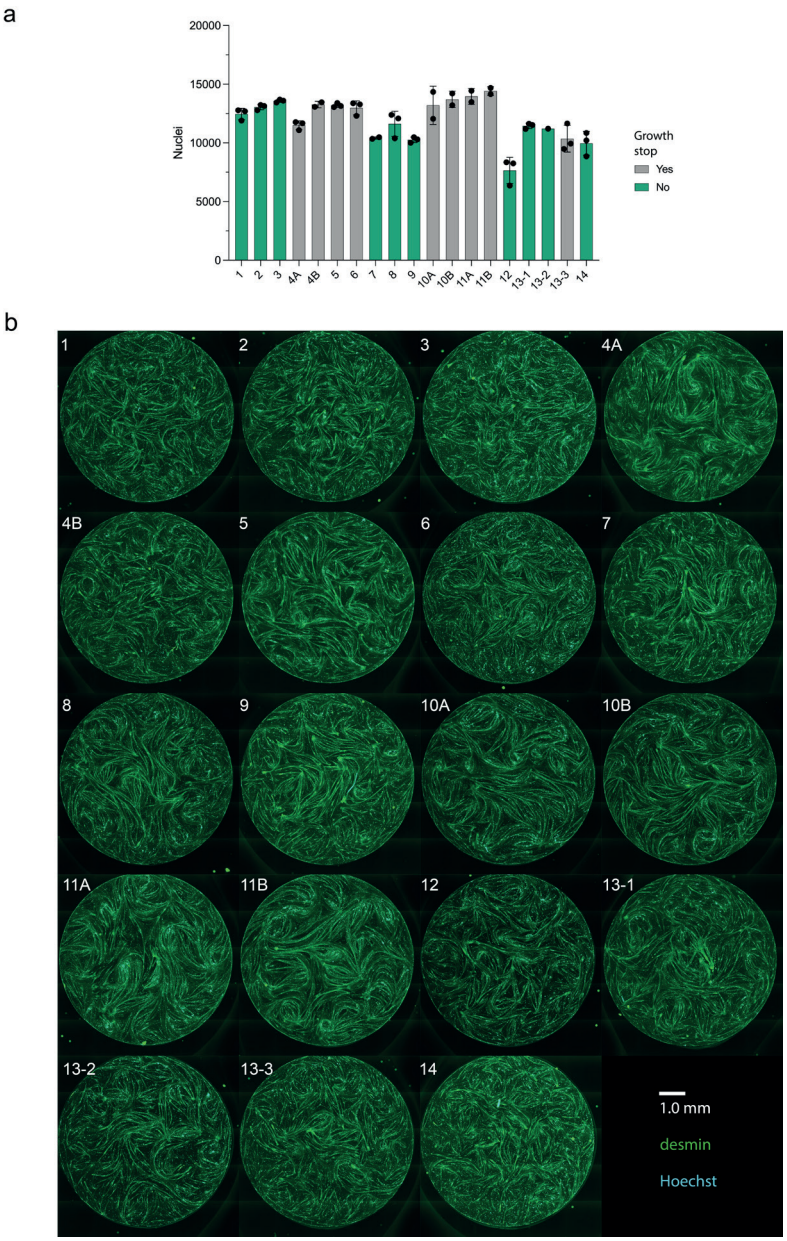

Supplementary Figure 1: Differentiation capacity at passage 2 (related to Figure 2).
a) Nuclei count related to Figure 2a, green bars indicate cultures that continue to proliferate beyond 30 PDs; n = 3; b) Representative fluorescent staining for desmin in culture after 96 h in SFDM + SCH772984, corresponding to (a).

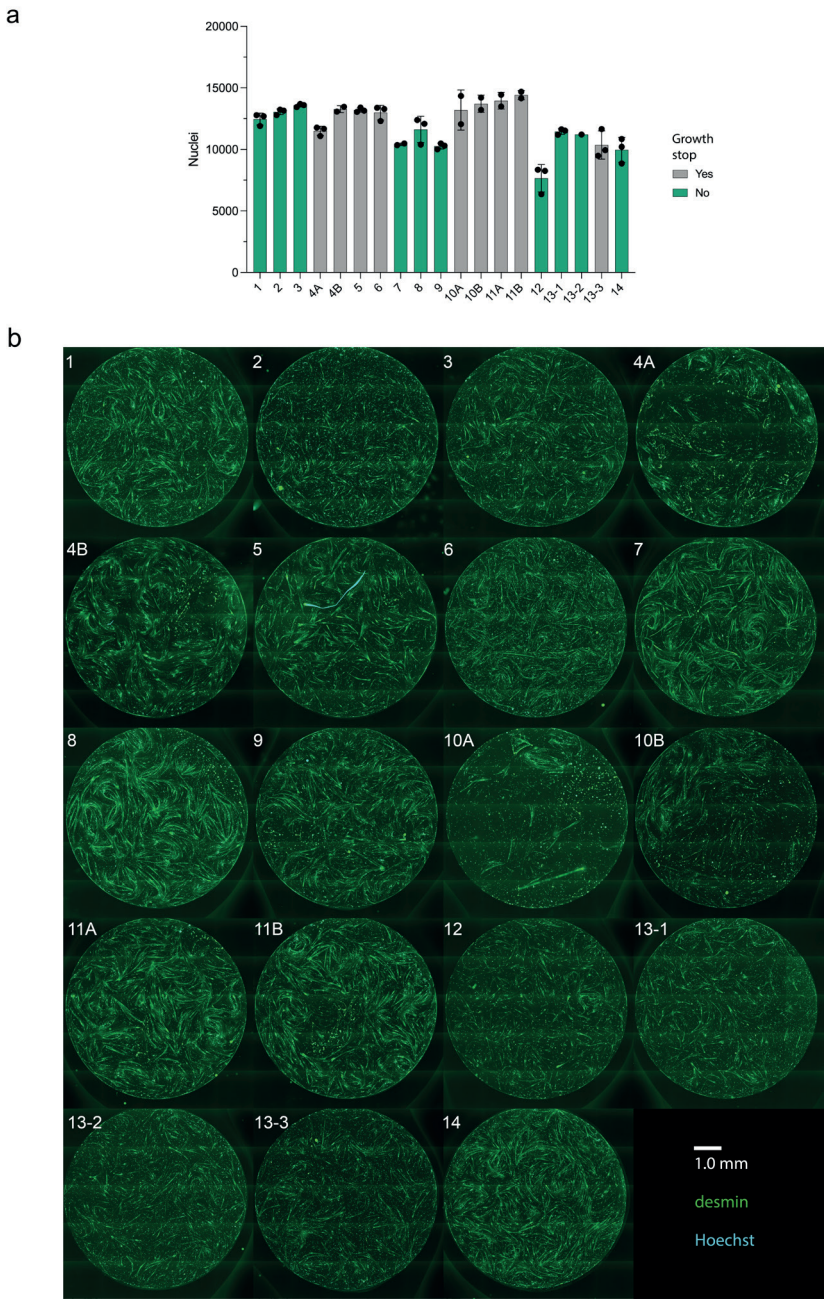

Supplementary Figure 2: Differentiation capacity at passage 6 (related to Figure 2).
a) Nuclei count related to Figure 2b, green bars indicate cultures that continue to proliferate beyond 30 PDs; n = 3; b) Representative fluorescent staining for desmin in culture after 96 h in SFDM + SCH772984, corresponding to (a), areas with myotube detachment prior to fixation (4A, 10A, 10B) were excluded from fusion index quantification.

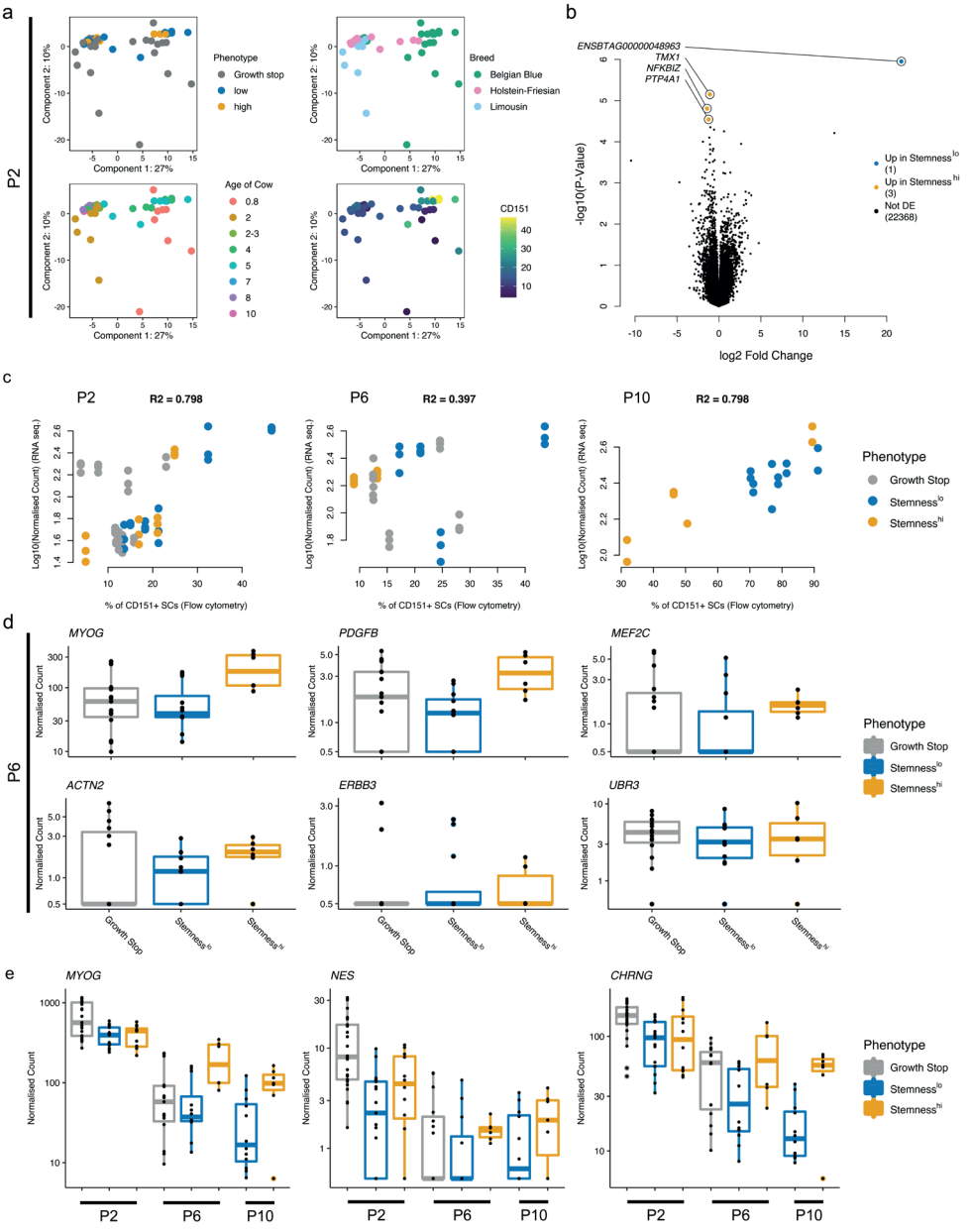
a
P2
Component 2: 10%
Component 1: 27%
Phenotype
Growth stop
low
high
Breed
Belgian Blue
Holstein-Friesian
Limousin
Age of Cow
0.8
2
2-3
4
5
7
8
10
CD151
40
30
20
10
b
ENSBTAG00000048963
TMX1
NFKBIZ
PTP4A1
-log10(P-Value)
log2 Fold Change
Up in Stemness lo (1)
Up in Stemness hi (3)
Not DE (22368)
c
P2
R2 = 0.798
P6
R2 = 0.397
P10
R2 = 0.798
Log10(Normalised Count) (RNA seq.)
% of CD151+ SCs (Flow cytometry)
Phenotype
Growth Stop
Stemness lo
Stemness hi
d
P6
MYOG
PDGFB
MEF2C
ACTN2
ERBB3
UBR3
Normalised Count
Growth Stop
Stemness lo
Stemness hi
Phenotype
e
MYOG
NES
CHRNG
Normalised Count
P2
P6
P10
Phenotype
Growth Stop
Stemness lo
Stemness hi

► Supplementary Figure 3: Transcriptomic analysis of SC cultures at passage 2 and 6 (related to Figure 5).
a) Principal component analysis (PCA) of cultures at passage 2 based on the 500 most variable genes, coloured by phenotype (topleft), donor breed (topright), donor age (bottom left) or proportion of quiescent ($CD151^+$) SCs; b) Volcano plot showing differentially expressed genes (points) at passage 2 between cultures with low and high stemness; c) Correlation of CD151 expression determined by RNA sequencing with CD151-positivity as measured by flow cytometry for passage 2 (left), 6 (centre) and 10 (right), colours indicate phenotype, R-squared (R2) values are given for pearson correlations d) Boxplots showing size factor-corrected gene expression counts (log10-scale) for indicated genes at passage 6, samples (points) grouped by phenotype, e) Boxplot showing size factor-corrected gene expression counts (log10-scale) for muscle-related genes at passage 2, 6 and 10, samples (points) grouped by phenotype.

Supplementary Table 1: Media formulations.

#	Component	Reference	Concentration
Pre-sorting serum-free growth medium (ps-SFGM)			
1	DMEM/F-12	21331-020, Gibco	
2	α-linolenic acid	L2376, Sigma Aldrich	1.0 µg ml^{-1}
3	FGF-2	100-18B, Peprotech	10 ng ml^{-1}
4	Human Serum Albumin	Rc HA NW20, Richcore Lifesciences	5.0 mg ml^{-1}
5	HGF	100-39H, Peprotech	5 ng ml^{-1}
6	Hydrocortisone	H0135, Sigma Aldrich	36 ng ml^{-1}
7	IGF-1	100-11, Peprotech	100 ng ml^{-1}
8	IL-6	200-06, Peprotech	20 ng ml^{-1}
9	ITSE	00-101, biogems	1%
10	GlutaMax	35050-061, Gibco	1%
11	Glucose	G7021, Sigma Aldrich	17.7 mM
12	L-ascorbic acid 2-phosphate (Vitamin C)	A8960, Sigma Aldrich	155 µM
13	PDGF-BB	100-14B, Peprotech	10 ng ml^{-1}
14	Penicillin/Streptomycin/ Amphotericin (PSA)	17-745E, Lonza	1%
15	VEGF	100-20 Peprotech	10 ng ml^{-1}
Serum-free growth medium (SFGM)			
1	DMEM/F-12	21331-020, Gibco	
2	α-linolenic acid	L2376, Sigma Aldrich	1.0 µg ml^{-1}
3	FGF-2	100-18B, Peprotech	10 ng ml^{-1}
4	Human Serum Albumin	Rc HA NW20, Richcore Lifesciences	5.0 mg ml^{-1}
5	HGF	100-39H, Peprotech	50 ng ml^{-1}
6	Hydrocortisone	H0135, Sigma Aldrich	36 ng ml^{-1}
7	ITSE	00-101, biogems	1%
8	GlutaMax	35050-061, Gibco	1%
9	Glucose	G7021, Sigma Aldrich	17.7 mM
10	L-ascorbic acid 2-phosphate (Vitamin C)	A8960, Sigma Aldrich	155 µM
11	PSA	17-745E, Lonza	1%
12	Triiodothyronine	T6397, Sigma Aldrich	30 nM
Serum-free differentiation medium (SFDM)			
1	DMEM/F-12	21311-020, Gibco	
2	EGF-1	AF-100-15, Peprotech	10 ng ml^{-1}
3	Human Serum Albumin	Rc HA NW20, Richcore Lifesciences	0.5 mg ml^{-1}
4	ITSE	00-101, biogems	2%
5	L-ascorbic acid 2-phosphate (Vitamin C)	A8960, Sigma Aldrich	40 µM
6	Lysophosphatidic acid (LPA)	L7260, Sigma Aldrich	1 µM
7	MEM Amino Acids Solution	11130-051, ThermoFisher	0.50%
8	$NaHCO_3$	P2256, Sigma Aldrich	6.5 mM
9	PSA	17-745E, Lonza	1%
10	Soy hydrolysates	58903C, Merck	1%

Chapter 5

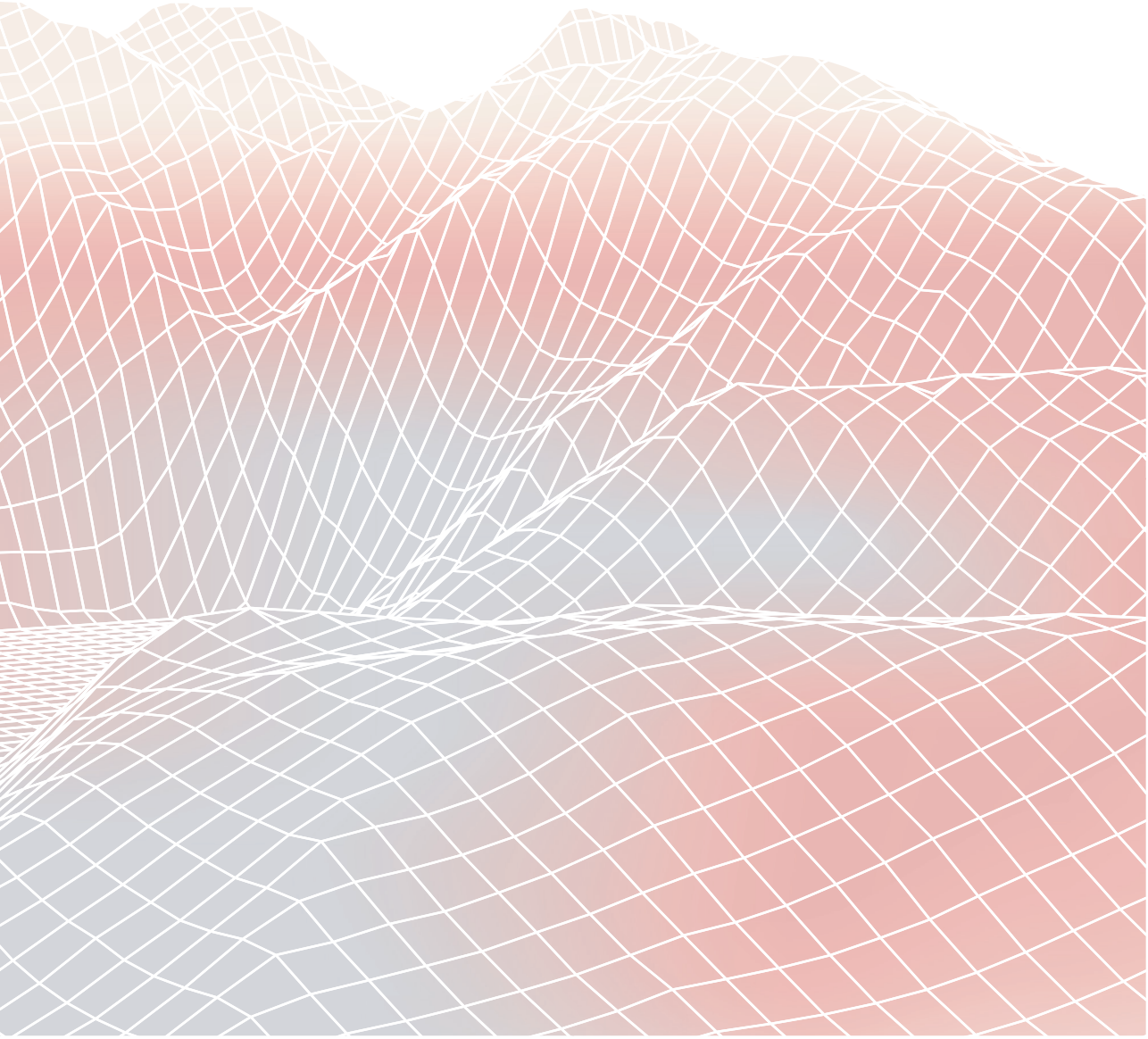

OPTIMISED P38α/β INHIBITION FOR MAINTENANCE OF SC STEMNESS IN AN UPSCALED CULTURED MEAT BIOPROCESS

Tobias Meßmer
Lieke Schaeken
Dhruv Raina
Joanna Papadopoulos
Joana Pimenta
Lea Melzener
Sergio Spaans
Rui Hüber
Mark Post
Joshua Flack

5.1 ABSTRACT

The production of commercially relevant quantities of cultured meat from primary adult stem cells, such as bovine satellite cells (SCs), requires a large number of population doublings ex vivo. However, self-renewal capacity and the ability for effective differentiation, the two primary hallmarks of stemness, decline upon prolonged in vitro cell culture. Transgene-free, small molecule-based interventions can affect the stemness of SCs by targeting a variety of cellular pathways, including through the inhibition of p38α/β-MAPK (p38i) by SB203580. Although well established in cell culture, it is unclear whether these interventions translate to an animal component-free bioprocess, which includes serum-free cell expansion in upscaled suspension cultures and the construction of alginate-based bioartificial muscles. Here, we characterised p38i by studying the effect of SB203580 during long-term serum-free culture. We found that proliferation rate and late differentiation capacity were increased by p38i through SB203580 when cells were cultured on laminin-coating, but not on vitronectin-coating as used in microcarrier-based spinner cultures. This coating dependency was circumvented by using the more selective p38α/β inhibitor PH797804, suggesting potential off-target effects of SB203580. Assessment of transcriptomic changes upon p38i further indicated that commitment towards myogenic fate was suppressed during proliferation, pointing to a possible mechanism of action. Together, these findings suggest that maintenance of SC stemness through p38i is preserved under serum-free conditions but that the compound SB203580 is incompatible with a bioprocess involving vitronectin coating.

5.2 INTRODUCTION

Cultivated meat technology aims to produce edible skeletal muscle from stem cells that are proliferated and differentiated ex vivo.[1,2] The commercialisation of this novel technology requires solving a multitude of interconnected scientific, technical and logistic challenges, including removal of animal-derived components from the bioprocess, reduction of cost and scaling up production from proof of concept to significant quantities.[3–6] The development of low-cost, serum-free media for proliferation and differentiation indicates significant progress in the field.[7–9] However, creating large amounts of functional cell mass from relatively small initial sample sizes requires a high replicative capacity of cells. For instance, a 1 mg starting cell population (which could feasibly be derived from one muscle biopsy) needs to divide at least 30 times to create approximately 1 ton of cultured meat.[5] During this period, cultured cells undergo a variety of genetic, epigenetic, morphological and metabolic changes including reduced proliferation rate, hypertrophy, protein misfolding or DNA damage, which may limit their applicability in the cultured meat bioprocess.[10]

Immortalised cell lines, induced pluripotent stem cells and adult stem cells have been proposed as cell sources for producing skeletal muscle in vitro, with distinct advantages and disadvantages in respect to their application in cultured meat technology.[11] While cell lines and pluripotent stem cells possess a high regenerative potential, their creation usually utilises genetic modification, and complex protocols are necessary to reach a sufficient extent of myogenic maturation.[12–16] By contrast, adult stem cells possess a strong ability to differentiate into functional tissue but their capacity to self-renew and effectively differentiate may be exhausted during long-term in vitro culture, a phenomenon described as loss of stemness.[17]

Bovine satellite cells (SCs), the precursors of skeletal muscle fibres, considerably decrease in stemness at 20-25 population doublings (PDs) in vitro (Chapter 4).[7,18] Therefore, to produce commercially relevant quantities of cultured meat, it is necessary to identify transgene-free interventions that maintaining proliferation and differentiation capacity beyond 25 PDs. Various compounds have been reported to affect SC proliferation and differentiation in vivo or in vitro by targeting key cellular pathways including ERK,[19,20] p38α/β,[18] Wnt signalling,[21] Notch signalling,[22] TGF-β / SMAD,[23] and others. Most prominently, inhibition of p38α/β increases the expression of stemness-marker Pax7, as well as fusion indices of bovine SCs at higher PDs in culture conditions that include animal-derived coatings and serum-containing media.[18]

Few studies have been conducted in consideration of a full, serum-free bioprocess that includes in vitro expansion, high-volume cultures such as spinner flasks or bioreactors, and animal component-free tissue formation. We therefore screened compounds for their potential of increasing the stemness of bovine SCs in a serum-free long-term culture, and assessed a promising candidate, the p38α/β inhibitor SB203580, for its potential usage in an approximated production process of cultivated skeletal muscle.

5.3 RESULTS

5.3.1 Inhibition of p38α/β increases proliferation rate and extents differentiation capacity

We first set up a screening experiment involving compounds that target a variety of pathways including p38, MEK/ERK, TGF-β, SMAD, JAK/STAT, PI3K/Akt, and others (Supplementary Table 1, Fig. 1a). Amongst these, only 9 out of 40 compounds led to cell survival beyond 6 experimental passages and the addition of 10 µM SB203580 resulted in the highest cumulative population doublings (PDs).

Based on this preliminary screen, and given its well-described effects on the stemness of bovine SCs (in serum-containing media), we studied the effect of p38-inhibitor SB203580 (p38i) in more detail throughout 10 passages in serum-free growth medium. Within a 35-day culture period, SCs gained more PDs when cultured with p38i ($p = 0.018$, Fig. 1b) due to a faster proliferation rate compared to control that also declined slower after passage 8 ($p = 0.020$, Fig. 1c). This observation was consistent with previous reports in serum-containing media.[18,24] Concurrently, CD151 expression marking a 'quiescent' in vitro SC state (Chapter 3) was consistently lower in p38i ($p = 0.048$, Fig. 1d), while the proportion of senescent cells tended to decrease at P5 ($p = 0.052$, Fig. 1e) and was significantly reduced at P8 ($p = 0.047$, Fig. 1f, Supplementary Fig. 1). Moreover, differentiation of SCs into myotubes, measured as fusion index, was increased by 11% ($p = 0.01$) at P10 in the presence of p38i during cell expansion, showing that differentiation capacity at high PDs was effectively preserved (Figs. 1g, h).

The stimulatory effects on proliferation rate were preserved across a variety of p38i compounds, and even more pronounced upon the addition of 10 µM PH797804 and 10 µM PD169316 compared to 10 µM SB203580, whereas naturally-occurring p38i compounds such as astaxanthin or tangeretin showed only a minor effect (Fig. 1i). These results suggested that p38i effectively improved the stemness in a serum-free environment and that a variety of compounds were able to stimulate this effect.

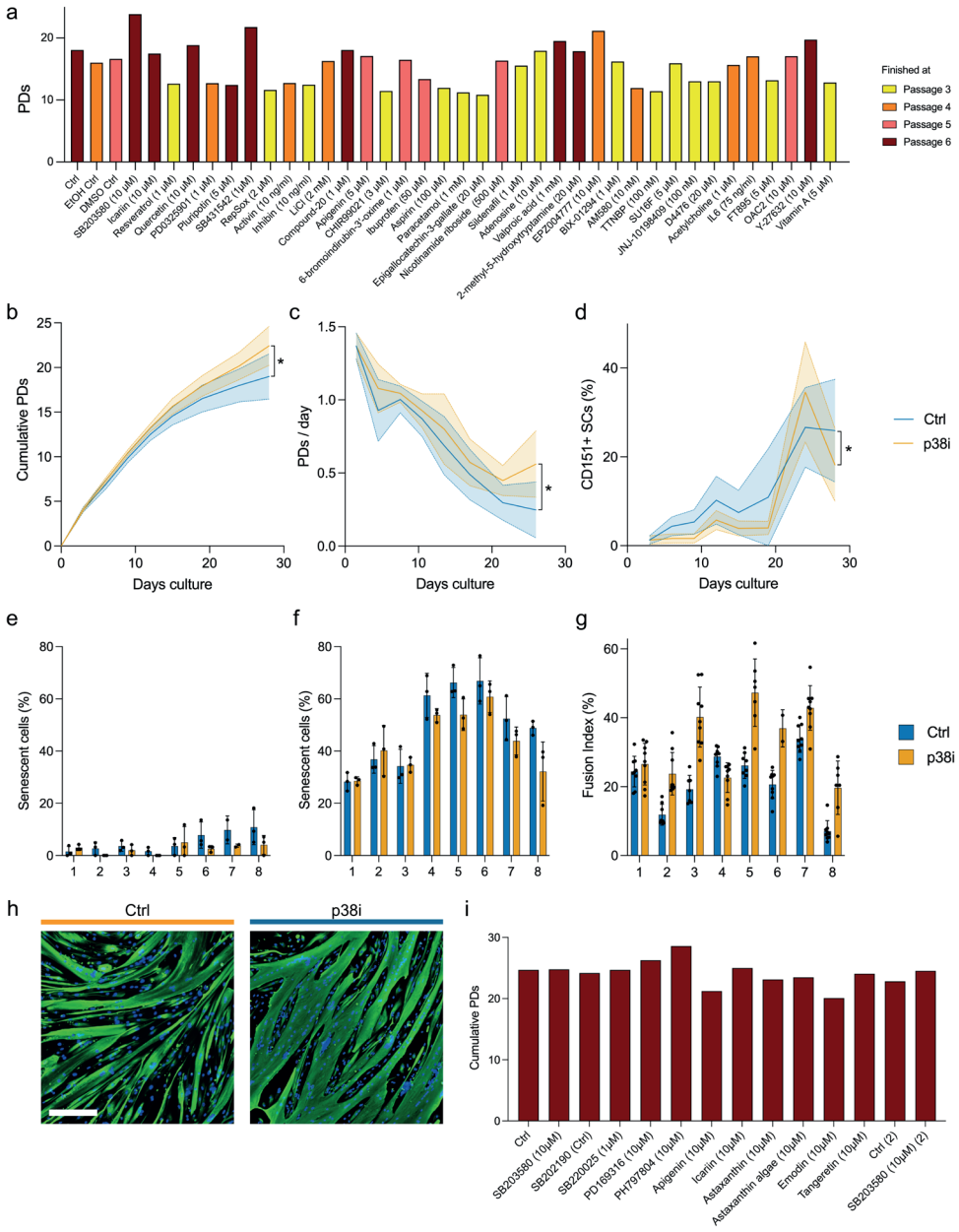

Figure 1: Supplementation of serum-free growth media with p38-inhibitor SB203580 increases proliferation rate and preserves differentiation capacity.
a) Cumulative population doublings (PDs) after the final harvest at indicated passage (colours) for denoted conditions; b) Mean cumulative population doublings of bovine SCs with (orange) or without (blue) 10 µM SB203580 (p38i) over time; shaded areas within dashed lines indicate standard deviation around the mean, significance was estimated using a two-way ANOVA, n = 8; c) As (b) but showing mean proliferation rate, measured as PDs per day

for each passage; d) Similar to (c) but showing mean percentage of CD151$^+$ SCs, determined via flow-cytometry; e) Percentage of senescent SCs at P5, measured using β-galactosidase staining; points indicate measurement from one image of the same well; numbers on x-axis indicate biological replicate; f) As (e) but at P8; g) Fusion indices of n = 8 SC cultures derived from different animals after 10 passages in SFGM with or without p38i, differentiated in SFDM for 96 h; points indicate measurement from one image of the same well; numbers on x-axis indicate biological replicate; h) Representative fluorescent images corresponding to (g), green = desmin, blue = Hoechst, scale bar = 500 µm; i) Cumulative PDs of indicated p38-inhibiting compounds as media supplements to SFGM after 27 days of in vitro culture; * $p < 0.05$.

5.3.2 Inhibition of p38α/β suppresses transcriptomic signatures for myogenic differentiation

To study cellular mechanisms underlying the preservation of stemness upon p38i, we analysed the transcriptomes of SCs at P2, P4, P7, P10 and P13 over a long-term culture supplemented with SB203580. Again, the proliferation rate upon p38i was increased while CD151 positivity was consistently lower than in the control condition (Supplementary Figs. 2a-c).

We next performed dimensionality reduction via principal component analysis of the 500 most variable genes. In the first principal component, the samples clustered neither by treatment nor by culture passage. In the second principal component, the samples of P7 and P10 treated with p38i clustered with the control samples at P2 and P4, suggesting the p38i-treated samples showed fewer transcriptional signs of cellular ageing than the same time points in control (Fig. 2a). While expression of mitotic genes decreased over time for both conditions, the expression of quiescence-marker *FN1* (Chapter 3) was consistently lower in p38i (Supplementary Fig. 2d). Differential expression analysis between all control and p38i samples showed that 937 genes were significantly upregulated by p38i, while 832 genes were significantly downregulated (Fig. 2b). As indicated by pathway enrichment analysis using GO biological processes the downregulated genes were predominantly related to muscle differentiation and contraction (Fig. 2c).[25] This indicates that p38i impeded commitment of SCs towards differentiation when cells reached confluence. Indeed, the average expression of genes related to differentiation (GO:0006936, Fig. 2d), as well as the expression of differentiation-related genes (Supplementary Fig. 2e) from P2 to P13 indicated that SC myogenic commitment tends to increase over time with passaging, but in a reduced fashion in p38i compared to control. Microscopic images of SCs at the end of the passage (Fig. 2e) supported this observation as the emergence of myotubes was suppressed by p38i, which was previously described in serum-containing conditions.[18]

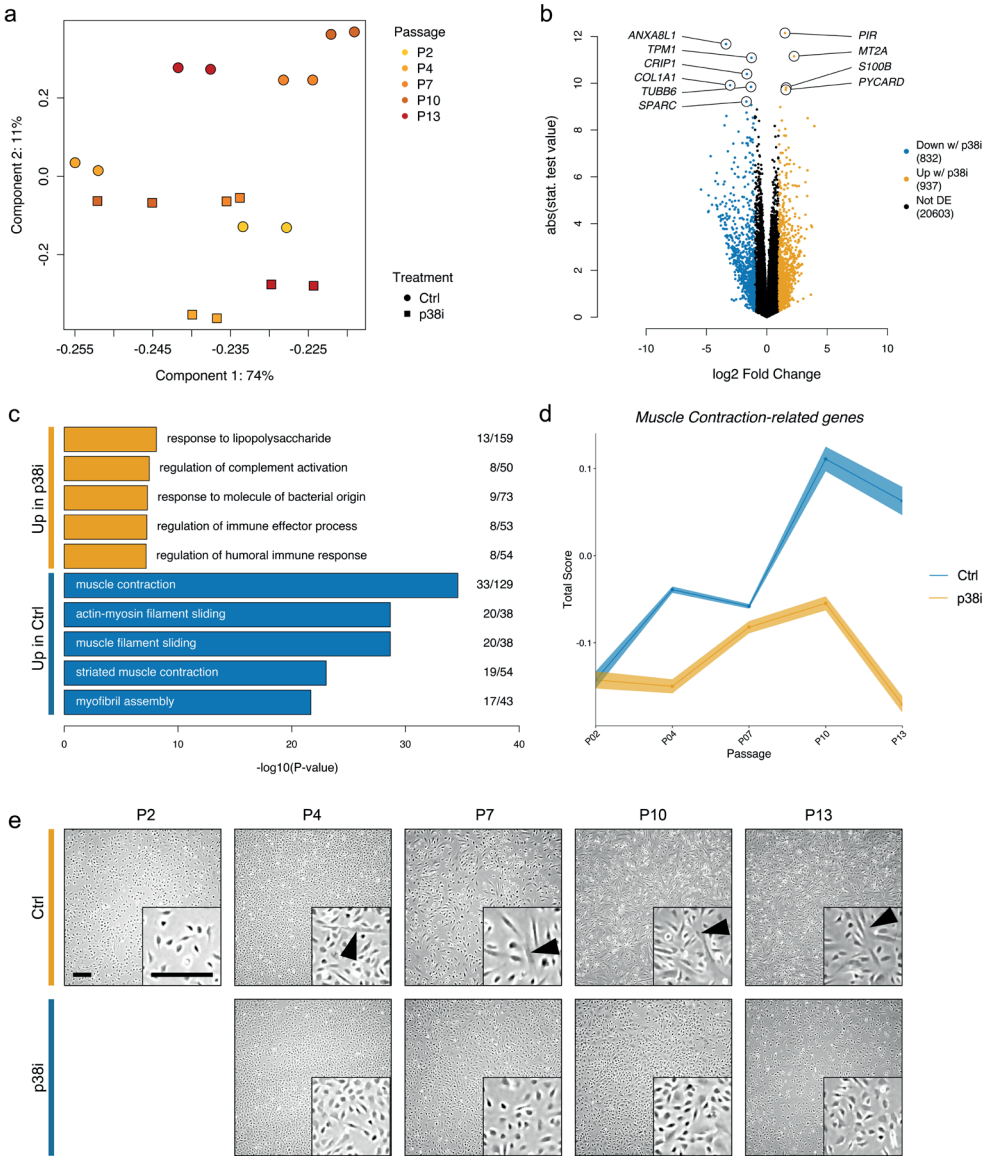

Figure 2: Inhibition of p38α/β suppresses premature differentiation of SCs during proliferation.
a) Principal component analysis of 500 most variable genes throughout different timepoints (colors) of long-term culture with (squares) and without (points) p38, quantified by RNA sequencing; b) Volcano plot showing differentially expressed genes (colored points) between Ctrl and p38i-treated SCs; c) GO-terms corresponding to significantly upregulated (orange) and downregulated (blue) genes from (b); d) Mean-expression of genes related to muscle contraction (GO:0006936); shaded area indicates standard deviation around mean, n = 3, e) Brightfield images after indicated passages with and without p38i, arrowheads in enlarged images point to committed SCs, scale bar = 200 µm.

5.3.3 p38i during proliferation increases muscle-specific protein expression in BAMs

Production of cultivated meat requires myogenic differentiation of SCs in three-dimensional (3D) constructs rather than on a two-dimensional (2D) surface. Thus, we next assessed whether the preservation of differentiation capacity through p38i would translate to animal component-free, RGD-alginate-based bioartificial muscles (BAMs).

We fabricated BAMs at P4, P6, P8, and P10, corresponding to 11, 16, 23, and 27 average PDs, respectively (Fig. 3a) and studied the extent of differentiation by determining total protein yield and the expression of muscle-specific proteins by ELISA and immunofluorescent stainings. First, total protein yield per BAM decreased over time, but was significantly higher in p38i than in control at P8 (Fig. 3b). Second, BAMs from SCs cultured in p38i formed more defined and enlarged myofibres than in control, and showed an increased expression of muscle-specific proteins desmin, myosin-HC and actin (Fig. 3c). Third, quantification of desmin (Fig. 3d) and myosin-7 (Fig. 3e) protein levels indicated a significant increase at P8 in p38i over control. This trend was also observed at P10, although insufficient numbers of control BAMs survived until the end of the BAM differentiation period to allow statistical testing between the conditions. Similar results were obtained in a second replicate (Supplementary Fig. 3).

Together, these data suggested that the increased stemness following p38i observed with 2D differentiation translated to BAM constructs, suggesting its benefit for producing cultured meat at lab-scale in an animal component-free environment.

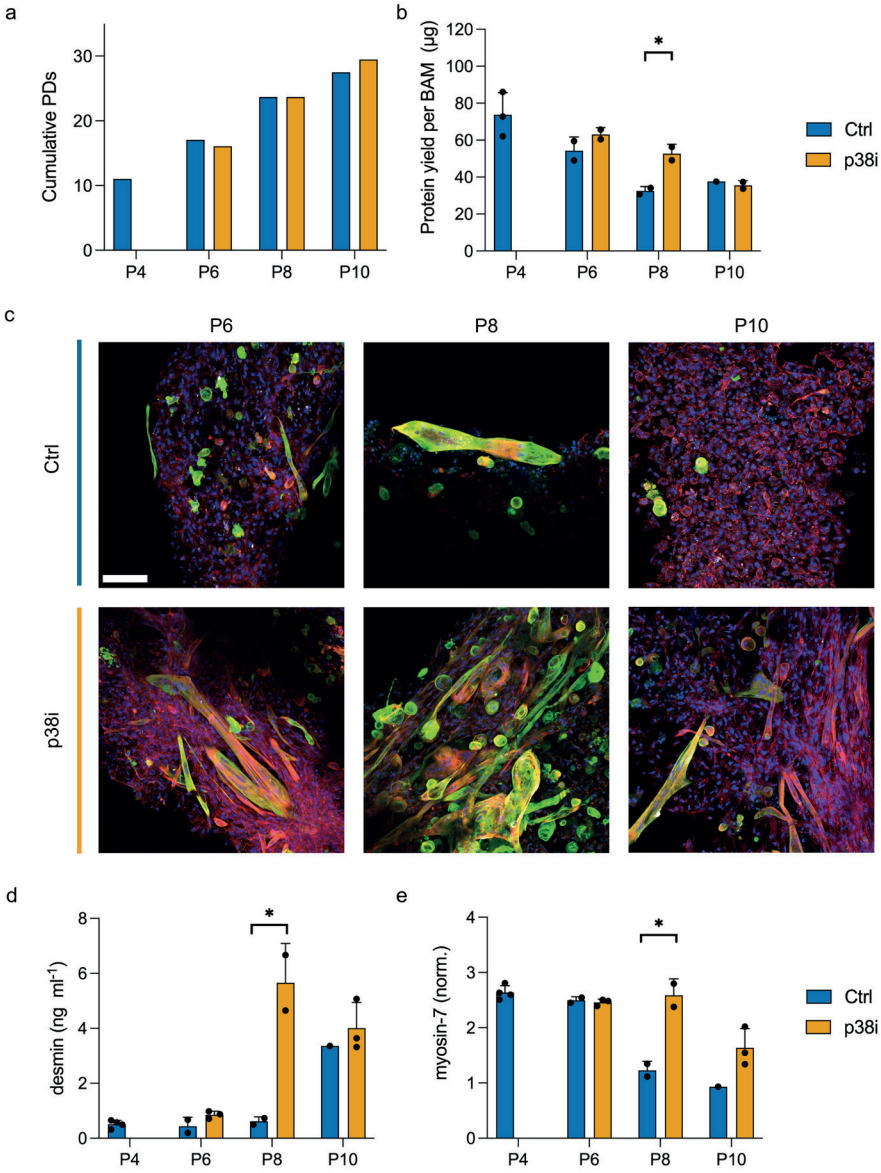

Figure 3: Preservation of differentiation capacity within animal component-free bioartificial muscles (BAMs) is improved by p38i during long-term culture.
a) Cumulative PDs of SCs grown with (orange) and without (blue) 10 µM SB203580 (p38i) before being used for BAMs at P4, P6, P8 and P10; b) Mean protein dry weight per BAM resulting from SCs grown with (orange) and without (blue) 10 µM SB203580; c) Immunofluorescent images of BAMs after 6, 8 and 10 passages with (bottom) and without (top) p38i, green = myosin-1, red = F-actin, blue = Hoechst, scale bar = 100 µM; d) Quantification of desmin expression in 20 µg ml^{-1} total protein solution in BAMs corresponding to (b), determined via ELISA; e) Quantification of myosin-7 expression normalised against meat lysate in BAMs corresponding to (b), determined via ELISA; * $p < 0.05$.

5.3.4 Off-target effects of SB203580 might cause coating-dependent decrease in proliferation

Finally, to make sufficient numbers of SCs to produce cultivated meat at commercial level, cells need to be grown in 3D vessels such as spinner flasks or bioreactors. To test whether the beneficial effect on proliferation rate and differentiation capacity at higher PDs is preserved on vitronectin(VN)-coated microcarriers in spinner flasks,[26] we ran three independent cultures with and without p38i using SB203580 as p38α/β inhibitor. To our surprise, we found that the confluence on the microcarriers was consistently lower in p38i ($p = 0.032$, Fig. 4a) due to a slower proliferation rate in each of the three replicates (Fig. 4b), indicating hampered cell growth through p38i. This observation was supported by the analysis of metabolites in the culture media, where we observed an increase in glucose consumption over time (indicated by a decrease in glucose concentration) in control but not in p38i (Fig. 4c), as well as lower concentrations of metabolic products including lactate (Fig. 4d) and LDH (Fig. 4e). Moreover, differentiation at the end of each spinner culture did not show a clear trend and was more pronounced for p38i in replicate A, but diminished in replicate B and C (Fig. 4f), suggesting that the preservation of differentiation capacity observed in 2D was not preserved in spinner cultures.

We considered coating of the microcarriers with VN as opposed to lam-521 used in the culture flask as well as off-target effects of SB203580 as possible explanations for this observation. We therefore cultured SCs on 2D flasks coated with lam-521 or VN and included PH797804 as an alternative inhibitor of p38α/β. We found that proliferation between lam-521 and VN was comparable in control but was hampered through p38i by SB203580 on VN (Fig. 4g). This effect was rescued by PH797804, where PDs were consistently higher than in control on both VN and lam-521. We then analysed p38α/β activity through measuring the phosphorylation of p38-target HSP27 via western blot (Fig. 4h).[27] While p38 levels were similar across samples, p-HSP27 decreased in SB203580 and completely diminished in PH797804, independently of whether the cells were grown on lam-521 or VN. This hints towards off-target effects of SB203580, rather than reduced inhibition of p38α/β on VN, that might explain its coating-dependency.

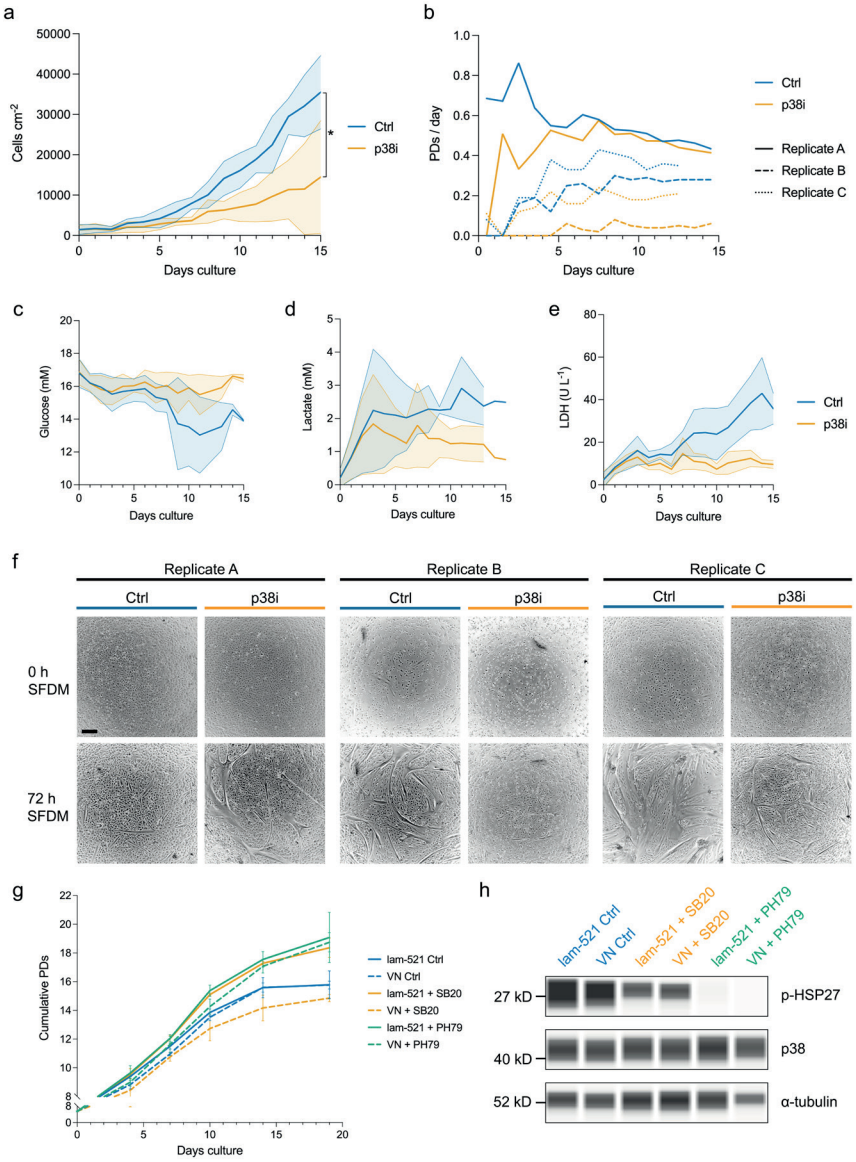

Figure 4: Growth reduction through p38i in vitronectin-coated microcarrier-based spinner flask cultures.
a) Mean cell density on microcarriers during spinner flask cultures with (orange) and without (blue) 10 µM SB203580, shaded areas within dashed lines indicate standard deviation around the mean, n = 3; b) Proliferation rate in each separate replicate of spinner flask cultures with (orange) and without (blue) 10 µM SB203580; c) Mean glucose concentration in the growth media corresponding to (a), n = 3; d) Mean lactate concentration in the growth media corresponding to (a), n = 3; e) Mean lactate dehydrogenase (LDH) concentration in the growth media corresponding to (a), n = 3; f) Brightfield images of SCs at the end of each spinner culture after 0 h and 72 h in SFDM, scale bar = 200 µm; g) Growth rate of SCs grown on Iam-521 (solid lines) or VN (dashed lines) in control media (blue) or with p38i via SB203580 (10 µM, orange) or PH797804 (10 µM, green), n = 2; h) Western blot of SCs after 48h on Iam-521 or VN in SFGM with DMSO (Ctrl), SB203580 or PH797804.

5.4 DISCUSSION

The pivotal challenge for advancing cultured meat technology towards commercialisation is the development of a robust, animal component-free, scalable and cost-effective bioprocess. Cells used in this process must be capable of a large number of cell divisions while maintaining the ability to differentiate. The term 'stemness' defines the ability of stem cells to self-renew while maintaining their capacity to make effective fate decisions. However, bovine SCs are limited both in continuous proliferation and in differentiation capacity and it is therefore essential to maintain stemness more efficiently during prolonged in vitro cultures.

Interventions to maintain a functional phenotype have to be compatible with a consumer-accepted bioprocess and should therefore be free from genetic modification.[28] Modification of cell behaviour for instance through culture media, coating, or physical parameters are likely less prone to consumer scrutiny.[7,29–32] In the preliminary screen of small molecule compounds and proteins that theoretically affect stemness, we tested primarily for continuous proliferation as one of the two hallmarks of stemness, using a serum-free growth medium. As shown in Chapter 4, the proliferation rate of bovine SCs decreases after 20 PDs in serum-free culture conditions and only a subset of cultures reach more than 30 PDs. Thus, rescuing proliferation capacity was considered a necessary prerequisite for stemness-maintaining compounds, and we assumed that compounds that increase proliferation rate have a high likelihood of also preserving differentiation capacity, as observed through p38α/β-MAPK inhibition, FGF2 or YAP activation in SCs, or for hypoxic conditions in mesenchymal stem cells.[18, 33-35] However, it needs to be acknowledged that this experimental setup has two main limitations. First, it may identify compounds that preserve differentiation capacity but attenuate proliferation rate as false negatives, which has been observed for high levels of HGF[36] or the Sirt1 activator resveratrol in C2C12, although these studies did not systematically assess in vitro differentiation in a long-term setup.[37] Second, interventions that increase or preserve proliferation rate may be independent of or negatively affect differentiation capacity. This may lead to the identification of false positive stemness compounds as observed for TGFβ1[38] or Notch signalling[39], which can be mitigated by testing for differentiation capacity in follow-up experiments.

Despite these limitations, our initial screen identified SB203580 as a potential stemness compound. Given its well-described role in serum-containing conditions,

we followed-up by studying additional readouts including differentiation, CD151-positivity, and cellular senescence. Indeed, p38α/β inhibition positively affected all measured parameters, leading to the conclusion that the maintenance of stemness through SB203580, which is well described under serum-containing conditions,[18,24] is preserved in a serum-free culture. Exploring the cellular mechanisms correlated with this effect via RNA sequencing and flow cytometry, we found p38i both kept SCs in a more activated ($CD151^-$) in vitro state by hampering transitions towards a quiescent ($CD151^+$) state (Fig. 1), and suppressed commitment towards differentiation (Fig. 2).

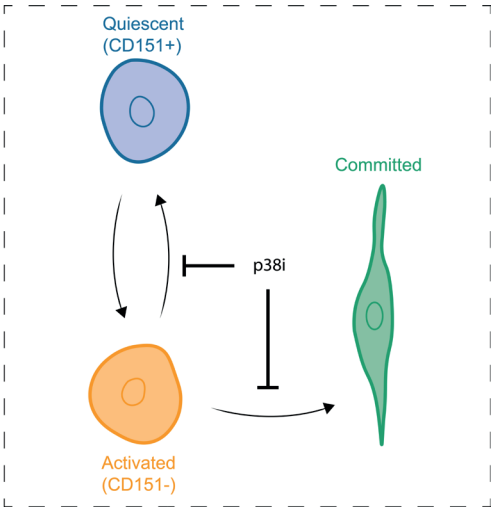

Figure 5: Effect of p38α/β inhibition on SC states.
In vitro, SCs transition between a quiescent-like ($CD151^+$) and an activated-like ($CD151^-$) state, which they may exit towards irreversible differentiation. Inhibition of p38α/β increases the proportion of activated SCs by hampering the transitions towards the quiescent and towards the committed state.

We speculate that p38i may have increased proliferation capacity while limiting the exhaustion of SCs capable of efficient differentiation, respectively (Fig. 6). However, while this study has demonstrated a strong correlation between the activated state and preservation of stemness, a causal relationship has not been established yet. Further studies are required to assess whether suppression of quiescence and suppression of myogenic commitment are needed in combination to maintain stemness or whether either is sufficient. The identification of compounds separating these effects (e.g. by lowering the ratio of $CD151^-$/$CD151^+$ SCs without suppressing

differentiation, or vice versa) may provide deeper insights into these mechanisms. Furthermore, studying the effect of p38α/β activation on differentiation (e.g. by TNF-α, IL-1 or CSF-1)[40] or preventing myogenic commitment by different measures, e.g. via different pathways or by passaging before cells reach confluence, may shed further light on the role of pre-differentiation on stemness.[41,42]

It is most likely that the suppression of the quiescent state and myogenic commitment are merely two of multiple factors by which p38i improves stemness, and that SC ageing comprises more than changes in SC states. Studying the effect of p38i on a single-cell level, e.g. by single-cell RNA sequencing as opposed to bulk RNA sequencing, may give better insights into alterations beyond cell states. Intracellular changes other than SC state dynamics, such as DNA damage, epigenetic alterations, or mitochondrial dysfunction, are key hallmarks of in vitro ageing but have not been assessed in this study.[43] Although we have not observed major changes on a DNAlevel within 12 in vitro passages (Chapter 4), studying whether and how p38i affects genetic, epigenetic and metabolic changes during SC ageing would be necessary to expand our understanding of the underlying molecular mechanisms by which it maintains SC stemness.

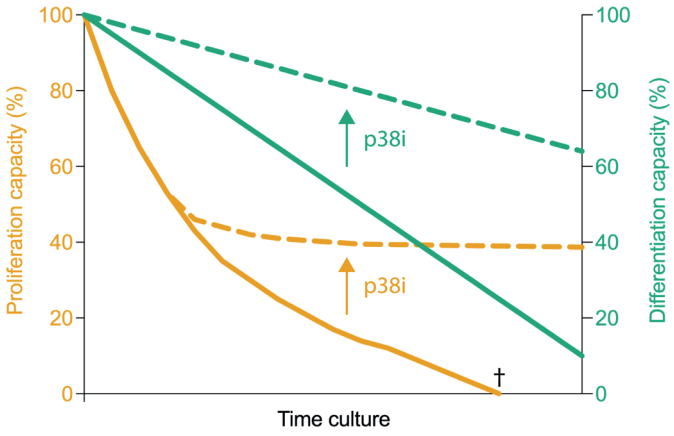

Figure 6: Effect of p38α/β inhibition on SC stemness.
In vitro ageing leads to a loss of stemness, which can be measured through assessing proliferation and differentiation capacity. Differentiation capacity gradually decreases with prolonged culture. Loss of proliferation capacity may lead to proliferative exhaustion (†), e.g. due to cellular senescence, apoptosis, or repeated cell cycle exit upon terminal differentiation. Two effects of p38α/β Inhibition are the increases of proliferation and differentiation capacity.

Tissue culture flasks provide a biologically meaningful but insufficient model for a cultured meat production process, as both the large-scale expansion as well as the final tissue construction need to be performed in bioreactor environments.[44] Therefore, we next assessed the process compatibility of p38i by studying differentiation in 3D constructs (Fig. 3) and proliferation in an upscaled system such as spinner-flask cultures (Fig. 4). While the preservation of differentiation capacity translated to 3D animal component-free BAMs yielding higher total protein and increased expression of sarcomere-related proteins, we observed detrimental effects on the proliferation rate and late differentiation in spinners. As a major difference from the 2D model, we hypothesised that coating microcarriers with VN may have caused opposite effects of p38i through SB203580. Effects of coatings on SC stemness have been previously reported but to our knowledge, there is no published data on the interaction between p38α/β inhibition efficacy and the extracellular environment, i.e. coating.[45,46] When we tested this hypothesis, we found that the decline of proliferation rate on VN upon p38i was compound-dependent and could be rescued by PH797804, which has a higher potency and selectivity than SB203580.[47,48] As neither the activity of p38 nor its inhibition were differentially affected by the coatings, we assume that off-target effects might have been responsible for the opposing proliferation outcome. For instance, In the concentration used in this study, SB203580 has been shown to impede Akt/PKB activity, a pathway involved in SC proliferation and differentiation.[49,50] Given the association of vitronectin with IGF-binding proteins upstream of Akt/PKB, this pathway may indicate a possible link to the coating-dependency of these off-target effects.[51] Nevertheless, reduced proliferation rates through SB203580 on VN-coated flasks and a curbed subsequent differentiation suggested that maintenance of SC stemness through p38i by SB203580 was dependent on the used coating solution. For this reason, we conclude that p38i by SB203580 is not compatible with a VN-based upscaled cell production system, demanding a switch to either PH797804 or to an alternative suspension culture system, for instance with different microcarriers, microcarrier-coating or as aggregates.[52]

Lastly, to ensure the compatibility of p38i usage in a food-production process, it will be necessary to determine whether trace elements of the small molecules can be detected in the final food product, and if so, whether these are below or above limits potentially harmful for human consumption. Alternatively, we have found that other p38i compounds may have a similar effect to SB203580. These may potentially be used in lower concentrations due to a higher potency (PD169316,

PH797804), or have a lower health concern due to their natural occurrence in edible plants such as astaxanthin or tangeretin, although these plant-derived compounds would need to show a higher efficacy than those tested in this study.

In conclusion, the presented data exemplifies a workflow to identify potential stemness-promoting compounds in a testing environment that can be expanded to high-throughput screens, and moreover, to assess such compounds in a setting that resembles the bioprocess of cultured meat production. The efficacy of p38 inhibition appears context-dependent suggesting that surface coating or compound-specificity need to be adjusted when applying this intervention for optimal efficacy. In bovine SCs for instance, p38i by SB203580 was ineffective with vitronectin coating but worked well on cells cultured on laminin, while PH797804 showed high efficacy on both coatings. Inhibition of p38α/β MAPK allowed SC cultures to maintain 3D-differentiation capacity beyond 20 experimental PDs. Testing a multitude of compound libraries in a fashion similar to this study may further expand the in vitro boundaries of primary SC culture for its application in cultured meat.

5.5 MATERIALS & METHODS

5.5.1 Satellite cell isolation

Satellite cells (SCs) were isolated and purified as previously described (Chapter 2). In short, semitendinosus muscle was digested using collagenase (CLSAFA, Worthington; 1 h; 37°C) before being filtered with cell strainers. Red blood cells were lysed with Ammonium-Chloride-Potassium (ACK), and cells were plated in a pre-sorting serum-free growth medium (ps-SFGM, Supplementary Table 2) on vessels coated with fibronectin (4 µg cm^{-2} bovine fibronectin; F1141, Merck/Sigma).

After 72 h, the cell mixture was harvested, stained for ITGA7 (APC) and ITGA5 (PE) and sorted by FACS for ITGA7+/ITGA5- SCs using a MACSQuant Tyto Cell Sorter (Miltenyi).

5.5.2 Cell culture

Culture vessels for SCs were coated with laminin-521 (0.5 µg cm^{-2}, LN521-05, Biolamina) for 1 h before plating. SCs were plated at a density of 5 x 10^3 cm^{-2} in serum-free growth medium (SFGM, Supplementary Table 2) and harvested when approaching confluence (every 3-5 days). SB203580 (10 µM, S1076, Selleck) or PH797804 (10 µM, S2726, Selleck) was added to SFGM where denoted.

5.5.3 Long-term proliferation assay

For long-term proliferation assays (Figs. 1, 3), SCs were cultured as described above over the course of indicated days or passages with denoted compounds. At the end of each passage, each condition was counted (Countess 3, Thermo Fisher) and reseeded (at 5 x 10^3 cells cm^{-2}) if the cells grew >1 PDs during the passage. Myogenic differentiation assays, immunofluorescent staining, or flow cytometry assays were performed where denoted.

5.5.4 Flow cytometry

SC purity was assessed after each passage via flow cytometry using a MACSQuant10 Flow Analyzer (Miltenyi Biotec) by staining for ITGA5 (PE) and ITGA7 (APC). In addition, the cells were stained for CD151 (PE/Cy-7) to assess their cell state.

5.5.5 Myogenic differentiation assay

To assess differentiation capacity, SCs were plated in SFGM at a density of 5 x 10^4 cells cm^{-2} on vessels coated with 0.5% Matrigel. After 24 h, the cells were washed with PBS and differentiation was induced by switching to a serum-free differentiation media (SFDM, Supplementary Table 2). After 120 h in SFDM, the cells were fixed and stained for desmin as described under 5.5.7.

Fusion indices were computed by dividing nuclei within desmin-positive areas by the total amount of nuclei.[53]

5.5.6 RNA sequencing

5.5.6.1 Sample preparation

SCs were cultured with and without p38i (SB203580, 10 µM) over the course of 13 passages. After passage 2, 4, 7, 10 and 13, 5 x 10^5 cm^{-2} cells were pelleted and lysed in Lysis/Binding Buffer of the Dynabeads mRNA DIRECT Micro Kit (Invitrogen). Next, mRNA was isolated following the kits suggested workflow, and reverse transcribed using the PCR-cDNA Barcoding Kit (SQK-PCB109, Oxford Nanopore Technologies). The cDNA libraries were barcoded, loaded on SpotOn flow cells and sequenced using a MinION sequencer (Oxford Nanopore Technologies).

5.5.6.1 Data processing and analysis

The sequencing reads were mapped to the bosTau9 (ARS UCD1.2.98) reference genome using minimap2[54] and quantified using Salmon[55]. Gene counts were transformed to transcripts per million and normalised using the varianceStabilizingTransformation function (DESeq2)[56]. The samples were clustered using principal component analysis (PCA) based on the 500 most variable genes. Differentially expressed genes between all samples of control and p38i were computed using Wald's significance test.

5.5.7 Immunofluorescent staining

To study the expression of desmin, myosin-1 and F-actin during 2D and 3D differentiation, cells on plates (Fig. 1) and in BAMs (Fig. 2) were fixed using 4% paraformaldehyde, permeabilized in 0.5% Triton X-100, and blocked with 2% bovine serum albumin (BSA). The cells on plates were stained with primary antibodies for desmin (D1033, Sigma Aldrich) and secondary antibody α-Mouse-AF488 (Sigma Aldrich). BAMs were stained for myosin-1 (M7523, Sigma Aldrich) and secondary antibodies α-Mouse-AF488 (Sigma Aldrich), and for F-actin using Phalloidin-490LS (14479, Sigma Aldrich). Hoechst 33342 (Thermo Fisher) was added to stain nuclei prior to imaging. Images of 2D plates were captured using the ImageXpress Pico Automated Cell Imaging System (Molecular Devices), whereas BAMs were imaged using a Stellaris 5 confocal microscope (Leica Microsystems).

5.5.8 Animal component-free BAM fabrication

To create animal-component-free bioartificial muscles (BAMs), SCs were harvested as described and resuspended in SFDM + 10 mM lactate at 12 x 10^6 cells ml^{-1}. The cell solution was mixed 1:1 with 1.8 wt% functionalized alginate (0.9 mol% RGD) and injected around steel pillars.[57] Immediately after injection, the solution was crosslinked by immersing the pillars in 100 mM $CaCl_2$ for 5 min. The crosslinking solution was removed, and the BAMs were washed and then incubated in SFDM + 10 mM Lactate. Medium was exchanged on day 3 and day 7, which from day 3 onwards additionally contained 10 µM acetylcholine. After a total of 10 days, the BAMs were harvested for protein quantification and confocal microscopy.

5.5.9 Protein extraction & quantification

The harvested BAMs were washed, resuspended in an extraction buffer (600 mM NACl, 100 nM NaOH, complete mini protease inhibitors (Roche)[58]), homogenised using

a rotating pestle, and lysed with two freeze-thaw cycles. Cell debris was removed by transferring only the supernatant subsequent to centrifugation. For quantifying the protein yield per BAM, the samples were denatured at 60°C for 10 min and by adding SDS-TEABC (5% SDS, 50 mM TEABC (T7408, Sigma)). The concentration was determined using the Pierce BCA Protein Assay Kit (23235, Thermo Fisher), measuring absorbance at 570 nm on a Victor X-5 plate reader (Perkin Elmer).

Samples for western blot analysis (Fig. 4h) were harvested after 48 h in SFGM by washing twice with ice-cold PBS before adding RIPA protein lysis buffer (sc24948, Santa Cruz Biotechnology), supplemented with additional phosphatase inhibitor (78420, Thermo Fisher). The lysates were centrifuged, yielding supernatants that were used for protein quantification. BCA assay was used as described above to adjust protein concentrations for equal loading. The protein samples were separated using a 12-230kDa fluorescence separation module (SM-FL001, biotechne), stained for p-HSP27 (1:25, 9709, Cell Signalling), p-p38 (1:25, 9211, Cell Signalling), p38 (1:25, 8690, Cell Signalling), and α-tubulin (ab4074, abcam) and developed using a Jess automated western blotting system (biotechne).

5.5.10 Enzyme-linked immunosorbent assay

Relative concentrations of myosin-7 and desmin were determining using an enzyme-linked immunosorbent assay (ELISA). First, total protein was extracted from BAMs and quantified as described above. Capture antibodies (SMH1M, MAB1628, Merck; desmin, ab227651, Abcam, diluted in tris-buffered saline (TBS)) were coated on a Maxisorp 96-well plate (44-2404-21, Invitrogen) and blocked with TBS + 1% BSA. Dilution standards and protein samples were diluted in TBS containing 0.1% tween-20 and incubated for 120 h. The plate was washed three times with TBS-T and incubated with biotin-conjugated detection antibodies for myosin-7 or desmin for 1 h, again washed three times, and incubated with streptavidin-HRP. After incubation and washing, the was developed with 1-Step Ultra TMP-ELISA Substrate Solution (Thermo Fisher) until the reaction was stopped with 2 M H_2SO_4, and absorbance was measured at 450nm on a Victor X-5 (Perkin Elmer). Protein concentrations were computed by subtracting background values before performing linear regression of the standard curve. For myosin-7, concentrations were normalised against relative myosin-7 concentrations from a meat lysate.

5.5.11 Spinner-flask cultures

For large-scale experiments, cells were grown on Cytodex1 microcarriers (Corning), maintained in either 125 ml plastic spinner flasks (Corning), or 125 ml glass spinner flasks (Bellco) with a paddle-impeller. A custom-made magnetic platform was used for agitation. Microcarriers were conditioned with SFGM and 1 µg ml^{-1} vitronectin (Peprotech) for 1 h before cell seeding. For all replicates, initial cell seeding density was maintained between 1-3 x 10^5 cells cm^{-2}. Spinner culture agitation regime was as follows: 72 h at intermittent stirring (30 min off; 5 min on at 45 rpm), followed by continuous stirring at 45 rpm until the end of the culture. Medium exchanges were performed every 48 to 72 h (between day 3 and day 8 of the culture) or on a daily basis (day 8 onwards) to ensure adequate supply of nutrients and removal of waste products. Cultures were monitored daily by directly imaging microcarriers using an EVOS M5000 Imaging System (Thermo Fisher), as well as by performing a cell count using the Nucleocounter NC-200 (Chemometec) according to manufacturer's instructions.

5.5.12 Senescence assay

Senescence was measured with a β-galactosidase activity assay using the Senescence Detection Kit (QIA117, Sigma-Aldrich). In summary, cells were fixed with Fixative Solution, washed, and incubated in the Staining Solution Mix at 37°C overnight. Percentage of senescence cells was quantified by dividing cells with blue stainings by total cells. Positive control consisted of cells incubated with 100 nM doxorubicin for 72 h, negative control (at P8) consisted of SCs at P2.

5.5.13 Statistical analyses

Statistical analysis was performed in Prism 9 (Graphpad Software). For growth curves, proliferation rates and CD151 positivity over time (Figs. 1, 4), two-way ANOVAs were carried out with culture time and treatment as independent variables and replicates consisting of SCs from different animals. Significance of changes in relative protein expression (Fig. 3, Supplementary Fig. 3), senescence (Figs. 1e, f), and fusion indices (Fig. 1g) between control and p38i was assessed using paired two-tailed t-tests. Replicates consisted of cells from different donor animals (Figs. 1, 4) or of cells from the same donor animal cultured in different vessels or BAM constructs (Figs. 2, 3).

5.6 BIBLIOGRAPHY

1. Datar, I. & Betti, M. Possibilities for an in vitro meat production system. *Innov. Food Sci. Emerg. Technol.* **11**, 13–22 (2010).
2. Post, M. J. Cultured beef: medical technology to produce food. *J. Sci. Food Agric.* **94**, 1039–1041 (2014).
3. Parodi, A. *et al.* The potential of future foods for sustainable and healthy diets. *Nat. Sustain.* **1**, 782–789 (2018).
4. Post, M. *et al.* Scientific, sustainability and regulatory challenges of cultured meat. *Nat. Food* **1**, 403–415 (2020).
5. Melzener, L., Verzijden, K. E., Buijs, A. J., Post, M. J. & Flack, J. E. Cultured beef: from small biopsy to substantial quantity. *J. Sci. Food Agric.* **101**, 7–14 (2021).
6. Hubalek, S., Post, M. J. & Moutsatsou, P. Towards resource-efficient and cost-efficient cultured meat. *Curr. Opin. Food Sci.* **47**, 100885 (2022).
7. Stout, A. J. *et al.* Simple and effective serum-free medium for sustained expansion of bovine satellite cells for cell cultured meat. *Commun. Biol.* **5**, 1–13 (2022).
8. Messmer, T. *et al.* A serum-free media formulation for cultured meat production supports bovine satellite cell differentiation in the absence of serum starvation. *Nat. Food* **3**, 74–85 (2022).
9. Kolkmann, A., Essen, A., Post, M. & Moutsatsou, P. Development of a Chemically Defined Medium for in vitro Expansion of Primary Bovine Satellite Cells. *Front. Bioeng. Biotechnol.* **10**, (2022).
10. Ogrodnik, M. Cellular aging beyond cellular senescence: Markers of senescence prior to cell cycle arrest in vitro and in vivo. *Aging Cell* **20**, e13338 (2021).
11. Specht, E. A., Welch, D. R., Rees Clayton, E. M. & Lagally, C. D. Opportunities for applying biomedical production and manufacturing methods to the development of the clean meat industry. *Biochem. Eng. J.* **132**, 161–168 (2018).
12. Su, Y. *et al.* Establishment of Bovine-Induced Pluripotent Stem Cells. *Int. J. Mol. Sci.* **22**, 10489 (2021).
13. Genovese, N. J., Domeier, T. L., Telugu, B. P. V. L. & Roberts, R. M. Enhanced Development of Skeletal Myotubes from Porcine Induced Pluripotent Stem Cells. *Sci. Rep.* **7**, 41833 (2017).
14. Shoji, E., Woltjen, K. & Sakurai, H. Directed Myogenic Differentiation of Human Induced Pluripotent Stem Cells. *Methods Mol. Biol. Clifton NJ* **1353**, 89–99 (2016).
15. Xu, N., Wu, J., Ortiz-Vitali, J. L., Li, Y. & Darabi, R. Directed Differentiation of Human Pluripotent Stem Cells toward Skeletal Myogenic Progenitors and Their Purification Using Surface Markers. *Cells* **10**, 2746 (2021).
16. Bar-Nur, O. *et al.* Direct Reprogramming of Mouse Fibroblasts into Functional Skeletal Muscle Progenitors. *Stem Cell Rep.* **10**, 1505–1521 (2018).
17. Ancel, S., Stuelsatz, P. & Feige, J. N. Muscle Stem Cell Quiescence: Controlling Stemness by Staying Asleep. *Trends Cell Biol.* **31**, 556–568 (2021).
18. Ding, S. *et al.* Maintaining bovine satellite cells stemness through p38 pathway. *Sci. Rep.* **8**, 10808 (2018).
19. Hindi, S. M. & Kumar, A. TRAF6 regulates satellite stem cell self-renewal and function during regenerative myogenesis. *J. Clin. Invest.* **126**, 151–168.

20. Shea, K. L. *et al.* Sprouty1 Regulates Reversible Quiescence of a Self-Renewing Adult Muscle Stem Cell Pool during Regeneration. *Cell Stem Cell* **6**, 117–129 (2010).
21. Otto, A. *et al.* Canonical Wnt signalling induces satellite-cell proliferation during adult skeletal muscle regeneration. *J. Cell Sci.* **121**, 2939–2950 (2008).
22. Gioftsidi, S., Relaix, F. & Mourikis, P. The Notch signaling network in muscle stem cells during development, homeostasis, and disease. *Skelet. Muscle* **12**, 9 (2022).
23. Lamarche, É. *et al.* SMAD2 promotes myogenin expression and terminal myogenic differentiation. *Development* **148**, dev195495 (2021).
24. Charville, G. W. *et al.* Ex Vivo Expansion and In Vivo Self-Renewal of Human Muscle Stem Cells. *Stem Cell Rep.* **5**, 621–632 (2015).
25. The Gene Ontology Consortium. The Gene Ontology Resource: 20 years and still GOing strong. *Nucleic Acids Res.* **47**, D330–D338 (2019).
26. Chen, A. K.-L., Chen, X., Choo, A. B. H., Reuveny, S. & Oh, S. K. W. Critical microcarrier properties affecting the expansion of undifferentiated human embryonic stem cells. *Stem Cell Res.* **7**, 97–111 (2011).
27. Fragoso, G. *et al.* Inhibition of p38 mitogen-activated protein kinase interferes with cell shape changes and gene expression associated with Schwann cell myelination. *Exp. Neurol.* **183**, 34–46 (2003).
28. Bryant, C., van Nek, L. & Rolland, N. C. M. European Markets for Cultured Meat: A Comparison of Germany and France. *Foods* **9**, 1152 (2020).
29. Burton, N. M., Vierck, J., Krabbenhoft, L., Bryne, K. & Dodson, M. V. Methods for animal satellite cell culture under a variety of conditions. *Methods Cell Sci.* **22**, 51–61 (2000).
30. Park, S. *et al.* Effects of Hypoxia on Proliferation and Differentiation in Belgian Blue and Hanwoo Muscle Satellite Cells for the Development of Cultured Meat. *Biomolecules* **12**, 838 (2022).
31. Liu, W. *et al.* Hypoxia promotes satellite cell self-renewal and enhances the efficiency of myoblast transplantation. *Dev. Camb. Engl.* **139**, 2857–2865 (2012).
32. Danoviz, M. E. & Yablonka-Reuveni, Z. Skeletal Muscle Satellite Cells: Background and Methods for Isolation and Analysis in a Primary Culture System. *Methods Mol. Biol. Clifton Nj* **798**, 21–52 (2012).
33. Pawlikowski, B., Vogler, T. O., Gadek, K. & Olwin, B. B. Regulation of skeletal muscle stem cells by fibroblast growth factors. *Dev. Dyn.* **246**, 359–367 (2017).
34. Liu, Z. *et al.* YAP Promotes Cell Proliferation and Stemness Maintenance of Porcine Muscle Stem Cells under High-Density Condition. *Cells* **10**, 3069 (2021).
35. Fotia, C., Massa, A., Boriani, F., Baldini, N. & Granchi, D. Hypoxia enhances proliferation and stemness of human adipose-derived mesenchymal stem cells. *Cytotechnology* **67**, 1073–1084 (2015).
36. Yamada, M. *et al.* High concentrations of HGF inhibit skeletal muscle satellite cell proliferation in vitro by inducing expression of myostatin: a possible mechanism for reestablishing satellite cell quiescence in vivo. *Am. J. Physiol.-Cell Physiol.* **298**, C465–C476 (2010).
37. Wang, L. *et al.* Sirtuin 1 promotes the proliferation of C2C12 myoblast cells via the myostatin signaling pathway. *Mol. Med. Rep.* **14**, 1309–1315 (2016).
38. Girardi, F. *et al.* TGFβ signaling curbs cell fusion and muscle regeneration. *Nat. Commun.* **12**, 750 (2021).

39. Pasut, A. *et al.* Notch Signaling Rescues Loss of Satellite Cells Lacking Pax7 and Promotes Brown Adipogenic Differentiation. *Cell Rep.* **16**, 333–343 (2016).
40. Zarubin, T. & Han, J. Activation and signaling of the p38 MAP kinase pathway. *Cell Res.* **15**, 11–18 (2005).
41. Judson, R. N. *et al.* Inhibition of Methyltransferase Setd7 Allows the In Vitro Expansion of Myogenic Stem Cells with Improved Therapeutic Potential. *Cell Stem Cell* **22**, 177-190.e7 (2018).
42. Bruyère, C. *et al.* Actomyosin contractility scales with myoblast elongation and enhances differentiation through YAP nuclear export. *Sci. Rep.* **9**, 15565 (2019).
43. Spehar, K., Pan, A. & Beerman, I. Restoring aged stem cell functionality: Current progress and future directions. *STEM CELLS* **38**, 1060–1077 (2020).
44. Allan, S. J., De Bank, P. A. & Ellis, M. J. Bioprocess Design Considerations for Cultured Meat Production With a Focus on the Expansion Bioreactor. *Front. Sustain. Food Syst.* **3**, (2019).
45. Wilschut, K. J., Haagsman, H. P. & Roelen, B. A. J. Extracellular matrix components direct porcine muscle stem cell behavior. *Exp. Cell Res.* **316**, 341–352 (2010).
46. Ishii, K. *et al.* Recapitulation of Extracellular LAMININ Environment Maintains Stemness of Satellite Cells In Vitro. *Stem Cell Rep.* **10**, 568–582 (2018).
47. Xing, L. *et al.* Discovery and characterization of atropisomer PH-797804, a p38 MAP kinase inhibitor, as a clinical drug candidate. *ChemMedChem* **7**, 273–280 (2012).
48. Clerk, A. & Sugden, P. H. The p38-MAPK inhibitor, SB203580, inhibits cardiac stress-activated protein kinases/c-Jun N-terminal kinases (SAPKs/JNKs). *FEBS Lett.* **426**, 93–96 (1998).
49. Lali, F. V., Hunt, A. E., Turner, S. J. & Foxwell, B. M. The pyridinyl imidazole inhibitor SB203580 blocks phosphoinositide-dependent protein kinase activity, protein kinase B phosphorylation, and retinoblastoma hyperphosphorylation in interleukin-2-stimulated T cells independently of p38 mitogen-activated protein kinase. *J. Biol. Chem.* **275**, 7395–7402 (2000).
50. Schiaffino, S. & Mammucari, C. Regulation of skeletal muscle growth by the IGF1-Akt/PKB pathway: insights from genetic models. *Skelet. Muscle* **1**, 4 (2011).
51. Latres, E. *et al.* Insulin-like growth factor-1 (IGF-1) inversely regulates atrophy-induced genes via the phosphatidylinositol 3-kinase/Akt/mammalian target of rapamycin (PI3K/Akt/mTOR) pathway. *J. Biol. Chem.* **280**, 2737–2744 (2005).
52. Bodiou, V., Moutsatsou, P. & Post, M. J. Microcarriers for Upscaling Cultured Meat Production. *Front. Nutr.* **7**, (2020).
53. Ozawa, E. Transferrin as a muscle trophic factor. *Rev. Physiol. Biochem. Pharmacol.* **113**, 89–141 (1989).
54. Li, H. Minimap2: pairwise alignment for nucleotide sequences. *Bioinformatics* **34**, 3094–3100 (2018).
55. Patro, R., Duggal, G., Love, M. I., Irizarry, R. A. & Kingsford, C. Salmon provides fast and bias-aware quantification of transcript expression. *Nat. Methods* **14**, 417–419 (2017).
56. Love, M. I., Huber, W. & Anders, S. Moderated estimation of fold change and dispersion for RNA-seq data with DESeq2. *Genome Biol.* **15**, 550 (2014).
57. Hunt, N. C. *et al.* 3D culture of human pluripotent stem cells in RGD-alginate hydrogel improves retinal tissue development. *Acta Biomater.* **49**, 329–343 (2017).
58. Mæhre, H. K., Dalheim, L., Edvinsen, G. K., Elvevoll, E. O. & Jensen, I.-J. Protein Determination-Method Matters. *Foods Basel Switz.* **7**, E5 (2018).

5.7 SUPPLEMENTARY INFORMATION

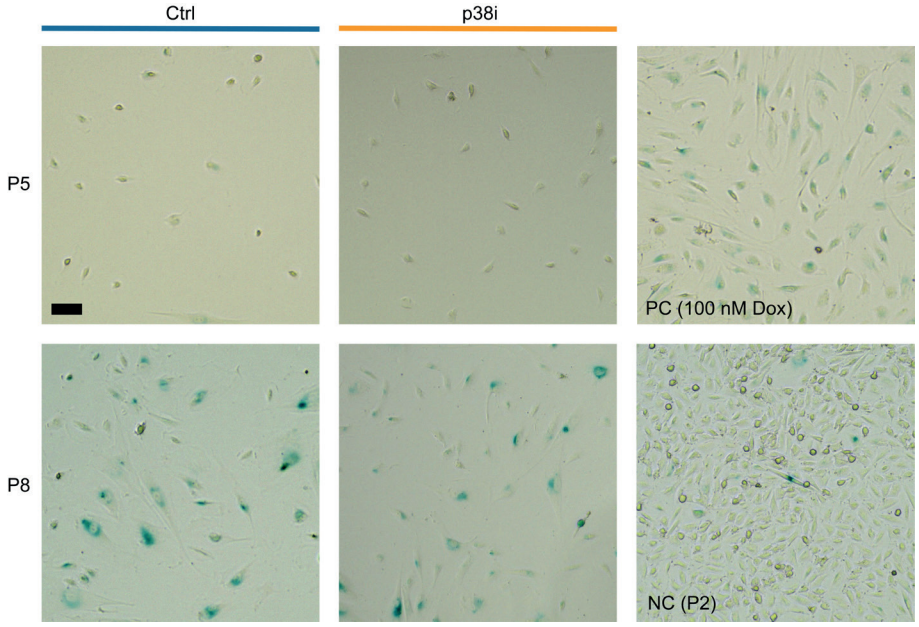

Supplementary Figure 1: Effect of p38i on cellular senescence (related to Figure 1). Representative images of SCs at passage 4 (top) and passage 8 (bottom) cultured without (blue) and with (orange) 10 µM SB203580; stained using a β-galactosidase activity assay; PC = positive control, NC = negative control.

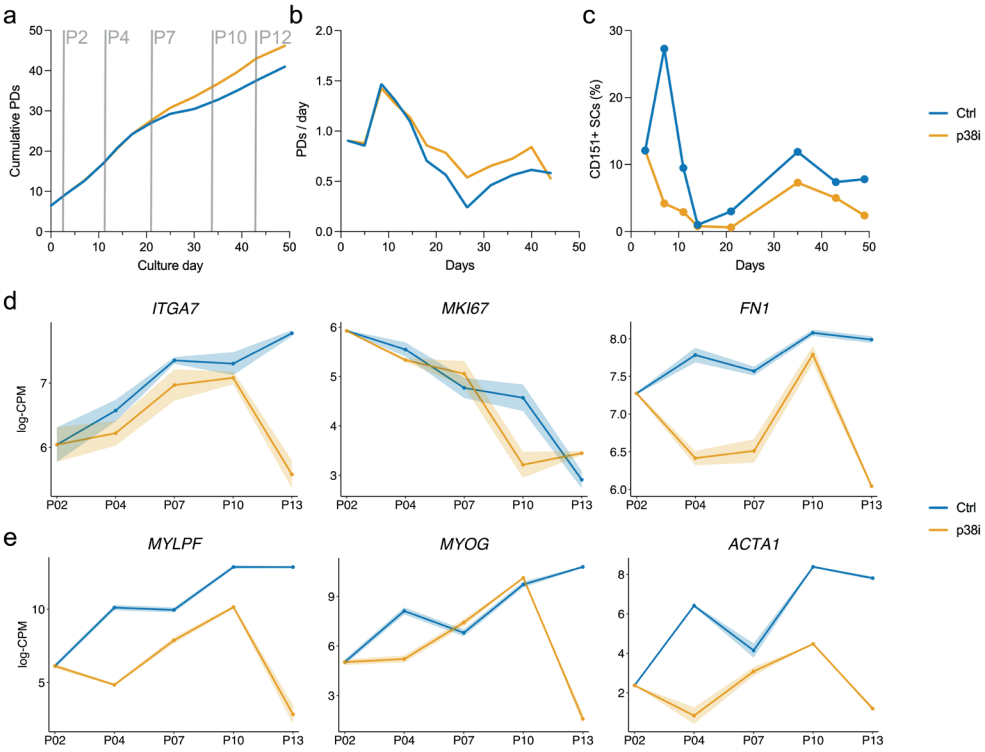

Supplementary Figure 2: Gene expression analysis of SCs proliferated with and without p38i (related to Figure 2).
a) Cumulative PDs of SCs grown with and without p38i; straight grey lines indicate time point collected for RNA sequencing; b) Proliferation rate of SCs from (a); c) Percentage of CD151^{+} SCs from (a), determined via flow cytometry; d) Expression of depicted genes (as $\log_2$ count per million) at the end of shown passages; e) Similar to (d) but showing representative differentiation-related genes.

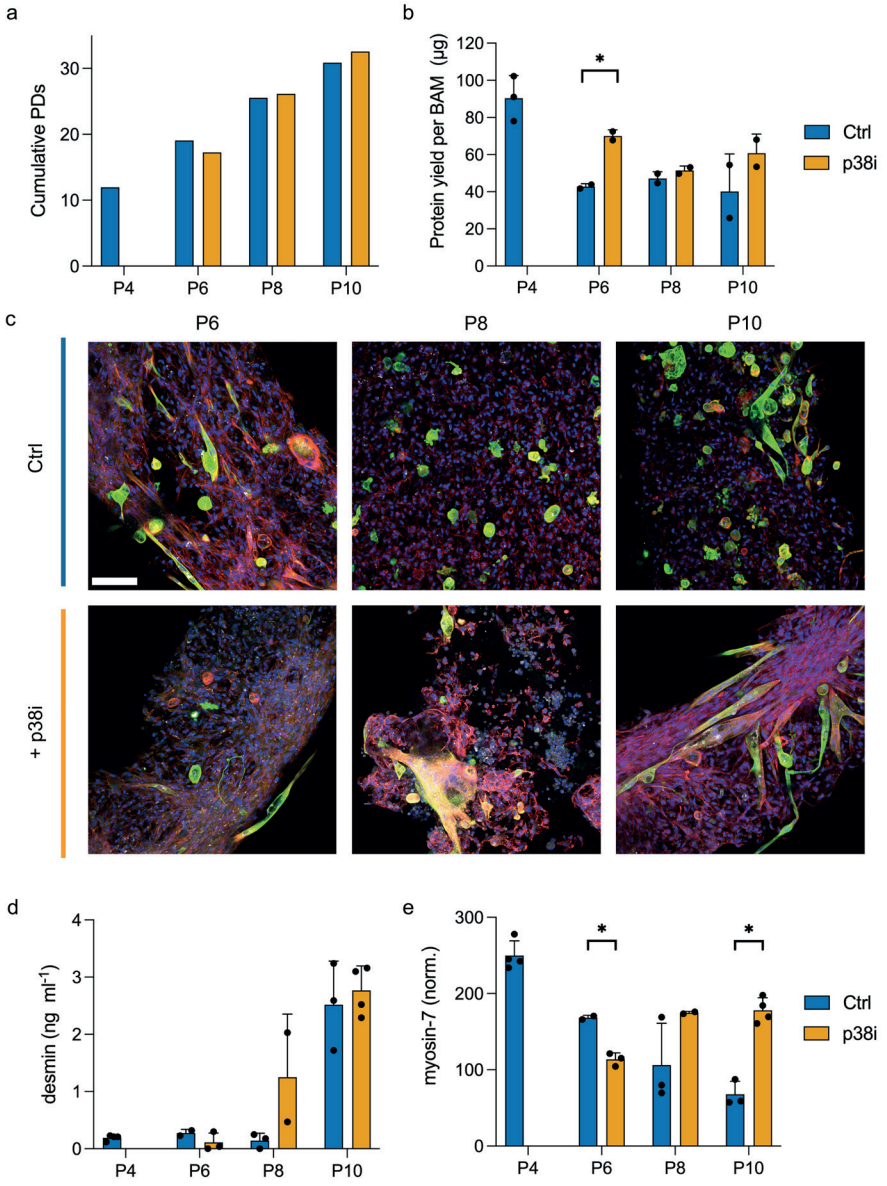

Supplementary Figure 3: Animal component-free BAMs from second replicate of SCs cultured with and without p38i (related to Figure 3).
a) Cumulative PDs of SCs grown with (orange) and without (blue) 10 µM SB203580 (p38i) before being used for BAMs at P4, P6, P8 and P10; b) Mean protein dry weight per BAM resulting from SCs grown with (orange) and without (blue) 10 µM SB203580; c) Immunofluorescent images of BAMs from SCs after 6, 8 and 10 passages with (bottom) and without (top) p38i, green = myosin-1, red = F-actin, blue = Hoechst, scale bar = 100 µM; d)Quantification of desmin expression in 20 µg ml^{-1} total protein solution in BAMs corresponding to (b), determined via ELISA; e) Quantification of myosin-7 expression normalised against meat lysate in BAMs corresponding to (b), determined via ELISA.

Supplementary Table 1: Overview of compounds and pathways to target SC stemness (related to Figure 1).

#	Pathway / Biological process	Compound	Effect
1	p38α/β-MAPK	SB203580	p38α/β inhibition
2	p38α/β-MAPK	Icariin	p38α/β inhibition
3	MEK/ERK	Resveratrol	Undefined
4	MEK/ERK	Quercetin	Undefined
5	MEK/ERK	PD0325901	MEK1/2 inhibition
6	MEK/ERK	Pluripotin	ERK1 inhibition
7	TGF-β	SB431542	ALK5 inhibition
8	TGF-β	RepSox	ALK5 inhibition
9	SMAD	Activin	Activin type 1 / 2 receptors agonist
10	SMAD	Inhibin	Activin type 1 / 2 receptors antagonist
11	Wnt	LiCl	GSK3 inhibitor
12	PKC-θ	Compound-20	PKC-θ inhibition
13	JAK/STAT	Apigenin	Multiple targets
14	PI3K/Akt	CHIR99021	GSK3β inhibition
15	PI3K/Akt	6-bromoindirubin-3'-oxime	GSK3β inhibition
16	Inflammation	Ibuprofen	COX inhibitor
17	Inflammation	Aspirin	COX inhibitor
18	Inflammation	Paracetamol	COX inhibitor
19	Catechin	Epigallocatechin-3-gallate	Antioxidant
20	Mitochondrial activity	Nicotinamide riboside	NAD^+ precursor
21	cGMP-PKG	Sildenafil	Phosphodiesterase 5 inhibition
22	Purinergic signalling	Adenosine	Class of adenosine receptors agonist
23	Epigenetic modification	Valproic acid	Histone deacetylase inhibition
24	Epigenetic modification	2-methyl-5-hydroxy-tryptamine	5-hydroxytryptamine receptor agonist
25	Epigenetic modification	EPZ004777	Methyltransferase inhibition
26	Epigenetic modification	BIX-01294	Methyltransferase inhibition
27	Epigenetic modification	FT895	HDAC11 inhibitor
28	Retinoic acid signalling	AM580	Retinoic acid receptor agonist
29	Retinoic acid signalling	TTNBP	Retinoic acid receptor agonist
30	PDGF	SU16F	PDGFR-β inhibition
31	PDGF	JNJ-10198409	PDGFR-α/β inhibition
32	TGF-β	D4476	Casein kinase inhibition
33	Muscle contraction	Acetylcholine (ACh)	ACh receptor agonist
34	JAK/STAT, MEK/ERK	IL6	IL6R-gp130 agonist
35	Pluripotency	OAC2	OCT4 activation
36	Rho-associated kinase	Y-27632	ROCK inhibition
37	Retinoic acid signalling	Vitamin A	Retinoic acid receptor agonist

Supplementary Table 2: Media formulations.

#	Component	Reference	Concentration
Pre-sorting serum-free growth medium (ps-SFGM)			
1	DMEM/F-12	21331-020, Gibco	
2	α-linolenic acid	L2376, Sigma Aldrich	1.0 µg ml^{-1}
3	FGF-2	100-18B, Peprotech	10 ng ml^{-1}
4	Human Serum Albumin	Rc HA NW20, Richcore Lifesciences	5.0 mg ml^{-1}
5	HGF	100-39H, Peprotech	5 ng ml^{-1}
6	Hydrocortisone	H0135, Sigma Aldrich	36 ng ml^{-1}
7	IGF-1	100-11, Peprotech	100 ng ml^{-1}
8	IL-6	200-06, Peprotech	20 ng ml^{-1}
9	ITSE	00-101, biogems	1%
10	GlutaMax	35050-061, Gibco	1%
11	Glucose	G7021, Sigma Aldrich	17.7 mM
12	L-ascorbic acid 2-phosphate (Vitamin C)	A8960, Sigma Aldrich	155 µM
13	PDGF-BB	100-14B, Peprotech	10 ng ml^{-1}
14	Penicillin/Streptomycin/ Amphotericin (PSA)	17-745E, Lonza	1%
15	VEGF	100-20 Peprotech	10 ng ml^{-1}
Serum-free growth medium (SFGM)			
1	DMEM/F-12	21331-020, Gibco	
2	α-linolenic acid	L2376, Sigma Aldrich	1.0 µg ml^{-1}
3	FGF-2	100-18B, Peprotech	10 ng ml^{-1}
4	Human Serum Albumin	Rc HA NW20, Richcore Lifesciences	5.0 mg ml^{-1}
5	HGF	100-39H, Peprotech	50 ng ml^{-1}
6	Hydrocortisone	H0135, Sigma Aldrich	36 ng ml^{-1}
7	ITSE	00-101, biogems	1%
8	GlutaMax	35050-061, Gibco	1%
9	Glucose	G7021, Sigma Aldrich	17.7 mM
10	L-ascorbic acid 2-phosphate (Vitamin C)	A8960, Sigma Aldrich	155 µM
11	PSA	17-745E, Lonza	1%
12	Triiodothyronine	T6397, Sigma Aldrich	30 nM
Serum-free differentiation medium (SFDM)			
1	DMEM/F-12	21311-020, Gibco	
2	EGF-1	AF-100-15, Peprotech	10 ng ml^{-1}
3	Human Serum Albumin	Rc HA NW20, Richcore Lifesciences	0.5 mg ml^{-1}
4	ITSE	00-101, biogems	2%
5	L-ascorbic acid 2-phosphate (Vitamin C)	A8960, Sigma Aldrich	40 µM
6	Lysophosphatidic acid (LPA)	L7260, Sigma Aldrich	1 µM
7	MEM Amino Acids Solution	11130-051, ThermoFisher	0.50%
8	$NaHCO_3$	P2256, Sigma Aldrich	6.5 mM
9	PSA	17-745E, Lonza	1%
10	Soy hydrolysates	58903C, Merck	1%

Chapter 6

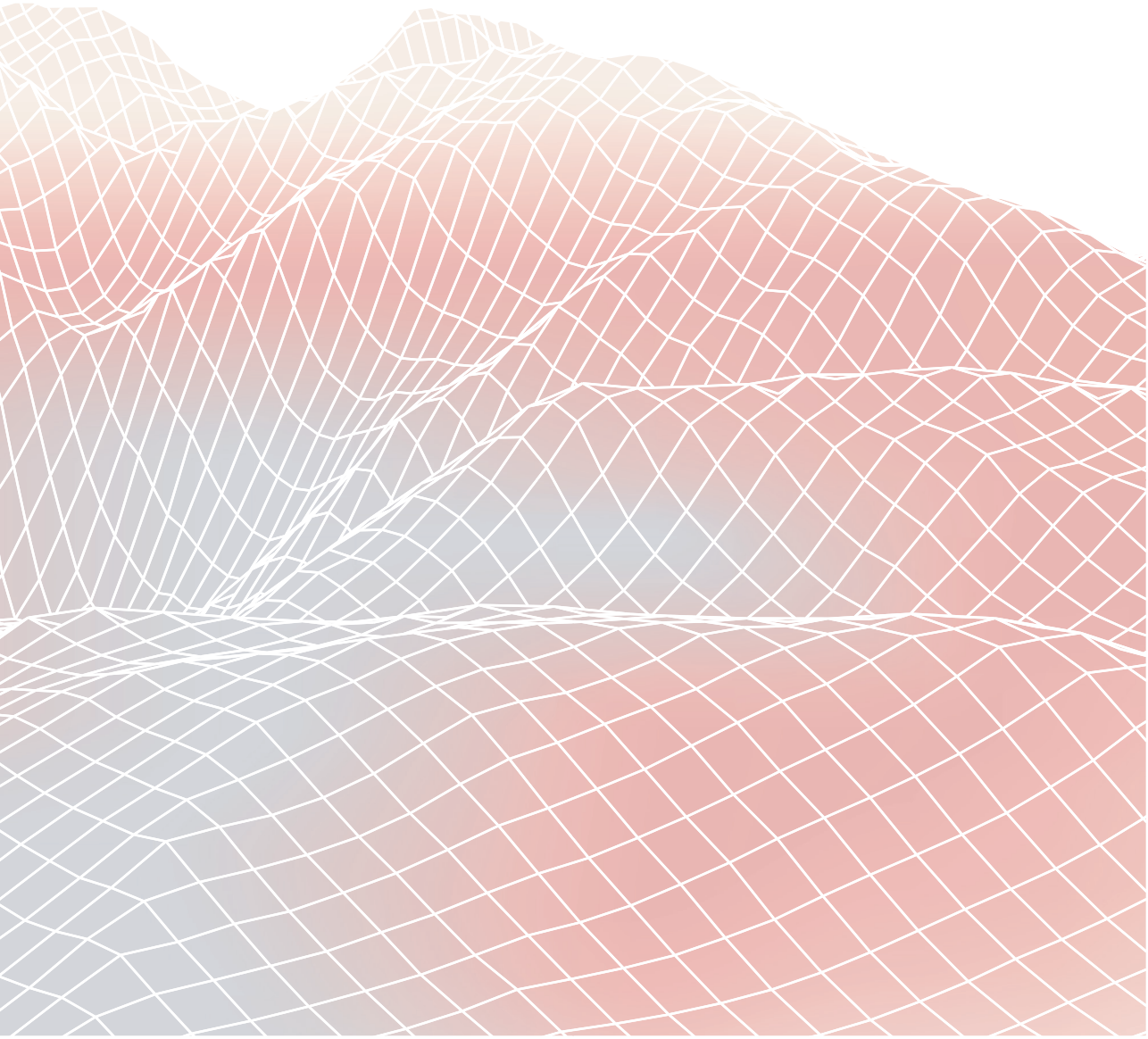

GENERAL DISCUSSION

6.1 DISCUSSION

Primary satellite cells (SCs) have a high proliferative and myogenic potential in vitro without requiring genetic modification and are therefore a promising cell source to produce culture meat. However, they rely on animal components for myogenic differentiation and lose stemness during prolonged culture, which restricts their applicability for commercial cultured meat production.

In the presented work, we leveraged transcriptomics and other bioinformatic tools to address and understand in vitro limitations of bovine SCs. We provide insights into differentiation, the cellular heterogeneity of muscle and derived cultures, the variability between SC cultures and the in vitro ageing process. This chapter contextualises the findings from this thesis, evaluates them in the context of their application in cultured meat and discusses the questions that remain unanswered by the presented data.

6.1.1 Overgrowth during serum-free proliferation can be rescued by adjusting culture conditions

Several serum-free media formulations for the proliferation of bovine SCs have been developed in recent years.[1,2] This thesis shows that long-term proliferation in a serum-free environment is a complex part of the bioprocess, irrespective of growth considerations in high-volume vessels.

We performed single-cell RNA sequencing on freshly isolated muscle tissue and derived cultures grown under serum-free conditions (Chapter 3). This identified at least 11 cell types in the bovine skeletal muscle. Analysing transcriptional heterogeneity in the derived cultures showed that despite separating these cell types by cell sorting, few unselected cells may remain in the post-sort cultures. Together with the selective effect of serum-free growth media on different cell types, this can lead to overgrowth of undesired populations during long-term proliferation. This issue has previously been reported in serum-containing cultures but may be exacerbated under chemically defined conditions.[3] Based on differentially upregulated surface receptors on cell types of interest, we increased the selectivity of the sorting protocol. In addition, we adjusted the serum-free growth media to maintain the purity of SCs by providing ligands to those receptors. We conclude that culture purity must be considered in studies that evaluate the long-term in vitro behaviour of primary cells and monitoring it during proliferation (e.g. by flow cytometry) must be an integral

part of the cultured meat bioprocess. Furthermore, we found that differences in proliferation capacity can emerge under prolonged serum-free culture. For example, some SC cultures grew beyond 35 PDs and retained their differentiation capacity, outperforming reported culture durations of bovine SCs both in serum-containing and serum-free media.[1,2,4–8] In contrast, a subset of cultures stopped proliferating at 20-25 PDs (Chapter 4). Using RNA sequencing on cultures with these different phenotypes, we found that genes related to differentiation are overexpressed in cultures more prone to proliferative exhaustion. Future work needs to clarify whether the expression of these genes has a predictive value for long-term culture behaviour. It is also necessary to study underlying mechanisms that lead to the observed proliferative differences in more depth and to clarify whether cultures exhibiting proliferative exhaustion are senescent or are merely in a reversible state of growth arrest (such as in vitro quiescence).

6.1.2 Bovine SCs can perform myogenic differentiation under serum-free conditions

Next to exogenous expression of myogenic regulators, serum starvation is the most commonly used protocol for inducing myogenic differentiation in vitro.[9–11] We studied the gene expression underlying differentiation using RNA sequencing and identified surface receptors that were differentially upregulated upon serum starvation. Supplementing ligands to those receptors enabled the formulation of a medium that allows the serum-free differentiation of bovine SCs (Chapter 2). Importantly, the extent of differentiation as well as the gene expression profile under serum-free conditions were comparable to serum starvation. However, we also found that up to 60% of SCs do not participate in myogenic fusion. Increasing the extent of differentiation and with this, the protein content in the final cultured meat product, is a pivotal objective of future work. The unfused cells likely have myogenic potential but are hindered from differentiating, e.g. by pro-mitotic signals that prevent efficient cell cycle exit or by cell-to-cell contacts with emerging myocytes that lead to the formation of a reserve cell population.[12,13] Studying this phenomenon on a single-cell or single-nucleus level rather than with bulk RNA sequencing may offer insights into the cellular heterogeneity during differentiation and indicate paths to exploit the full myogenic potential of SCs.[14,15] Future research may also establish whether the developed formulations can induce differentiation in other species relevant to cultured meat, such as porcine, avian, or ovine SCs.

Moreover, further work is necessary to characterise serum-free myogenic differentiation in bioartificial muscles (BAMs) in more detail. While the developed serum-free differentiation media supported fusion in BAMs based on collagen/matrigel (Chapter 2) or RGD-alginate (Chapters 4 & 5), it remains open to what extent the tissue maturation of these constructs compares to in vivo grown myofibres. Again, single-nucleus RNA sequencing or spatial transcriptomic analysis of BAMs may increase our understanding of potential cellular and spatial heterogeneity during differentiation. In addition, involvement of other cell types, such as endothelial cells or fibro-adipogenic progenitors, may influence SC alignment or myotube formation.[16,17] Whether co-cultures during differentiation are beneficial to the behaviour of SCs or contribute to texture or taste of the final product needs to be evaluated.

6.1.3 Inter- and intrastate changes occur during SC in vitro ageing

Producing commercially relevant quantities of cultured meat from primary SCs is mainly limited by in vitro cellular ageing, a multifaceted process that manifests in the loss of stemness. A central objective of this thesis is to understand the underlying mechanisms that affect this process. During muscle regeneration, SCs switch from a quiescent to an activated state before committing to myogenic differentiation. We speculated that a similar heterogeneity exists in vitro and that changes between or within these states might be connected to the observed loss of stemness. Therefore, we used single-cell RNA sequencing and flow cytometry to study cellular heterogeneity during serum-free proliferation (Chapters 3 & 4). We identified three in vitro states and found that SCs have the ability to dynamically switch between them. Alluding to the in vivo nomenclature, we labelled them ‘quiescent’, ‘activated’, and ‘committed’, although we acknowledge considerable differences between these states in vitro and in vivo (such as persistent expression of *Pax7* or *Myf5* in both the activated and the quiescent in vitro states). By correlating these states to proliferation and differentiation behaviours, we found that in vitro ageing of SCs is composed of changes between those states (interstate) as well as changes within them (intrastate).

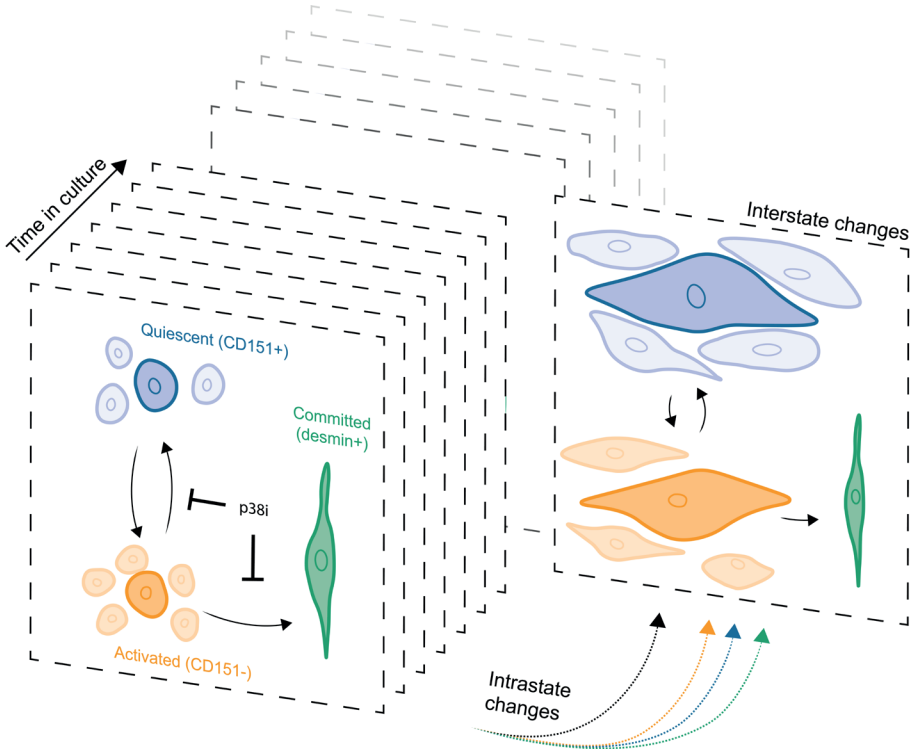

Figure 1: In vitro ageing comprises inter- and intrastate changes.
Within each passage (dashed squares), SCs transition between activated (orange) and quiescent (blue) states, which they may exit towards myogenic commitment (green) when becoming confluent. Upon prolonged in vitro proliferation, cells transition between states less frequently, indicating interstate alterations. In addition, the cells experience state-specific (coloured dashed arrows) and state-agnostic (black dashed arrow) intrastate changes such as hypertrophy, decline in proliferation capacity, or the increased expression of extracellular matrix proteins. Interventions that affect the stemness of SCs, such as the inhibition of p38α/β MAPK (p38i) may target either or both inter- and intrastate changes.

6.1.3.1 Transitions between in vitro states occur more slowly in aged SCs

We studied the ratios of quiescent, activated, and committed states in SCs at different PDs and in respect to proliferation or differentiation behaviours. Contrary to our expectation, we did not see a robust change in the ratios of these states upon in vitro ageing nor between SC cultures with different stemness. Instead, we found that the rate of transitions between those states decelerates over time, suggesting a connection to the decline of proliferation and/or differentiation capacity (Fig. 2).

Within each passage, we showed that SCs transition dynamically between the quiescent and activated state, which was measured by staining for CD151 via flow

cytometry. However, the in vitro role of CD151 and its involvement in SC ageing remains open. First of all, it is unclear whether CD151 itself has a functional role in driving these states, or is merely associated with them. Next, there is only a minor correlation between CD151 positivity measured via flow cytometry and *CD151* gene expression (Chapter 4). As CD151 can be rapidly internalised,[18] the transition between the CD151^{+} (quiescent) and CD151^{-} (activated) states might thus be regulated downstream of the transcriptional level, for example by the interaction of surface proteins with its environment. CD151 is a tetraspanin involved in cell motility and morphology, and colocalizes with other transmembrane proteins that communicate with the extracellular environment.[19,20] Given the increased expression of several extracellular matrix (ECM) proteins in CD151^{+} SCs, we speculate that CD151 could be linked to quiescence in vivo but that SCs may fail to recreate this state in vitro.[21,22] In line with this, culture conditions benefiting SC growth (such as coating with laminin instead of collagen, Chapter 3) or stemness (such as inhibition of p38α/β, Chapter 5) lowered the proportion of CD151^{+} cells. This suggests a potential application as a marker for SC culture optimisation. However, this is complicated by the lack of a strong correlation between CD151 positivity and in vitro ageing as well as by the high variability of CD151 positivity between SC cultures (Chapter 4). Further investigation of CD151 is therefore necessary, for example by studying the effect of CD151 knock-out or overexpression on the SC phenotype or by live-imaging of SCs with GFP-tagged CD151 during short- and long-term proliferation.[23]

SCs regularly transition towards a committed state despite being cultured in pro-mitotic conditions, as previously described.[4,24,25] Suppression of this transition has been proposed as a possible mechanism by which p38α/β inhibition maintains SC stemness.[4,25] Using bulk RNA sequencing, we found that SCs with a proliferative phenotype show lower expression of differentiation-related genes (Chapter 4) and that myogenic commitment is suppressed by p38α/β inhibition (Chapter 5). We speculate that SCs might irreversibly exit the cell cycle upon entering the committed state, which may gradually lower the number of SCs capable of proliferation or affect non-committed SCs through cell-cell interactions, e.g. through Notch signalling.[26] As our results were obtained by bulk-RNA sequencing, we could not conclude whether this lower expression of differentiation markers was driven by a constitutive decrease in the whole population or by the suppressed transition of a subpopulation of SCs towards myogenic commitment (Chapter

5). Therefore, future research is necessary to elucidate the connection between myogenic commitment and stemness. For instance, investigating aged SCs with different stemness by single-cell RNA sequencing might indicate whether late differentiation potential can be connected to differences in the size or expression patterns of the committed state. Furthermore, it may indicate whether the emergence of additional subpopulations might be involved in the loss of stemness.

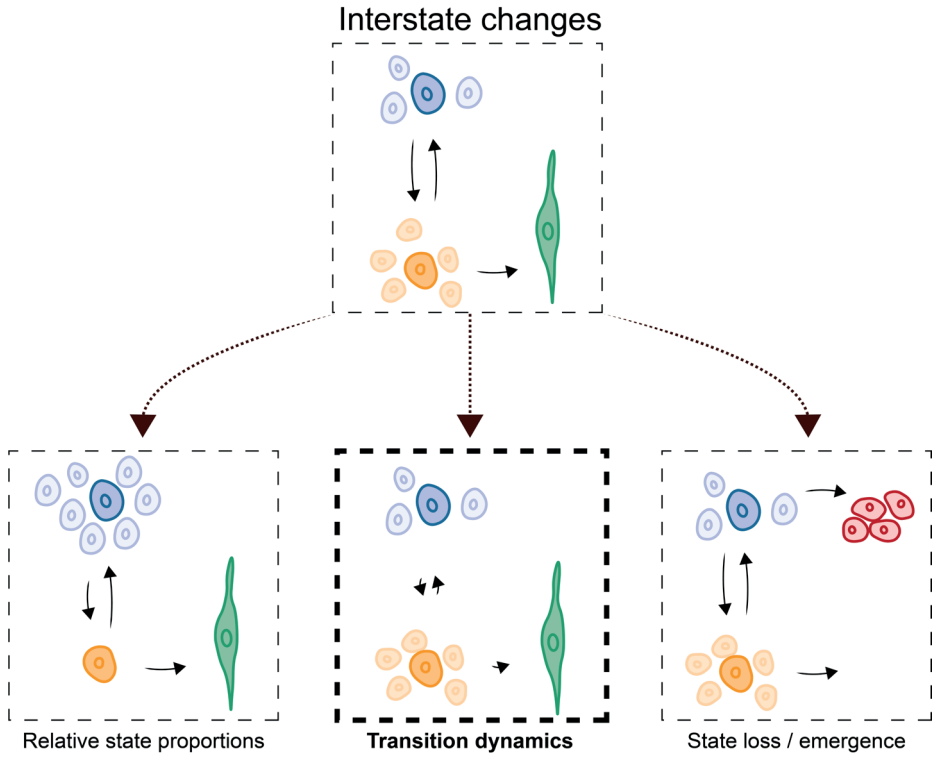

Figure 2: Possible interstate changes upon long-term in vitro proliferation.
In vitro ageing may change the heterogeneity of cultured SCs by shifting the ratios of quiescent (blue), activated (orange) and committed (green) states (shown in left square), by altering the transition frequency (centre square) or by the emergence of new states (red cells) / loss of states (right square). In this thesis, we found evidence for the reduction of transition dynamics (bold).

6.1.3.2 SC states change after prolonged in vitro culture

Aged SCs exhibit a markedly different phenotype compared to freshly isolated cells. Alterations responsible for this aged phenotype occur within all SC states as a potential result of replication stress (Fig. 3).[27] The most prominent differences we observed throughout this thesis were changes in cell size and morphology, as

well as decrease in proliferation rate. Within a few PDs, SCs change from a round, small shape, to an elongated cytoplasm with an up to 10-fold increase in length. Concurrently, we measured up to fourfold increases in doubling times in aged SCs.

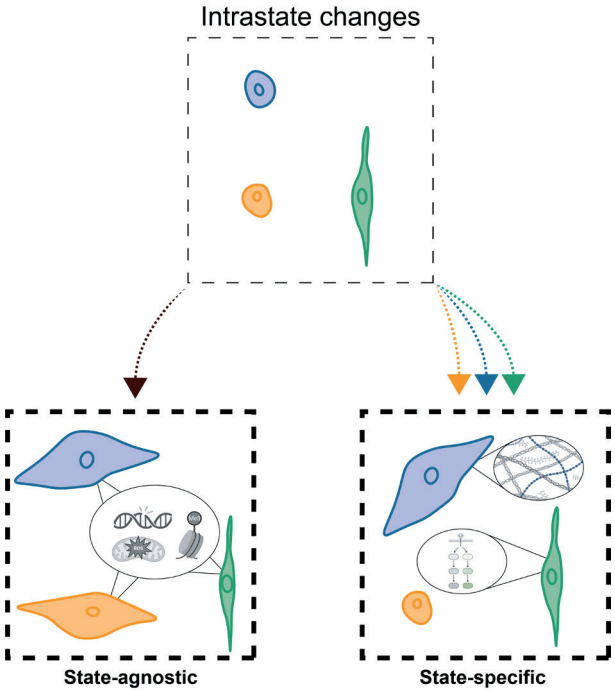

Figure 3: Possible intrastate changes during long-term proliferation.
Aged SCs exhibit changes that occur for all cells, which may manifest either dependently or independently of the current state. Observed state-agnostic changes include increased cell size and altered cell shape, while DNA damage, epigenetic drifting, and metabolic shift were not sufficiently assessed. State-specific changes can be detected for each state, such as increased expression of extracellular matrix proteins in the aged quiescent SCs.

Comparison of gene expression profiles between young and aged SCs using single-cell RNA sequencing showed pronounced differences within each state, such as increased expression of genes related to ECM upon ageing or the downregulation of genes related to transcription and translation (Chapters 3 & 4). We speculate that the ECM, which is considerably less complex in vitro than in their niche compartment in vivo, might play an important role in these population-wide ageing effects.[28] A better understanding of ageing as changes of states themselves and of the entire cell population is crucial to develop interventions to mitigate these changes. Tools with a single-cell resolution are necessary to build this understanding, as many

of the intrastate alterations might otherwise be confounded by gene expression differences between cells in different states.

Several other population-wide changes described in literature were not or only rudimentarily assessed in this work, including epigenetic, metabolic and genetic alterations.[27] For example, we did not find a connection between genetic structural variation or global DNA methylation with different ageing profiles. However, higher-resolution techniques are necessary to adequately study the phenotypic differences between SC cultures or between young and aged SCs. On a DNA level, these include techniques that detect genetic and epigenetic alterations on a single-nucleotide resolution, such as whole genome, exome or methylation sequencing.

6.1.4 Maintenance of stemness is context-dependent

Throughout this thesis, we studied stemness by measuring proliferation and differentiation capacity over time. Initial investigations of these processes under serum-free conditions were hindered by overgrowth with other cell types (Chapters 2 & 3). By increasing purity through improved sorting and selective culture conditions, we were able to characterise pure SCs over prolonged culture. This led to the observation that loss of proliferation capacity and loss of differentiation capacity occurred at different speeds with increasing culture duration (Chapter 4). In particular, three phenotypes emerged upon prolonged in vitro passaging: SC cultures that lost their proliferation capacity, cultures that maintained proliferation capacity but lost their differentiation capacity, and cultures that maintained both proliferation and differentiation capacities. Inhibition of the p38α/β MAPK pathway under serum-free conditions increased proliferation rate and extended the differentiation capacity. Whether this intervention is sufficient to rescue cultures from proliferative exhaustion is subject to future investigation. Moreover, we found that the effect of p38α/β was context-dependent. While the compound SB203580 improved stemness on laminin coating, it led to reduced growth rates when used on vitronectin, both in 2D tissue and 3D suspension cultures. This detrimental effect on vitronectin was rescued by PH797804, indicating that off-target effects may manifest depending on the surface coatings. These behaviours show that the ability to maintain stemness may be inherently different between batches of SCs and between culture conditions. Interventions to prevent the loss of stemness must therefore be assessed under conditions as similar to the bioprocess as possible to ensure their efficacy is preserved in upscaled culture systems.

6.2 CONCLUSION AND FUTURE DIRECTIONS

Removal of non-replicative animal components, improvement of product complexity, upscaling, and reduction of production costs are pivotal challenges for bringing cultured meat to market.

In this thesis, we showed that bovine SCs can proliferate and differentiate under animal component-free conditions. We investigated the complexity of bovine skeletal muscle and developed protocols to purify, culture and monitor several muscle-resident cell types, which may allow the construction of complex cultured meat constructs consisting of multiple cell types. We characterised the proliferation and differentiation capacity of SCs over prolonged serum-free expansion and showed that at least a subset of primary bovine SC cultures has the potential to generate sufficient mass for commercial production. Finally, we evaluated p38α/β inhibition as a means to maintain SC stemness under serum-free, upscaled culture conditions to lower the relative cost by producing larger batches of cultured meat.

These advances mark an important step towards the realisation of cultured meat. However, our findings also show that additional effort is needed to reliably produce the vast number of differentiation-competent SCs needed for a commercially viable process.

6.2.1 Towards large quantities of differentiation-competent SCs

In Chapter 4, we observed differences of in vitro ageing between SC cultures with direct consequences for a cultured meat production process. On average, 2.8×10^4 SCs were purified from 1 g of digested muscle tissue, corresponding to an estimated cell mass of 28 µg.[29] Assuming a 10-fold increase in mass during the differentiation phase, it would require at least 12 population doublings (PDs) to produce an equal quantity of cultured meat compared to the sourced animal tissue. Therefore, cultures that stopped proliferating before 20 PDs would yield no more than 10 to 100 g of cultured meat per 1 g of digested tissue. For the residual cultures, differentiation at 22 PDs would yield 1 kg of cultured meat per 1 g of tissue, which is insufficient for large-scale production.[30] Only cultures that still showed differentiation beyond 32 PDs (21% of those tested in Chapter 4) would yield cultured meat quantities over 1 ton. Meanwhile, the decline in proliferation and differentiation capacity results in smaller yields per batch or lower product quality

due to inefficient muscle formation, respectively. A viable bioprocess must resolve these limitations by one or a combination of the following three approaches (Fig. 4).

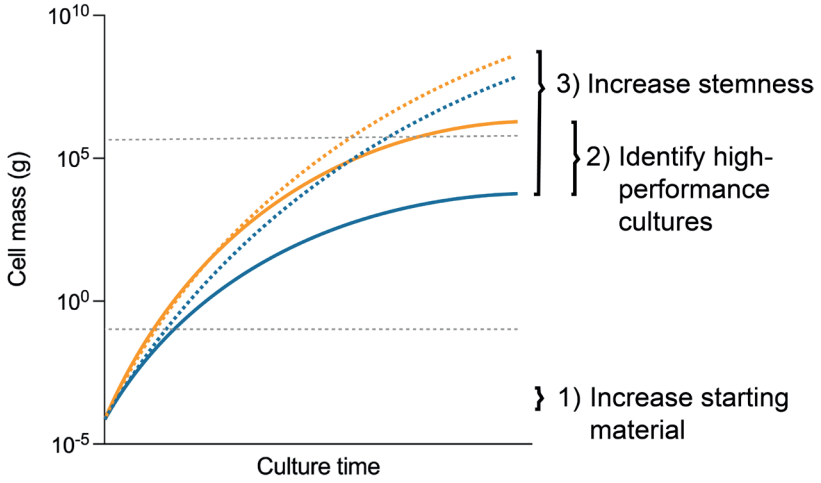

Figure 4: Approaches to increase final cell mass.
The total number of SCs capable of myogenic differentiation can be maximised (1) by starting with a higher cell mass, (2) by selecting high-performance (orange) over low-performance (blue) cultures or (3) by increasing the stemness of all cultures (dashed lines). Above lower grey line more cell mass is produced than put in, upper grey line indicates exemplified threshold for industrial relevance.

Starting with a bigger cell population would require fewer PDs to create commercially relevant quantities of meat, either by increasing the amount of SCs derived per tissue mass through improved isolation and purification protocols, by increasing the volume of initial digested tissue, or by combining the cell batches from multiple animals into cell pools.[31] This trivial approach may increase final product quantity. However, as the multiplication factor of the cells remains unaffected, it would not enable cost reduction through the economics of scale, nor remove significant numbers of animals from the food system.[32]

Therefore, a second approach may aim to identify high-performance cultures early in the bioprocess to select them for upscaled production. This requires measurable parameters with strong predictive power for future culture behaviour. We investigated CD151 as a potential maker for proliferation and/or differentiation potential but found no significant correlation. Instead, we detected increased expression of muscle-related genes as a possible prediction factor to exclude

cultures with a higher risk of proliferative exhaustion, but more research, such as whole exome sequencing, is needed to establish tools that explain or robustly predict the stemness of a culture.

The third approach is to identify conditions that prevent phenotypic differences in proliferation or differentiation behaviour from manifesting upon long-term culture. Interventions that maintain the stemness of SCs, e.g. through pathways such as Notch, p38 MAPK, JNK, PDGF, or EGF or through inhibition of differentiation, can delay proliferative exhaustion or loss of differentiation capacity.[4,33–36] However, future studies need to investigate whether such interventions, or combinations thereof, are capable of rescuing low-performance phenotypes. This requires the establishment of large-scale, automated screening platforms to test compound libraries for their potential to maintain stemness. As shown in Chapter 5, a solely proliferation-based screen may be sufficient to identify candidate compounds. In parallel, it is essential to gain a deeper understanding of underlying mechanisms of stemness-maintaining compounds such as inhibitors of p38α/β MAPK. In the example of p38α/β inhibition, further work may focus on how its effect on stemness depends on surface coatings and to what extent it is connected with the suppression of differentiation during proliferation. These insights might enable recreation of similar stemness-promoting effects through alternative interventions and help prevent failures of translation to upscale systems.

6.2.2 Towards a commercially viable product

SCs have a sufficient proliferation and differentiation capacity under serum-free conditions to produce cultured meat on a scale relevant for commercialisation. Nevertheless, many additional challenges in a range of scientific areas have to be overcome to create a viable product. While there is no defined benchmark for the extent of maturation or structural complexity needed to satisfy the sensory experience during consumption, animal component-free bioartificial muscle constructs do not yet compare to the protein content and composition of conventionally grown meat. To construct cultured meat that fully resembles skeletal muscle, this technology must resolve known challenges of tissue engineering such as pronounced maturation, vascularisation or co-differentiation of multiple cell types. Moreover, much of the work presented was performed in 2D tissue culture flasks. Expanding cell production to high bioreactor volumes introduces a variety of additional stresses to the cells and increases the risk of

contamination. It is unknown whether growth on microcarriers, in aggregates, or as single-cell suspensions in these dimensions affects cell behaviours such as the stemness of SCs, as observed for other cell types.[37] Finally, cultured meat will need to achieve price parity with conventionally grown meat. This can only be accomplished by replacing the components of the serum-free culture media with low-cost, food-grade alternatives without compromising cell performance, as well as by developing methods to recycle media in bioreactor cultures.

This extensive yet incomplete list of challenges highlights the necessity of additional research to realise cultured meat as viable food technology. The presented work demonstrates the potential of bioinformatic analysis to support this scientific endeavour and may contribute to the goal of considerably reducing livestock in the global food system.

6.3 BIBLIOGRAPHY

1. Kolkmann, A., Essen, A., Post, M. & Moutsatsou, P. Development of a Chemically Defined Medium for in vitro Expansion of Primary Bovine Satellite Cells. *Front. Bioeng. Biotechnol.* **10**, (2022).
2. Stout, A. J. *et al.* Simple and effective serum-free medium for sustained expansion of bovine satellite cells for cell cultured meat. *Commun. Biol.* **5**, 1–13 (2022).
3. Ding, S. *et al.* Characterization and isolation of highly purified porcine satellite cells. *Cell Death Discov.* **3**, 17003 (2017).
4. Ding, S. *et al.* Maintaining bovine satellite cells stemness through p38 pathway. *Sci. Rep.* **8**, 10808 (2018).
5. Baquero-Perez, B., Kuchipudi, S. V., Nelli, R. K. & Chang, K.-C. A simplified but robust method for the isolation of avian and mammalian muscle satellite cells. *BMC Cell Biol.* **13**, 16 (2012).
6. Loiben, A. M. *et al.* Long-term high-yield skeletal muscle stem cell expansion through staged perturbation of cytokine signaling in a soft hydrogel culture platform. 2020.06.04.134056
7. Benedetti, A. *et al.* A novel approach for the isolation and long-term expansion of pure satellite cells based on ice-cold treatment. *Skelet. Muscle* **11**, 7 (2021).
8. Zhu, H. *et al.* Production of cultured meat from pig muscle stem cells. *Biomaterials* **287**, 121650 (2022).
9. Genovese, N. J., Roberts, R. M. & TELUGU, B. P. V. L. Method for scalable skeletal muscle lineage specification and cultivation. (2016).
10. Das, M., Wilson, K., Molnar, P. & Hickman, J. J. Differentiation of skeletal muscle and integration of myotubes with silicon microstructures using serum-free medium and a synthetic silane substrate. *Nat. Protoc.* **2**, 1795–1801 (2007).
11. Guo, X. *et al.* In vitro Differentiation of Functional Human Skeletal Myotubes in a Defined System. *Biomater. Sci.* **2**, 131–138 (2014).
12. Yoshida, N., Yoshida, S., Koishi, K., Masuda, K. & Nabeshima, Y. Cell heterogeneity upon myogenic differentiation: down-regulation of MyoD and Myf-5 generates 'reserve cells'. *J. Cell Sci.* **111**, 769–779 (1998).
13. Laumonier, T., Bermont, F., Hoffmeyer, P., Kindler, V. & Menetrey, J. Human myogenic reserve cells are quiescent stem cells that contribute to muscle regeneration after intramuscular transplantation in immunodeficient mice. *Sci. Rep.* **7**, 3462 (2017).
14. Petrany, M. J. *et al.* Single-nucleus RNA-seq identifies transcriptional heterogeneity in multinucleated skeletal myofibers. *Nat. Commun.* **11**, 6374 (2020).
15. Williams, K., Yokomori, K. & Mortazavi, A. Heterogeneous Skeletal Muscle Cell and Nucleus Populations Identified by Single-Cell and Single-Nucleus Resolution Transcriptome Assays. *Front. Genet.* **13**, (2022).
16. Rao, N. *et al.* Fibroblasts influence muscle progenitor differentiation and alignment in contact independent and dependent manners in organized co-culture devices. *Biomed. Microdevices* **15**, 161–169 (2013).
17. Ben-Arye, T. *et al.* Textured soy protein scaffolds enable the generation of three-dimensional bovine skeletal muscle tissue for cell-based meat. *Nat. Food* **1**, 210–220 (2020).

18. Liu, L. *et al.* Tetraspanin CD151 promotes cell migration by regulating integrin trafficking. *J. Biol. Chem.* **282**, 31631–31642 (2007).
19. Yamada, M. *et al.* The tetraspanin CD151 regulates cell morphology and intracellular signaling on laminin-511. *FEBS J.* **275**, 3335–3351 (2008).
20. Palmer, T. D. & Zijlstra, A. CD151. *AFCS-Nat. Mol. Pages* **2011**, 10.1038/mp.a004123.01 (2011).
21. De Micheli, A. J. *et al.* Single-Cell Analysis of the Muscle Stem Cell Hierarchy Identifies Heterotypic Communication Signals Involved in Skeletal Muscle Regeneration. *Cell Rep.* **30**, 3583-3595.e5 (2020).
22. De Micheli, A. J., Spector, J. A., Elemento, O. & Cosgrove, B. D. A reference single-cell transcriptomic atlas of human skeletal muscle tissue reveals bifurcated muscle stem cell populations. *Skelet. Muscle* **10**, 19 (2020).
23. Jankovicova, J. *et al.* Expression and distribution of CD151 as a partner of alpha6 integrin in male germ cells. *Sci. Rep.* **10**, 4374 (2020).
24. Baroffio, A., Bochaton-Piallat, M.-L., Gabbiani, G. & Bader, C. R. Heterogeneity in the progeny of single human muscle satellite cells. *Differentiation* **59**, 259–268 (1995).
25. Ono, Y. *et al.* BMP signalling permits population expansion by preventing premature myogenic differentiation in muscle satellite cells. *Cell Death Differ.* **18**, 222–234 (2011).
26. Kitzmann, M. *et al.* Inhibition of Notch signaling induces myotube hypertrophy by recruiting a subpopulation of reserve cells. *J. Cell. Physiol.* **208**, 538–548 (2006).
27. Ogrodnik, M. Cellular aging beyond cellular senescence: Markers of senescence prior to cell cycle arrest in vitro and in vivo. *Aging Cell* **20**, e13338 (2021).
28. Thomas, K., Engler, A. J. & Meyer, G. A. Extracellular matrix regulation in the muscle satellite cell niche. *Connect. Tissue Res.* **56**, 1–8 (2015).
29. Bianconi, E. *et al.* An estimation of the number of cells in the human body. *Ann. Hum. Biol.* **40**, 463–471 (2013).
30. Melzener, L., Verzijden, K. E., Buijs, A. J., Post, M. J. & Flack, J. E. Cultured beef: from small biopsy to substantial quantity. *J. Sci. Food Agric.* **101**, 7–14 (2021).
31. Metzger, K., Tuchscherer, A., Palin, M.-F., Ponsuksili, S. & Kalbe, C. Establishment and validation of cell pools using primary muscle cells derived from satellite cells of pig skeletal muscle. *Vitro Cell. Dev. Biol. - Anim.* **56**, 193–199 (2020).
32. Hubalek, S., Post, M. J. & Moutsatsou, P. Towards resource-efficient and cost-efficient cultured meat. *Curr. Opin. Food Sci.* **47**, 100885 (2022).
33. Contreras, O., Córdova-Casanova, A. & Brandan, E. PDGF-PDGFR network differentially regulates the fate, migration, proliferation, and cell cycle progression of myogenic cells. *Cell. Signal.* **84**, 110036 (2021).
34. Golding, J. P., Calderbank, E., Partridge, T. A. & Beauchamp, J. R. Skeletal muscle stem cells express anti-apoptotic ErbB receptors during activation from quiescence. *Exp. Cell Res.* **313**, 341–356 (2007).
35. Conboy, I. M. *et al.* Rejuvenation of aged progenitor cells by exposure to a young systemic environment. *Nature* **433**, 760–764 (2005).
36. Ishii, K. *et al.* Recapitulation of Extracellular LAMININ Environment Maintains Stemness of Satellite Cells In Vitro. *Stem Cell Rep.* **10**, 568–582 (2018).
37. Phillips, B. W. *et al.* Attachment and growth of human embryonic stem cells on microcarriers. *J. Biotechnol.* **138**, 24–32 (2008).

Appendices

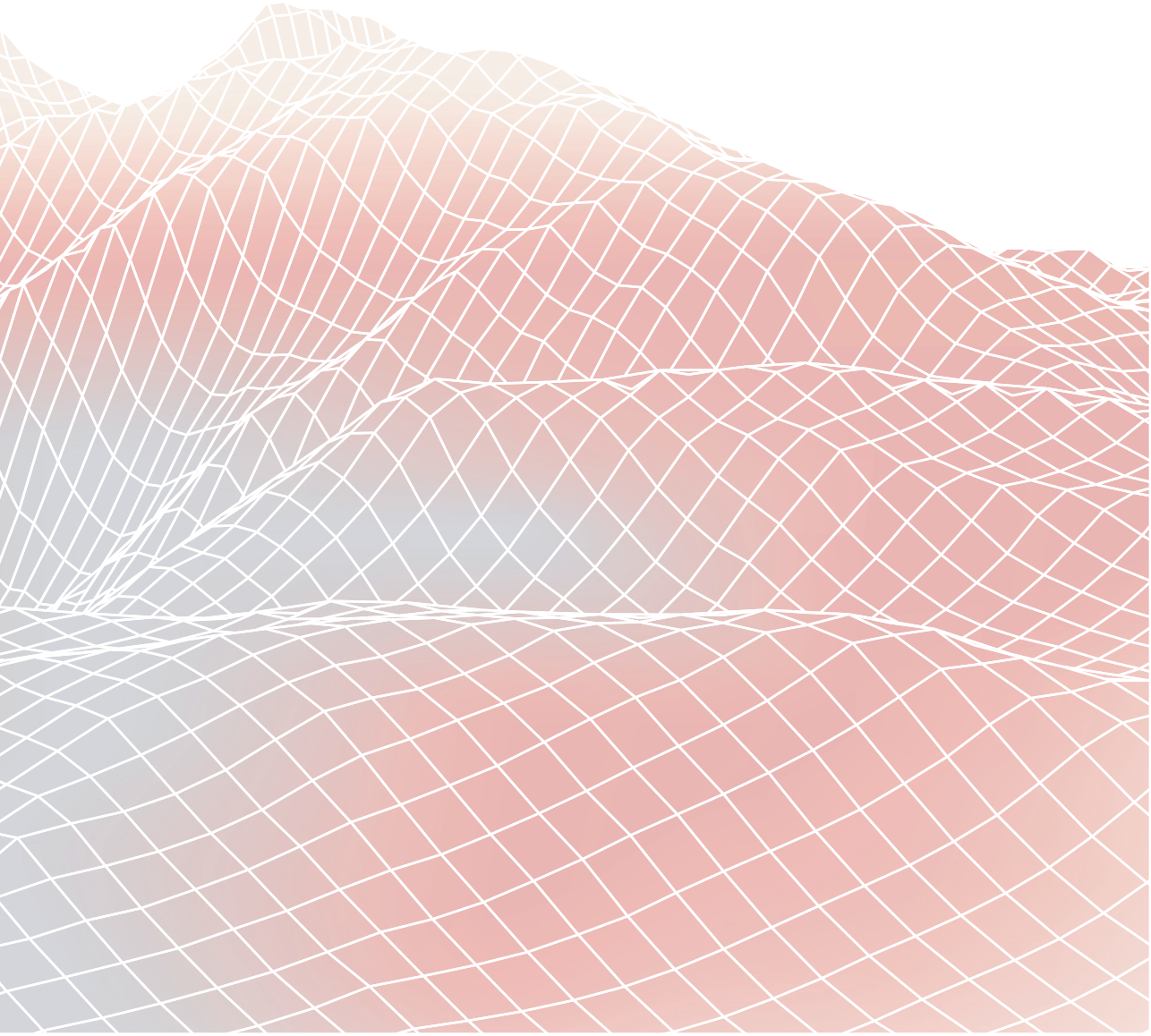

SUMMARY

A growing world population and increased per capita consumption have quadrupled the global production of meat since 1960, a trend that is expected to continue for the upcoming decades. Industrial livestock production is required to satisfy this demand but comes at high environmental cost. As a potential solution for this issue, cultured meat technology utilises ex vivo grown stem cells to recreate skeletal muscle tissue for human consumption. The production of cultured meat omits livestock husbandry and slaughter, and is projected to emit less greenhouse gases and require less land and fresh water.

While several proofs of concept have shown its small-scale feasibility, commercialisation of cultured meat faces numerous challenges. Many biological issues are directly related to the cell source, which affects the entire downstream process steps including proliferation and myogenic differentiation. Bovine satellite cells (SCs) are a promising candidate to produce cultured beef. However, protocols to purify, proliferate and differentiate primary SCs traditionally include animal-derived components, which is antithetical to the aim of reducing livestock from the food chain. In addition, SCs experience loss of stemness during long-term in vitro expansion, limiting the maximum quantities that can be produced from a starting sample. In this thesis, we studied SCs in proliferation and differentiation with the help of bioinformatic tools, in particular RNA sequencing, to inform the development of a large-scale, animal component-free cultured meat production process.

Existing transgene-free protocols to induce myogenic differentiation of SCs rely on the reduction of foetal bovine serum concentrations, a process referred to as serum-starvation. In **Chapter 2**, we characterised the transcriptomic and proteomic changes of SCs during serum-starvation. This showed that genes related to cell cycling were downregulated, while the expression of myogenic regulatory factors was increased. In addition, several surface receptors were increasingly expressed during serum-starvation. Supplementation of ligands to those surface receptors enabled myogenic differentiation in the absence of serum, but to a comparable extent and with a similar gene expression profile as through serum-starvation. For the first time, we therefore showed the ability of SCs to perform serum-free and transgene-free myogenic differentiation both on two-dimensional plates and in three-dimensional bioartificial muscles.

Skeletal muscle is a complex tissue containing numerous different cell types, many of which undergoing strong transcriptional changes during muscle regeneration. In **Chapter 3**, we used single-cell RNA sequencing to gain insights into the heterogeneity of bovine muscle tissue and derived cultures that were sorted using canonical SC makers. This identified at least 11 cell types in the bovine skeletal muscle niche with differentially expressed genes. By filtering for surface receptors within those markers, we developed a strategy for fluorescent-activated cell sorting that enabled the simultaneous selection of SCs, fibro-adipogenic progenitors (FAPs), endothelial cells, and smooth muscle mesenchymal cells. Within sorted SC cultures, we noted that a small population of contaminating cell types, in particular FAPs, may be sufficient to overgrow an entire culture under serum-free proliferation conditions. By studying the gene expression of SCs and FAPs, we adjusted the serum-free growth medium to be more selective for SCs, enabling long-term growth with high purity. Finally, we noted three different in vitro states within purified SCs: quiescent, activated, or committed. Transitions between those states happen dynamically within one passage, but occur less frequently upon prolonged culture, indicating that SC ageing manifests in changes of state dynamics.

SCs have a limited proliferation and differentiation capacity in vitro. This necessitates regular sourcing of new cell batches, introducing variability to the bioprocess. In **Chapter 4**, we assessed this variability by studying proliferation and differentiation capacity of cultures derived from 14 donor animals over a prolonged serum-free expansion. We observed three phenotypes: cultures that stopped proliferating between 20-25 PDs, cultures that continued to proliferate but stopped differentiating, and cultures that maintained both proliferation and differentiation capacity beyond 35 PDs. We then analysed in vitro readouts at low PDs, as well as genetic structural variation, DNA methylation and the transcriptional profiles of multiple passages of SCs in order to understand and predict this phenotypic variability.

Finally, in **Chapter 5,** we established a workflow to screen candidate compounds for maintaining SC stemness and to assess their compatibility in a cultured meat production process. We studied the effects of p38α/β inhibitor SB203580 on proliferation and differentiation during a long-term serum-free culture and used RNA sequencing to gain insights into the effect of p38α/β-inhibition on stemness. We found that p38α/β-inhibition increased proliferation speed and prolonged differentiation capacity both on two-dimensional plates and in animal component-free bioartificial muscles. Finally, we tested the application of p38α/β inhibition in

an upscaled bioprocess and observed that its effect is context-dependent, being affected by plate coating and off-target effects of the specific compound.

In conclusion, the detailed study of SC proliferation and differentiation through RNA sequencing enabled considerable improvements to the cultured meat bioprocess. We designed serum-free conditions for high-purity growth and differentiation up to sufficient PDs for an industrial bioprocess, but additional optimisation is needed to achieve this robustly. Bioinformatic tools with single-cell resolution can inform this path leading towards robust, high-performance SC cultures for producing cultured meat.

SAMENVATTING

Door een groeiende wereldpopulatie en een toenemende consumptie per capita is de productie van vlees verviervoudigd sinds 1960, een trend die zich naar verwachting de komende decennia zal voortzetten. Momenteel voorziet industriële veehouderij deze groeiende vraag met de bijbehorende, nadelige effecten op klimaatverandering. Een potentiële oplossing voor dit probleem is kweekvlees. Deze technologie maakt gebruik van stamcellen om skeletspierweefsel voor humane consumptie te kweken. Middels kweekvleesproductie is veeteelt en het laten slachten hiervan niet meer nodig en dit gaat naar verwachting gepaard met een reductie in broeikasgasuitstoot, en het behoeft minder land en water.

Hoewel verschillende 'proof of concepts' de haalbaarheid op kleine schaal hebben aangetoond, staat de commercialisering van kweekvlees voor tal van uitdagingen. Veel biologische problemen houden direct verband met de cel waarvan wordt uitgegaan. Deze startcel bepaalt verschillende downstream processen waaronder proliferatie en myogene differentiatie. Satellietcellen (spierstamcellen, SCs) zijn een veelbelovende startcel voor kweekvleesproductie. Traditionele protocollen voor het zuiveren, prolifereren en differentiëren van primaire SCs bevatten echter dierlijke componenten, wat in strijd is met het doel om vee uit de voedselketen te verwijderen.

Bovendien vertonen SCs verlies van 'stemness' (verlies van stamcelidentiteit en differentiatiepotentieel) gedurende langdurige in vitro expansie, waardoor de maximale hoeveelheid die uit een startsample geproduceerd kan worden beperkt is. In dit proefschrift hebben we SCs tijdens proliferatie en differentiatie bestudeerd met behulp van bioinformatica-tools, voornamelijk RNA-sequencing, met als doel de ontwikkeling van een grootschalig en dierlijk-vrij kweekvlees productie proces te ondersteunen.

Bestaande transgeen vrije protocollen om myogene differentiatie van SCs te induceren maken gebruik van een methode die ook wel wordt aangeduid als serum-onttrekking ('serum starvation'). Celkweken vereisen normaliter foetaal runder serum in het groeimedium, zodra de concentratie van het serum wordt verlaagt zal differentiatie worden geinduceerd. In **Hoofdstuk 2** hebben we de veranderingen op eiwit- en genniveau van SCs tijdens serum onttrekking gekarakteriseerd. Hieruit is gebleken dat genen die worden geassocieerd met de celcyclus verminderd tot expressie kwamen, terwijl de expressie van

myogeen regulerende factoren verhoogd was. Bovendien werden verschillende oppervlakte receptoren in toenemende mate tot expressie gebracht tijdens serum onttrekking. Het toevoegen van liganden specifiek voor deze oppervlakte receptoren maakte myogene differentiatie mogelijk in de afwezigheid van serum. De myogene differentiatie was in vergelijkbare mate en met een vergelijkbaar genexpressieprofiel als gezien wordt in serum-starvatie. We hebben hiermee voor het eerst aangetoond dat SCs het vermogen hebben om serumvrij en transgeen-vrij te differentiëren zowel op tweedimensionale kweekplaten als in driedimensionale biologisch kunstmatige spieren.

De skeletspier is een complex weefsel dat talloze verschillende celtypen bevat, waarvan er vele sterke transcriptionele veranderingen ondergaan tijdens spierregeneratie. In **Hoofdstuk 3** hebben we single-cell RNA sequencing gebruikt om inzicht te krijgen in de heterogeniteit van runder spierweefsel en de daaruit geïsoleerde celkweken welke werden gesorteerd met behulp van klassieke SC markers. Hiermee hebben we tenminste 11 celtypen geïdentificeerd in runder skeletspieren aan de hand van verschillen in gen profielen. We hebben een nieuwe strategie ontwikkeld voor fluorescentie-geactiveerde cell sortering (FACS) door te filteren op oppervlakte receptoren binnen deze markers. Dit maakt het mogelijk om tegelijkertijd te selecteren voor SCs, fibro-adipogene progenitors (FAPs), endotheel cellen en smooth muscle mesenchymal cells. We hebben geconstateerd dat binnen deze gesorteerde SC-kweken een kleine populatie van ongewilde celtypen, in het bijzonder FAPs, voldoende kan zijn om een volledige celkweek te overwoekeren in serumvrij groeimedium. Door het bestuderen van gen expressie van SCs en FAPs was het mogelijk om ons serumvrije groeimedium aan te passen zodat deze selectiever is voor SCs, waardoor langdurige groei met een hoge zuiverheid mogelijk is. Ten slotte hebben we drie verschillende in vitro cel toestanden vastgesteld binnen een gezuiverde SCs populatie: quiescent (in rust), geactiveerd of toegewijd. Overgangen tussen deze toestanden zijn dynamische en vinden plaats binnen één passage, maar nemen in frequentie af bij een langdurige kweek. Dit duidt erop dat SC veroudering zich manifesteert in veranderingen van deze cel toestanden.

SCs hebben een beperkte proliferatie en differentiatie capaciteit in vitro. Dit zorgt ervoor dat een regelmatige aanvoer van nieuwe cel batches vereist is, wat extra variabiliteit introduceert tijdens het bioproces. In **Hoofdstuk 4** hebben we deze variabiliteit onderzocht door het proliferatie- en differentiatievermogen

te bestuderen van kweken afkomstig van 14 donor runderen gedurende een langdurige serumvrije expansie. We hebben drie fenotypes waargenomen: kweken welke stopte met proliferatie na 20-25 populatie verdubbelingen, kweken welke aanhoudende proliferatie lieten zien maar waarbij de differentiatiecapaciteit verloren ging, en kweken welke zowel proliferatie en differentiatie capaciteit behielden tot tenminste 35 populatie verdubbelingen. Vervolgens zijn verschillende in vitro readouts geanalyseerd bij lage populatie verdubbelingen, evenals genetische structurele variatie, DNA methylatie en transcriptie profielen van verschillende passages van SCs om de fenotypische variabiliteit te begrijpen en te voorspellen.

Ten slotte hebben we in **Hoofdstuk 5** een workflow opgezet om kandidaat compounds te screenen voor het behoud van SC stemness en om de compatibiliteit in een kweek vlees productie proces te testen. We hebben het effect van de p38α/β-remmer SB203580 op proliferatie en differentiatie bestudeerd tijdens een langdurige serumvrije kweek. Tevens hebben we RNA-sequencing gebruikt om inzicht te krijgen in het effect van p38α/β-remming op stemness. We ontdekten dat p38α/β-remming de proliferatiesnelheid en het differentiatievermogen verbeterde zowel op tweedimensionale kweekplaten als in driedimensionale biologisch kunstmatige spieren. Tot slot hebben we de toepassing van p38α/β-remming in een bioproces getest en hierbij is vastgesteld dat het effect contextafhankelijk is en kan worden beïnvloed door plaat coating en off-target effecten van de specifieke compound.

Concluderend, de gedetailleerde studie van SC proliferatie en differentiatie door middel van RNA-sequencing heeft aanzienlijke verbeteringen mogelijk gemaakt in het bioproces van kweekvlees. We hebben serumvrije omstandigheden ontwikkeld voor groei met een hoge zuiverheid en het behoud van differentiatievermogen tot voldoende populatie verdubbelingen behaald zijn voor een industrieel bioproces. Aanvullende optimalisatie is echter nodig om voldoende robuustheid te bereiken in dit proces. Bioinformatica-tools, waarbij wordt gekeken op het niveau van individuele cellen, kunnen bijdragen aan het bereiken van robuuste en hoogwaardige SC kweken voor de productie van kweekvlees.

IMPACT

Production of livestock to satisfy the growing demand for meat comes with great cost for the environment, accounting for over 13.5% of global greenhouse gas emissions, 38.5% of habitable land usage and 30.2% of fresh water consumption.[1,2] Cultured meat technology offers a chance to drastically improve the environmental footprint of meat by producing muscle from stem cells using tissue engineering techniques. However, a multitude of scientific challenges must be overcome to bring this novel food technology to market.

The aim of this thesis is to use bioinformatic tools to address the biological limitations of satellite cells, one of the most promising cell types that can be used for producing cultured meat. These are stem cells that have the ability to form new muscle fibres in animals but also outside of an animal when grown as cell cultures.

Scientific impact

Satellite cells (SCs) have traditionally been grown in cell culture using compounds derived from animals, a major obstacle for their application in cultured meat. The results of this thesis show that it is possible to remove animal components from SC cultures derived from cows, both for their growth and their differentiation, i.e. the formation of muscle structures. The development and optimisation of animal component-free media for growth and differentiation of SCs are important steps for the cultured meat field. Beyond its application in cultured meat, the underlying approach to develop and optimise animal component-free media can also be extended to medical basic research, where animal components are still in frequent use to culture mammalian cells.

Just as animals alter as they age, the behaviour of SCs is subject to change during long-term growth in culture. During this ageing process, they gradually lose the ability to divide or to differentiate, which restricts the quantity of cultured meat that can be produced. In this thesis, we analyse the changes that occur to SCs during prolonged culture on a single-cell and a population-wide level. Our findings indicate that it is possible to produce enough functional cells for commercially relevant quantities of cultured meat but further optimisation is needed to achieve this robustly. The ability to create large amounts of cell mass, and from those, maturated and complex tissues, is equally relevant for other applications in the field of tissue engineering, such as the growth of organs for patient-derived cells.

This thesis demonstrates how to use existing bioinformatic tools to understand cell behaviour during these processes and how to leverage gained insights to improve them. Although there is only limited transferability of results from cells cultured outside an animal to their natural environment, the detailed characterisation of SCs in this work can also contribute to a better understanding of skeletal muscle biology necessary for treating muscle-related syndromes such as sarcopenia or duchenne muscular dystrophy.

Social impact

The revenue generated in the global meat market amounted to over 1.1T USD in 2021, of which meat substitutes had a share of less than 1%.[3] This creates a strong incentive for commercial parties aiming to enter the market with a food technology that promises environmental and ethical benefits over conventionally grown meat. This vast market opportunity resulted in the founding of 107 cultured meat-related startup companies by the end of 2021.[4] However, the challenges of producing cultured meat on a commercial scale are too numerous and complex to be solved by one company alone. Meanwhile, the opportunities offered by this technology outweigh mere financial interests and justify collaborative efforts beyond the boundaries of private institutions.

The realisation of cultured meat on an industrial scale may have a dramatic impact on society. If the estimations of early life cycle assessment studies hold true, it may reduce greenhouse gas emissions, land and fresh water usage, deforestation and loss of biodiversity. It may contribute to global food security by requiring fewer crops to produce equal calories of meat. It may lower the risk of animal-borne diseases and antibiotic resistance by reducing the number of animals used for food production. Just as importantly, it may reinstate the social contract between livestock animals and humans, where the harvest of animal goods is exchanged for protection from nature and disease. This social contract is out of balance in today's industrial meat production, where livestock animals are considered merely a product. In contrast, cultured meat technology presents the chance to return the rights to these animals by harvesting their cells, rather than their lives, for the production of meat.

The research presented in this thesis aims to support environmental and societal change through advancing the development of the field, but it also shows that

the path to produce substantial quantities of cultured meat might be long and convoluted. In an area dominated by privately funded companies, open-access research and scientific dialogue across institutions remain key to drive innovation along the entire product chain. Therefore, the results of this thesis have not only contributed to the filling of three patents (applications pending)[5] but were shared in peer-reviewed journals,[6] open-access repositories,[7] scientific conferences,[8,9] lectures, blog posts,[10,11] social media platforms and podcasts.[12] By promoting open-access science and engaging in public education, we want to create a technology that is comprehensible, inclusive and transparent. This may pave the way for a new, sustainable and more ethical relation to our food.

REFERENCES

1. Heinke, J. *et al.* Water Use in Global Livestock Production—Opportunities and Constraints for Increasing Water Productivity. *Water Resour. Res.* **56**, e2019WR026995 (2020).
2. Ritchie, H. & Roser, M. Meat and Dairy Production. *Our World Data* (2017).
3. The Business Research Company. *Meat Products Global Market Opportunities And Strategies To 2031: COVID-19 Impact And Recovery*. (2022).
4. Cultivated meat state of the industry report - GFI Europe. https://gfieurope.org/resource/cultivated-meat-state-of-the-industry-report/.
5. Cruz, H. *et al.* Serum-Free Medium for Differentiation of a Progenitor Cell. (2022).
6. Messmer, T. *et al.* A serum-free media formulation for cultured meat production supports bovine satellite cell differentiation in the absence of serum starvation. *Nat. Food* **3**, 74–85 (2022).
7. Messmer, T. *et al.* Single-cell analysis of bovine muscle-derived cell types for cultured meat production. 2022.09.02.506369 Preprint at https://doi.org/10.1101/2022.09.02.506369 (2022).
8. International Scientific Conference on Cultured Meat. *International Scientific Conference on Cultured Meat* https://www.culturedmeatconference.com.
9. IFHN-2022 | Food Conferences | Food Technology Conferences | Barcelona. https://foodscience-nutrition.org/.
10. Cultivating beef without FBS. *Mosa Meat* https://mosameat.com/blog/cultivating-beef-without-fetal-bovine-serum.
11. Heim, D. J. Building a kinder future with cellular agriculture. *ProVeg International* https://proveg.com/blog/building-a-kinder-future-with-cellular-agriculture/ (2022).
12. Tobias Messmer of Mosa Meat by Cultured Meat and Future Food Podcast. *Anchor* https://anchor.fm/futurefoodshow/episodes/Tobias-Messmer-of-Mosa-Meat-e1ctkhq.

ACKNOWLEDGEMENTS

My first and foremost thanks go to my supervisor Josh. Your scientific ingenuity and your ability to grasp complex ideas within seconds have impressed me since the first day we worked together. Thank you for everything you have taught me, for your rigorous reviewing and for always pushing me forwards (both in the lab and on the bike). Most importantly, thank you for the huge fun along the way. You were the best supervisor I could have wished for and above all, a mentor and friend. Keep engaging your core.

Mark, building a company is a massive undertaking by itself but despite this, you took on the extra effort to enable me and my colleagues to earn a PhD. I want to express my deep gratitude for this opportunity. You have always remained a scientist at heart, and are an inspiration to each one in our company and to the entire field of cultured meat.

It would have been impossible to gather all the data in this work without a team of committed and supportive colleagues. Richard, Lea, Rui, Lieke, Joana, Joanna, Dhruv, Sergio, Carin, Christoph, Arın, and the entire Cell Biology team - not only could I always rely on your help, you also made the past three and a half years most enjoyable. Huge thanks for your effort, ideas and critical thinking – I could not have done it without you.

Mosa Meat provides an environment in which everyone can be their best self and do the exciting groundwork to make cultured meat happen. Every morning, I'm looking forward to coming to work. Thanks to everyone in our company for making this possible and for sharing the excitement to work on this great endeavour.

Thanks also to the many great collaborators outside of our company who have contributed to this thesis: Kasper and Wanwisa at the Genome Services Maastricht, Ronnie, Hans and Carmen at the M4I, and Latifa, Manon, Alice and Wouter at University Liège.

Special thanks also go to my assessment committee - Judith Sluimer, Chris Evelo, Marius Henkel, Fabien Le Grand and Tim Snijders - for having spent their valuable time on thoroughly reviewing this thesis.

Finally, I would like to express my deepest thanks to those who fill my life with music and colour.

My friends from Lake Constance, Heidelberg, and Maastricht, you have either been there as long as I can remember or joined my journey somewhere along the way, making me the person I am today. Thanks for having my back no matter what, I love you guys.

Viktoria, of the many discoveries over the past years, finding you was the one that mattered the most. Your positivity makes the lives of everyone around you brighter, and I feel grateful for every moment we share.

Petra und Josef, Christian and Isabella. You are my backbone, my safe haven. You have taught me what is important in life, and I would be nowhere without you. This thesis is dedicated to you.

ABOUT THE AUTHOR

Tobias Meßmer was born on 22nd September, 1992 in Tettnang, Germany. In 2012, he graduated from secondary school with majors in physics and biology, for which he received the Karl-von-Frisch award. After travelling through Asia for 7 months, he studied Molecular Biotechnology at Heidelberg University for both his Bachelor and Master of Science. During these studies, Tobias completed laboratory rotations studying hematopoietic stem cells at the German Cancer Research Institute (DKFZ) with Prof. Andreas Trumpp, murine neuroscience at the Harvard Center for Brain Science with Prof. Bence P. Ölveczky and analysing single-cell RNA sequencing data of induced pluripotent stem cells at Cambridge University with Prof. John Marioni. In 2018, he performed an internship at Maastricht University in the group of Prof. Mark Post under the supervision of Dr. Shijie Ding. After completing his M.Sc. thesis on cancer stem cells at the Heidelberg Institute for Stem Cell Technology and Experimental Medicine in 2019, he started as a Ph.D. student in the Cell Biology team of Mosa Meat, the first European cultured meat start-up company founded by Mark Post and Peter Verstrate. In 2020, Tobias established the Cellular Agriculture Online Symposium (CAOS), an online platform to facilitate scientific exchange in the cellular agriculture space, and co-founded the non-profit organisation Cell-Ag Germany. Outside of the lab, he enjoys snowboarding, triathlon, and climbing, and is an enthusiast of music and film.

PUBLICATIONS

Published

Messmer, T., Klevernic, I., Furquim, C., Ovchinnikova, E., Dogan, A., Cruz, H., Post, M.J., Flack, J.E. A serum-free media formulation for cultured meat production supports bovine satellite cell differentiation in the absence of serum starvation. *Nat Food* **3**, 74–85 (2022).

Dohmen, R.G.J., Hubalek, S., Melke, J., **Messmer, T.**, Cantoni, F., Mei, A., Hueber, R., Mitic, R., Remmers, D., Moutsatsou, P., Post, M.J., Jackisch, L., Flack, J.E. Muscle-derived fibro-adipogenic progenitor cells for production of cultured bovine adipose tissue. *npj Sci Food* **6**, 6 (2022).

Submitted for publication

Messmer, T., Dohmen, R.G.J., Schaeken, L., Melzener, L., Hueber, R., Godec, M., Post, M.J., Flack, J.E. Single-cell analysis of bovine muscle-derived cell types for cultured meat production.
Preprint available at: https://doi.org/10.1101/2022.09.02.506369

Prepared for submission

Messmer, T., Dohmen, R.G.J., Schaeken, L., Melzener, L., Pimenta, J., Bister, A., Martins, B., Gouveia, M., Shirley, S., Papadopoulos, J., Raina, D., Hueber, R., Bouchet, B., Flack, J.E. Scientific advances and technical challenges of cell production for cultured meat.

Messmer, T., Schaeken, L., Papadopoulos, J., Melzener, L., Hueber, R., Boerlin, C., M., Post, M.J., Flack, J.E. Variability in proliferation and differentiation between satellite cell cultures emerges during long-term expansion.

Melzener, L, **Messmer, T.**, Schaeken, L., Fros, M., Kiessling, A., Raina, D., Remmers, D., Wijler, G., Spaans, S., M., Post, M.J., Flack, J.E. Reprogramming of reserve cells enables optimized myogenic differentiation for cultured meat production.